Technical Report *June 1973*

Slanting for Combined Nuclear Weapons Effects: EXAMPLES WITH ESTIMATES, AND AIR BLAST ROOM FILLING

For:

DEFENSE CIVIL PREPAREDNESS AGENCY
WASHINGTON, D.C. 20301

Contract DAHC20-71-C-0292
DCPA Work Unit 1154H

SRI Project 1219-1

STANFORD RESEARCH INSTITUTE
Menlo Park, California 94025 · U.S.A.

SECURITY CLASSIFICATION OF THIS PAGE (When Data Entered)

REPORT DOCUMENTATION PAGE

READ INSTRUCTIONS BEFORE COMPLETING FORM

1. REPORT NUMBER: (none)

2. GOVT ACCESSION NO.:

3. RECIPIENT'S CATALOG NUMBER:

4. TITLE (and Subtitle): SLANTING FOR COMBINED NUCLEAR WEAPONS EFFECTS: EXAMPLES WITH ESTIMATES, AND AIR BLAST ROOM FILLING

5. TYPE OF REPORT & PERIOD COVERED: Technical Report

6. PERFORMING ORG. REPORT NUMBER:

7. AUTHOR(s): H. L. Murphy and J. E. Beck

8. CONTRACT OR GRANT NUMBER(s): DAHC20-71-C-0292

9. PERFORMING ORGANIZATION NAME AND ADDRESS:
Stanford Research Institute
Facilities and Housing Research Dept.
Menlo Park, California 94025

10. PROGRAM ELEMENT, PROJECT, TASK AREA & WORK UNIT NUMBERS: DCPA Work Unit 1154H

11. CONTROLLING OFFICE NAME AND ADDRESS:
Defense Civil Preparedness Agency
Washington, D. C. 20301

12. REPORT DATE: June 1973

13. NO. OF PAGES: 280

14. MONITORING AGENCY NAME & ADDRESS (if diff. from Controlling Office):

15. SECURITY CLASS. (of this report): UNCLASSIFIED

15a. DECLASSIFICATION/DOWNGRADING SCHEDULE:

16. DISTRIBUTION STATEMENT (of this report):
Approved for public release; distribution unlimited.

17. DISTRIBUTION STATEMENT (of the abstract entered in Block 20, if different from report):

18. SUPPLEMENTARY NOTES:

19. KEY WORDS (Continue on reverse side if necessary and identify by block number):
Protective Shelter, Nuclear Weapon Effects
Slanting
Combined Nuclear Effects Slanting
Protective Shelter, Natural Disasters
Nuclear Attack Shelter
Nuclear Attack
Protective Shelter Costs
Shelter Costs

20. ABSTRACT (Continue on reverse side if necessary and identify by block number):

This report provides updated and expanded versions of, and thus replacements for, Chapter 8 (Slanting the Building) and Appendix E (Room Filling from Air Blast) in the latest of a series of feasibility studies* on slanting (design modification) of basements in new buildings, to provide shelter against combined nuclear weapons effects - air blast and initial nuclear, thermal and fallout radiation. As in the overall feasibility study, the two parts of this report were written solely for the guidance of building design professionals (archi-

DD FORM 1 JAN 73 1473
EDITION OF 1 NOV 65 IS OBSOLETE

19. KEY WORDS (Continued)

20 ABSTRACT (Continued)

tects and engineers). *Full slanted basement shelters, as presented in these reports, more than meet requirements for protection against all natural disasters except floods, even those designed for as low as 5 or 10 psi air blast overpressure and related radiation effects.*

This first part of this report, entitled Chapter 8 (Slanting the Building), uses the study Scope and Stipulations sections, plus weapons effects data and engineering protective design guidance provided by earlier chapters, applying such data and guidance to slanting four buildings in a total of eighteen modifications from the buildings as originally designed. The first eight modifications are for 15 psi design peak overpressure and related effects; additional slanting applications are for 5, 10, and 20 psi on two buildings ("open" shelter), and 20 and 30 psi on two others of the four buildings ("closed" shelter). Floor plans show both original layouts and slanting layouts, with the latter keyed to tables showing the specific modifications and the additional estimated cost of each.

The second part of the report, entitled Appendix E (Room Filling from Air Blast), provides the theory, equations, and practical simplifications necessary to solve the problem of estimating the behavior of air blast inside shelters, including locating zones of drag pressure or wind hazard (jet effect) and developing the pressure/time history of the average overpressure buildup and subsidence within the shelter (room filling). An interactive computer program (FORTRAN) listing is included.

* Murphy, H. L., Feasibility Study of Slanting for Combined Nuclear Weapons Effects (Revised), Volumes 1 and 2, SRI Technical Report for OCD (DCPA), July 1971 (AD-734 831 and 2), and an updating report:
Murphy, H. L., and J. R. Rempel, Slanting for Combined Nuclear Weapons Effects: FIRE HAZARD REDUCTION, Stanford Research Institute Technical Report for Defense Civil Preparedness Agency, August 1971 (AD-762 472).

STANFORD RESEARCH INSTITUTE
Menlo Park, California 94025 · U.S.A.

Technical Report *June 1973*

Summary

Slanting for Combined Nuclear Weapons Effects: EXAMPLES WITH ESTIMATES, AND AIR BLAST ROOM FILLING

By: H. L. MURPHY
J. E. BECK
Facilities and Housing Research

For:

DEFENSE CIVIL PREPAREDNESS AGENCY
WASHINGTON, D.C. 20301

Contract DAHC20-71-C-0292
DCPA Work Unit 1154H

SRI Project 1219-1

SUMMARY

This report provides updated and expanded versions of, and thus replacements for, Chapter 8 (Slanting the Building) and Appendix E (Room Filling from Air Blast) in the latest of a series of feasibility studies* on slanting (design modification) of basements in new buildings, to provide shelter against combined nuclear weapons effects - air blast and initial nuclear, thermal and fallout radiation. In addition, the Preface and Summary from the feasibility study have been combined and appear in the pages following the Preface of this report, in order to give the reader an orientation on the purpose and results of the full feasibility study. Another updating report† has been published since the latest complete version of the feasibility study.*

As in the overall feasibility study, the two parts of this report were written solely for the guidance of the design professionals (architects and engineers), who may be called upon to design shelter to protect people in the basement of a new building or other adaptable structure situated below grade. This report, therefore, is not intended to be a comprehensive or even complete discussion of all aspects of the two subjects in its title: It is limited in scope to suit the purpose just described.

It is emphasized that protective shelter of the kind contemplated in full slanting - i.e., to protect against 15 psi nuclear air blast and related radiation effects (or even much lower than 15 psi) - provides excellent (full) protection against such natural disasters as earthquakes, hurricanes (including cyclones), and tornadoes. Also, such protective shelter provides fire protection at a level equaling, in most aspects exceeding, fire codes, because fire codes assume continuing availability of professional fire departments and water supply, while their nonavailability is assumed in full slanting. *In short, full slanted basement shelters more than satisfy requirements for protection against all natural disasters except floods.*

---

* Murphy, H. L., Feasibility Study of Slanting for Combined Nuclear Weapons Effects (Revised), Volumes 1 and 2, SRI Technical Report for OCD (DCPA), July 1971 (AD-734 831 and 2).

† Murphy, H. L., and J. R. Rempel, Slanting for Combined Nuclear Weapons Effects: FIRE HAZARD REDUCTION, Stanford Research Institute Technical Report for Defense Civil Preparedness Agency, August 1971 (AD-762 472).

For updating a copy of the latest slanting report,* Chapter 8 and Appendix E herein are total replacements for Chapter 8 and Appendix E of the slanting report; and page 11-38.1 herein is an addition to the slanting report* and replaces the updating page 11-38.1 provided by an intervening updating report.†

This first part of this report, entitled Chapter 8 (Slanting the Building), uses the study Scope and Stipulations sections, plus weapons effects data and engineering protective design guidance provided by earlier chapters, applying such data and guidance to slanting four buildings in a total of eighteen modifications from the buildings as originally designed. The first eight modifications are for 15 psi design peak overpressure and related effects; additional slanting applications are for 5, 10 and 20 psi on two buildings ("open" shelter), and 20 and 30 psi on two others of the four buildings ("closed" shelter). Floor plans show both original layouts and slanting layouts, with the latter keyed to tables showing the specific modifications and the additional estimated cost of each. Summaries are provided in tables (one for each overpressure just mentioned) that show estimated cost subtotals for four categories of modifications - structural, blast doors, ventilation (including emergency exit tunnels, if any), and other - as well as overall totals. In addition, the summary tables show estimates for nondeferrable slanting items in each of the four categories, meaning those items that judgment dictated must be incorporated at the time the building is built. The tables also provide various percentages, as well as costs per square foot for various (calendar) times. An air blast room filling application is shown in the case of the larger of the two open shelters. Other sections briefly discuss such things as baffle walls and drag pressures; a comparison of two centerline support systems; and three blast door schemes (with cost estimates) used in the slanting applications. The results clearly show the feasibility of building protective shelter, for 15 psi air blast peak overpressure and related nuclear weapons effects, at an additional or incremental cost of not more than $6/sf as of January 1968, or a comparable current criterion (about $7.74/sf as of June 1973).

The second part of the report, entitled Appendix E (Room Filling from Air Blast), provides the theory, equations, and practical simplifications necessary to solve the problem of estimating the behavior of air blast inside shelters, including locating zones of drag pressure or wind hazard (jet effect) and developing the pressure/time history of the average overpressure buildup and subsidence within the shelter (room filling).

---

* Same footnote as preceding page.

† Same footnote as preceding page.

The appendix also includes guidance on text material that may be skipped without loss of continuity and on choice of calculational methods offered, plus an interactive (or conversational) computer program in a FORTRAN commercial time-sharing version with both a listing and user guidance.

The report authors prepared Chapter 8 as a considerable expansion of the original chapter by the senior author; the indicated author of Appendix E, J. R. Rempel, also prepared the earlier published version.

Authors

Except for Appendix E and two specialized areas in Chapter 8 where preparation by colleagues is indicated by footnote, the report senior author prepared all original[3] and revised text material herein and supervised all project work. The junior author carried out the work of correcting any discrepancies found in the eight earlier case studies (building examples of slanting), including the associated data tables and floor plans, then completed the considerable amount of new work in ten new case studies, all for air blast peak overpressures other than 15 psi. For both the original eight studies and the new ten, Mr. C. K. Wiehle made a substantial contribution by completing the dynamic design of most of the structural elements in the slanting versions of the buildings.

The named author of Appendix E was also the author of the earlier published version.[3]

Acknowledgments

Through suggestions, guidance, or supporting work, the technical help of many persons was freely given and is gratefully acknowledged: G. N. Sisson, N. A. Meador, and M. A. Pachuta, U.S. Defense Civil Preparedness Agency; Prof. W. J. Hall, University of Illinois; and J. R. Rempel, C. K. Wiehle, and G. G. Hoskins, Stanford Research Institute.

PREFACE AND SUMMARY FROM THE FEASIBILITY STUDY ON FULL SLANTING[3]

The feasibility study and results described in this report had two principal goals:

- To determine the general feasibility of slanting for combined nuclear weapons effects, within a specified scope and stipulated conditions prescribed by the U.S. Office of Civil Defense.

- To organize the work and resulting report in such a manner that, should the general question of feasibility be answered affirmatively by this study, the later preparation of a prototype guide or manual for use by architects and engineers would be facilitated.

Because of the latter goal, this report is organized as a guide and the word "guide" is used frequently; nonetheless, the report is intended only to cover a feasibility study, not to provide a guide for protective design.

Publication of a report at this stage of work thus has two broad purposes:

- To demonstrate the possibility that full slanting is achievable, i.e., modification of usual building designs to provide protection in basements against 15 psi overpressure and associated nuclear weapons effects appears possible within the prescribed (added cost) limitation of $6/sf (January 1968) of shelter space.

- To serve as a clearly defined point of departure in the further work of several researchers, including not only those working directly on the project but also those working on associated U.S. Office of Civil Defense research projects that are expected to contribute inputs to this work.

It is hoped that readers will feel free to provide constructive technical comments to the author by whatever means is most convenient to the reviewer. A discussion of planned further work is included at the end of the report (Chapter 11).

Chapter 1 includes introductory material and sections on Scope, Stipulations, Approach, Preliminary Building Selection for Slanting, and Acknowledgments. Chapters 2 through 6 provide nuclear effects data and design methodology needed by the architect or professional engineer for combined nuclear effects slanting design. Chapters 7 and 8 constitute applications of the data and methodology to certain buildings selected for use as examples or case studies, and for which complete design drawings were at hand. Chapters 9 and 10 will attempt to draw together lessons learned from the case studies. The Appendices, Volume 2, contain supporting data too voluminous to include in Volume 1.

The revised feasibility study includes discussion of open shelter - concept, problems, and types - with two types included as case studies (applications of full slanting, with cost estimates and floor plans); also an open shelter case study of the two below-grade levels of a large parking garage was completed, except for needed review work in some high cost areas such as ventilation, showing a tremendous potential for combined effects shelter. Each case study slanting cost estimate was summarized into four major categories: structural, blast doors, ventilation, and other. An estimate is also shown for that work which must reasonably be performed at the time of original building construction, i.e., non-deferrable work.

Included too are typical designs, using a detailed final design procedure, for simply supported one-way reinforced concrete slabs. Designs using all combinations of three concrete strengths, two dynamic steel strengths, and four positive moment steel ratios are shown by graphs; a graph for one steel ratio shows total estimated steel quantities. All design graphs have scales for slab clear span, effective depth, positive and negative moment steel ratios, and stirrup steel ratio.

REFERENCES USED IN THE PREFATORY MATERIAL

1. Murphy, H. L., Feasibility Study of Slanting for Combined Nuclear Weapons Effects, Stanford Research Institute Technical Report for U.S. Office of Civil Defense (now Defense Civil Preparedness Agency or DCPA), June 1969 (AD-692 312).

2. Murphy, H. L., Feasibility Study of Slanting for Combined Nuclear Weapons Effects (Revised), Volumes 1 and 2, SRI Interim Report for OCD (DCPA), October 1970 (AD-724 711 and 2).

3. Murphy, H. L., Feasibility Study of Slanting for Combined Nuclear Weapons Effects (Revised), Volumes 1 and 2, SRI Technical Report for OCD (DCPA), July 1971 (AD-734 831 and 2).

4. Murphy, H. L., and J. R. Rempel, Slanting for Combined Nuclear Weapons Effects: FIRE HAZARD REDUCTION, Stanford Research Institute Technical Report for Defense Civil Preparedness Agency, August 1972 (AD-763 472).

Chapter 8

SLANTING THE BUILDING

The following sections briefly present the approach and rationale applied to the full slanting in each case study. Preslanting and post-slanting basement floor plans are used, as are tables listing the specific slanting changes (keyed to the appropriate floor plan) and the estimated additional cost of each tabulated item.* These costs clearly show the considerable impact of structural blast-resistant design, and selection of an ultimate deflection criterion μ for flexural structural members strongly affects such design. Selection of this criterion is discussed in the section of Chapter 6 entitled "General Comments on Blast-Resistant Design of a Structural Element," which includes mention of design charts in Ref. 2 tailored to μ=3; the design charts were frequently used in the slanting case studies (examples) described in this Chapter, but the modest conservatism introduced thereby is considered to be balanced by other items that might have been overlooked, or that are mentioned but not estimated. A reasonable upper bound on cost was sought; therefore, use of alternative structural designs, design optimization techniques, or both, is likely to show lower slanting costs than those presented herein. Designs herein were only complete enough, and often only of sample members, for comparative cost estimating.

Case studies shown as Buildings 1A, 1B, and 2A considered only closed shelter, because the room filling prediction method available at the time of the studies did not merit sufficient confidence in its reliability, for predicting even the average room pressure rise-time, to warrant its use for back-loading on a wall or slab in hopes of reducing the member load, design, and related cost. Appendix E presents a later version on room filling than was available for these first three case studies. The concept of open shelter (at least one entry open to shelterees until one full minute or more after arrival of the blast wave; see

---

* That is, the cost of the slanted (modified design) item minus the cost of the similar item in the original design. Dollar values were tabulated as estimated and do not imply accuracy beyond the usual degree inherent in such estimating.
General note concerning all floor plans herein: any framing indicated is generally for the floor system above the shelter space(s) shown in the floor plan; each slanting scheme (except Bldg. 1A) is described by a table keyed to the floor plan, and the table may describe any modification, whether framing above the space(s) or footings below or any other item(s).

Open Shelter section of this chapter) has many advantages including the important one of making unnecessary a decision as to when and in whose face the shelter door is to be closed. Open shelter is included in full slanting of later case study buildings. Later studies of all the buildings also consider overpressures other than 15 psi. At 15 psi, potential debris loads from the specific case buildings were considered as not controlling on shelter structural design; while this consideration might be inapplicable at 5 or 10 psi, it was nevertheless similarly applied, in the interests of obtaining relative costs for the general case (low-rise buildings).

Figure 8-0A schematically shows a shelter fresh air intake/emergency exit that was used several times, particularly in the first three case studies. Figure 8-0B indicates a version offering more protection against a vehicle being rolled onto and blocking the emergency exit. Figure 8-0C shows a window-well version. Figure 8-0D suggests a ventilation duct/emergency exit scheme; the blast doors are for an "open" shelter discussed later herein. Figure 8-0E illustrates three blast door schemes, all of which were used in full slanting of case study buildings described later in this chapter; further details and cost estimates are provided in a later section of this chapter.

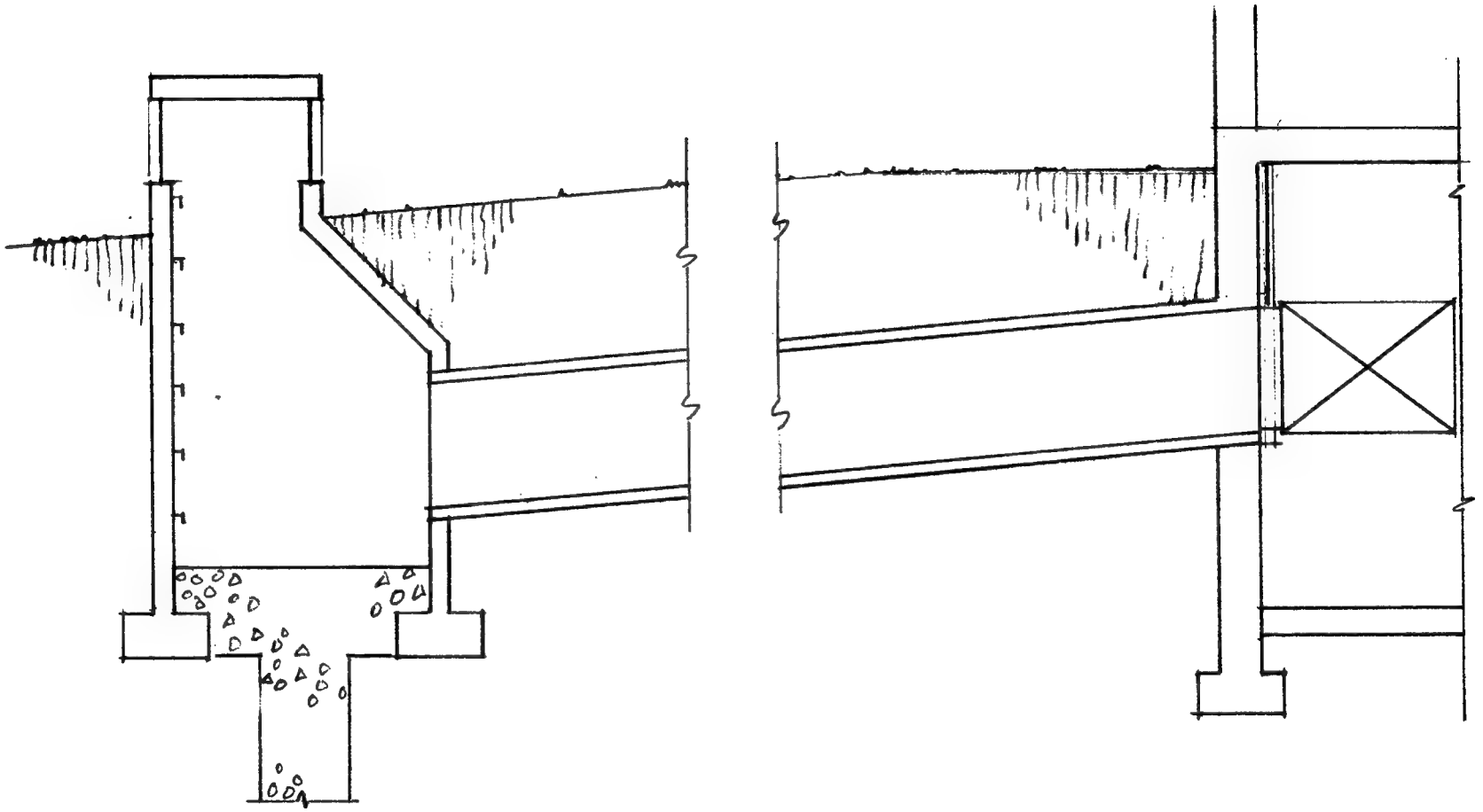

FIG. 8-0A FRESH AIR INTAKE/EMERGENCY EXIT SCHEME

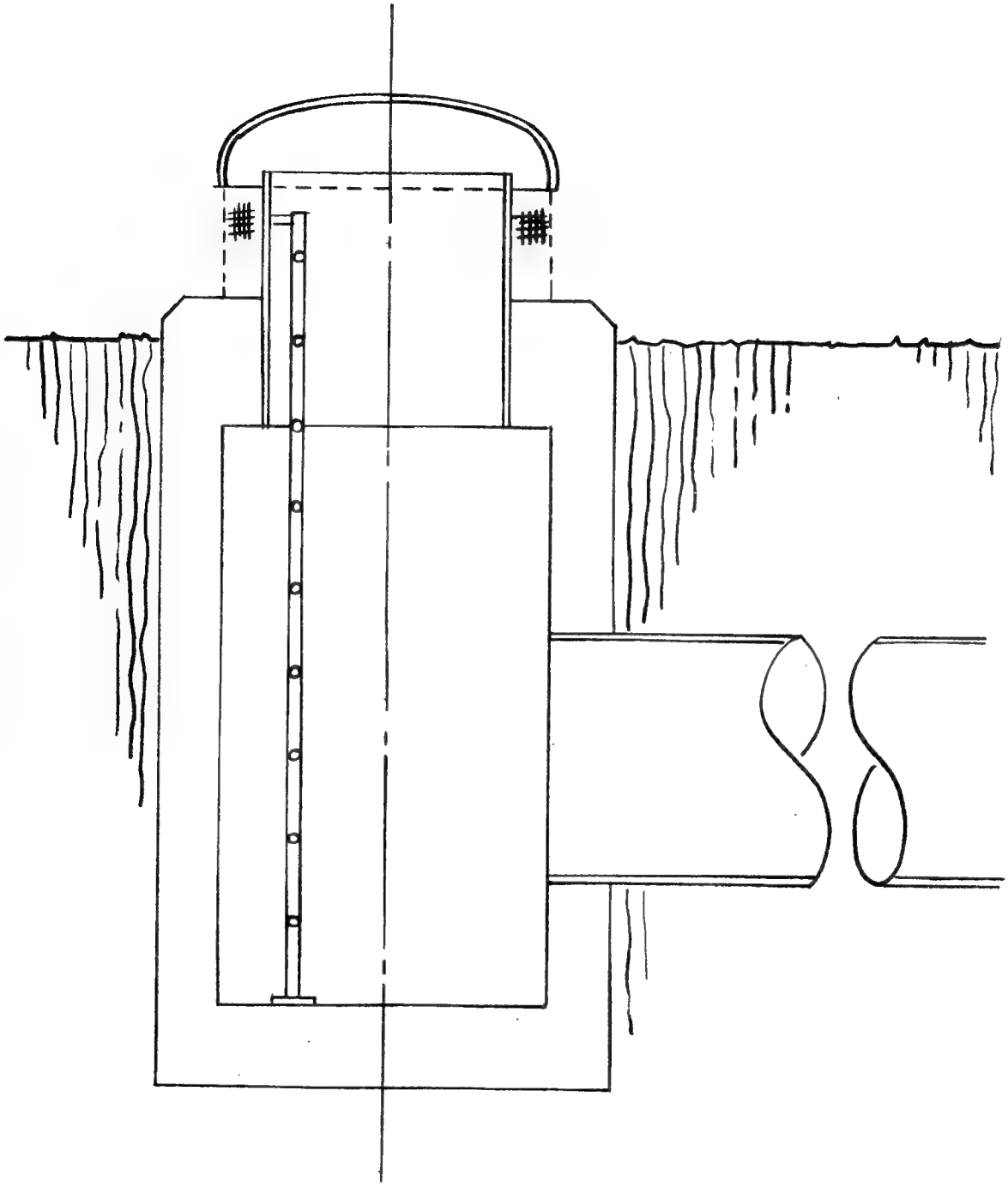

FIG. 8-0B FRESH AIR INTAKE/EMERGENCY EXIT ALTERNATE SCHEME

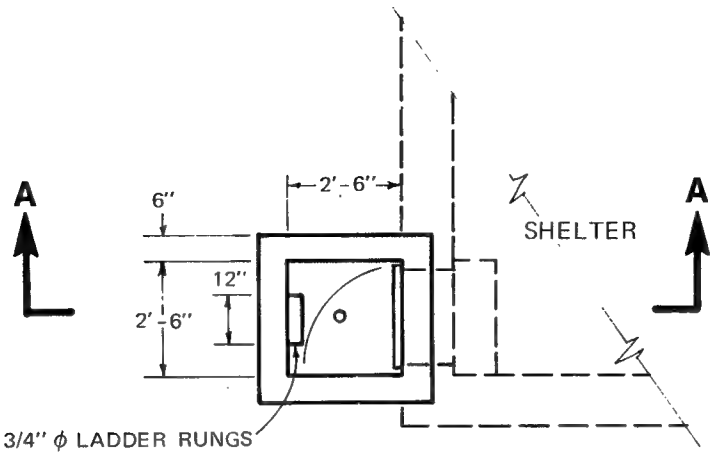

PLAN

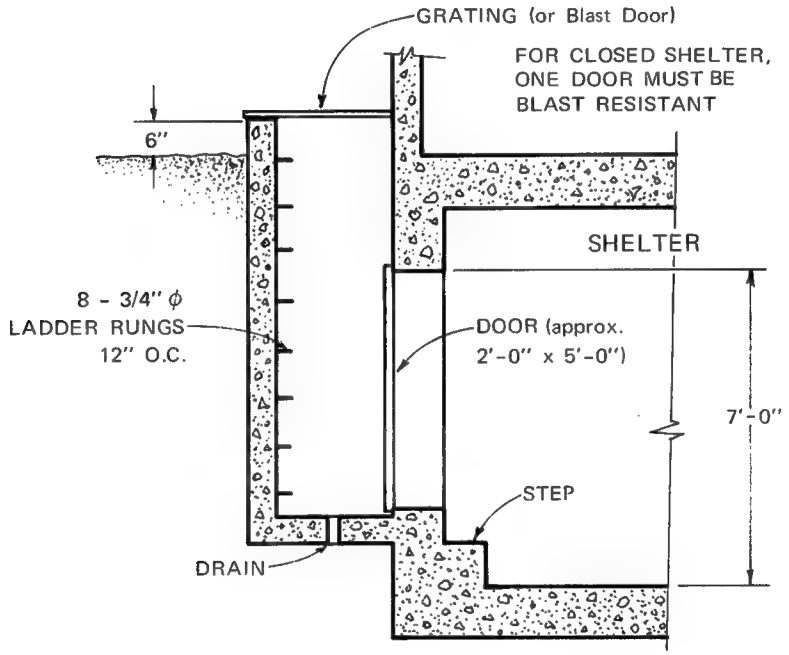

SECTION A–A

SOURCE: Reference 25, plus modifications

FIG. 8-0C BASEMENT SHELTER WINDOW-WELL ESCAPE EXIT

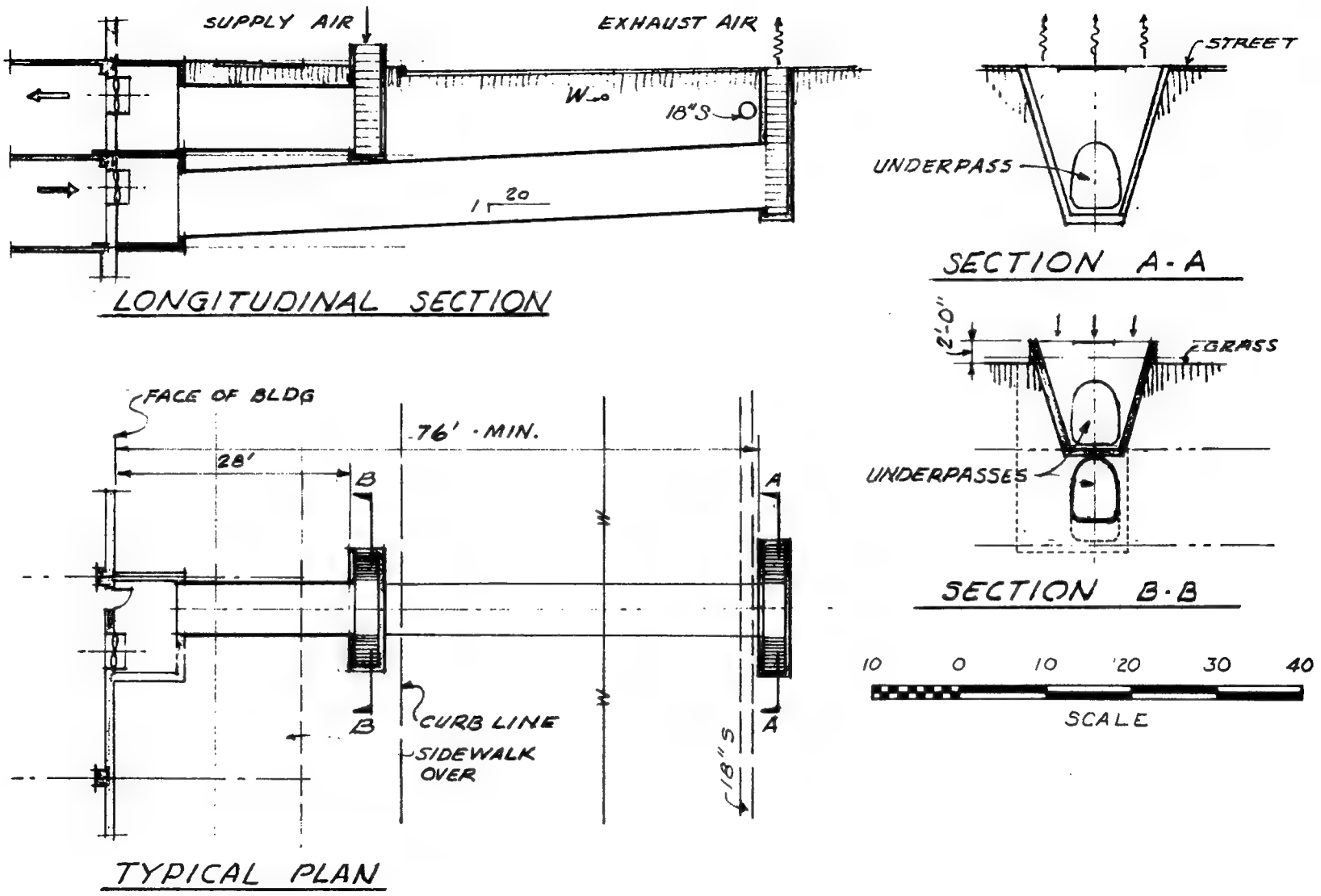

FIG. 8-0D VENTILATION/EMERGENCY EXIT SCHEME – OPEN SHELTER VERSION

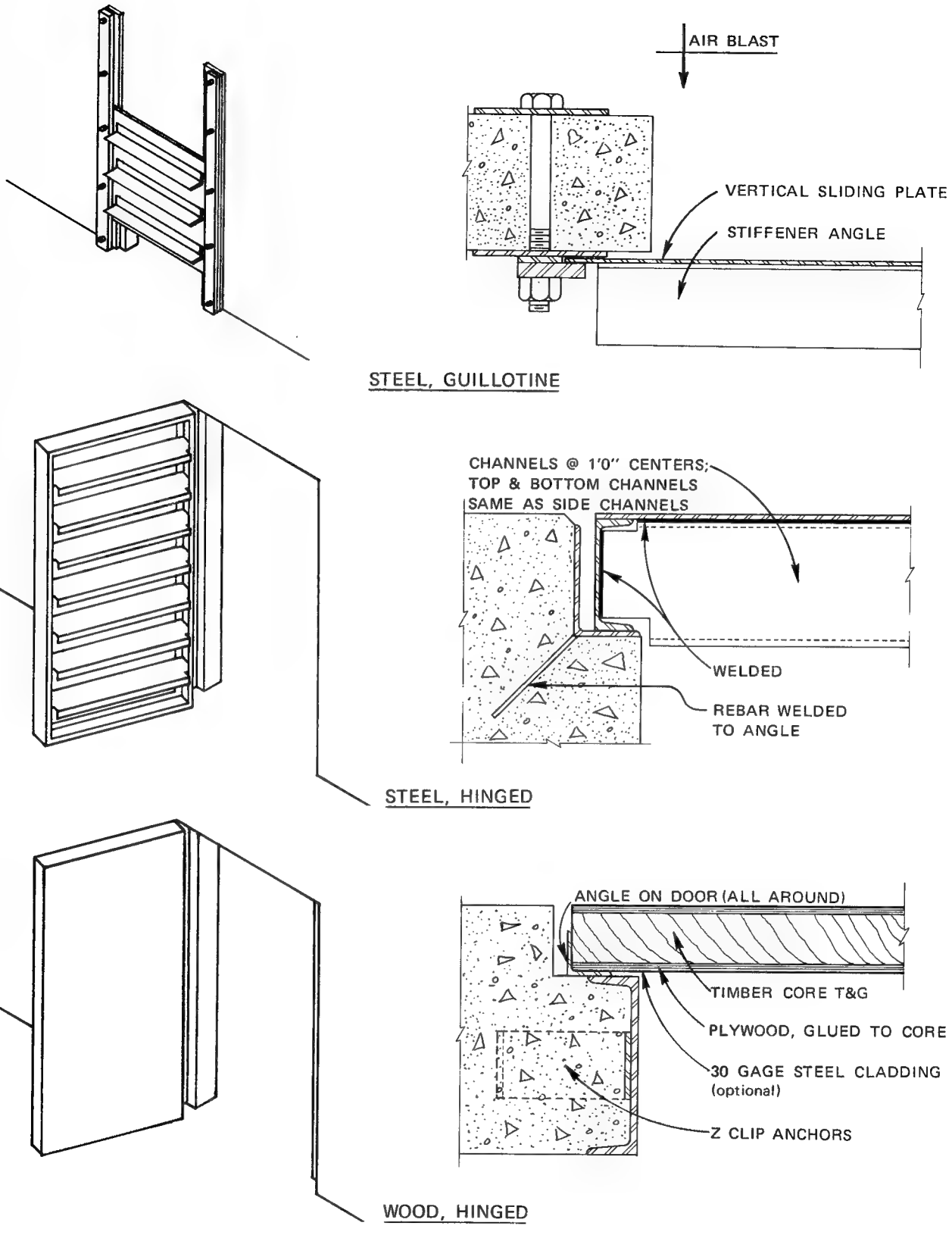

a. ISOMETRIC VIEWS

b. HORIZONTAL SECTIONS IN VERTICAL DOORS

FIG. 8-0E BLAST DOOR SCHEMES USED FOR ESTIMATING

Building 1A

The building is described in general terms in Chapter 7. The designed basement floor plan is shown in Figure 8-1. The slanted version is shown in Figure 8-1A (black lines show slanting changes), the shelter area being L-shaped minus an interior stairwell. A list of slanting changes is not included herein for Building 1A because the estimated additional cost of slanting was many times the Scope limit. The estimates served to confirm what was fairly foreseeable: that too much interior blast-resistant wall was required by this L-shaped shelter and excluded stairwell. The example was useful, however, in learning rough boundaries of possible slanting measures versus the Scope cost limitation; the latter would certainly preclude consideration of this case for any slanting incentive program.

FIG. 8-1

BUILDING 1 BASEMENT FLOOR PLAN

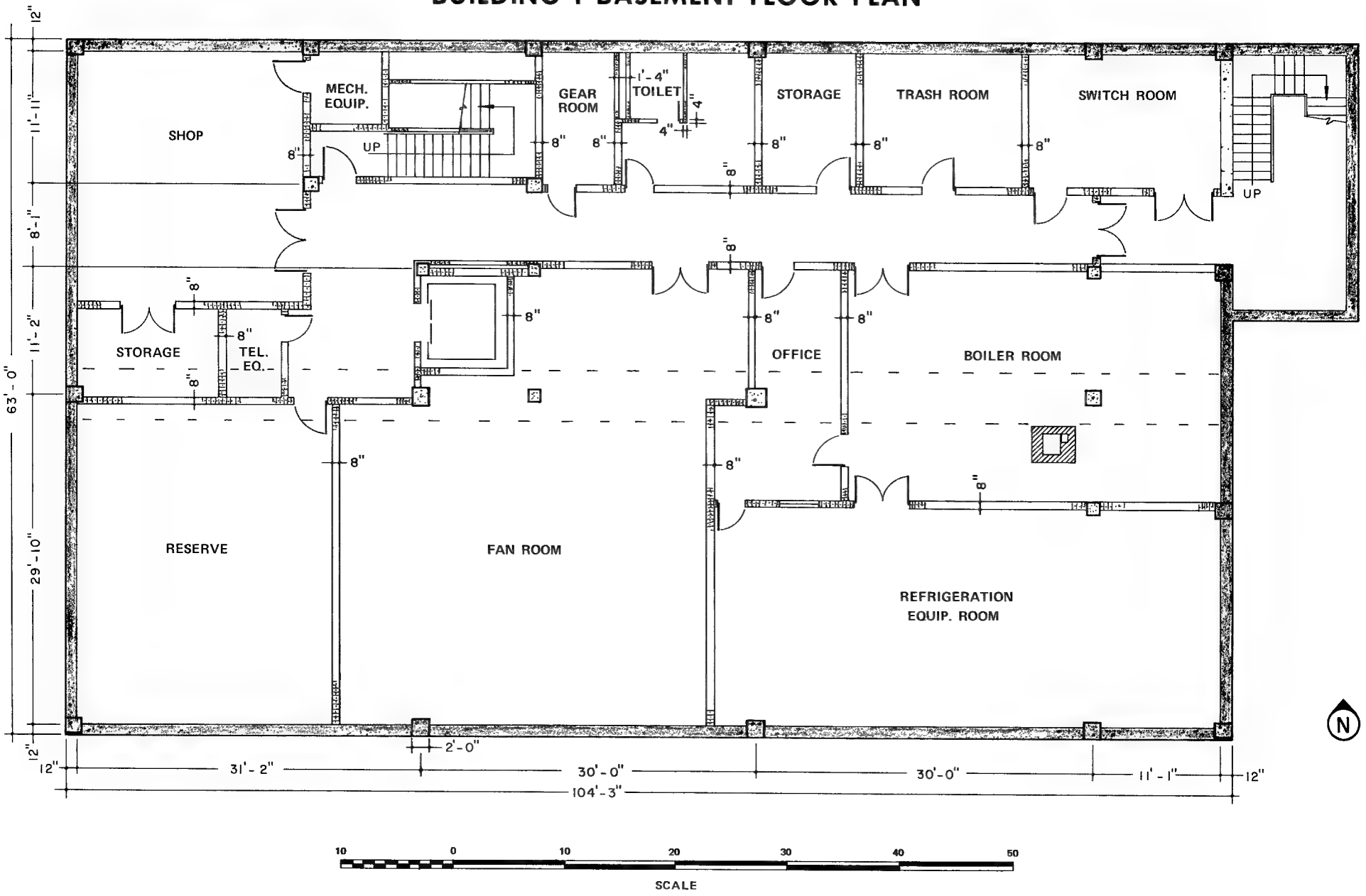

FIG. 8-1A

BUILDING 1A BASEMENT FLOOR PLAN

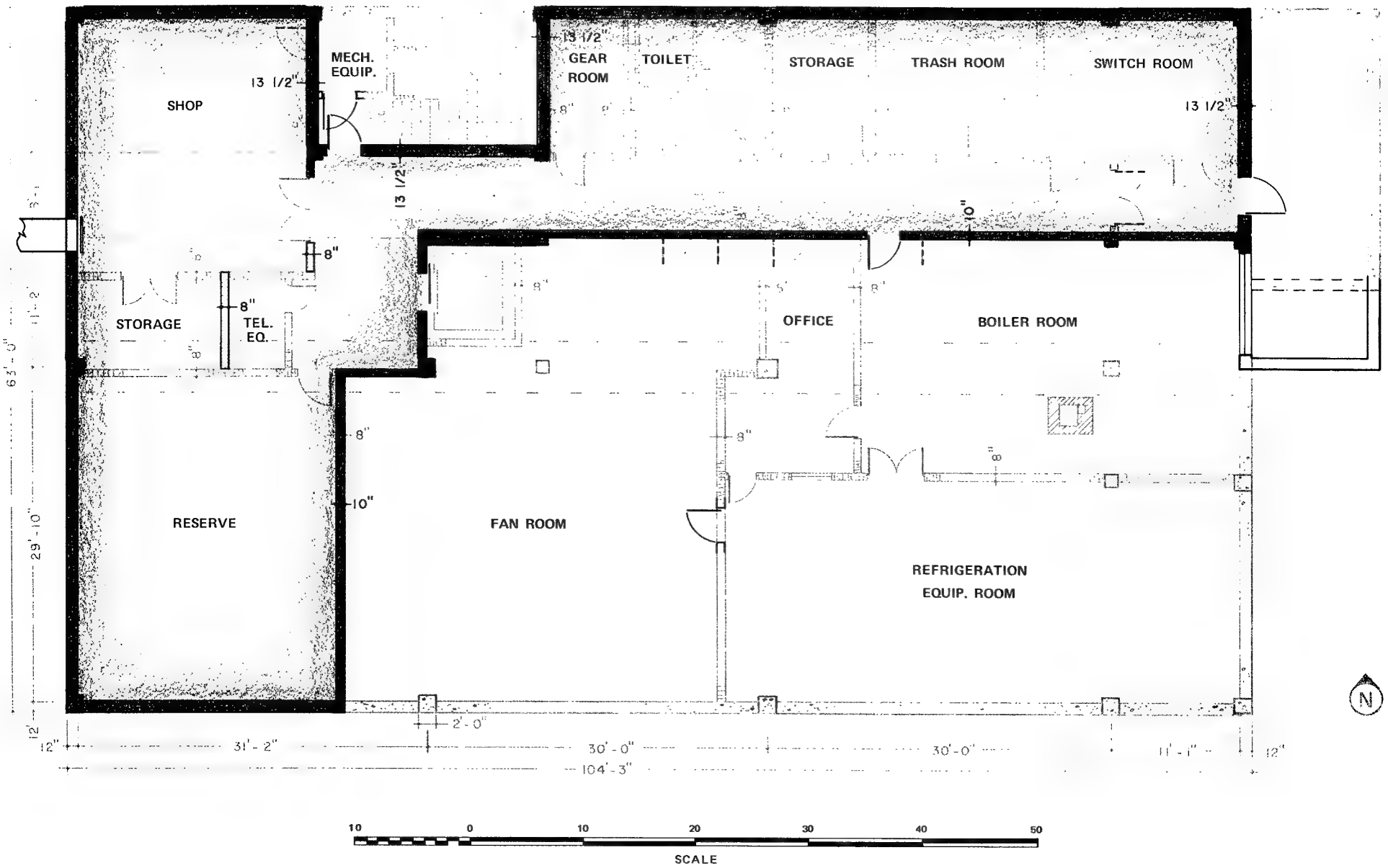

Building 1B

The building is described in general terms in Chapter 7.* The designed basement floor plan is shown in Figure 8-1, the slanted version in Figure 8-1B (black lines show slanting structural and layout changes, gray lines show the original design), the shelter being the large rectangular area across the west end. Table 8.1B provides a list of slanting changes, keyed to Figure 8-1B, as well as the estimated additional cost of each change item. Interior shelter walls are not blast-resistant.

The ducted air conditioning from central fan-coil units in the basement and penthouse, plus a boiler room, necessitate about half of the planned partial basement under this building. A slanting change to a four-pipe system (Chapter 6) was not applied because the total basement space requirement might then have been logically reduced. Instead, the many penetrations of the first floor slab for air ducts, pipes, and stairwell were left in a nonshelter area. Items 2 and 9-13, Table 8.1B, describe the slanted shelter ventilation system. The shelter fresh air intake/emergency exit is described in Item 10 and schematically shown by Figure 8-0A.

The second case study results helped in learning the effect of slanting changes versus the Scope cost limitation, in that the estimated additional cost of slanting was improved to about twice the Scope limit. The study illustrates the cost penalty of the fixed cost of Item 10 being borne by a rather small shelter, thereby inordinately increasing unit slanting costs. Further review of the concept and details of this fixed cost item was indicated.

* This second slanting use of the Newnan Post Office has a different shelter layout than the first, Building 1A, in order to reduce the amount of interior blast resistant wall required.

FIG. 8-1B

BUILDING 1B BASEMENT FLOOR PLAN

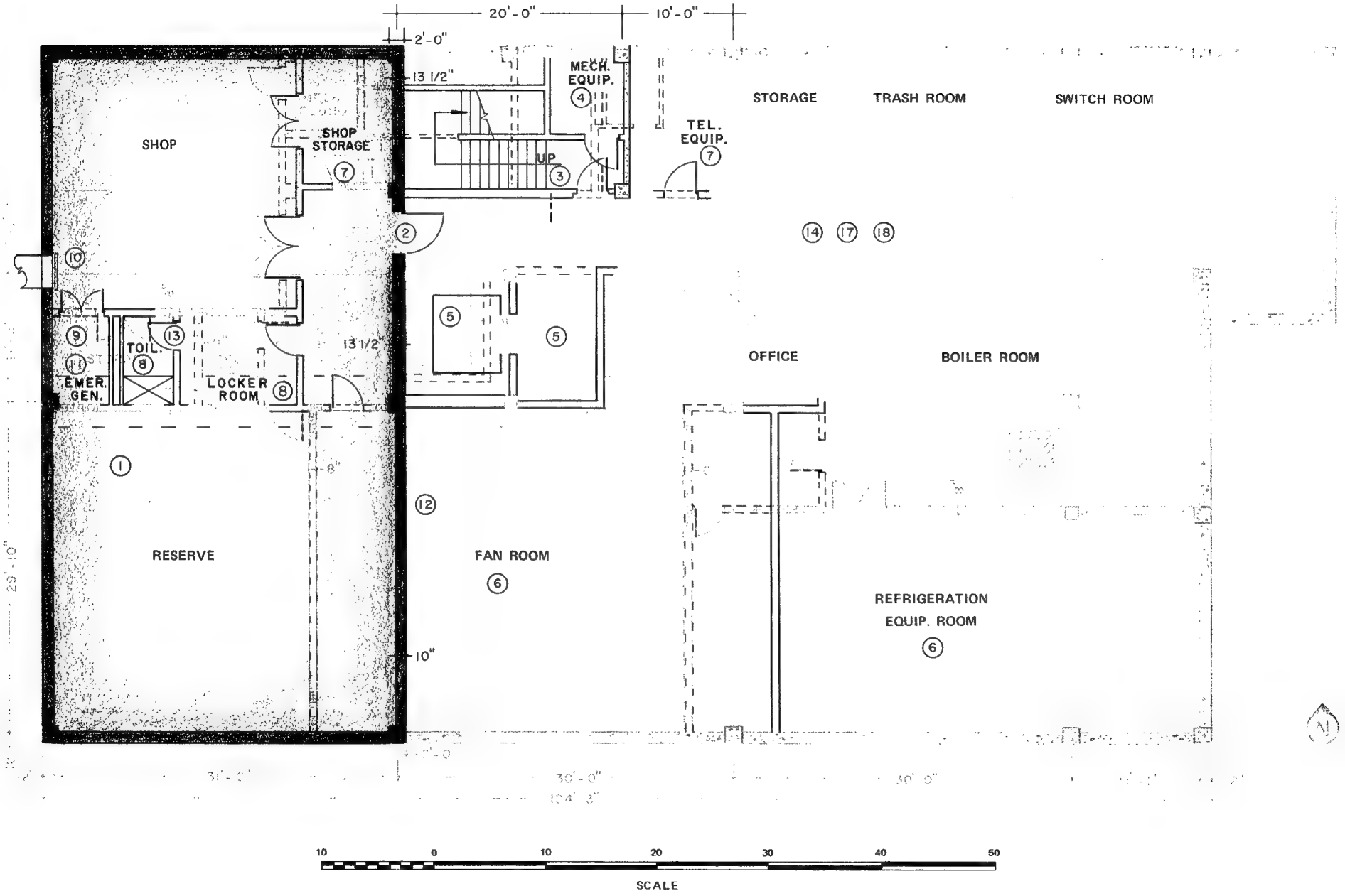

Table 8.1B

BUILDING 1B SLANTING
(Post Office, Newnan, Georgia)

1.	Provide blast walls as shown ($4,385); with blast slab above (15-1/2" thick) and centerline girder increased to 46" overall depth in shelter area ($9,498). All interior partitions in shelter to be nonbearing and detailed to remain so, even with large deflection of slab and/or girder above, say 6" or more.	$13,883
2.	Provide blast door to corridor ($760); with 1'x 4' exhaust air vent ($40) and its own vertical sliding blast door ($160) (both above corridor door). Exhaust air vents into a corridor duct.	960
3.	Relocate stair 10 ft east, as shown; revise stair layout to 3 flights to land at door shown.	*
4.	Relocate Mechanical Equipment Room as shown.	*
5.	Provide elevator with a rear door for basement use only ($1,800); and relocate basement lobby as shown, using space under ducts from Fan Room (*).	1,800
6.	Relocate Fan Room 7'9" to east, maintaining same clear width, as shown. Refrigeration Room can be reduced in size by offsetting two coolers as needed to provide space for disassembly.	*
7.	Relocate Shop Storage and Telephone Equipment Room, as shown.	*
8.	Provide Toilet Room (shower optional) and Mechanic and Labor Locker Room, as shown.	*
9.	Add Generator Room (*) for emergency power unit (5 kva) ($1,400) for shelter lighting and emergency ventilating (fans only; 3500 cfm) (*); provide engine exhaust vent ($100) at grade just outside building wall.	1,500

* Design modification considered achievable at little (<<$100) or no additional cost.

Table 8.1B (concluded)

10.	Provide fresh air intake tunnel, 36" diam. by 55' long ($1,538); plus manhole ($2,204); for use at all times for shelter area, plus emergency use as an exit. Provide vertical sliding blast door in inside face of shelter wall ($394) (dismantle fresh air duct to use tunnel as exit).	$ 4,136
11.	Provide separate air handling system for shelter area use (both normal and emergency), with fan-coil unit located overhead in Generator, Reserve or Shop Storage Room (*). In normal use, unit is to be supplied with HW and CW from existing system. In emergency use, only the fan operates, using emergency power (conduit, wire, and switches: $100).	100
12.	All nonshelter ductwork is to be outside the shelter space.	*
13.	Vent toilet with own fan, and duct out through above-door vent and new duct (#2).	135
14.	Allow no flammable wall and/or ceiling treatment in basement, inside or outside shelter.	*
15.	Metal venetian blinds with fire resistant tapes are to be used on all windows, at least on entire floor above basement.	*
16.	Roof should be Class A or B fire rating (probably normal design).	*
17.	Plumbing vent pipes should be metal (or pass 100 psi internal pressure test) and be tightly grouted (expansion type) for full depth through slab over shelter.	*
18.	All duct risers from nonshelter areas of the basement should have standard fire dampers at first floor slab level.	*
		$22,514
(June 1968)	1,911 sf	$11.78/sf

* Design modification considered achievable at little (<<$100) or no additional cost.

Building 2A

The building is described in general terms in Chapter 7. The designed basement floor plan is shown in Figure 8-2, and the slanted version in Figure 8-2A (black lines show slanting structural and architectural changes, gray lines show the original design), the shelter occupying the full basement excluding the interior stairwell and the exit hallway leading to exterior stairs. Table 8.2A provides a list of slanting changes, keyed to Figure 8-2A, as well as the estimated additional cost of each change item. Interior shelter walls are not blast-resistant. Figures 8-2.1 and 8-2A.1 provide perspective views of the building basements, as originally designed and after slanting, respectively (i.e., comparable to the floor plans of Figures 8-2 and 8-2A).

The original, natural cross-ventilation scheme contemplated for the large, open basement portion was slanted to forced fresh air ventilation of the entire basement, as described under Items 2 and 8-12, Table 8.2A. Item 17 covers an unestimated alternate, an air conditioning scheme for the shelter area. The fresh air intake/emergency exit is described in Item 9 and schematically shown by Figure 8-0A.

Table 8.2A (15 psi shelter) was used first for estimates based on June 1968 costs, then later for estimates based on June 1970 costs. Both sets of estimates were shown in the latest version of the complete combined effects slanting study/guide.[50] Only the June 1970 estimates were retained for this Chapter 8 revision, but estimates for new studies of 20 and 30 psi shelters were added.

For this third case study, estimated additional slanting costs were within the Scope limit of $6/sf (about 4% below, when both are corrected to the same time period). The study indicated the need for further review of slanting measures, aimed at reduction in ventilation and blast door costs.

FIG. 8-2

BUILDING 2 BASEMENT FLOOR PLAN

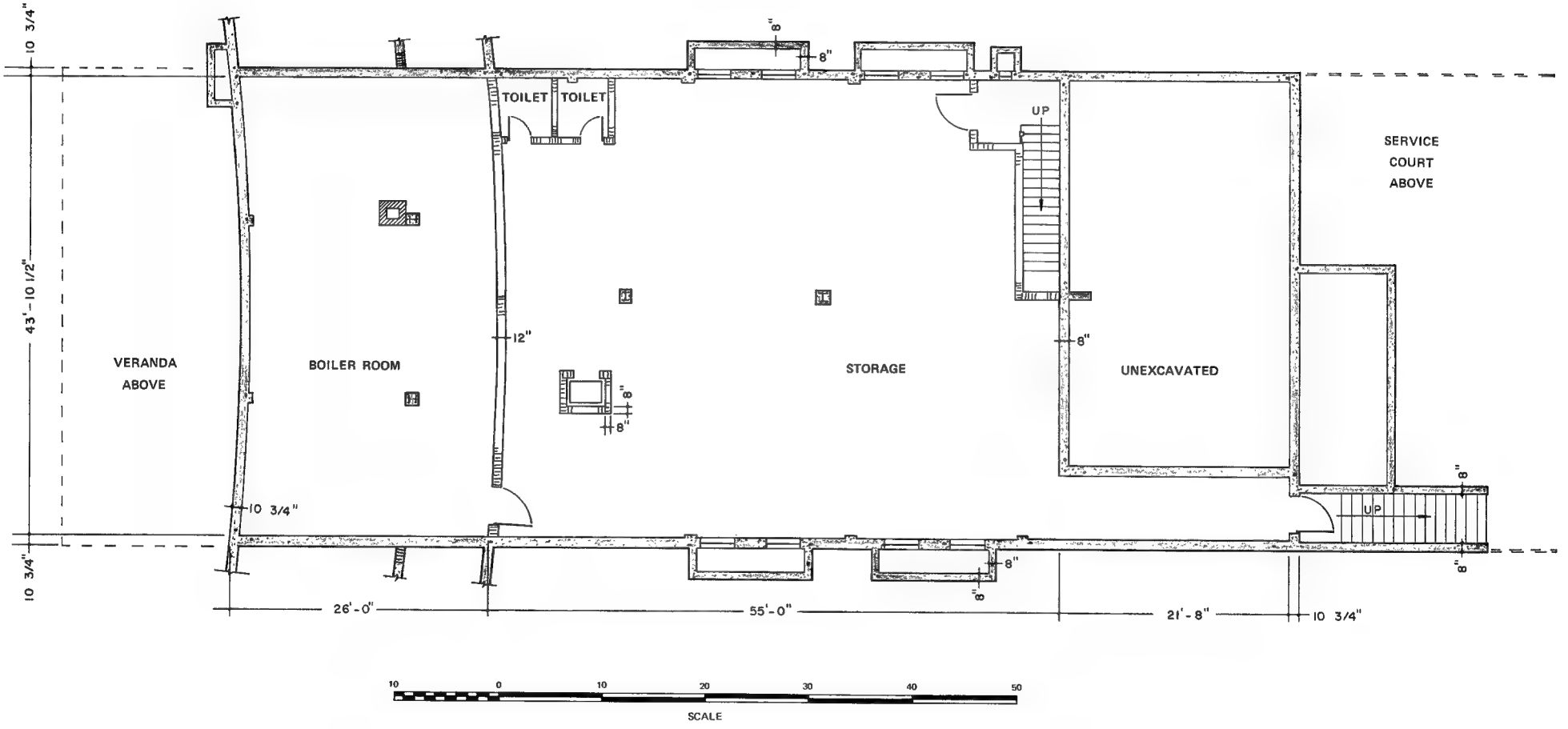

FIG. 8-2A

BUILDING 2A BASEMENT FLOOR PLAN

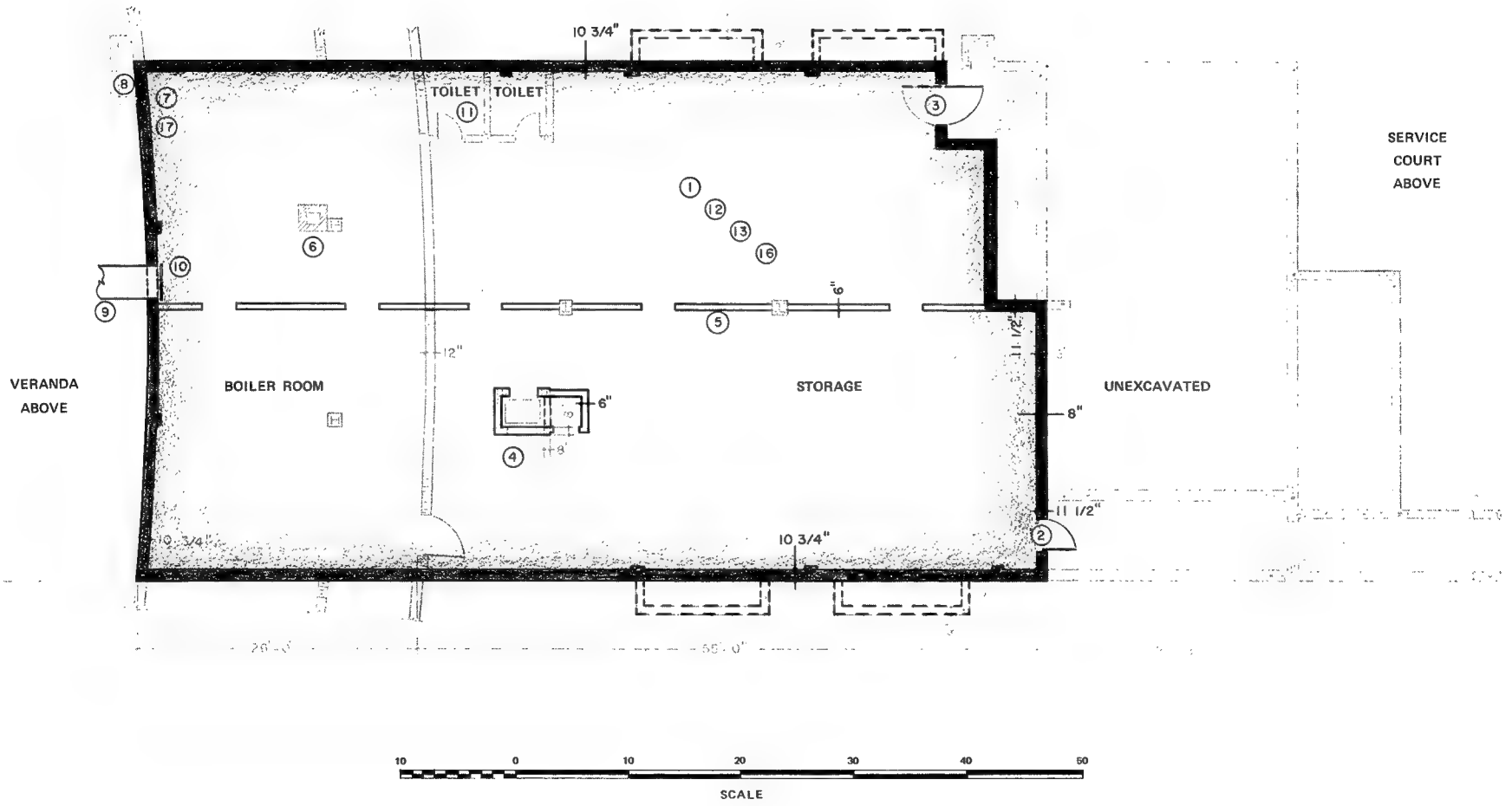

Table 8.2A

BUILDING 2A SLANTING
(Brentwood Rehabilitation Center, Asheville, N.C.)

		15 psi shelter	20 psi shelter		30 psi shelter	
1.	Provide blast walls (10-3/4" and 11" thick) as shown (-$99), with blast slab above (14-1/2" thick) ($8,385).	$8,286	(10-3/4" and 12") ($415)(17")($10,587)	$11,002	(12-1/2"and 13-1/2") ($2,166)(20")($13,460)	$15,626
2.	Provide blast door ($747), to also serve as exhaust vent for part of room air by holding door part way open using adjustable door closure ($74).	821	($750) ($74)	824	($755) ($74)	829
3.	Provide blast door between interior stairway and shelter.	747		750		755
4.	Provide blast enclosure (6" thick) around dumbwaiter and laundry chute ($1,174), with vertical sliding blast doors ($99).	1,273	(6") ($1,215) ($105)	1,320	(6") ($1,251) ($111)	1,362
5.	Provide bearing wall (6" thick) along longitudinal column line, with openings as desired.	4,894	(6")	5,074	(6")	6,547
6.	Harden chimney (in shelter) for blast (*), and provide manual blast door ($182) at breeching	182	($210)	210	($257)	257
7.	Provide 7.5 KVA emergency generator ($1,700 + panel + labor), in separate room, for lighting and ventilating.	2,270	($1,700 + +)	2,270	($1,700 + +)	2,270
8.	Convert one remaining areaway (see Plan) into exhaust for room air (passed out through generator room) and generator exhaust; estimate 24" diameter exhaust duct ($99), plus blast door ($182).	281	($99)($210)	309	($99)($257)	356
9.	Provide fresh air intake tunnel, 36" diameter by 55' long ($1,759), leading to manhole ($2,392) in clear area in front of building, to serve as emergency exit as well; vertical sliding blast door ($447) in inside face of shelter wall (dismantle duct for use as exit).	4,598	($1,759)($2,392) ($464)	4,615	($1,759)($2,392) ($519)	4,670
10.	Provide air handling system for entire shelter area, to serve normally as well as in an emergency; 4800 cfm fan ($686), ducts ($1,027) in fan room leading to wall of shelter area; air flows toward stair well, through openings in new center wall and back through boiler room door to vent system. Provide for varying mix of recirculated and fresh air.	1,713	($686)($1,027)	1,713	($686)($1,027)	1,713

Table 8.2A (concluded)

		15 psi shelter	20 psi shelter	30 psi shelter
11.	Vent toilets with own fan and ducts out through areaway (#8)	$ 307	$ 307	$ 307
12.	Delete all present exhaust risers to roof ventilators	*	*	*
13.	Allow no flammable wall and/or ceiling treatment in basement.	*	*	*
14.	Metal venetian blinds with fire resistant tapes are to be used on all windows of building wing above the basement.	*	*	*
15.	Roof of entire building should be Class A or B fire rating (probably not normal design).	*	*	*
16.	Plumbing vent pipes should be metal (or pass 100 psi internal pressure test) and be tightly grouted (expansion type) for full depth through slab over shelter. All heating pipes should be similarly grouted.	*	*	*
17.	If water well is economically available (at least for industrial water), an alternate ventilation system scheme could be considered, using only 1000 cfm fresh air mixed into same 4800 cfm in 10 above, but using well water coils to cool the entire air supply (this scheme not estimated). With this scheme, well water could be used for generator engine radiator cooling, and a blast closure valve could be used over the fresh air intake (it would be reduced enough in vent size).			
18.	Provide for all gas, water, fuel oil, etc., supply lines serving the entire facility to first enter through the Boiler Room, and have cut off valves at entry points.	†	†	†
		$25,372	$28,394	$34,692
	(June 1970 costs) 3,378 sf	$7.51/sf	$8.41/sf	$10.27/sf

* Design modification considered achievable at little (<<$100) or no additional cost.

† Costs not estimated, but probably minor.

FIG. 8-2.1

BUILDING 2 BASEMENT PERSPECTIVE

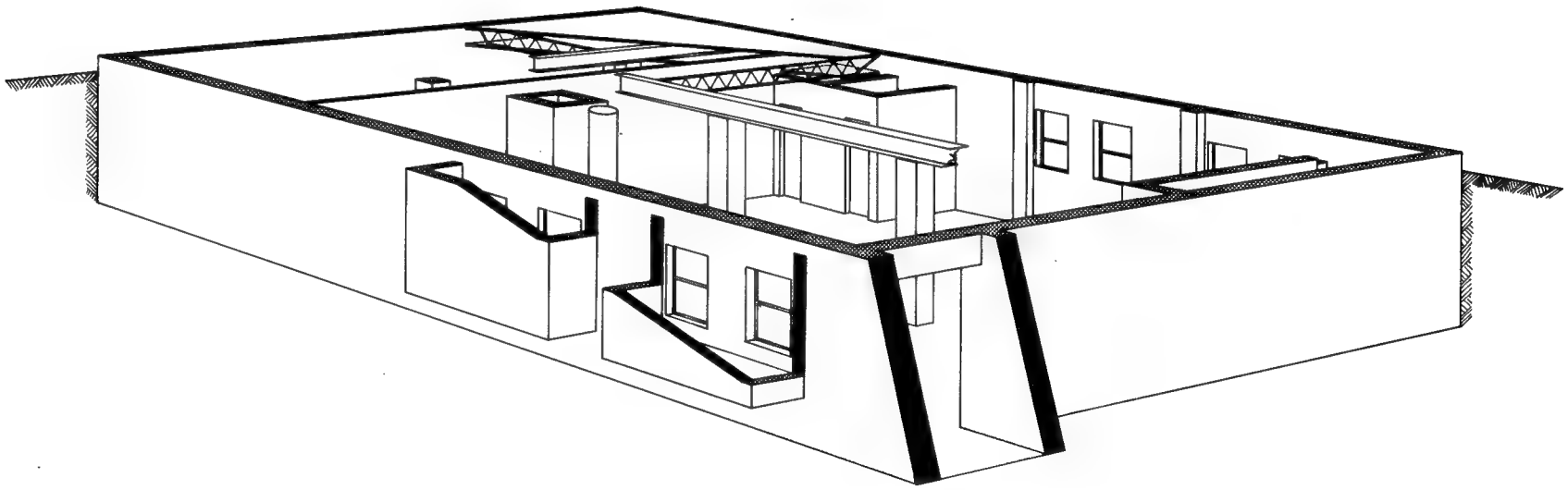

FIG. 8-2A.1

BUILDING 2A BASEMENT PERSPECTIVE

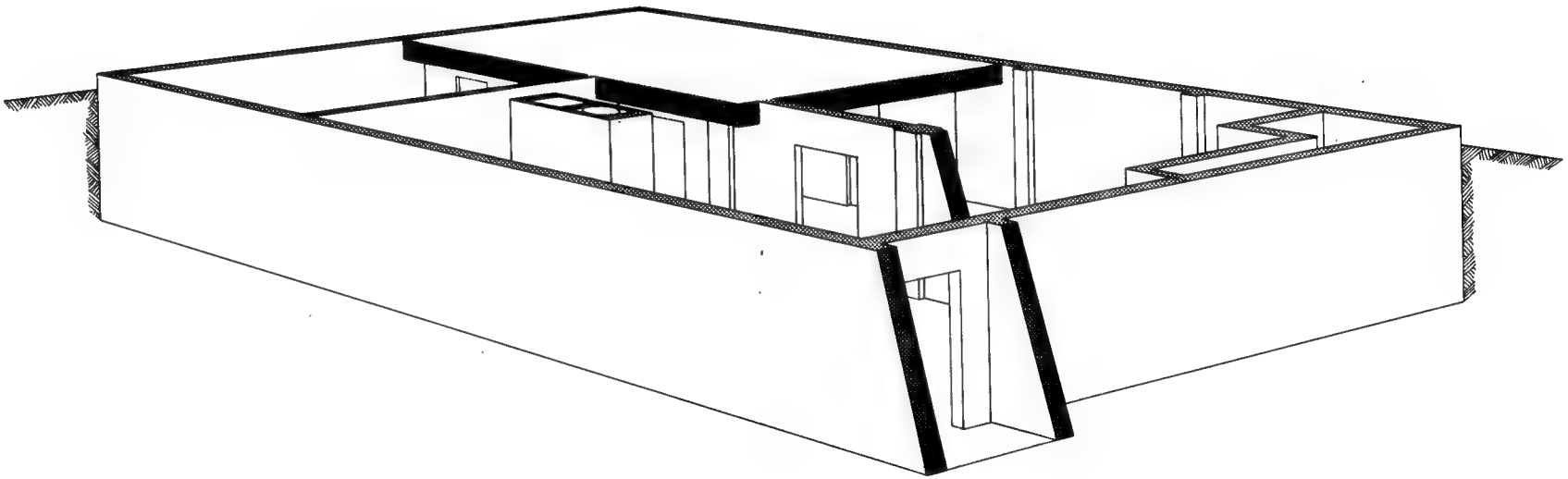

Questions Raised by Early Case Studies

Questions arising from these early case studies include:

- Are there slanting ventilation schemes that are more cost-effective (e.g., PVK and Kearny pump) than those used?

- Is the fresh air intake/emergency exit tunnel really required (for blast debris and fire hazards reduction) in an austere, survival shelter situation? Can its cost be markedly reduced by design studies? Are multiple window-wells better? Does the concept of knock-outs in first floor slab have any ventilation potential?

- Can the cost of blast doors be reduced by design studies or eliminated by an open-shelter approach?

- Are the loading assumptions and/or design techniques used on the buried exterior shelter walls too conservative?

Open Shelter

Closed shelters,* as in Buildings 1A, 1B, and 2A, pose the inevitable question: When will the shelter door be closed? This question is avoided in the open shelter concept, defined for purposes herein as shelter where at least one entrance door remains open to shelterees until one full minute or more after the nuclear detonation. Open shelter also merits consideration for its possible lower unit slanting cost, even though the shelterees may face a greater variety of hazards in open than in closed shelter.

Open shelter might be discussed under the following four types:

I. What amounts to a closed shelter but is closed only to the blast wave and other direct nuclear effects, not to people - for example, by having each entrance be a system where people can enter more or less continuously into either of two parallel hallways (really entry locks), with one alternately open to new arrivals while the other is closed to new arrivals but is open to empty an earlier arriving group into the shelter. The alternating is accomplished by sliding doors interlocked so that there is never a passageway for air blast to enter the shelter. Other examples exist.[36]

II. What approaches a closed shelter but is closed only after an early part of the blast wave has entered the shelter - for example, by having an entrance door or doors that are slammed closed by the blast wave, thereby shortening the duration (but not reducing the peak pressure) of the entering air blast to an extent that shelterees (probably prone) will not be accelerated enough to cause injuries/deaths by being thrown into walls or other objects. (Granted that the door may be slammed onto someone rather than going fully closed; in either case the air inflow is reduced quickly and considerably.)

III. An open shelter, but with only one or perhaps two entrance doors open, all other openings being closed not later than during the time interval between nuclear detonation and blast wave arrival at the shelter.

IV. An open shelter with multiple openings (windows and doors) remaining open at least during passage of the blast wave, probably longer for ventilation and access purposes. Openings such

* Defined, for use herein, as shelter closed before air blast arrival to all further ingress.

as those for chimneys and ventilation ducts could also remain open, provided that protection is included against chimney and duct parts becoming missiles in the shelter.

No quick conclusions should be drawn about these four types of open shelter. Type I might have all the slanting costs of a closed shelter (such as Building 2A) plus the cost of an elaborate entrance system, leading to a (premature) conclusion that the other types would all cost less than Type I. In Type I, interior walls need not be blast resistant. In the other three types, they must be blast resistant to some degree, a cost item in favor of Type I. Because of such interrelationships among slanting costs, personnel protection, weapons effects, etc., these matters as they relate to the open shelter types are examined in more detail below.

For convenience, the four open shelter types are summarized with shortened descriptions, as follows:

I. Shelter closed to blast but allowing continuous shelteree ingress

II. Shelter with few openings and internal blast duration shortened

III. Shelter with one or two entrances open

IV. Shelter with many openings

The remainder of this section on open shelter is devoted to discussion of certain weapons effects in terms of open shelter and to such general considerations in open shelter as blast resistant construction needed; certain necessary shelter stocks and their storage; and some aspects of shelter management and early recovery tasks applicable to open shelter. A recapitulation closes the section.

A. Weapons Effects and Open Shelter

The shelter designer must exercise care in considering not just the design peak overpressure (15 psi) or higher values and related other effects, but also the full range of all effects <u>below</u> the design level. For example, the fire potential in stories over the basement shelter is likely to be much greater at some overpressure range lying just <u>below</u> an overpressure capable of making debris of the upper stories than at blast levels <u>above</u> this overpressure.

Air Blast - Exterior. At some p_{so} around or above 7 psi, from a surface or air burst, there is a high probability of extensive damage, possibly even collapse, to the entire building above the basement. Also, at p_{so} of about 7 psi or more, from a surface burst, fallout contaminant is likely, even upwind or crosswind from the burst point.[1(Sec.9.87)] At p_{so} of about 1 to 3 psi, exterior and interior aboveground walls may become debris along with the building contents, perhaps blocking egress through downwind window-wells/doors, but providing additional fallout shielding on the shelter (basement) roof. The floors, and perhaps the roof, may not be collapsed, and would contribute to the fallout protection for the shelter. At p_{so} down to about 1/2 psi, there will still be much damage (minor at the lower p_{so} values) to equipment, interiors, and many building elements. All window glass will be shattered.

Air Blast - Interior. This effect is inapplicable to Type I. For the other types, it poses critical problems of estimating interior flow velocities* on shelterees and blast loadings on structure surfaces and shelter equipment, problems that can be only partially solved by Appendix E methods and the present state of knowledge in the field; however, directly applicable research, analytical and experimental, is under way.

Present knowledge suggests that Types III and IV shelter will contain at least some areas of low survival probability and that these types may not meet the 85% to 95% survival probability called for in the Stipulations section herein, unless special efforts are made to vacate dangerous areas before arrival of the air blast. This conclusion is based on calculations such as those discussed in Appendix E, showing that drag forces may be high enough and last long enough to cause prone shelterees to be thrown into walls or other fixed objects with lethal speeds.

For example, when peak free field overpressure is 15 psi, dynamic pressure (jet) in every opening may reach as high as 3.2 psi, enough to accelerate a prone human body to approximate lethal skull impact speed (15 fps)[38 39] in approximately 46 msec. Maximum dynamic pressure in an opening follows a brief diffraction episode of relatively low dynamic pressure and is in turn succeeded by a slow decline of dynamic pressure as the room fills. In a large room the highest values of dynamic pressure are thought to be located within a straight jet issuing from the opening, although a swirling motion entraining most of the air in the room may also occur.

Since, even with all openings open (Type IV shelter), filling time for the basement of Building 2 is approximately 130 msec, it is clear that

---

* Really need dynamic pressures; or, more strictly, drag pressures.

shelterees in the neighborhood of an opening will be threatened. If, in an attempt to spare a large part of the shelter area from these high winds, all but one opening is blast sealed (Type III shelter), the duration of the dangerous inflow is lengthened to approximately 600 msec during which time even relatively weak drag forces remote from the main jet may have the opportunity to accelerate the human body to lethal speed. A steady jet, issuing through an aperture the size of an ordinary door from a reservoir at 15 psi overpressure, will expand, after about 55 ft of travel in an infinite atmosphere, reducing the dynamic pressure to approximately 1.0 psi* (still equivalent to a hurricane wind of about 200 mph).

These approximate and preliminary calculations do not demonstrate that open shelter is infeasible, but they do demonstrate that open shelter of the kind (Type IV) represented by Building 2B presents a survival hazard to some shelterees at the 15 psi range. The magnitude of the hazard and an evaluation of the usefulness of the shelter are matters requiring further knowledge and study. The interior air blast hazard receives a lengthy discussion in the later section herein dealing with Building 4A.

Improved prediction techniques for interior air blast behavior offer a potential for structural savings as well. For example, back pressure on the concrete slab over the basement shelter might have a negligible effect on the slab design when rather small ultimate deflections are considered; however, at the large deflections for longer span slabs, say about 20 ft, the time to maximum deflection becomes of the order of 0.2 sec, which may be sufficient to allow a back pressure build-up of consequence.

Initial Nuclear Radiation. This effect presents no hazard† in an air burst (Figure 2-3), but a surface burst delivers a free-field, gamma-plus-neutron dose of about 450 rads (Figure 2-6, for 1 Mt and 15 psi). The surface burst radiation is likely to be much reduced by shielding from other buildings, but should be considered carefully in relation to protection around all shelter openings. Window-wells and entrances should have only a scattering, not line-of-sight (streaming) hazard because of the low sight angle of even maximum probable height surface bursts.‡ Even then, shelteree mortalities should be improbable and sickness unlikely.

---

* Calculated using Equation 36, Appendix E.

† Using the Scope yield of 1 Mt; if say 200 kt is assumed, the hazard from initial nuclear radiation (INR) may be considerable (Chapter 2), perhaps overshadowing air blast as a structural design criterion.

‡ For air bursts, maximum vertical sight angles (above the horizon) versus air blast peak overpressure might be: 30 psi, 43°; 20 psi, 36°; 15 psi, 33°; and 10 psi, 31°. These values came from considering HOBs to maximize the range for each overpressure (i.e., considering the "knees" of the curves in Figures 3.67a and 3.67b, Reference 1).

Fallout Radiation. This effect was first discussed in connection with exterior air blast and is further discussed below under protective action by shelterees. It should present no serious problems in considering open versus closed shelter.

Thermal Radiation and Secondary Fires. Fires and air blast present the greatest hazards to shelterees within the Scope of this guide.*

The thermal radiation reaching the shelter building exterior should, in a high probability of cases, have been reduced if not eliminated through shielding by other structures and hills. The risk of thermal radiation setting interior fires in the floor above the shelter must be countered by preattack countermeasures (e.g., fire-retardant treatment) and shelteree firefighting capabilities (Chapter 3); the latter are further discussed below. Even at the range of about 2.5 to 3 psi overpressure, the thermal radiation (Figure 2-2) may be sufficient to start fires in the floor above the basement shelter. As the overpressure and thermal radiation levels increase, however, rubble replaces or covers what were exposed building interiors, and there is serious doubt as to whether blast-caused rubble can ignite and burn so as to be a serious threat to shelter occupants. Certainly the threat, if any, is not well understood.

The secondary fire hazard must be countered by the means discussed just above and in Chapter 3, and as discussed further below. This hazard may well be worst at and beyond ranges where overpressures will make debris out of walls and interior equipment and furnishings.

B. General Considerations in Open Shelter†

At least some of the general considerations applicable to open shelter require review in relation to protective shelter design. The more important ones might include those discussed in the paragraphs below.

Blast Resistant Construction Needs. Some of the blast resistant construction needed in and around an open shelter includes:

- All structural elements located in the open shelter space must be blast resistant, including interior walls/partitions (which should therefore be reduced in number to the extent possible).

---

* Footnote † on the preceding page applies here as well.

† Entire section has little application to Type I "open" shelter (closed to air blast, by definition), the exception being some guidance that is useful to both open and closed shelter situations.

- All fixed equipment in the open shelter space must also be blast resistant, both in mounting and as to the equipment itself flying apart.*

- Entranceways, window-wells, and any other openings require attention to blast resistance, generally and for strength around each opening into the shelter.

  Doors should be fire-resistive, capable of being anchored in a protected (open) position for the blast passage, then of being quickly closed as necessary for fire protection. If flying debris, from materials or building elements near but outside the open shelter space, presents a hazard, grating doors may be required in nonentry doors of Type IV shelters.

  Windows should be detailed so that their glazing and other components present no missile hazard to shelterees - for example, glazed sashes could be removable and, at time of shelter occupancy, be moved out of the shelter or to a blast-protected closed space. (Or the sashes might be designed to be anchored safely in an open position, perhaps including use of a new high-strength glazing.)

  Window-wells serving the open shelter should have walls blast strengthened, at least in the walls common to the shelter. The strengthening should extend to all walls in each window-well that may be needed as an emergency exit. Each window-well should have a top grating† for protection against flying debris, but removable for emergency exit use if such use is planned. Window-well bottoms should be sufficiently below their window sills to give protection against direct fallout radiation from contaminant falling onto the bottoms.

- Some closed shelter space appears to be required even in the open shelter concept - if not for people then at least for certain stocks.‡ Examples include the OCD water drums and PVKs (package ventilating kits) in current use.

---

* However, for the blast loading on such equipment, the better interior air blast prediction techniques, mentioned earlier as a subject of ongoing research, are badly needed.

† Sloping, if exterior wall will support upper edge.

‡ Again, better prediction techniques for interior air blast behavior could change this need.

Shelter Stocks. Certain shelter supplies and equipment aspects seem to indicate the following:

- Stocks must not become missiles in the personnel shelter - they must either be removed from the shelter at time of occupancy or must be provided with blast resistant anchorage.* Supplies that cannot be so anchored and cannot withstand air blast damage - such as the water drums and PVKs - must be removed to protected closed space.

- Stocks must be in a space or spaces accessible to the shelterees, both after the direct nuclear effects and without receiving an unacceptable fallout dose.

- Stocks, at least the vital ones, must be protected from destruction by thermal radiation or secondary fires, as well as blast.

- Stocks should include such structural recovery items as building jacks, crowbars, wedges, and sledges.

Shelter Management. For success of an open shelter, shelterees must be informed (and willing) to:

- Move all unanchored items out of the shelter before the blast arrives.

- Move all stocks needing protected shelter to such space.

- Close all blast doors in any closed shelter spaces, either before the detonation or during the few seconds (available with large weapon yields) between detonation and arrival of the air blast wave.

- Take prone positions† at assigned locations, probably with close spacing to provide mutual protection.

- Perform radiation monitoring (for fallout contaminant) on tools, supplies, workers' clothing, etc., to control/reduce the amount of fallout contaminant carried or tracked into the shelter; this

---

* Again, better prediction techniques for interior air blast behavior could change this need.

† Again, better interior air blast prediction techniques could indicate other body positions, as well as specific locations in the shelter.

hazard is considered slight. Also monitor for poor fallout protection places within the shelter, resulting from unexpected contaminant deposition or wind redeposition.

- Work at recovery tasks, including those discussed below.

Early Recovery Tasks and Open Shelter. Many early recovery tasks are vital to the success of an open shelter concept - shelterees must be able to:

- Control fires in spaces adjacent to the shelter, at the same or any lower level and on the level above, or at least keep them small.*

- Control fires elsewhere as necessary to keep the heat on shelterees low enough for survival. This task is magnified in importance if there is a fallout hazard, otherwise the shelter could be evacuated if the heat becomes truly unbearable; even with fallout, evacuation from heat threat may be necessary.

- Clear emergency exits of any building or other debris blocking them.

- Clear any threatening fallout contaminant (that is, perform localized decontamination - e.g., sweeping, washdown, shaking, or brushing) in or near doorways, or deposited on debris in window-wells so as to be dangerously near window-sill height.

- Pile up "clean" debris or shelter stocks wherever needed to create fallout radiation barriers, e.g., near doorways and in window-wells.

Recapitulation. Table 8.0 provides a recapitulation of the general considerations in open shelter.

---

* Shelter building requirements have been stated earlier herein for general fire-resistive construction and fire-resistive or fire retardant treated equipment in, near, and above the shelter.

Table 8.0

OPEN SHELTER GENERAL CONSIDERATIONS
(Recapitulation)

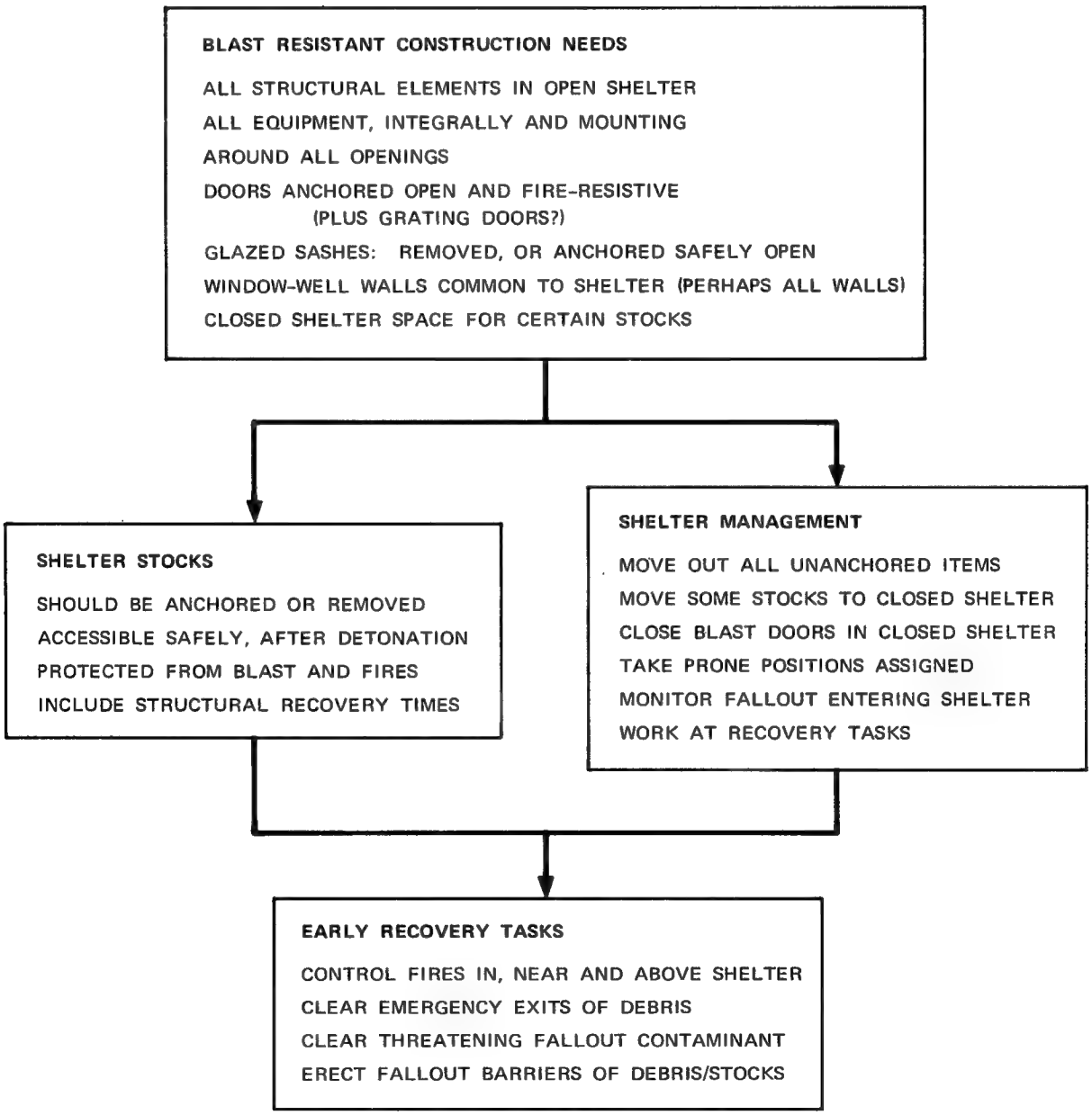

Building 2B

The first application of the open shelter concepts just described was to Building 2, already studied as a closed shelter; the benefits of reuse of Building 2 were economy and a potential for cost comparisons (after two years, a fresh estimate of Building 2A (closed shelter) additional costs for slanting was necessary because of rapidly changing construction costs).

Building 2A costs (from both June 1968 and June 1970 estimates) could be attributed to structural (56%), blast doors (10%), ventilation (25%), and fresh air intake/emergency exit tunnel (18%), the last item being of benefit to ventilation, fire protection, and blast protection, thus rather difficult to assign in terms of the preceding three categories.

Open shelter seemed to offer some potential slanting cost reductions in blast doors, in ventilation (at some increased fire risk), and perhaps in structural changes. However, such reductions may be substantially offset by the cost of closed shelter space required for certain equipment and stocks. Some fire test results[37] were reviewed that seemed to indicate that the noxious gases hazard from fires above the shelter might not be as great as accepted in the past. (See Appendix B.) However, safe ventilation of open shelter in a fire environment requires continuous monitoring of the air taken in and also the capability of changing the source of ventilation air to some extent (or at least the capability of stopping ventilation temporarily if all the sources become contaminated).[51] With such a proviso a well-type escape exit, Figure 8-0C, was considered for use (if used on several basement walls) as an open shelter alternative to the (expensive) fresh air intake/emergency exit tunnel, Figures 8-0A and 8-0B, used in Buildings 1B and 2A. Depending on the fireload on the floors above a basement there may be some danger to basement shelterees from heat. Basement roof slab thickness of one foot appears to be ample to prevent this. For a fuller discussion of all aspects of the fire hazard, see Chapter 3 and Appendix B.

Type IV of the open shelter conceptual types appeared most promising in terms of lower slanting costs, if not in terms of protection provided. Type IV was therefore used for the first case study among the open shelter types.

At the time of writing, serious questions remain concerning the feasibility of Type IV shelter, as discussed in the Open Shelter section of this Chapter. The purpose of this case study, therefore, was to make

some approximate cost comparisons between closed and open shelter, whether or not the latter was of questionable feasibility from a survival standpoint at the time of the study.

Building 2 is described in general terms in Chapter 7. The designed basement floor plan is shown in Figure 8-2 and the slanted version in Figure 8-2B (black lines show slanting structural and architectural changes, gray lines show the original design). The shelter occupies the full basement, excluding the interior stairwell and the exit hallway leading to the exterior stairs. Table 8.2B provides a list of slanting changes, keyed to Figure 8-2B, as well as the estimated additional cost of each change item. Interior shelter walls are blast resistant.

In contrast to Building 2A, Building 2B uses the original, natural cross-ventilation scheme contemplated for the large, open, basement portion used in the slanted version as open shelter. Supplementary ventilation needs could be met by OCD packaged equipment. Some closed shelter space was considered necessary because of the type of equipment in the boiler room and the need for blast resistant storage for certain supply items. However, because the ratio of closed to open shelter areas (49%) is probably atypical, a later summary (Table 8.0A) shows separate estimates for the open, closed, and total shelter areas of Building 2B, in order that the unit costs may be approximately applied to other ratios than 49%.

For this fourth case study, estimated additional slanting costs were close to the Scope limit of $6/sf (about 7% below, when both are corrected to the same time period).

Later work, using this building as the example, made a brief comparison of the centerline support system used in slanting (beams, columns and column footings) with an alternative system (wall and wall footings). The work is described and results provided in a later section of this chapter. The alternative system indicated a potential savings in estimated slanting costs for Building 2B of $3,078 (or about 13% of the total slanting estimate shown in Tables 8.2B and 8.0A).

FIG. 8-2B

BUILDING 2B BASEMENT FLOOR PLAN

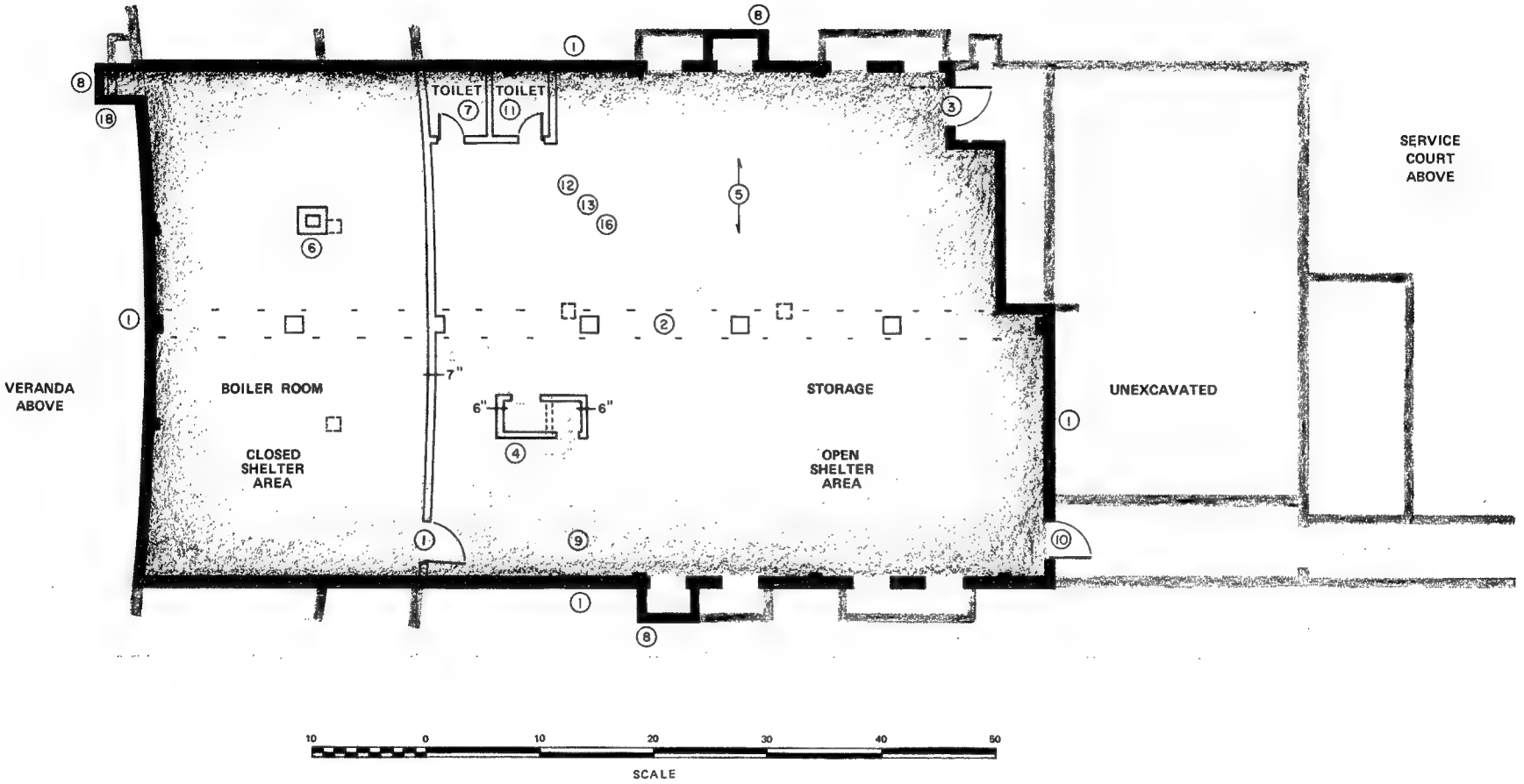

Table 8.2B

BUILDING 2B SLANTING (Type IV Open Shelter)
(Brentwood Rehabilitation Center, Asheville, N.C.)

		15 psi shelter	5 psi shelter		10 psi shelter		20 psi shelter	
1.	Provide blast walls: outer wall (10-3/4" thick)* all around ($3,204), plus main transverse wall 7" thick separating closed and open shelter areas ($1,933), plus blast door ($584). Shelterees allowed in both shelters, but only in prone position in open shelter during blast.	$5,721	(10-3/4") ($859)(7") ($1,412)($574)	$2,845	(10-3/4") ($2,331)(7") ($1,668)($579)	$4,579	(10-3/4") ($4,263)(9.5") (2,342)($590)	$7,195
2.	Provide R/C beam (45" x 24" deep) ($2,539), with R/C columns (tied, 18" square) plus ftgs & end pilasters ($5,145), deleting existing columns	7,684	(45" x 15")($1,200) (10")($1,335)	2,535	(45" x 20")($1,934) (13.5")($3,122)	5,056	(45"x28.5")($3,137) (20")($8,457)	11,594
3.	Provide hardware to anchor stairway door in open position	†		†		†		†
4.	Provide blast enclosure (6" thick) around dumbwaiter and laundry chute ($1,174), with 2 blast doors ($99).	1,273	(6") ($960)(90)	1,050	(6") ($996)($95)	1,091	(6") ($1,215)($105)	1,320
5.	Provide blast slab (13-1/2" thick) over both open and closed shelter areas.	7,558	(8.5")	3,165	(11.5")	5,397	(15.5")	9,421
6.	Harden chimney (only in shelter) for blast (†), and provide manual blast door at breeching ($182).	182	($105)	105	($149)	149	($210)	210
7.	Harden toilet spaces: Anchor toilet equipment for blast ($138); detail each door and jamb to open door flat onto a wall and be locked in open position for blast (†); strengthen walls (7" thick) ($889). Prone shelterees allowed during blast.	1,027	($138) (7")($709)	847	($138) (7")($810)	948	($138) (7")($994)	1,132
8.	Convert two areaways, or portions, to Shelter Escape Exits (Figure 8-0C) ($376); convert areaway off Boiler Room to Shelter Escape Exit and into exhaust for all building room air in normal use ($343), with blast door ($373); strengthen all such areaway walls (7" thick) (†).	1,092	($318) ($309)($369) (7")	996	($346) ($326)($371) (7")	1,043	($396) ($350)($375) (7")	1,121

* East wall 11" thick around stairway and main doorway, 8" thick adjacent to remaining (unexcavated) area and at stairwell.

† Design nodification considered achievable at little (<<$100) or no additional cost.

Table 8.2B (concluded)

	15 psi shelter	5 psi shelter	10 psi shelter	20 psi shelter
9. Provide for blast on all fixed equipment (e.g., laundry tubs), that cannot be moved out during warning periods, by either:	*	*	*	*
a. Blast resistant mounting, with equipment "defanged" (modified as necessary so that no parts can become missiles during blast, or caged in grating heavy enough to contain missiles during blast, preferably the former); OR,				
b. Provide lockable casters and easily unhooked utility connections (as on home washers), so that equipment can be moved during warning period, either to closed shelter or outside both shelters.				
10. Take remedial measures about main entrance doorway, based on air blast behavior analysis - at least provide a sliding fire door, mounted and anchored-open-for-blast on inside surface of shelter wall.	*	*	*	*
11. Provide ventilation in toilets:	†	†	†	†
a. Fan in each toilet, ducted out through Boiler Room exhaust areaway (item 8); OR				
b. Something modified for compatibility with item 9 or no missile hazard; OR				
c. Some other solution (some ventilation is needed in normal use of building).				
12-16. As in Table 8-2A.	†	†	†	†
17. As in Table 8-2A.				
18. Provide for all gas, water, fuel oil, etc., supply lines serving the entire facility to first enter through the Boiler Room, and have cut off valves at entry points.	*	*	*	*
	$24,537	$11,543	$18,263	$31,993
(June 1970 costs) 3,378 sf	$7.26/sf	$3.42/sf	$5.41/sf	$9.47/sf

* Costs not estimated, but probably minor.

† Design modification considered achievable at little (<<$100) or no additional cost.

Building 2C

Continuing the application of the open shelter concepts, Building 2C represents a Type I open shelter, thus being like the Building 2A closed shelter (Figure 8-2A) except for having one entrance lock at a time that remains open to entering shelterees. Thus the text remarks under Building 2A apply to Building 2C as well, as does Figure 8-2. Figure 8-2C shows (in black lines) the slanting structural and architectural changes (gray lines show the original design), as applied to the Figure 8-2 basement floor plan. Table 8.2C provides a list of the slanting changes, keyed to Figure 8-2C, as well as the estimated additional cost of each change item. Interior shelter walls are not blast resistant.

For this fifth case study, estimated additional slanting costs were well above the Scope limit of $6/sf (about 25% high, when both are corrected to the same time period); however, the certainty of the protection level provided was high for an "open" shelter concept.

Table 8.2C

BUILDING 2C SLANTING (Type I Open Shelter)
(Brentwood Rehabilitation Center, Asheville, N.C.)

1 and 3 to 18. Same as in Table 8.2A.		$24,551
19. Provide special airlock entrance structure (slab 6" thick) ($6,559) with 3 blast doors ($2,286) and necessary electrical-mechanical changes ($365)		9,210
		$33,761
(June 1970 costs)	3,465 sf	$9.74/sf

FIG. 8-2C

BUILDING 2C BASEMENT FLOOR PLAN

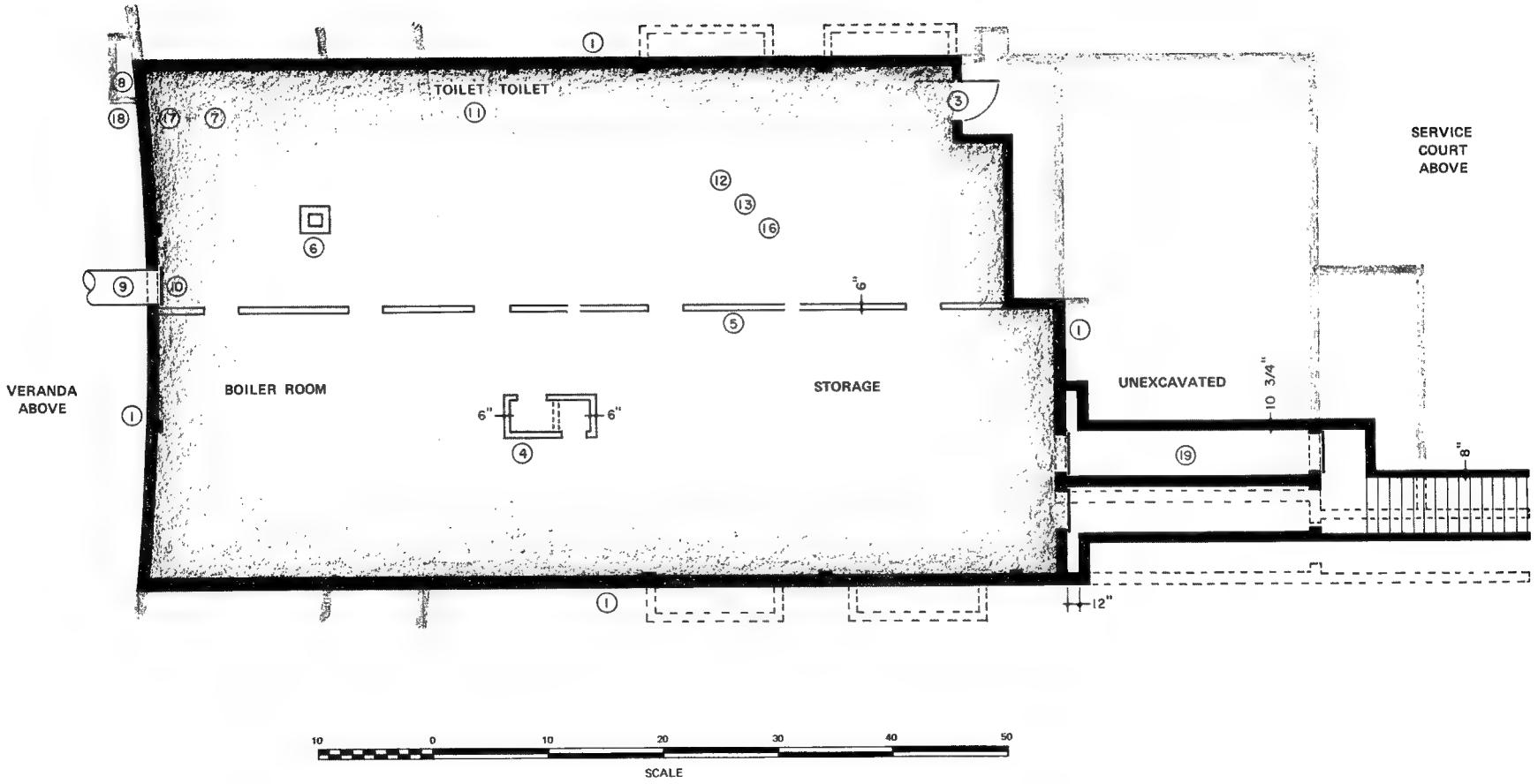

Building 3A

Pursuing slanting case studies into somewhat larger closed shelters seemed appropriate after the lessons of Buildings 1A, 1B, and 2A, to gain some measure of possible lower slanting unit costs with increasing shelter size.

The building is described in general terms in Chapter 7. The designed basement floor plan is shown in Figure 8-3, and the slanted version in Figure 8-3A (black lines show slanting structural and architectural changes, gray lines show the original design). The shelter occupies the full basement excluding the two interior stairwells to upper floors, the elevator shafts, and the police elevator well (no door). Table 8.3A provides a list of slanting changes, keyed to Figure 8-3A, as well as the estimated additional cost of each change item. Interior shelter walls are not blast resistant, except those enclosing the interior stairwells/elevator shafts.

While Items 4, 5, 6, 8, 9, and 10 of Table 8.3A deal with ventilation changes, some further comments on the environmental aspects alone appear to be appropriate. The mechanical plans for the building show a 20,000 cfm exhaust fan that provides cooling air to the transformer vault or removes radiation losses from the emergency diesel-electric set during an emergency. A modified environmental control plan was devised that provides for air conditioning of normally occupied spaces in the basement and also uses this 20,000 cfm of air for ventilating the basement when all habitable spaces are to be densely populated during an attack. For normal use, the central system provides air conditioning for two zones, the Emergency Operating Center (EOC) zone and the Elevator Lobby/Storage Room zone, each of which is supplied with about 5,000 cfm of treated air. With 50% recirculation, the required capacity of the water chiller is about 34 tons. For shelter use, the speed of the zone fans would be doubled and, consequently, the total ventilation rate would be increased to 20,000 cfm, which is about 15 cfm per shelteree (based on 10 sf per person). As early as possible in the postattack period, shelterees in the EOC zone would presumably be relocated to permit EOC personnel to function more effectively. The fan for the EOC zone would then return to normal low speed, and air conditioning would be restored. High speed operation of the fans may be accompanied by objectionable noise. To accommodate requirements for densely populated spaces in the basement shelter, only two changes appeared to be needed in the environmental control system: first, two-speed motors and controllers for the zone supply fans and second, zone supply fans with Class 2 (rather than Class 1) construction that provides reliable operation at high speed.

For this sixth case study, estimated additional slanting costs were under the Scope limit of $6/sf (about 21% below with mezzanine, about 16% below without mezzanine, when all are corrected to the same time period).

FIG. 8-2B

BUILDING 2B BASEMENT FLOOR PLAN

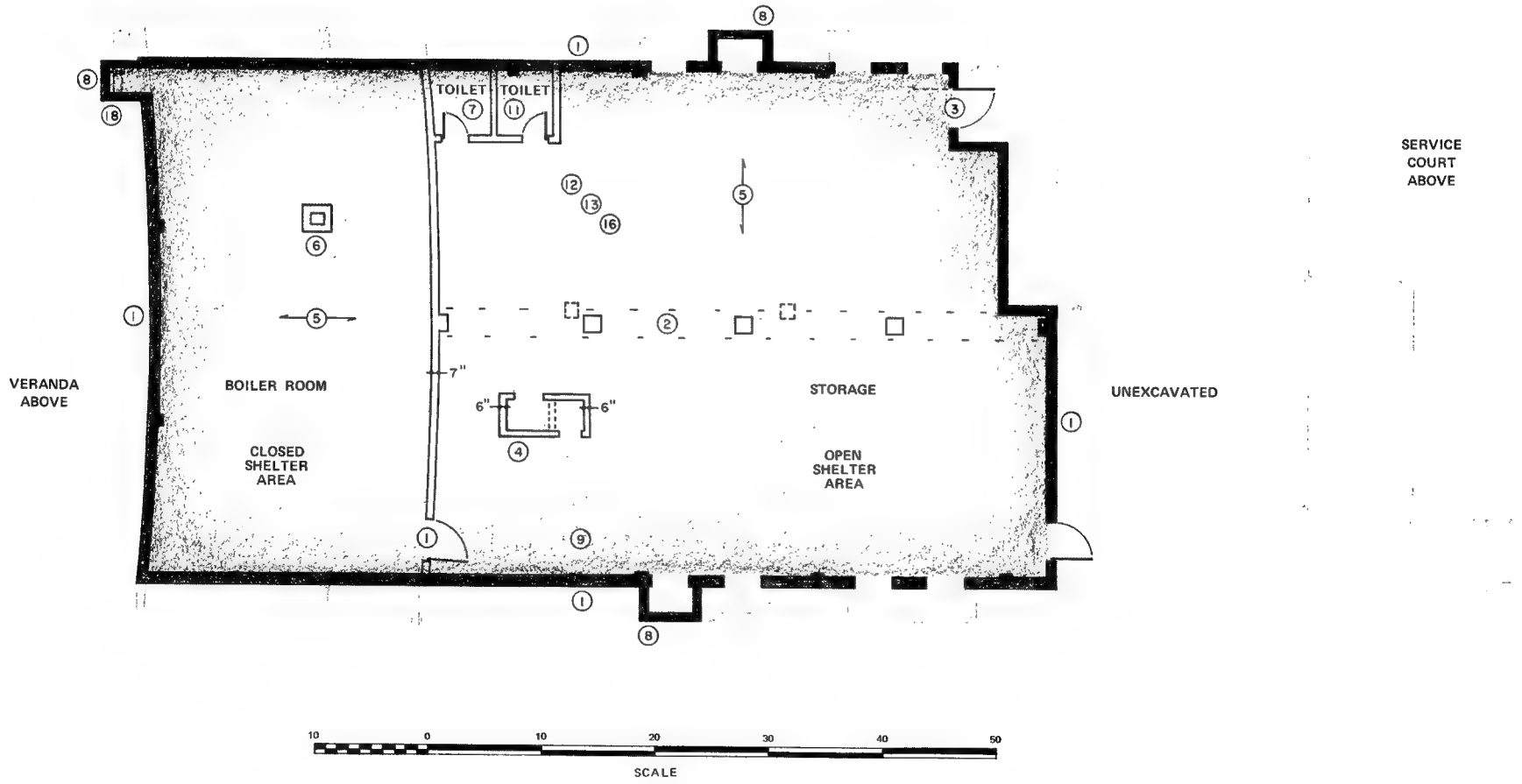

FIG. 8-3A

BUILDING 3A BASEMENT FLOOR PLAN AND SECTION

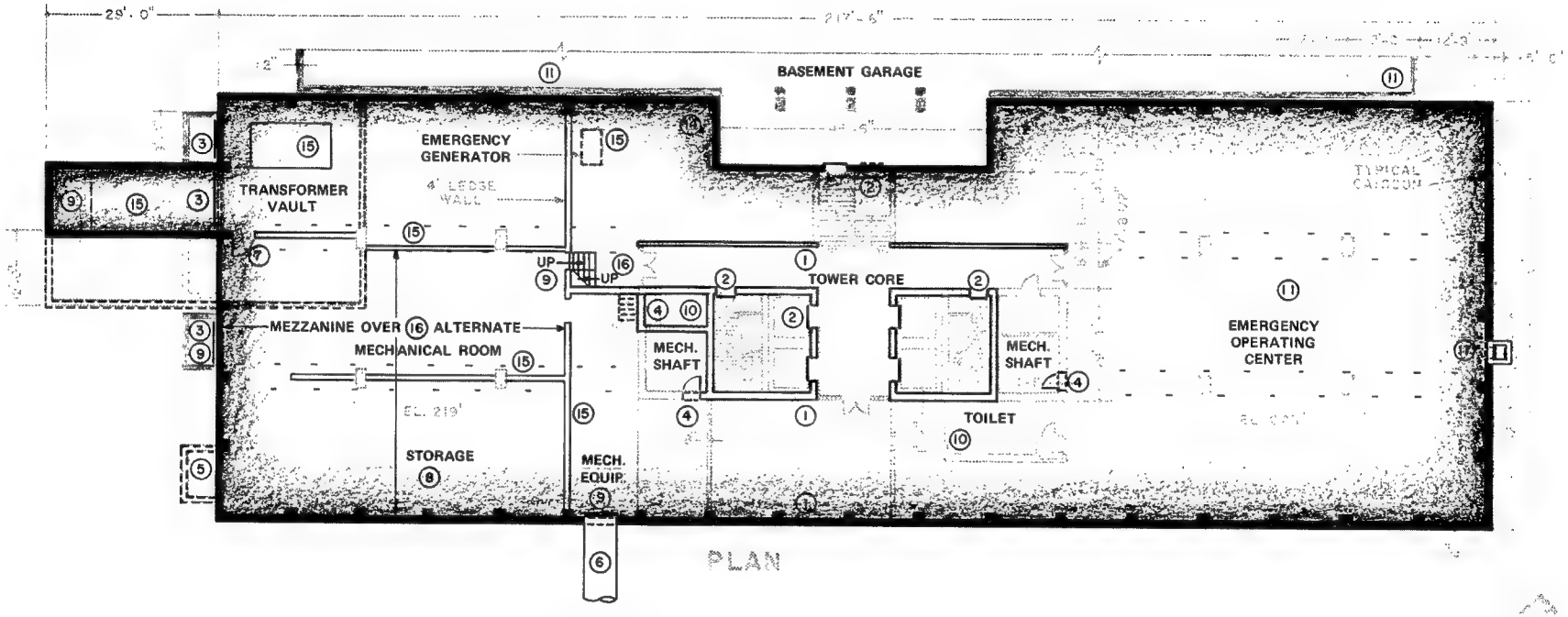

NOTE: The two elevator–stairwell areas are nonshelter areas, thus their surrounding walls and doors are blast-resistant

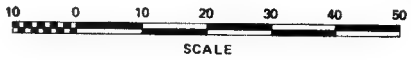

Table 8.3A

BUILDING 3A SLANTING
(Columbus-Muskogee County Court House, Columbus, Ga.)

		15 psi shelter	.20 psi shelter		30 psi shelter	
1.	Strengthen exterior walls (12" thick) for blast ($7,623). Provide interior blast walls enclosing two stairwells (N&S, 13" thick; E&W, 14" thick) and three elevator shafts ($4,200); interior support walls (8" thick with pilaster outer ends) and strengthened columns and footings ($3,709); and blast slab (9" to 14-1/2" thick)*($32,318) and supporting beams (54" x 37" deep)($4,895).	$52,745	(12")($10,508) (15")(15") ($4,687)(8") ($3,832) (10.5" to 16.5")($38,501) (54" x 42")($7,430)	$64,958	(12")($16,139 (18")(18") ($5,883)(8") ($4,016) (12.5" to 20")($49,185) (54" x 51")($12,264)	$87,487
2.	Provide 8 blast doors at existing doorways: 2 at interior stairways ($1,119); 2 at garage entrance doors ($1,093); and 4 at elevator doors ($10,738).	12,950	($1,209)($1,195) ($10,955)	13,359	($1,427)($1,395) ($13,410)	16,236
3.	Provide 3 horizontal blast doors (or hatches) at areaways.	2,485		2,537		3,100
4.	Modify mechanical shafts: Provide new door to each shaft ($361); close shafts with blast slab (9" thick) above ($1,260); provide R/C blast wall (14" thick) in lieu of existing masonry unit wall between west mechanical shaft and police elevator well (no door)($1,215). Shafts become available as shelter.	2,836	($361)(10-1/2") ($1,344)(15") ($1,322)	3,027	($361)(12-1/2") ($1,495)(18") ($1,471)	3,327
5.	Modify existing air intake #1 to serve ground floor only.	-2,732		-2,732		-2,732
6.	Provide fresh air intake/emergency exit tunnel, approx. 5.5' x 7' corrugated metal cattle-pass by 55' long ($8,862), leading to manhole ($3,712) in clear area south of tower building, with vertical sliding blast door ($727) on inside face of shelter wall.	13,301	($8,862) ($3,712) ($780)	13,354	($8,862) ($3,712) ($880)	13,454
7.	Provide new door into transformer vault to add to shelter space (assuming normal power shut off). Door must meet fire standards.	369		369		369

Table 8.3A (continued)

		15 psi shelter	20 psi shelter	30 psi shelter
8.	Modify ventilation system at and above ground floor level: Relocate AU-1, AU-2, and RA-1 systems to ground floor storage area (Room G-35)($-1,343); relocate storage to basement shelter; relocate return air louvers on all floors from east mechanical shaft to west (*); provide outside air supply openings at ground floor level to outside air plenum (*); duct toilet room exhausts (all floors except basement) via west mechanical shaft to 12th floor exhaust fan to permit open shaft to be used as normal return air duct for all floors ($1,208).	$ -135	$ -135 ($-1,343) ($1,208)	$ -135 ($-1,343) ($1,208)
9.	Relocate AU-3 unit into new mechanical equipment room; increase AU-3 size to provide required shelter ventilation; provide outside air from fresh air intake tunnel (Item 6); increase exhaust air system (in mechanical equipment room) to provide required shelter exhaust through areaways at transformer vault.	1,284	1,284	1,284
10.	Relocate basement toilet room exhaust duct (15" x 10") from west mechanical shaft to new emergency exit, Item 17 ($560); provide local exhaust fan ($263).	823	823 ($560) ($263)	823 ($560) ($263)
11.	Provide for all gas, water, fuel oil, etc., supply lines serving entire tower building and nearby garage areas to first enter facility through tower building basement (shelter), and have cut off valves (inside) at entry points.	375	375	375
12.	Grout all pipe penetrations through slab above shelter and through common walls to garage.	1,168	1,168	1,168
13.	If water well is economically available, its development should be considered for two purposes - the obvious one of an emergency water supply in lieu of stored water containers and a second one of a course of cooling water for emergency cooling use in the shelter.			

* Design modification considered achievable at little (<<$100) or no additional cost.

Table 8.3A (concluded)

		15 psi shelter	20 psi shelter	30 psi shelter
14.	Modify present electrical distribution of emergency power supply to provide separate cut-off of nonshelter circuits. Shelter emergency power to serve shelter lighting, heating, ventilation, water pump, and sewage ejector.	*	*	*
15.	Relocate transformers and emergency generator; construct new concrete block partitions for transformer vault and for new mechanical equipment room (Item 9), all to provide for proper shelter ventilation and exhaust circulation; relocate transformer tunnel (*).	$2,214	$2,214	$2,214
16.	Provide new concrete slab (6" thick) and support beams for mezzanine in new basement storage area to provide additional shelter area (2,753 sf) with metal access stairs.	11,646	11,646	11,646
17.	Provide new window-well emergency exit (east end) ($801), including blast door ($373).	1,174	1,176 ($375)	1,179 ($378)
		$100,503	$113,423	$139,795
June 1970 costs)	16,351 sf	$6.15/sf	$6.94/sf	$8.55/sf
Omitting mezzanine (Item 16):		$ 88,857	$101,777	$128,149
(June 1970 costs)	13,598 sf	$6.53/sf	$7.48/sf	$9.42/sf

* Design modification considered achievable at little (<<$100) or no additional cost.

Summary Comments - First Six Case Studies

The first six slanting examples include four closed and two open shelters; the latter are one Type I (closed to blast but open to ingress) and one Type IV (many openings). All of the entranceways have ample capacity (Table 1.1). None of the entranceway configurations was specifically checked for shielding adequacy in terms of initial nuclear and thermal radiation, or fallout, although all appear to be satisfactory if occupant countermeasures can be assumed to have been undertaken. All design changes (slanting) varied between schematic and preliminary, the goal being bare sufficiency to enable the estimator to make a reasonable cost estimate. All estimates were prepared by a professional estimator. For each slanting example, a full set of contract construction plans (i.e., of the original design) was available and used by both designers and the estimator. The usual rounding off of dollar values was not done in the estimates because of their extensive further use in calculations of percentages and other ratios, which were then used in various comparisons; the lack of rounding off does not imply any greater accuracy than usual for building cost estimates (see Cost Estimates section, Chapter 6).

The cost estimates for each of the six slanting examples were summarized into four major items - structural, blast doors, ventilation, and other - to facilitate comparisons and further study. A review was made for construction work that must be done at time of building construction versus work that could be completed later; the former was termed "nondeferrable" for discussion purposes. Percentages were calculated for ratios of each major item's cost to the total slanting cost and also of the nondeferrable to total cost for each major item and total slanting cost. Perhaps of most interest were the total additional costs per square foot of shelter space, for each example and all reduced to the same time period.

Table 8.0A shows the foregoing data.* Building 2B costs (columns 2 to 4) show open portion, closed portion, and total costs. Building 3A costs (columns 6 and 7) show two building options, with and without mezzanine. It should be obvious that many arbitrary decisions had to be made in preparing the table; however, the table was prepared and all estimates/descriptions of work items for all slanted buildings were reviewed by an architect colleague, both because of his diverse background encompassing architecture, structures, mechanical, and estimating experience and to gain another's viewpoint.

---

* Plus data from the case study that follows (Building 4A).

The data of Table 8.0A* indicate a potential for lowered slanting costs in open versus closed shelter, considering total, not nondeferrable, costs (note columns 2 and 1, $5.07 versus $5.78, a ratio of 88% for open over closed shelter). The data also indicate that about 60% of slanting costs in closed shelters is nondeferrable (Building 2C, open to shelterees but closed to blast, is more comparable to the closed shelters than to the other open shelter, Building 2B). Building 2B slanting costs (column 4) are about 95% nondeferrable as one might expect for an open shelter.

Considering the data for closed shelters, plus Building 2C (i.e., omitting Buildings 2B and 4A), nondeferrable work under the structural item amounts to 96% to 99% of the nondeferrable totals, but total work under structural amounts fo 57% to 67% of the building totals, blast doors 10% to 19%, and combined structural-blast doors 66% to 85%.

The sparse data indicate that:

- An open shelter (other than Type I such as Building 2C) should probably be considered only for complete work at the time of building construction, because deferrable work may amount to such a small portion of the total work (e.g., 5% in column 5); inflation may reinforce this thinking.

- The results of subsequent work showed that open shelter slanting costs are more sensitive to changes in design overpressure than closed shelter slanting costs. As shelters become smaller in floor area, say below 3000 sf, slanting costs begin to rise markedly.

---

* Holders of earlier versions of this table may note differences among the earlier versions and the version herein. Many new "designs" were required for this report, to cover the range of overpressures and related slanting estimates reported later in this Chapter. Frequently the design approach of the 15 psi shelter studies used for the current Table 8.0A had to be changed from that used earlier, in order to better suit use throughout an overpressure range, i.e., so that the calculation of estimate ratios, say for each overpressure versus a base overpressure, might have better validity. Such 15 psi re-designs, plus simply finding discrepancies in the earlier estimates, generally account for the differences among versions of the table.

Table 8.0A

SUMMARY OF SLANTING COST ESTIMATES (15 psi)

Building:		(1) 2A (closed)		(2) 2B (open portion)		(3) 2B (closed portion)		(4) 2B (total)		(5) 2C ("open")		(6) 3A (closed) with mezzanine		(7) 3A (closed) no mezzanine		(8) 4A (open)	
Cost Items		All	Non-deferrable	All	Non-deferrable	All	Non-deferrable	All	Non-deferrable	All	Non-deferrable	All	Non-deferrable	All	Non-deferrable	All	Non-deferrable
Shelter area (sf)		3,378		2,262		1,116		3,378		3,465		16,351		13,598		130,522	
Estimate date		6-70		6-70		6-70		6-70		6-70		6-70		6-70		6-70	
A. Structural	$	14,354	14,354	13,399	13,399	8,154	8,154	21,553	21,553	20,913	20,913	67,667	57,220	56,021	55,220	498,824	498,824
	$/sf	4.25	4.25	5.92	5.92	7.31	7.31	6.38	6.38	6.03	6.03	4.14	3.50	4.12	4.06	3.82	3.82
	%*	57	99	90	91	85	96	88	93	62	>99	67	96	63	96	63	64
	%†		*100*		*100*		*100*		*100*		*100*		*85*		*99*		*100*
B. Blast doors	$	2,478	--	99	--	1,139	--	1,238	--	3,943	--	17,265	--	17,265	--	22,738	9,730
	$/sf	.73	--	.04	--	1.02	--	.37	--	1.14	--	1.06	--	1.27	--	.17	.07
	%*	10	--	1	--	12	--	5	--	12	--	17	--	19	--	3	1
	%†		*0*		*0*		*0*		*0*		*0*		*0*		*0*		*43*
C. Ventilation (Incl. emergency exit tunnel, if any)	$	6,270	99	376	376	343	343	719	719	6,270	99	11,814	-760	11,814	-760	233,585	233,585
	$/sf	1.86	.03	.17	.17	.31	.31	.21	.21	1.81	.03	.72	-.05	.87	-.06	1.79	1.79
	%*	25	1	3	3	3	4	3	3	19	--	12	-1	13	-1	30	30
	%†		*2*		*100*		*100*		*100*		*<1*		*-6*		*-6*		*100*
D. Other	$	2,270	--	1,027	1,027	--	--	1,027	1,027	2,635	--	3,757	3,043	3,757	3,043	35,697	35,697
	$/sf	.67	--	.45	.45	--	--	.30	.30	.76	--	.23	.19	.28	.22	.27	.27
	%*	9	--	7	7	--	--	4	4	8	--	4	5	4	5	5	5
	%†		*0*		*100*		*0*		*100*		*0*		*81*		*81*		*100*
Total	$	25,372	14,453	14,901	14,802	9,636	8,497	24,537	23,299	33,761	21,012	100,503	59,503	88,857	57,503	790,844	777,836
	$/sf	7.51	4.28	6.59	6.54	8.63	7.61	7.26	6.90	9.74	6.06	6.15	3.64	6.53	4.23	6.06	5.96
	%†		*57*		*99*		*90*		*95*		*62*		*59*		*65*		*98*
‡ Jan. 68:	$/sf	5.78	3.29	5.07	5.03	6.64	5.86	5.59	5.30	7.49	4.66	4.73	2.80	5.03	3.25	4.66	4.58
‡ Jun. 73:	$/sf	9.69	5.51	8.50	8.44	11.14	9.82	9.37	8.90	12.57	7.82	7.93	4.69	8.43	5.45	7.81	7.69

* Percent ratio of item cost to total cost.

† Percent ratio of nondeferrable cost to item (All) cost.

‡ Using Engineering News-Record Building and Construction Cost Indexes (averaged) to convert totals from San Francisco area to EN-R's 20-cities average and from estimate date to date(s) shown.

Building 4A

Building 4 was selected for a case study of a very large, open shelter (Type IV - many openings), thus providing cost and study data to supplement earlier data on a small, open shelter (Building 2B) and to include a shelter some eight times larger than the largest earlier one (Building 3A), open or closed.

The building is described in general terms in Chapter 7. The two below-grade levels of this parking garage are shown, as designed, in Figures 8-4.1 and 8-4.2; the slanted version is shown in Figures 8-4A.1 and 8-4A.2 in which black lines show slanting changes (dashed lines or Xs for deletions) and gray lines show the original design. Slanting was planned to be independent of any slanting of the adjacent tower building (Building 3A), so that costs and problem areas might be more realistic for a general case.

The shelter occupies both sub-levels of the parking garage; however, during passage of the direct effects, it was planned to move personnel and movable equipment out of the more hazardous air blast areas discussed further below. It was considered necessary to cut off by blast doors the air blast that would enter the shelter spaces through stairwells, elevator shafts, and the proposed ventilation ducts/emergency exits; to do otherwise apparently leaves too few "safe" floor areas for the contemplated number of shelterees. Because four large (auto ramp) openings remain, however, the shelter is still an open shelter (Type IV - many openings).

Table 8.4A provides a list of slanting changes keyed to Figures 8-4A.1 and 8-4A.2, as well as the estimated additional cost of each change item. Also indicated in Table 8.4A is the blast loading assumed to act on each of many of the structural components. Such loadings considered results from room filling/jet effect calculations (Appendix E), but were finally based on the judgment of engineers with experience in blast-resistant design and full-scale nuclear tests. Cost data were added to Table 8.0A (column 9) to facilitate various cost comparisons.

For this seventh case study, estimated additional slanting costs were under the Scope limit of $6/sf (about 22% below the Scope limit when all costs are corrected to the same time period, January 1968).

For the cost estimates for full slanting of Building 4A for overpressures other than the initially used 15 psi, the large number of different structural members in this big shelter precluded as too costly the redesign of each member. Instead, a few members considered typical of their type (e.g., floor cover slabs, beams, walls, columns) were redesigned, then the ratio of their cost to that of the 15 psi design costs was applied to all members of that type.

FIG. 8-4.1

BUILDING 4 UPPER SUB-LEVEL FLOOR PLAN

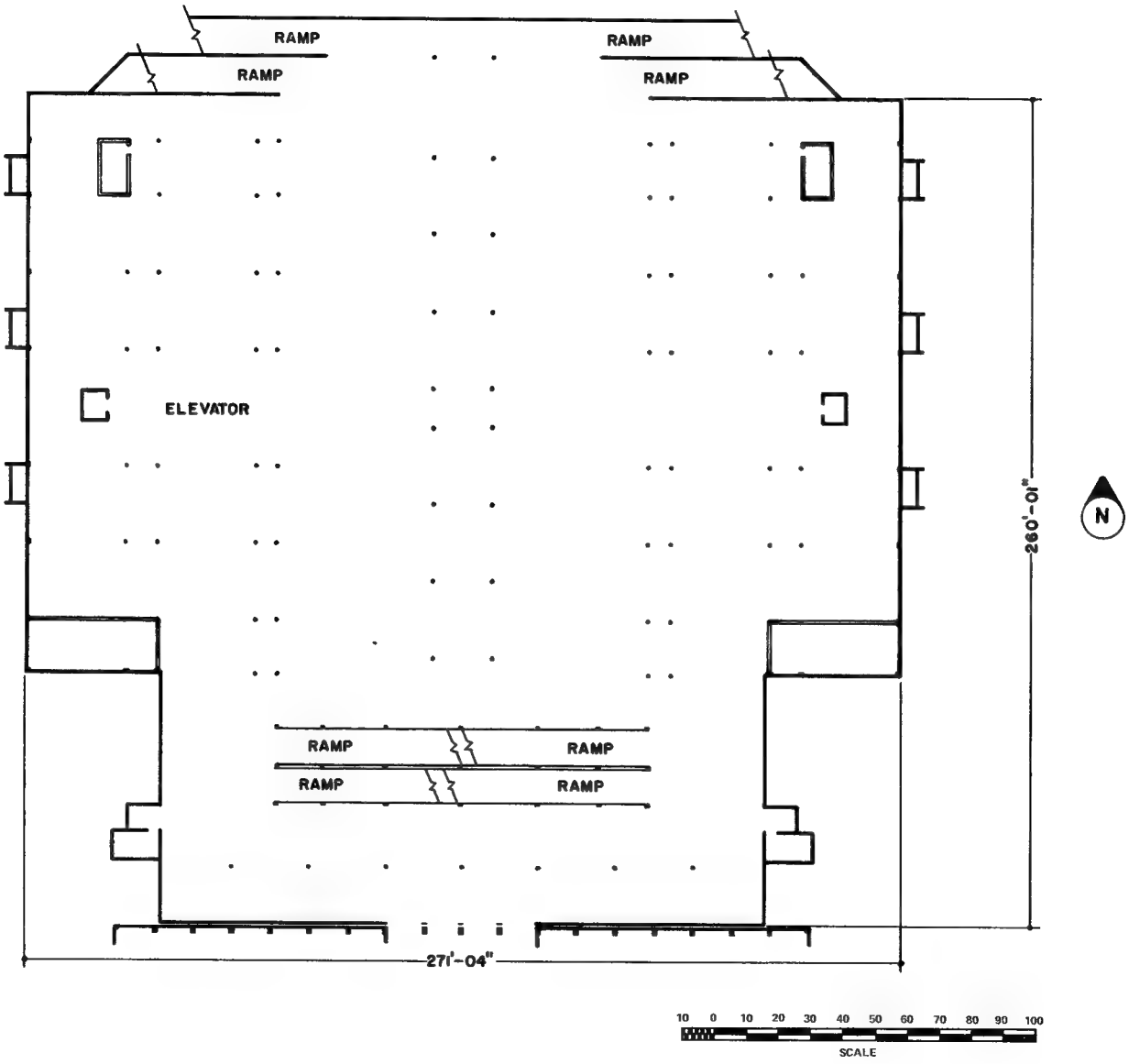

FIG. 8-4.2

BUILDING 4 LOWER SUB-LEVEL FLOOR PLAN

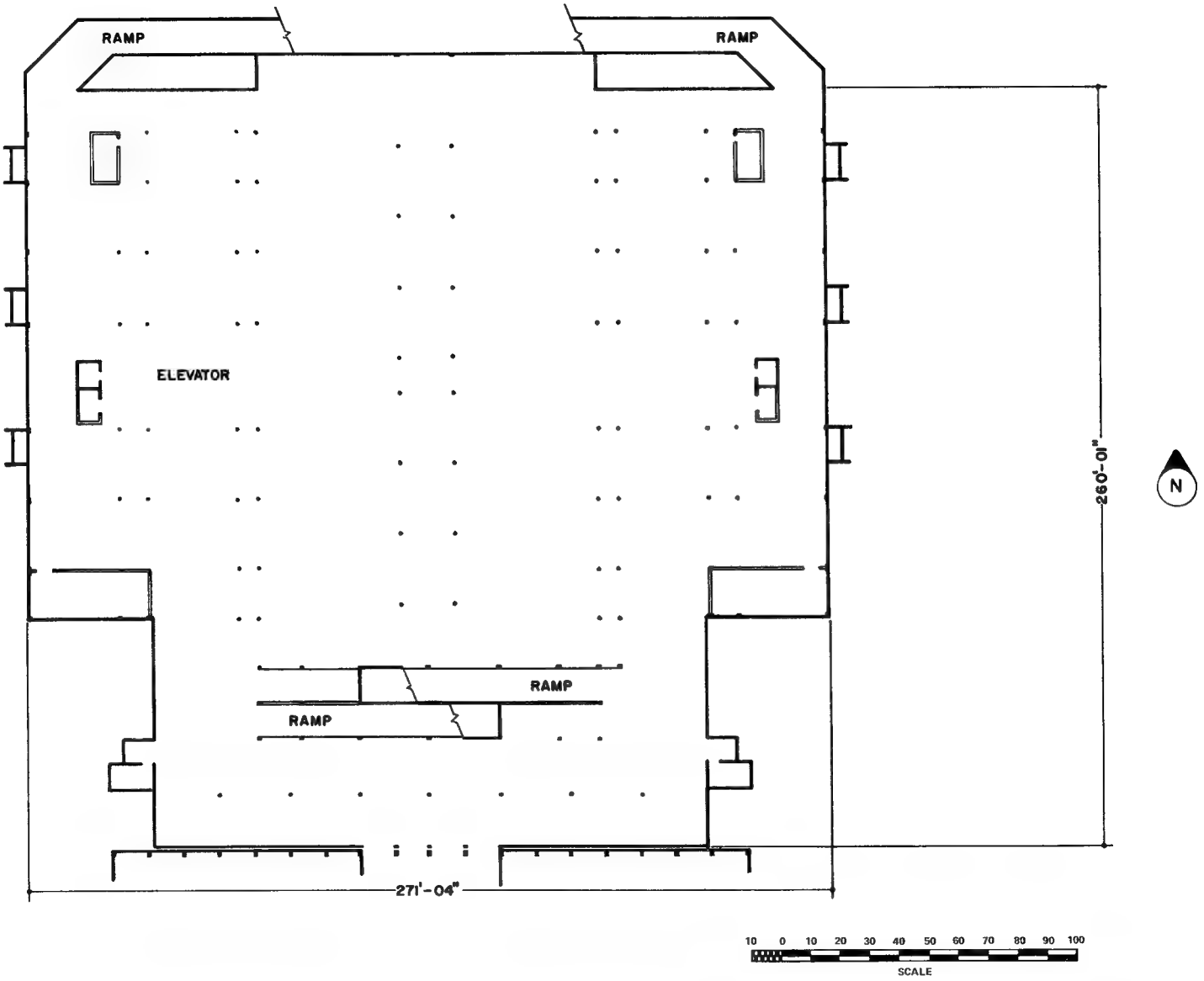

FIG. 8-4A.1

BUILDING 4A UPPER SUB-LEVEL FLOOR PLAN

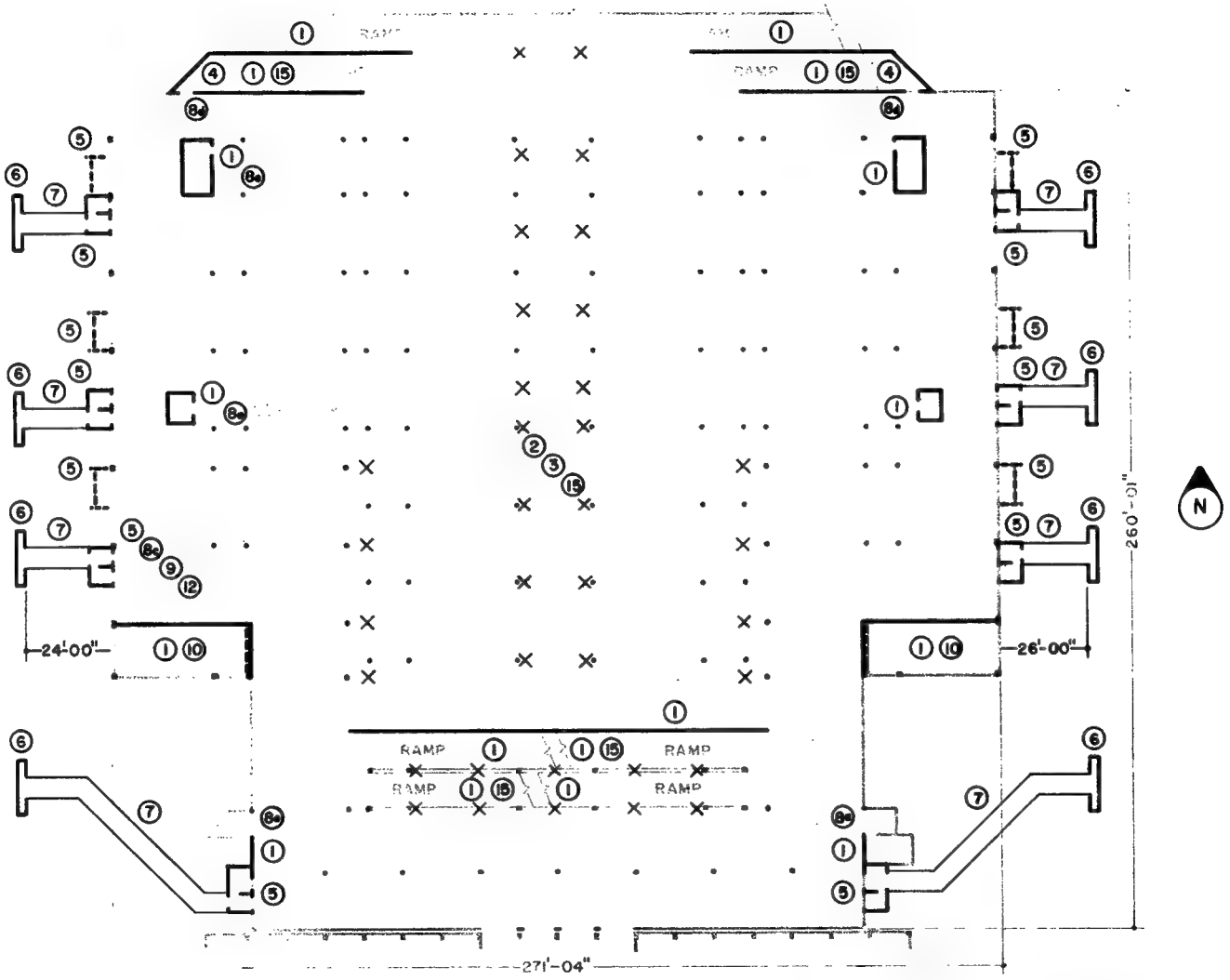

× INDICATES REMOVAL OF COLUMN

--- INDICATES REMOVAL OF WALL

10 0 10 20 30 40 50 60 70 80 90 100

SCALE

FIG. 8-4A.2

BUILDING 4A LOWER SUB-LEVEL FLOOR PLAN

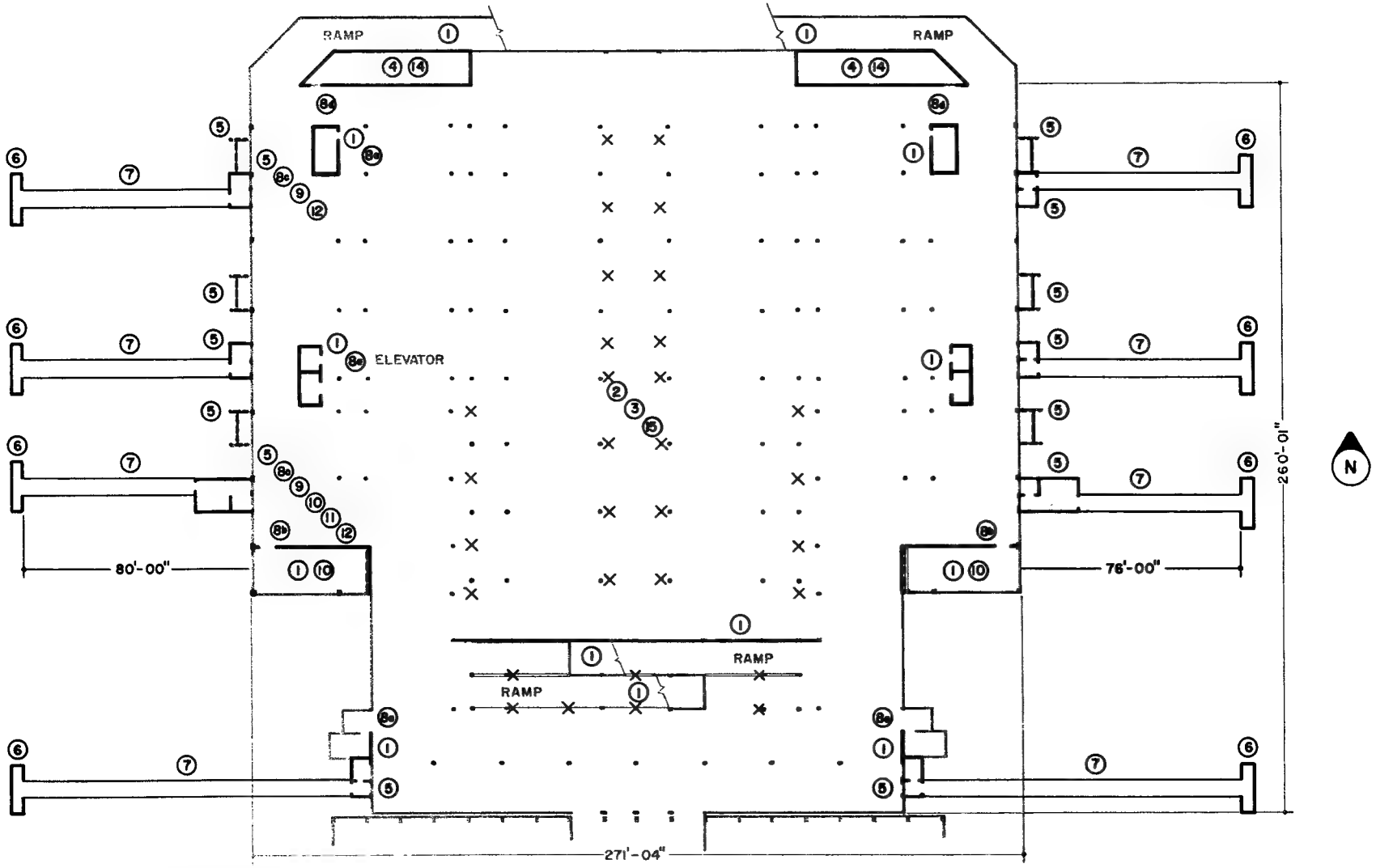

× INDICATES REMOVAL OF COLUMN

--- INDICATES REMOVAL OF WALL

10 0 10 20 30 40 50 60 70 80 90 100

SCALE

Table 8.4A

BUILDING 4A SLANTING
(Columbus-Muskogee County Court House, Columbus, Ga.)

	15 psi shelter	5 psi shelter	10 psi shelter	20 psi shelter
1. Strengthen for blast resistance:	$ 41,805	$ 31,715	$ 37,239	$ 45,914
a. No exterior shelter walls[a] (lateral soil coefficient used for airslap = 1/2); all (4) stairwells[a]; both (2) elevator shafts,[a] each with a machinery room on lower sub-level only; interior walls between garage and 2 mechanical equipment rooms[f] (blast loading either side); ($23,417);		($16,913)	($20,474)	($26,066)
b. Auto ramps serving upper[a] and lower[b] sub-levels ($6,267) and northernmost wall[a] (also closed openings) of south pair of ramps ($12,121); including their footings.[c] Stairwell, shaft, and mechanical room R/C walls replace concrete block construction.		($5,467) ($9,335)	($5,905) ($10,860)	($6,593) ($13,255)
2. Relocate interior columns under plaza for reduced spans. Strengthen for blast resistance, all interior columns[d] and their footings,[c] both sub-levels.	197,657	28,340	117,030	294,400
3. Strengthen for blast resistance: Floor slab and beams over upper sub-level (mostly 2-way slabs, 10" to 16-1/2" thick), using worst blast direction[a] ($203,970); floor slab and beams over lower sub-level[b,e] (mostly 2-way slabs, 6" to 12" thick)($52,596). Both floor slab-and-beam systems replace pan-joist-and-beam systems.	256,566	106,378 (7" to 12") ($68,174) (6" to 10")($38,204)	205,763 (9" to 15") ($159,679) (6" to 11")($46,084)	302,302 (11" to 18") ($243,832) (6" to 12")($58,470)
4. Replace unexcavated space (shown only on lower sub-level plan but extends partly into upper sub-level) with 2 storage rooms approx. 1-1/2 stories high having blast resistant[a] walls and footings; each room to have approx. 7,000 cf.	2,796	2,796	2,796	2,796
5. Replace 6 ventilation wells ($-27,429) with 8 blast resistant[a] ventilating vaults (2-story); two with adjacent generator rooms ($19,105), six without ($31,225), all located exterior to east and west exterior wall lines.	22,901	($-27,429) 20,339 ($18,168)($29,600)	($-27,429) 21,742 ($18,681)($30,490)	($-27,429) 23,945 ($19,487)($31,887)
6. Provide: 8 ventilation exhaust/emergency exit structures in midstreet ($36,744); and 8 ventilation intake/emergency exit structures in sidewalk ($23,192).	59,936	59,936 ($36,744) ($23,192)	59,936 ($36,744) ($23,192)	59,936 ($36,744) ($12,192)

Table 8.4A (continued)

	15 psi shelter	5 psi shelter	10 psi shelter	20 psi shelter
7. Provide: 8 corrugated steel cattle-pass tunnels (approx. 5'6" x 7'), each approx. 68' long, connecting Items 5 and 6 (exhaust at midstreet) ($113,871); and, 8 ditto, each approx. 20' long, connecting Items 5 and 6 (intake at sidewalk) ($25,165).	$139,036	$139,036 ($113,871) ($25,165)	$139.036 ($113,871) ($25,165)	$ 139,036 ($113,871) ($25,165)
8. Provide 68 blast doors[a] as follows:	22,738	22,106	22,422	23,054
a. One (3' x 7') at each stairwell and elevator shaft (Item 1), at each sub-level ($2,148);		($2,028)	($2,088)	($2,208)
b. One (3' x 7') for each mechanical room (Item 1), lower sub-level only ($358);		($348)	($353)	($363)
c. One (3'4" x 7') for each ventilating vault (Item 5) at each sub-level, between garage and vault ($5,888); one (5'4" square) for each vault, at each sub-level, between garage and ventilating fan ($6,448); one (4' x 6'8") for each vault, at each sub-level, between vault and cattle-pass ventilating duct ($6,560);		($5,728) ($6,288) ($6,400)	($5,808) ($6,368) ($6,480)	($5,968) ($6,528) ($6,640)
d. One (3' x 7') for each new storage room (Item 4) at lower sub-level and one (3' x 4') at upper sub-level ($1,336).		($1,314)	($1,325)	($1,347)
9. Provide mechanical equipment for each of 8 ventilation vaults (Item 5): one fan (27,000 cfm), 5-hp motor, and appurtenances for each vault, at each sub-level ($9,725); one recirculating air damper for each 2-story vault ($1,987).	11,712	11,712 ($9,725) ($1,987)	11,712 ($9,275) ($1,987)	11,712 ($9,725) ($1,987)
10. Relocate sump pumps from 2 mechanical equipment rooms (outside shelter) to emergency generator rooms (Item 5).	*	*	*	*
11. Provide emergency generators (2 @ 50 kw) and power distribution for ventilating, sump pumps, and partial shelter lighting (Item 5).	23,069	23,069	23,069	23,069
12. Provide shelter lights at each ventilating fan opening (Items 5 and 9), located behind blast door (Item 8c).	3,731	3,731	3,731	3,731
13. Provide normal-use garage lighting fixtures with features to facilitate preattack removal, e.g., hung by strap or chain that can be quickly cut with bolt cutters.	8,160	8,160	8,160	8,160

Table 8.4A (concluded)

	15 psi shelter	5 psi shelter	10 psi shelter	20 psi shelter
14. Provide minimal lighting in new storage rooms (Items 4 and 8d).	$ 737	$ 737	$ 737	$ 737
15. Provide draft curtains at ramps connecting ground level and upper sub-level, for postblast use.	†	†	†	†
16. Reroute all utilities serving complex to reduce or eliminate hazards to shelterees from ruptures.	*	*	*	*
17. If water well is economically available, its development should be considered for two purposes - the obvious one of an emergency water supply in lieu of stored water containers and a second one of a source of cooling water for emergency cooling use in the shelter.				
		$790,844	$458,055	$653,373	$938,792
(June 1970 costs)	130,522 sf‡	$6.06/sf	$3.51/sf	$5.01/sf	$7.19/sf

* Design modification considered achievable at little (<<$100) or no additional cost.

† Costs not estimated, but probably minor.

‡ See third footnote on page 1-2; area of ramps connecting sub-levels was counted, but area of ramps connecting upper sub-level and ground level was counted only for those portions lying directly below the ground level floor slab.

a. Blast loading: Design peak free-field overpressure (5, 10, 15 and 20 psi), zero rise-time, 1 Mt yield, no increase for reflection.

b. Blast loading: 1, 1.5, 1 and 1 psi peak, respectively, for design peak overpressure of 5, 10, 15 and 20 psi; zero rise-time, 1 Mt yield, no increase for reflection. 2 psi was used for both 15 and 20 psi design values because choking was assumed to occur above about 14 psi free-field.

c. Allowable bearing pressure for dynamic loading equals twice the conventional allowable static value plus the peak free-field soil pressure at foundation level.[2]

d. Upper sub-level column loading equal to twice the design peak overpressure[a] times loaded area. Lower sub-level column loading equal to twice the design (e.g., 15+2) peak overpressure[a,b] times loaded area.

e. Blast loading, for slabs over lower sub-level in vicinity of ramps: Design peak[b], zero rise-time, 70 msec duration (used for 2 psi peak[b]; proportional durations used for other peaks), no increase for reflection.

f. Blast loading: 15 psi peak, 100 msec rise-time, 1 Mt yield, no increase for reflection.

The shelter should be cleared of cars to the maximum extent possible following an alert notice. Any remaining cars should have windows open, be located in the "safer" floor areas with respect to the air blast behavior discussed further below, and may be occupied by shelterees. Reported results of recent tests of deliberately set fires in cars parked in an enclosed parking garage[44] showed a modest but entirely survivable fire hazard; the more significant test findings were as follows:

- Intensity and size of car interior fires are closely linked with the additional fire load of objects scattered inside the car.
- Generally the fire remains confined to the car for a very long time and will spread to adjacent cars only under certain conditions.
- Gas tank does not explode, even if the fire rages around the tank (tested at half to two-thirds full); the gasoline burns at the filler cap through the pressure release valve,* the burned-out tank seal and the melted seams.
- Rear tires of burning vehicle explode.
- Room temperature remained bearable† in all tests (but note that only one test fire was burning at any one time).
- With the automatic sprinkler system inoperative, smoke production did not impair visibility until some minutes after the fire had reached its full proportions, even when smoke production was deliberately heightened by burning smoke producing materials (celluloid waste, tires, motor oil).
- With the automatic sprinkler system operative, its opening caused complete smoke obscuration within a few seconds; breathing without auxiliary breathing apparatus was then impossible, as well could be evacuation and firefighting.

---

* Gas tank caps in modern U.S. and European cars are each equipped with a spring-loaded closure that opens, under extraordinary internal pressure, to exhaust vapor to the atmosphere. Under ordinary conditions, the spring holds the cap closed to the seal. It is understood that cars manufactured before 1965 do not have a pressure release valve built into the gas tank cap.

† Probably not if space were full of shelterees, however. The point is that gas tank hazard is not as severe as intuition might indicate, explosion hazard is nil, and time is available for fire countermeasures or evacuation.

- Automatic sprinkler system required a relatively high temperature at ceiling level to respond, could not extinguish a car interior fire, spread pools of burning gasoline and thus the fire, and caused the immediate smoke hazard just described.

Ventilation assumed major proportions because of the large size of this case study shelter. The ventilation planning and preliminary design work is described in Appendix H and is intended to serve as an illustrative example of such mechanical engineering work applied to full slanting of a building. Use of dual emergency generator rooms (Items 5 and 11, Table 8.4A) was adopted for increased reliability (either of the two 50-kw engine-generator sets could operate <u>all</u> of the ventilation fans at their lower or two-thirds speed, 1200 rpm) and because a fan serving a generator room would be inadequate (when operating at the lower speed) to provide sufficient cooling air for a single generator installation (100 kw). Figures 8-4A.3, 8-4A.4, and 8-4A.5 show the contemplated ventilation vaults, the latter figure including a generator room.

FIG. 8-4A.3

TYPICAL VENTILATION VAULT — WEST WALL

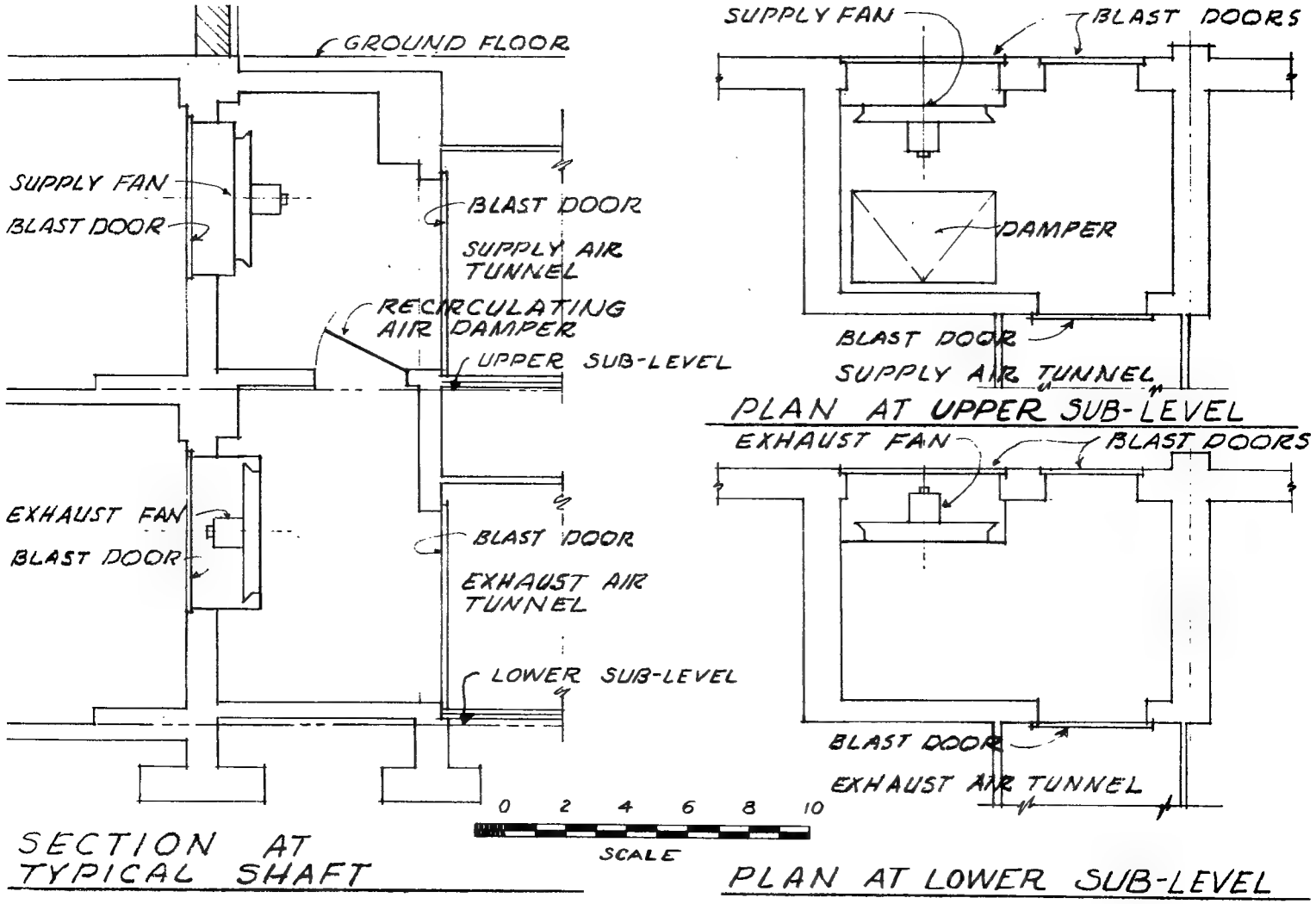

FIG. 8-4A.4

TYPICAL VENTILATION VAULT — EAST WALL

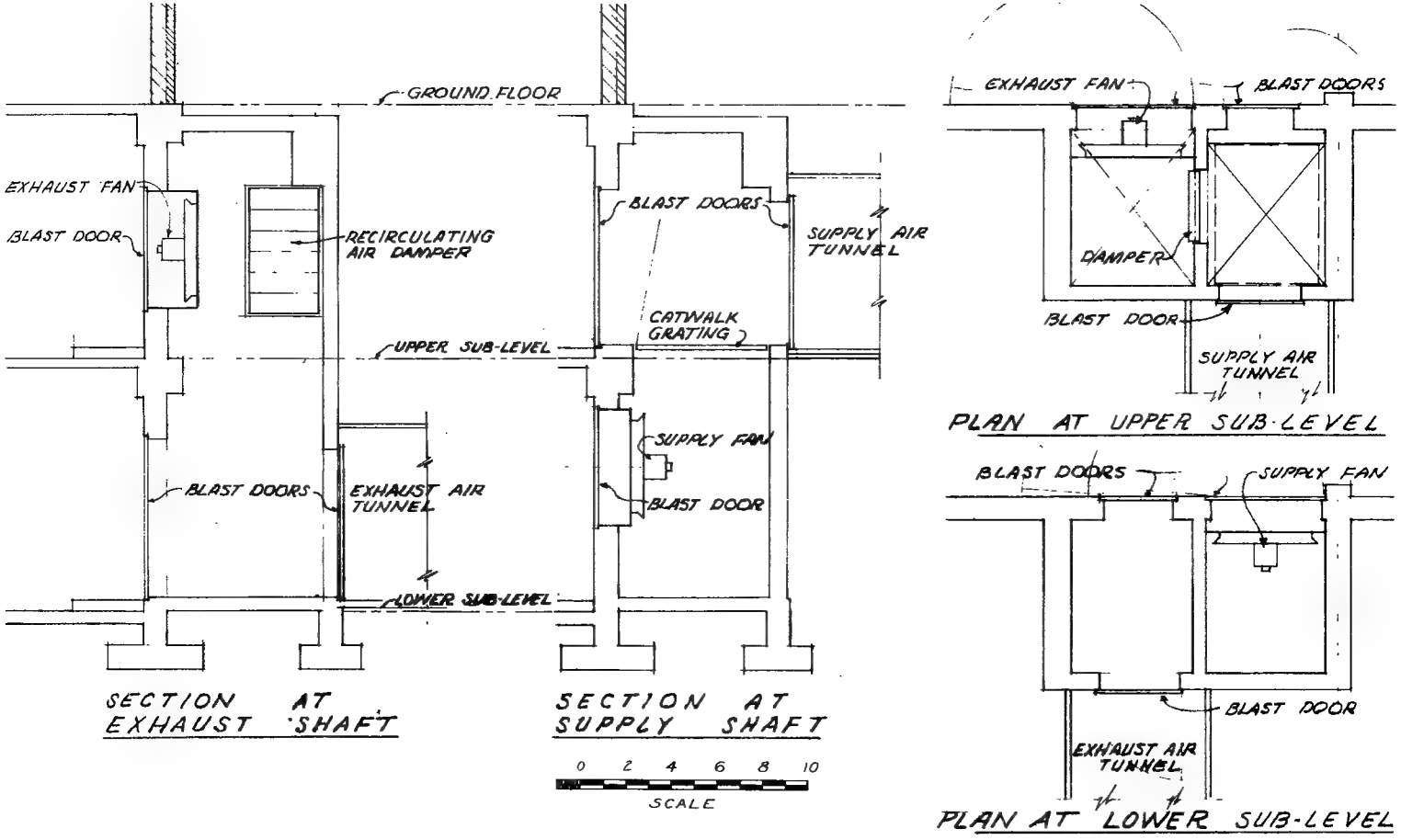

FIG. 8-4A.5

TYPICAL VENTILATION VAULT WITH GENERATOR ROOM

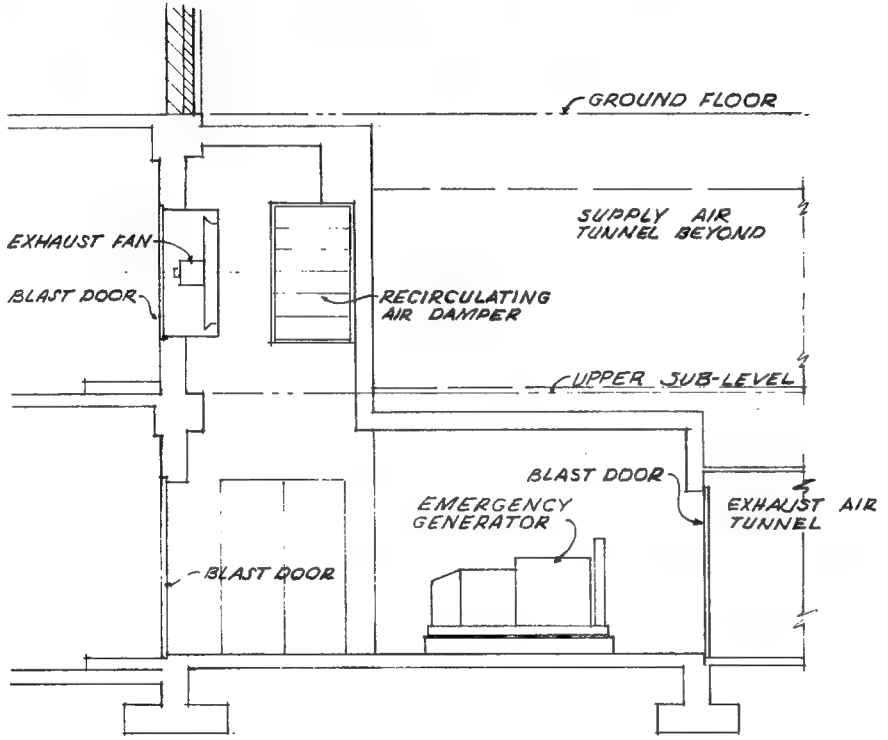

SECTION AT EXHAUST SHAFT & GENERATOR ROOM

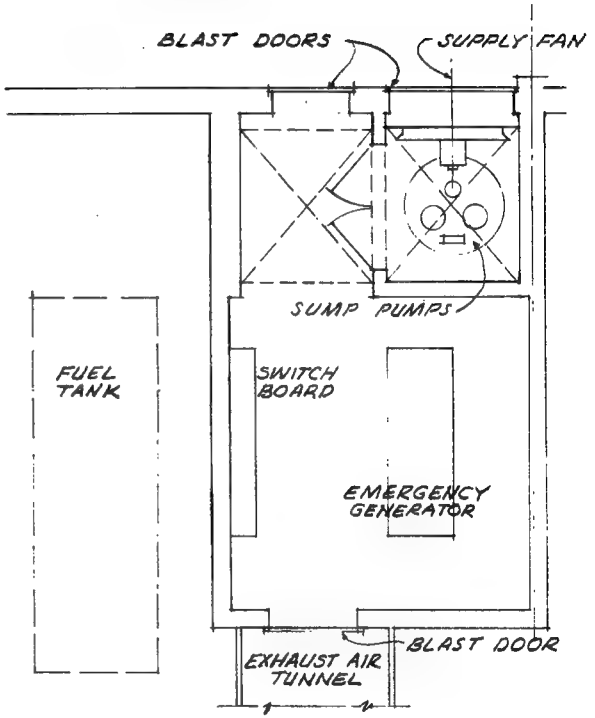

PLAN AT LOWER SUB-LEVEL

0 2 4 6 8 10

SCALE

For a review of interior air blast behavior in room filling and jet effects, the general method and theory in Appendix E were used. The work and results are briefly described in the following paragraphs.*

The building was subjected to a hypothetical nuclear blast, and the suitability of its two underground floors as open shelter was evaluated. Peak free-field overpressure was 15 psi, and positive phase duration about 2 sec.† Openings between shelter spaces and the free-field blast environment were assumed to remain free of debris or other obstruction to inflow. As part of the slanting, ramp sidewalls were assumed to have been closed off, at least on the side facing the large parking areas, and the openings from the ventilator wells into the two sub-levels to have been closed. Interior elevator shafts and stairwells were assumed to have been provided with blast doors. The only entries for air blast then would be through the auto ramps.

Detailed results are shown on outline floor plans, Figure 8-4A.6A.‡ In summary, it appears that approximately two-thirds of the upper sub-level area lies outside the more conservatively drawn danger zones and all of the lower sub-level is "safe" except for small areas (not shown in the figure) at the mouths of ramps between sub-levels.

---

* Prepared by a colleague, J. R. Rempel.

† See details below.

‡ Yields of 1 and 10 Mt (1.55 and 3.45 sec. blast duration) are shown, for reasons discussed in footnote of next text page. No estimated hazard areas found on lower sub-level.

FIG. 8-4A.6A

BUILDING 4A AIR BLAST JETS — 15 PSI

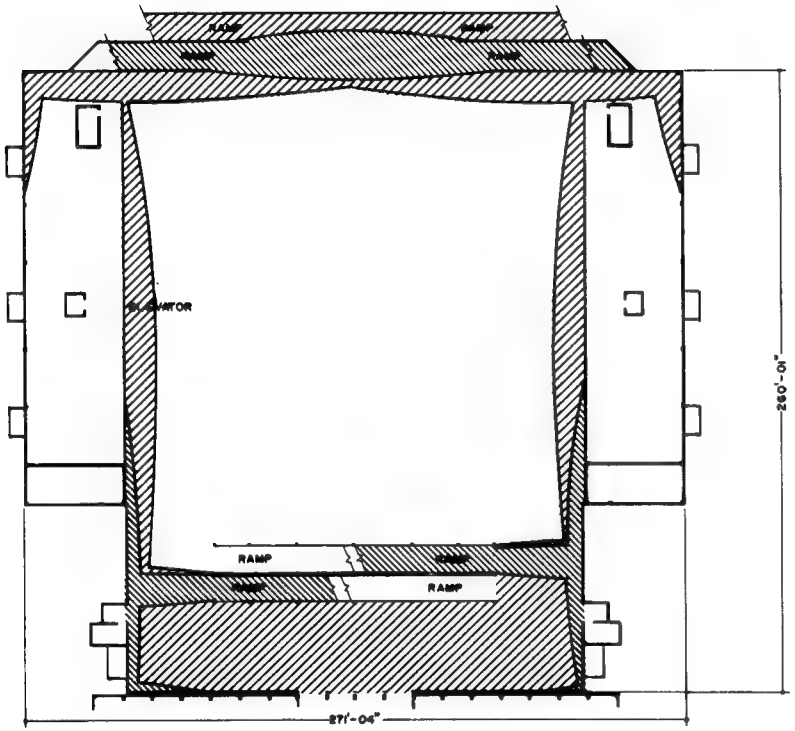

UPPER SUB-LEVEL
(1 Mt)

LEGEND
20 fps criterion
80 fps criterion

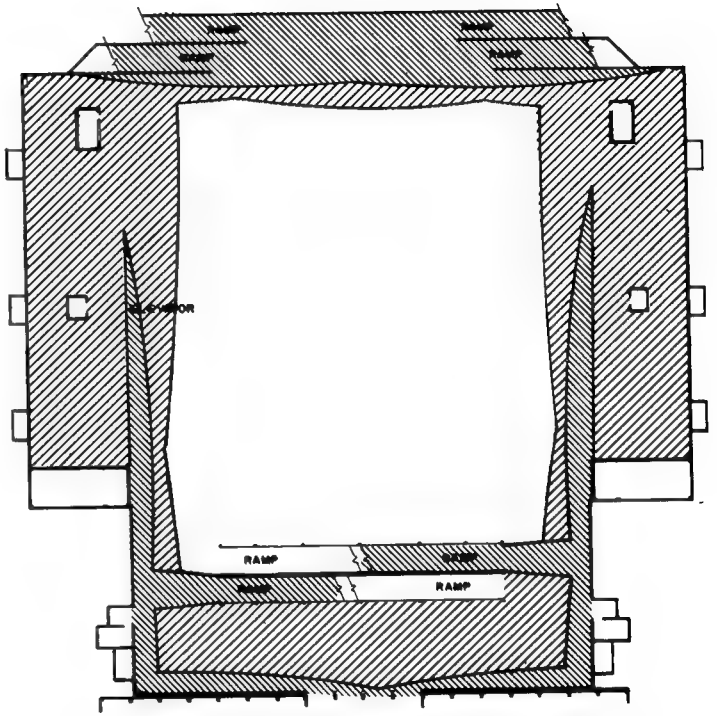

UPPER SUB-LEVEL
(10 Mt)

0 50 100
SCALE

For each opening expected to contribute significant air blast, two areas are outlined. A prone human body located athwart the blast jet within the smaller of the two areas, if not checked or restrained, may be accelerated by the blast wind to 80 fps; within the larger the final speed may be 20 fps. These values correspond approximately to speeds producing death in humans on collision with a massive rigid object: 80 fps for whole body impact, 20 fps for head impact.†

---

† Because of wide individual variability, biological hazard criteria cover a range of values. Available evidence[38,39] indicates that serious injury or death by head impact against a massive, hard object may occur at a speed between 10 and 20 fps. A few individuals will be seriously hurt or killed when stopped at only 10 fps and some not until a 20 fps speed is reached, but virtually all will experience serious injury or death at some speed within the range. A corresponding hazard range for whole body impact in a direction transverse to the spine (but with head and neck relatively protected) appears to lie near 80 fps but, at the present, data are insufficient to provide a meaningful range. Evidence for these values is presented and discussed in Reference 41. Such values for humans are not precisely known and they may well be subject to some adjustment in the light of further study.

Hazard ranges for impacts against yielding objects and in directions other than transverse to the spine have also been discussed along with some physical evidence in Ref. 41. For example, tolerance to longitudinal impact (in a direction along the spine) appears to lie between 20 and 80 fps; in these cases mortality is probably connected with relatively large displacements of viscera. However, without more detailed analysis of impact parameters, the two limits used in Figure 8-4A.6A are believed to be adequate to suggest the hazard to a prone sliding/rolling body, which will most likely be decelerated by transverse body impact. The results in the figure should be interpreted as showing that the chances of survival in the smaller danger zone (determined by the 80 fps criterion) are slight. However, in the larger danger zone, while some shelterees will be killed by blows to the head, many if not most others will probably survive with nothing worse than broken bones or dislocated joints as they are slammed into walls, pillars, furniture, or each other at speeds between 20 and 80 fps. Outside both zones, even broken bones should be exceptional.

The estimated hazard areas shown in Figure 8-4A.6A are conservative because the following were excluded from the calculations: less dangerous bodily orientations than athwart the blast; sliding friction; any benefit from packing of shelterees; and the possibilities of finding shelter directly under high openings in walls or of a body moving outside the danger area before reaching critical speed. To partly compensate for such conservatism, the upper value of the head impact hazard range, 20 fps, was used in determining the larger hazard areas of Figure 8-4A.6A.

Building 8-4A was also used as an example of a very large open shelter in studies with free-field air blast peak overpressures other than 15 psi, i.e., 5, 10, and 20 psi; the results are described in the next section. This use dictated a need for more estimates of hazard areas, which were made using the same approach as described above for the 15 psi slanting application. Further, the need for blast doors between the two garage levels and each level's 6 elevator and stair wells led to estimates of hazard areas with these 12 blast doors omitted.

Figures 8-4A.6B and C show estimated hazard areas for 20 and 5 psi peak overpressures, respectively, using 10 Mt weapon yield.* While these Figures show no blast doors on the 12 stair and elevator wells, the Figures can be used for study of hazard areas with the 12 blast doors used; the estimated hazard areas from the ramp entrances are about 10% larger when the 12 blast doors are used. Whether the 12 blast doors can or should be omitted, based on the estimated hazard areas shown in the Figures, is a matter of judgment that must in turn consider at least two key matters: the degree of accuracy that can be assigned to the room filling/jet effect calculational method presented by Appendix E; and a conclusion about the discipline of the shelterees in terms of taking carefully spotted locations on each garage level when so instructed.

---

* Positive phase durations of 3.06 and 5.27 psi, respectively, were used; they are for weapon yield of about 10 Mt, as calculated from Brode curves of Figure 2-1. While 1 Mt was used for structural components, they are nearly insensitive to change from 1 to 10 Mt; however, estimated hazard areas, at a single overpressure, vary about as positive phase durations (which in turn vary as cube root of yield). Thus, for 1 Mt positive phase durations, about 1.37 (20 psi) and 2.5 (5 psi) sec., estimated hazard areas would be a little less than half those shown in Figures 8-4A.6B and C (jet lengths would be about two-thirds).

FIG. 8-4A.6B

BUILDING 4A AIR BLAST JETS — 20 PSI

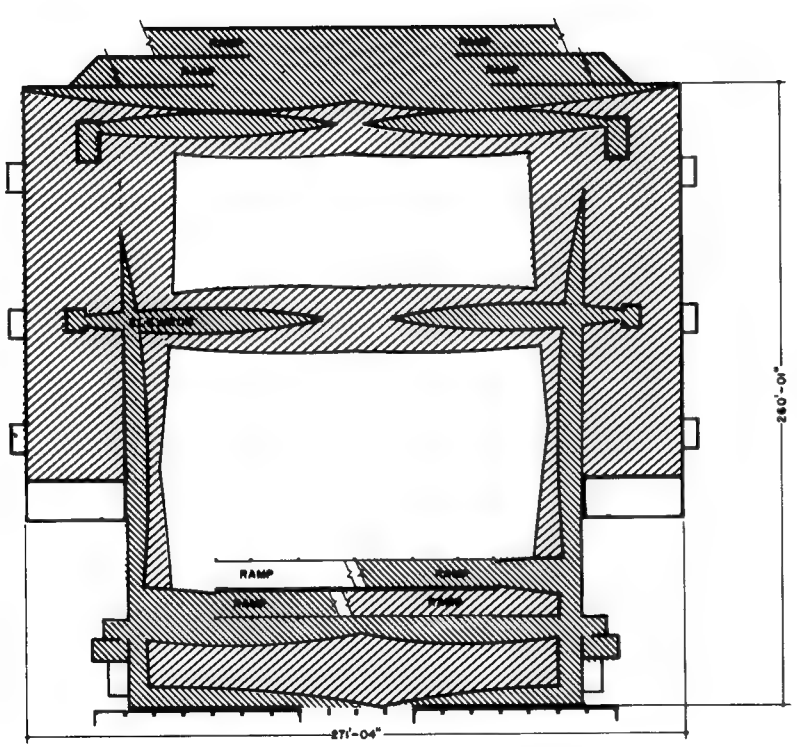

UPPER SUB-LEVEL

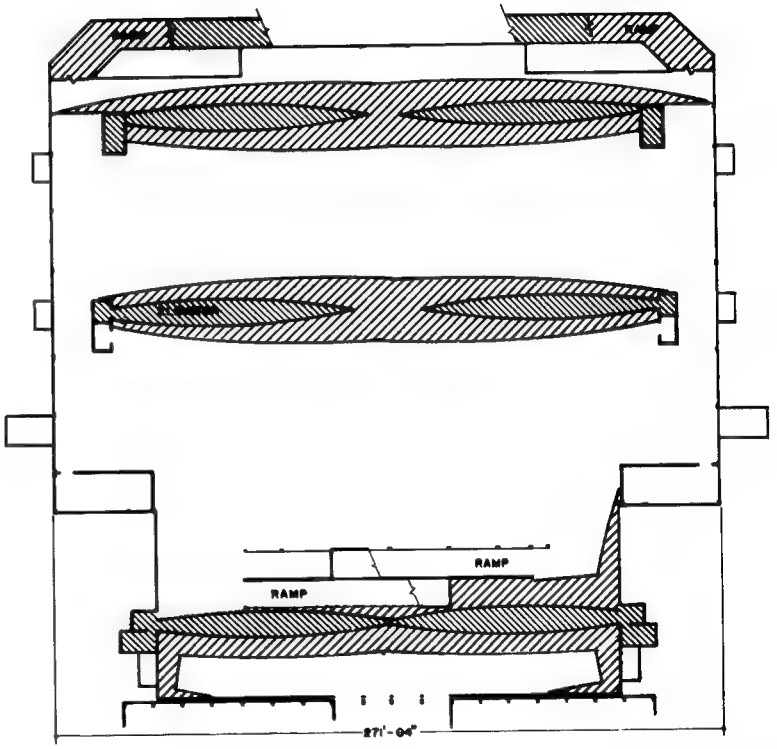

LOWER SUB-LEVEL

LEGEND

20 fps criterion

80 fps criterion

0 50 100

SCALE

FIG. 8-4A.6C

BUILDING 4A AIR BLAST JETS — 5 PSI

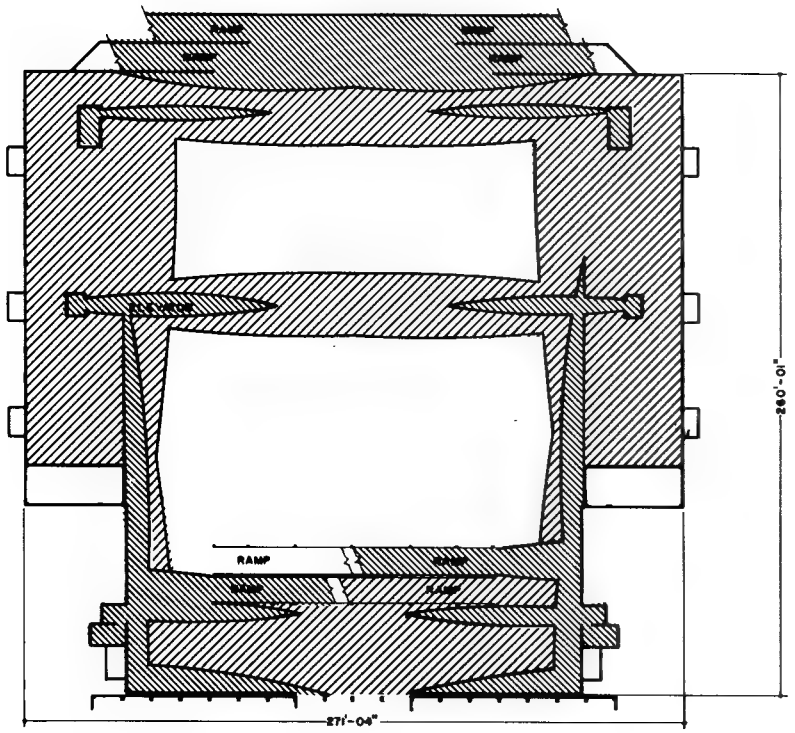

UPPER SUB-LEVEL

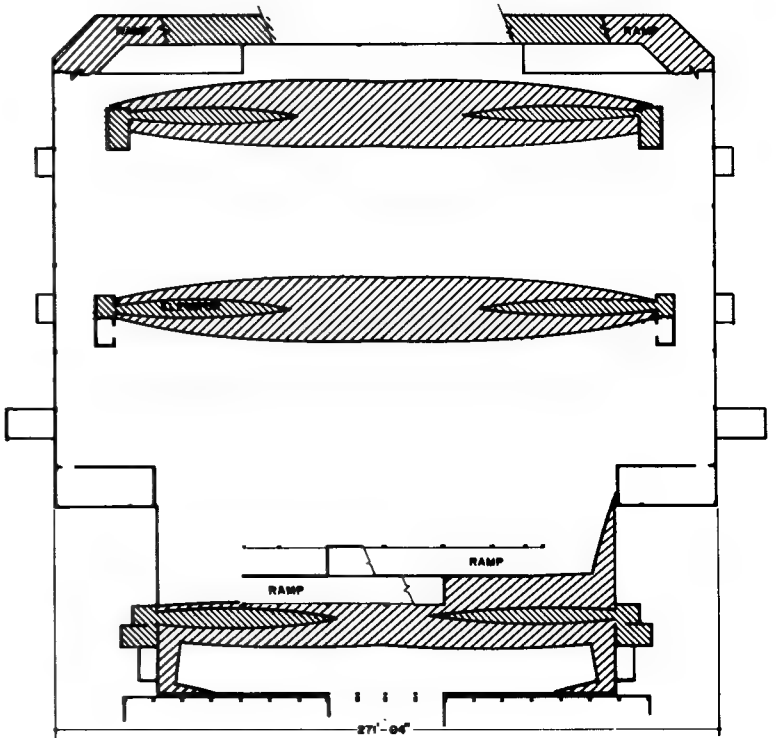

LOWER SUB-LEVEL

LEGEND

20 fps criterion

80 fps criterion

0 50 100

SCALE

Slanting Estimated Costs at Peak Overpressures Other Than 15 psi

The study work was extended to cover other peak overpressures than the 15 psi adopted as basic for the original feasibility study (Chapter 1 and other references herein). Two each open and closed shelter example buildings were used: Buildings 2A and 3A for closed, and Buildings 2B and 4A for open. Peak overpressures selected for study, in addition to the original 15 psi, were 5, 10 and 20 psi for the open shelters, and 20 and 30 psi for the closed.

Estimated cost results have been added to each building's estimates table as originally developed for 15 psi; i.e., Tables 8.2A, 8.2B, 8.3A and 8.4A. In addition, cost summary tables, similar to the 15 psi summary table (Table 8.0A), are included herein: Tables 8.0B, 8.0C, 8.0D and 8.0E for peak overpressures of 5, 10, 20 and 30 psi, respectively.

Table 8.0F contains, for each building, at each overpressure, ratios of estimated cost compared to that at 15 psi.

Tentative conclusions might include the following:

- Open shelter estimated slanting costs appear to be more sensitive (or at least equally sensitive) to peak overpressure design changes than those for closed shelters.

- Estimated slanting costs for the larger (open and closed) shelters (Buildings 3A and 4A) were under the Scope limit of $6/sf (4% to 11% below, when all costs are corrected to the same time period) for a design peak overpressure of 20 psi.

Table 8.0B

SUMMARY OF SLANTING COST ESTIMATES (5 psi)

Building:		2B (open portion)		2B closed portion)		2B (total)		4A (open)	
Cost Items		All	Non-deferrable	All	Non-deferrable	All	Non-deferrable	All	Non-deferrable
Shelter area (sf)		2,262		1,116		3,378		130,522	
Estimate		6-70		6-70		6-70		6-70	
A. Structural	$	4,952	4,952	3,979	3,979	8,931	8,931	169,229	169,229
	$/sf	2.19	2.19	3.57	3.57	2.64	2.64	1.30	1.30
	%*	80	81	75	93	77	86	37	38
	%†		*100*		*100*		*100*		*100*
B. Blast doors	$	90	--	1,048	--	1,138	--	22,106	9,418
	$/sf	.04	--	.94	--	.34	--	.17	.07
	%*	1	--	20	--	10	--	5	2
	%†		*0*		*0*		*0*		*43*
C. Ventilation	$	318	318	309	309	627	627	231,023	231,023
(Incl. emergency	$/sf	.14	.14	.28	.28	.19	.19	1.77	1.77
exit tunnel,	%*	5	5	6	7	5	6	50	52
if any)	%†		*100*		*100*		*100*		*100*
D. Other	$	847	847	--	--	847	847	35,697	35,697
	$/sf	.37	.37	--	--	.25	.25	.27	.27
	%*	14	14	--	--	7	8	8	8
	%†		*100*		*0*		*100*		*100*
Total	$	6,207	6,117	5,336	4,288	11,543	10,405	458,055	445,367
	$/sf	2.74	2.70	4.78	3.84	3.42	3.08	3.51	3.41
	%†		*99*		*80*		*90*		*97*
‡ Jan. 68:	$/sf	2.11	2.08	3.68	2.96	2.63	2.37	2.70	2.62
‡ Jun. 73:	$/sf	3.54	3.49	6.17	4.98	4.41	3.97	4.53	4.40
Cost ratio (5 psi/15 psi)	%	42	41	55	50	47	45	58	57

* Percent ratio of item cost to total cost.

† Percent ratio of nondeferrable cost to item (All) cost.

‡ Using Engineering News-Record Building and Construction Cost Indexes (averaged) to convert totals from San Francisco area to EN-R's 20-cities average and from estimate date to date(s) shown.

Table 8.0C

SUMMARY OF SLANTING COST ESTIMATES (10 psi)

Building:		2B (open portion)		2B (closed portion)		2B (total)		4A (open)	
Cost Items		All	Non-deferrable	All	Non-deferrable	All	Non-deferrable	All	Non-deferrable
Shelter area (sf)		2,262		1,116		3,378		130,522	
Estimate date		6-70		6-70		6-70		6-70	
A. Structural	$	9,544	9,544	5,905	5,905	15,449	15,449	362,828	362,828
	$/sf	4.22	4.22	5.29	5.29	4.57	4.57	2.78	2.78
	%*	87	88	81	95	85	91	56	57
	%†		*100*		*100*		*100*		*100*
B. Blast doors	$	95	--	1,099	--	1,194	--	22,422	9,574
	$/sf	.04	--	.98	--	.35	--	.17	.07
	%*	1	--	15	--	7	--	3	1
	%†		*0*		*0*		*0*		*43*
C. Ventilation	$	346	346	326	326	672	672	232,426	232,426
(Incl. emergency	$/sf	.15	.15	.29	.29	.20	.20	1.78	1.78
exit tunnel,	%*	3	3	4	5	4	4	36	36
if any)	%†		*100*		*100*		*100*		*100*
D. Other	$	948	948	--	--	948	948	35,697	35,697
	$/sf	.42	.42	--	--	.28	.28	.27	.27
	%*	9	9	--	--	5	6	5	6
	%†		*100*		*0*		*100*		*100*
Total	$	10,933	10,838	7,330	6,231	18,263	17,069	653,373	640,525
	$/sf	4.83	4.79	6.57	5.58	5.41	5.05	5.01	4.91
	%†		*99*		*85*		*94*		*98*
‡ Jan. 68:	$/sf	3.72	3.69	5.05	4.29	4.16	3.89	3.85	3.77
‡ Jun. 73:	$/sf	6.23	6.18	8.47	7.20	6.97	6.52	6.46	6.33
Cost ratio (10 psi/15 psi)	%	73	73	76	73	74	73	83	82

* Percent ratio of item cost to total cost.

† Percent ratio of nondefferable cost to item (All) cost.

‡ Using Engineering News-Record Building and Construction Cost Indexes (averaged) to convert totals from San Francisco area to EN-R's 20-cities average and from estimate date to date(s) shown.

Table 8.0D

SUMMARY OF SLANTING COST ESTIMATES (20 psi)

Building:		2A (closed)		2B (open portion)		2B (closed portion)		2B (total)		3A (closed) with mezzanine		3A (closed) no mezzanine		4A (open)	
Cost Items		All	Non-deferrable	All	Non-deferrable	All	Non-deferrable	All	Non-deferrable	All	Non-deferrable	All	Non-deferrable	All	Non-deferrable
Shelter area (sf)		3,378		2,252		1,116		3,378		16,351		13,598		130,522	
Estimate date		6-70		6-70		6-70		6-70		6-70		6-70		6-70	
A. Structural	$	17,291	17,291	18,355	18,355	10,480	10,480	28,835	28,835	80,071	69,624	68,425	67,624	645,412	645,412
	$/sf	5.12	5.12	8.15	8.15	9.39	9.39	8.54	8.54	4.90	4.26	5.03	4.97	4.94	4.94
	%*	61	99	92	92	87	97	90	94	71	97	67	97	69	70
	%†		*100*		*100*		*100*		*100*		*87*		*99*		*100*
B. Blast doors	$	2,563	--	105	--	1,175	--	1,280	--	17,781	--	17,781	--	23,054	9,886
	$/sf	.76	--	.05	--	1.05	--	.38	--	1.09	--	1.31	--	.18	.08
	%*	9	--	1	--	10	--	4	--	16	--	17	--	2	1
	%†		*0*		*0*		*0*		*0*		*0*		*0*		*43*
C. Ventilation (Incl. emergency exit tunnel, if any)	$	6,270	99	396	396	350	350	746	746	11,814	-760	11,814	-760	234,629	234,629
	$/sf	1.86	.03	.18	.18	.31	.31	.22	.22	.72	-.05	.87	-.06	1.80	1.80
	%*	22	1	2	2	3	3	2	2	10	-1	12	-1	25	25
	%†		*2*		*100*		*100*		*100*		*-6*		*-6*		*100*
D. Other	$	2,270	--	1,132	1,132	--	--	1,132	1,132	3,757	3,043	3,757	3,043	35,697	35,697
	$/sf	.67	--	.50	.50	--	--	.34	.34	.23	.19	.28	.22	.27	.27
	%*	8	--	6	6	--	--	4	4	3	4	4	4	4	4
	%†		*0*		*100*		*0*		*100*		*81*		*81*		*100*
Total	$	28,394	17,390	19,988	19,883	12,005	10,830	31,993	30,713	113,423	71,907	101,777	69,907	938,792	925,624
	$/sf	8.41	5.15	8.88	8.83	10.76	9.70	9.47	9.09	6.94	4.40	7.48	5.14	7.19	7.09
	%†		*61*		*99*		*91*		*96*		*63*		*69*		*99*
‡ Jan. 68:	$/sf	6.46	3.96	6.83	6.79	8.27	7.46	7.28	6.99	5.34	3.38	5.76	3.95	5.53	5.45
‡ Jun. 73:	$/sf	10.84	6.64	11.45	11.39	13.87	12.52	12.21	11.73	8.95	5.67	9.65	6.63	9.28	9.15
Cost ratio (20 psi/15 psi)	%	1.12	1.20	1.34	1.34	1.25	1.27	1.30	1.32	1.13	1.21	1.15	1.22	1.19	1.19

* Percent ratio of item cost to total cost.

† Percent ratio of nondeferrable cost to item (All) cost.

‡ Using Engineering News-Record Building and Construction Cost Indexes (averaged) to convert totals from San Francisco area to EN-R's 20-cities average and from estimate date to date(s) shown.

Table 8.0E

SUMMARY OF SLANTING COST ESTIMATES (30 psi)

Building:		2A (closed)		3A (closed) with mezzanine		3A (closed) no mezzanine	
Cost Items		All	Non-deferrable	All	Non-deferrable	All	Non-deferrable
Shelter area (sf)		3,378		16,351		13,598	
Estimate date		6-70		6-70		6-70	
A. Structural	$	23,424	23,424	102,900	92,453	91,254	90,453
	$/sf	6.93	6.93	6.29	5.65	6.71	6.65
	%*	68	100	74	98	71	98
	%†		*100*		*90*		*99*
B. Blast doors	$	2,728	--	21,324	--	21,324	--
	$/sf	.81	--	1.30	--	1.57	--
	%*	8	--	15	--	17	--
	%†		*0*		*0*		*0*
C. Ventilation	$	6,270	99	11,814	-760	11,814	-760
(Incl. emergency	$/sf	1.86	.03	.72	-.05	.87	-.06
exit tunnel,	%*	18	--	8	-1	9	-1
if any)	%†		*2*		*-6*		*-6*
D. Other	$	2,270	--	3,757	3,043	3,757	3,043
	$/sf	.67	--	.23	.19	.28	.22
	%*	7	--	3	3	3	3
	%†		*0*		*81*		*81*
Total	$	34,692	23,523	139,795	94,736	128,149	92,736
	$/sf	10.27	6.96	8.55	5.79	9.42	6.82
	%†		*68*		*68*		*72*
‡ Jan. 68:	$/sf	7.90	5.36	6.58	4.46	7.25	5.25
‡ Jun. 73:	$/sf	13.25	8.98	11.03	7.47	12.15	8.80
Cost ratio (30 psi/15 psi)	%	1.37	1.63	1.39	1.59	1.44	1.61

* Percent ratio of item cost to total cost.

† Percent ratio of nondeferrable cost to item (All) cost.

‡ Using Engineering News-Record Building and Construction Cost Indexes (averaged) to convert totals from San Francisco area to EN-R's 20-cities average and from estimate date to date(s) shown.

Table 8.0F

SLANTING COST RATIOS - OTHER OVERPRESSURES VS. 15 PSI SHELTERS

BUILDING:	2A Closed		3A w/mezz. Closed		2B Open			4A Open		
					(total shelter) *3,378* (open portion only)					
AREA, sf:	3,378		16,351		2,262			130,522		
OVERPRESSURE:	20	30	20	30	5	10	20	5	10	20
STRUCTURAL	1.20	1.63	1.18	1.52	*0.41* 0.42	*0.72* 0.71	*1.34* 1.37	0.34	0.73	1.29
BLAST DOORS	1.03	1.10	1.03	1.24	*0.92* 0.91	*0.96* 0.96	*1.03* 1.06	0.97	0.99	1.01
VENTILATION	1.00	1.00	1.00	1.00	*0.87* 0.85	*0.93* 0.92	*1.04* 1.05	0.99	1.00	1.00
OTHER	1.00	1.00	1.00	1.00	*0.82* 0.82	*0.92* 0.92	*1.10* 1.10	1.00	1.00	1.00
TOTAL	1.12	1.37	1.13	1.39	*0.47* 0.42	*0.74* 0.73	*1.30* 1.34	0.58	0.83	1.19

NOTE:

PF100 fallout protection generally means an 8.5" to 9.5" cover slab over basement (Table 5.1). In some cases - such as short spans and some of the lower overpressure medium spans - these PF100 thicknesses were controlling.

Support Systems - Beams, Columns and Footings vs. Wall and Wall Footing

Building 2B, a basement shelter offering an open area (2,262 sf) and a closed area (1,116 sf) as described earlier in this Chapter, was subsequently used to briefly compare the slanting costs of two interior support systems: beam, columns and column footings versus wall and wall footing. In this building, the support systems were used on the longitudinal centerline of the shelter, in both open and closed portions. Figure 8-2B shows use of the beam-column system, which in Table 8.2B is Item 2 and the shelter cover slab is Item 5. The interior wall "design" included blast resistance against the very short differential blast loading on its two faces, based on a blast wave incident to a building side parallel to the interior wall and therefore reaching the wall more quickly from openings in the building blastward side than from the leeward side. The following tabulation shows pertinent slanting estimated costs for the two support systems, as applied to Building 2B (15 psi shelter):

	BEAM-COLUMN			WALL		
	Shelter Area			Shelter Area		
	Open	Closed	Total	Open	Closed	Total
Cover slab	$5,195	2,363	7,558 (13.5"th.)	5,475	2,490	7,965 (14.5"th.)
Beam	1,672	867	2,539	-994	-393	-1,387
Columns	488	18	506	-225	-225	-450
Interior wall	-	-	-	3,081	1,285	4,366
Footings	3,157	1,482	4,639	1,185	485	1,670
TOTAL	$10,512	4,730	15,242	8,522	3,642	12,164

(The cover slab cost less in the beam-column than in the wall system, because of a shorter span to the very wide beam than to the wall.) The wall and wall footing system offered a savings of 20 percent compared to the beam, columns and column footings system in this one slanting application.

Blast Door Schemes Used for Estimating

Figure 8-0E shows three blast door schemes used in the case studies of this chapter. Selected details and cost estimates for the three door schemes are shown in Table 8.0G.

Design μ was most often used as 1.3 to 3, but 10 was used for the hinged steel blast doors to close up vents that had no emergency exit function. Designs were not detailed but only complete enough for comparative cost estimating purposes. With blast doors representing as much as about 20% of total slanting cost in a shelter, certainly an early candidate for finished standard designs would be a family of blast doors, should a slanting program be undertaken.

Preventive (not breakdown) maintenance methods would be an absolute requirement for any emergency shelter and components, and the adequacy of such maintenance should be subjected to independent scheduled inspections; this would be particularly applicable to blast doors.

The blast door schemes used were, of course, predicated on manual rather than automatic closing. Manual closing was considered appropriate to the basic nuclear attack and low cost assumptions stated in the Stipulations section of Chapter 1 (first and sixth stipulations). Blast-actuated or other automatic-closing blast doors are generally small, not amenable to the building basement's normal or non-shelter use, and very expensive (say one to two orders of magnitude greater than the doors contemplated herein).

Table 8.0G
BLAST DOORS SCHEMES USED FOR ESTIMATING

Building	Door	Jamb Steel	p_{so}	p_m	q	* Est. $/door	* Est. $/sf
STEEL, GUILLOTINE:							
2A	2'7"x2'7"x1/4" with C3X4.1 stiffeners	PL3/8X2 and PL3/8X3	15	19.5	20.5	44	6.6
2A	3'x3'x1/4" with same	" "	"	"	"	55	6.1
2A	2'7"x2'7"x1/4" with C4X5.4 stiffeners	" "	30	41.5	43.7	50	7.5
2A	3'x3'x1/4" with same	" "	"	"	"	61	6.8
STEEL, HINGED:							
3A	4'3"x8'x1/4" w/C4X5.4 and C5X6.7 stiffeners	L4X3X1/4	15	41.5	44	863	25.4
3A	4'3"x10'x1/4" w/same	"	"	"	"	1,067	25.1
3A	4'3"x8'x1/4" w/C4X5.4 and C6X8.2 stiffeners	"	20	59.5	62.6	879	25.9
3A	4'3"x10'x1/4" w/same	"	"	"	"	1,087	25.6
3A	4'3"x8'x5/16" w/C5X9.0 and C8X11.5 stiffeners	"	30	100.6	105.9	1,052	30.9
3A	4'3"x10'x5/16" w/same	"	"	"	"	1,304	30.7
WOOD (METAL-CLAD), HINGED:							
2A/2B	3'4"x7'3"x3-1/4"	C12X20.7	15	41.5	67.4	747	30.9
2A	" " 4-1/2"	"	30	71	115.4	755	31.2
2B	3'6"x6'11"x3"	C6X8.2	15	30	48.7	584	24.1
†2C	3'10"x6'11"x3-3/4"	C12X20.7	"	41.5	67.4	762	28.7
3A	3'6"x6'11"x2-1/4"	"	"	15	24.4	727	30.0
3A	" " 3-1/2"	"	"	41.5	67.4	735	30.4
3A	" " 3"	2 L6X4X1/2	30	30	48.7	880	36.4
3A	" " 4-1/2"	"	"	100.6	120.4	894	36.9

* June 1970 costs, San Francisco area; use multiple of about 1.29 to June 1973, ENR 20-cities.
† Sliding doors
Notation on structural shapes follows (approximately) AISC Manual of Steel Construction 7th ed., p. 1-10; e.g., C4X5.4 is 4" channel @5.4 plf, PL 3/8X2 is plate 3/8" thick by 2" wide.

Baffle Walls and Blast Drag Pressures (Jet Effect)

Appendix E provides calculational methods for predicting average air blast pressure rise versus time in a shelter space (room filling), as well as drag (wind) pressures for various locations within the shelter (jet effect). The final section of Appendix E describes the use of an interactive (conversational) computer program and includes a listing of the FORTRAN program.

Because of the jet effect hazard to humans, moved directly or by being hit by flying objects, an investigation was made to determine the potential of baffle walls for reducing the jet effect, as well as the usual purpose of turning its direction.

Briefly stated, baffle walls were found to offer only the possibility of flow division in shelter from megaton weapons, rather than reduction of the intrinsic hazard within the jet itself. Friction in any reasonable number of turns was found to be too small to be of any consequence. The study ignored the initial shock wave, which is very weak, thus considering (in many short increments of time) only the quasi-steady drag pressures; a discussion of this matter is included in Appendix E. Use of baffles to concentrate hazardous jets within a part of the shelter space should be considered.

After a series of measurements of dynamic pressure in model rooms exposed in a shock tube to overpressures in the range of 5 to 20 psi, Coulter* concluded that a baffle inside the entrance significantly reduced the dynamic pressure in the jet entering the room, although the baffle had no significant effect on the filling time of the room regardless of where in the room the filling time was observed. The mechanism of this reduction in dynamic pressure may be a slight delay in the formation of the jet into the room. It has not been shown that a significant reduction in dynamic pressure would appear in a full size room struck by air blast from a megaton weapon.† In any case, baffles may be valuable in diverting flow from occupied areas.

---

* Ref. 21 of Appendix E.

† See a discussion of baffles in Section IIC2 of Appendix E.

Room Filling Maximum Interior Pressure

Interest in shelter interior pressure buildup through room filling from a nuclear air blast wave - as it might occur in large spaces, such as caverns or mines, with few or many openings at various angles of incidence to the blast wave - led to the running of several solutions using the computer program shown in the last section of Appendix E.

Two values of free-field blast overpressure were assumed 10 and 20 psi,* and the ratio of total shelter volume (V, cf) to the sum of the area of all apertures/openings (A, sf) was used. Calculations were made for the limits represented by all openings being either hit side-on by the air blast, or hit by a fully reflected wave as if in the front wall of a block-house structure.

When the value of a graph showing all solutions became apparent, sufficient calculations were made to cover the range of V/A from 10 ft to 10^6 ft, and for both side-on and fully reflected angles of blast wave incidence. The results are shown by Figure 8-0F for maximum interior overpressure and by Figure 8-0G for time (seconds) to reach such maximum pressure.

The curves of Figure 8-0F are drawn to two scales of maximum interior pressure, with arrows to indicate which scale applies to each group of curves. In the V/A range of values from 10^3 to 10^4 there are curve groups for both scales. For example, when V/A equals 10^3 a maximum interior pressure value of 7.4 psi may be read on the left side scale for a free-field overpressure of 10 psi (side-on); using the similar curve from the upper group of curves, and reading on the right side scale, the value is 7.45 psi.

* Duration of positive pressure values were based on 5 Mt yield.

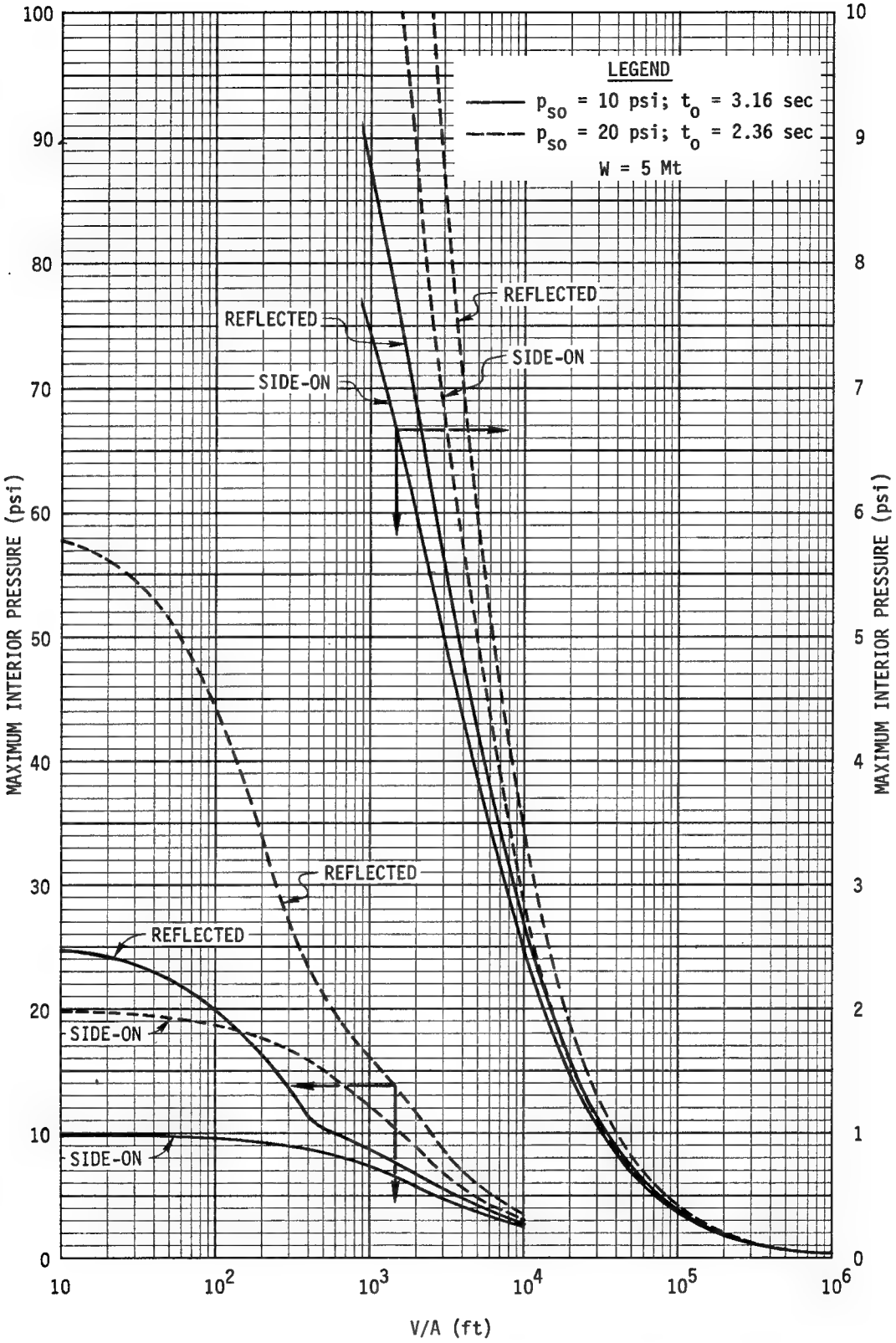

FIG. 8-0F MAXIMUM INTERIOR PRESSURE VERSUS V/A (ROOM VOLUME/TOTAL APERTURE AREA)

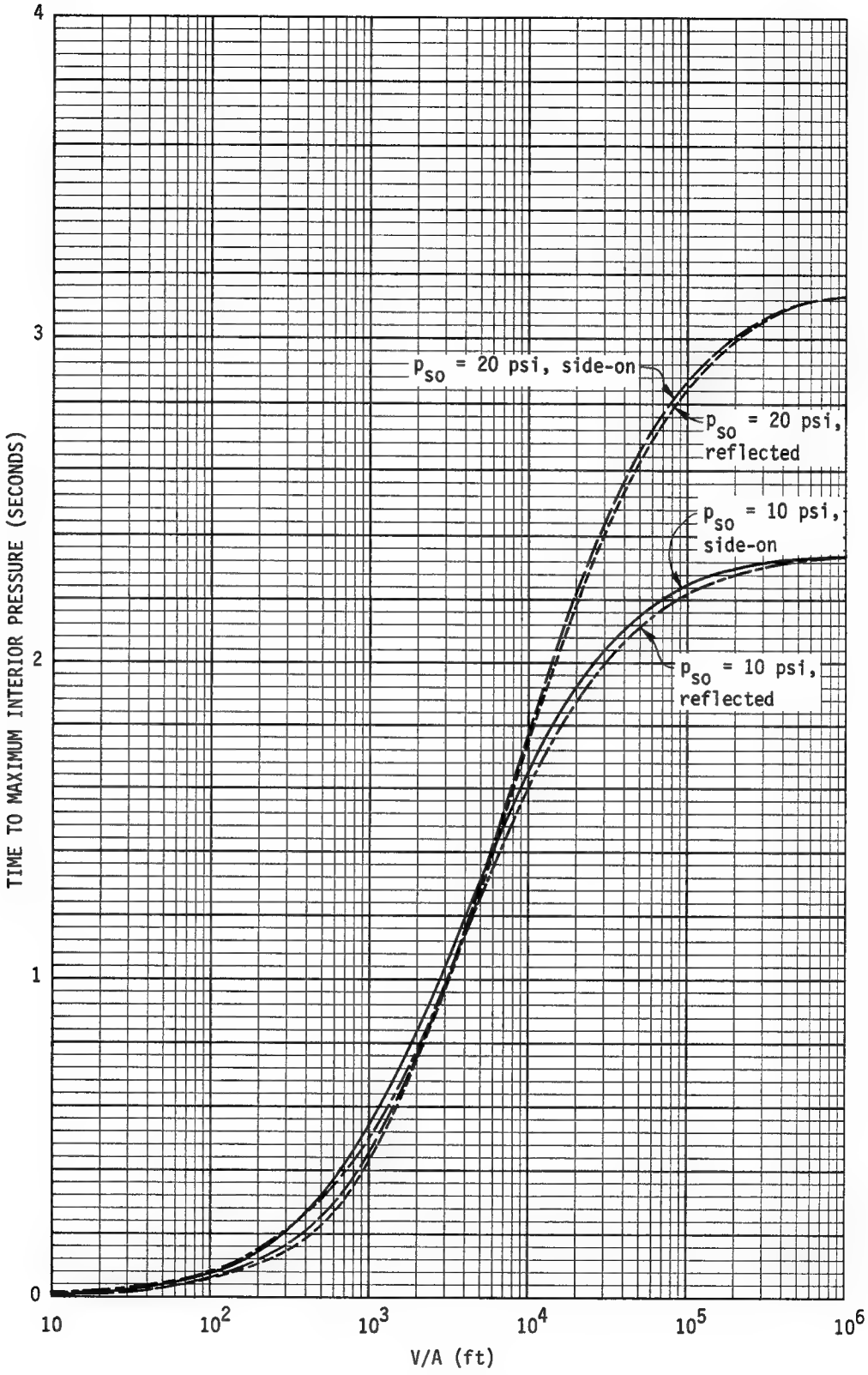

FIG. 8-0G TIME TO MAXIMUM INTERIOR PRESSURE VERSUS V/A (ROOM VOLUME/ TOTAL APERTURE AREA)

45. Guidelines for the Use of SI Units of Measurement in the Publications of the American Society of Civil Engineers (June 1972), A.S.C.E., New York, N.Y. (extracted from ASTM E380-70); ASTM E380-72, June 1972, was used for latest conversion values.

46. Engineering News-Record, October 26, 1972, page 16.

47. _____., December 21, 1972, page 27.

48. Progressive Architecture, July 1972, page 96.

49. Smith, Paul D., P.E., Fire Protection and Life Safety for Underground Buildings, Gage-Babcock & Associates, Inc., letter report (unpublished), March 1972.

50. Murphy, H. L., Feasibility Study of Slanting for Combined Nuclear Weapons Effects (Revised), Stanford Research Institute Technical Report, for U.S. Office of Civil Defense (now Defense Civil Preparedness Agency), 2 vols., July 1971. (AD-734 831 and 2)

51. Waterman, T. E., Fire Laboratory Test - Phase III, IIT Research Institute Final Technical Report for Defense Civil Preparedness Agency, February 1973.

Appendix E

ROOM FILLING FROM AIR BLAST

By J. R. Rempel

PREFACE

This appendix is intended to serve both as a source of immediately applicable methodology and as a guide to the underlying gas dynamic theory. Those interested more in applying the methodology than in derivations and comparisons of calculated and observed results will find the following parts of this appendix of particular importance:

Location	Description
Section IIA	The simplest and fastest method of estimating average pressure in a room as a function of time; adequate for many purposes. The room may have one or more openings to the outside pressure source or sources.
Section IIB3	Two different methods for a step-by-step, hand calculation providing average room pressure, as well as dynamic pressure in the opening; valid for all flows through a single opening into a single room when the outside pressure is known as a function of time. Either method may be used but Method F is recommended for inflow, Method D for outflow.
Section IIC	General formulas describing geometric extent of the jet created inside the room by inflowing air and for dynamic pressure distribution within the jet. Provides basis for calculation of jet distribution in Table E-3.
Table E-3	A computer program to calculate average pressure within a single room, as well as dynamic pressure distribution around as many as eight openings as functions of time when the single room has openings into several different pressure fields (e.g., a room with front, rear, and side windows struck by a blast on the front wall). If desired, follows translation of objects caught in jet.

Location	Description
Section IVB	A specific numerical example using one of the step-by-step procedures set forth in Section IIB3 for the calculation of average room pressure, as well as dynamic pressure in each opening, during filling of a single room through two openings into separate pressure fields. Also illustrates the calculation of certain nuclear blast wave parameters.

The Notation section near the end of this Appendix defines the symbols used in the methodologies just described; the computer program versions of some of these symbols appear also in the Notation section. Subscripts not explained there refer to physical spaces, i.e., subscript 1 indicates quantity is measured outside the room; other odd-numbered subscripts refer to interior of rooms and even-numbered subscripts refer to connecting ducts or openings.

CONTENTS

FIGURES

TABLES

Appendix E

ROOM FILLING FROM AIR BLAST
By J. R. Rempel

I Introduction

When a blast wave strikes a building, even should the structure withstand the initial impact, the resulting inflow of air through windows and other openings can be critical in determining the safety of any people sheltered by the structure and in determining the response of the structure itself to the blast impact. Although the physical laws obeyed by moving gases are well known and the course of the inflow in filling the building can in principle be calculated completely, any such calculation is far too lengthy to be practical for most purposes; fortunately, simplifications can be introduced which greatly shorten the labor of estimating effects of the blast inside the building and which give results in good to fair agreement with experiments done with small models. In general, the effect of the inflow is to provide a stream of fast moving air in the shelter space which may (1) endanger shelterees by hurling them against large relatively fixed objects or by hurling objects against them, (2) provide a back pressure on the inner surfaces of outside structure walls countering the blast pressures on their outer surfaces, and (3) provide pressure against interior walls.

Several factors enter into the calculation: the pressure outside each wall with openings and the time each opening becomes available, the area occupied by each opening and the volume of each room, the number of connected rooms and the area of each connection, and the ambient pressure and temperature in the building before the blast strikes. Perhaps the first of these to consider is what proportion of the wall exposed to the blast is open. If this fraction is greater than one half, the shock front leading the blast wave will pass into the building only slightly weakened and subsequent inside pressure should be estimated from a knowledge of shock pressure and the laws of shock reflection. Methods appropriate to this case are only touched upon here. On the other hand, should the fraction be less than one tenth, clearly the filling is not a shock process and the methods treated here are quite pertinent. Unfortunately, in many applications the fraction of open area will lie between these two extremes and, in these cases after the room filling calculation has been completed according to the methods suggested here, some thought must be given independently to the influence of the entering shock front.

When the source of the blast wave is an explosion and the location of the building in relation to the point of explosion is known or postulated, "free-field" pressure histories at the building site can be found in standard references,[1,2,15]* and from these histories well-known methods[1,3] are available to derive approximate histories on the outside of the walls of the building. Briefly, these methods account for a short-lived peak of pressure created by the impact of the front upon the wall nearest the explosion, the relatively fast erosion of this high pressure to a level which is the sum of the free field pressure plus a drag pressure on the wall due to the high winds behind the blast front. This quasi-steady pressure then decays slowly to zero as the blast wave moves onward past the structure.

Ordinary window glass breaks rather quickly, i.e., within 8 ms (milliseconds) or less when struck by blast overpressure of 1 psi (pound per square inch) or more.[4] Doors may withstand outside pressure longer, or even altogether. The time an opening becomes available with respect to the first impact of the blast upon the building becomes, then, the breaking time plus the time required by the wave to travel from the wall nearest the explosion to the opening. If the opening is in the wall nearest the explosion, travel time is of course zero. Strictly, the decay of the blast wave overpressure which occurs during this time must be taken into account, but when the blast arises from a nuclear explosion of yield greater than a few kt (kilotons), this decay is slight and negligible; that is, a single "free-field" pressure history for all openings may be assumed.

The methods given here are simplified and their use leads only to estimates. They are intended to provide: (1) calculations applicable to hand computation by those untrained in gas dynamics and (2) approximate results useful until more careful calculations are made. Only in the case of the simplest structural configurations and the simplest pressure history shapes can limits of error be suggested for these results. Such cases are the subject of the discussion immediately below.

II Classical Nuclear Blast Wave Incident upon a Single Room with Openings into Single Pressure Field

A. Estimation of Inside Pressure History

The "classical" blast wave from nuclear explosions consists of a steep pressure front or rise followed by a long-lasting decay phase, during which the pressure in the wave falls to zero. It is accompanied by high winds giving rise to dynamic pressure against objects in the stream. Striking a wall at normal or near normal incidence, it creates a high-pressure

---

* References for Appendix E are listed at the end of the appendix.

zone at the surface, which however is rapidly eroded as relief waves move across the wall face from the edges. As a first approximation in the calculation of room filling, this reflected phase can usually be neglected. Following the decay of the high reflected pressure, the quasi-steady pressure (free field plus drag) remains against the wall for hundreds of milliseconds to several seconds, depending on explosive yield. Generally filling is complete before this quasi-steady pressure has fallen more than a few percent; hence, as a first approximation the outside pressure may often be considered constant and, if only a single wall with opening is exposed to the blast, the time ΔT (in milliseconds) to complete filling may be computed as the ratio $\frac{V}{2A}$, where V is room volume in cubic feet and A is area of opening in square feet.* The average room pressure at any time t during the filling process is then simply the fraction of the quasi-steady outside pressure given by the ratio $\frac{t}{\Delta T}$. For the purposes of this calculation, areas of several openings in the same wall should be added together to form the quantity A.†

In case there are two or more walls with openings exposed to the blast and each such wall sustains a different outside pressure history (as will happen, for example, when the drag coefficient is different for two walls), the calculation is more complicated but first estimates of filling time and average inside pressure during filling can be found by adding interior pressures calculated as if each wall alone were exposed. As an example, consider a room of volume 30'x10'x10' = 3000 ft^3 in which the front wall has total openings of 36 sf and side walls have total openings of 60 sf. The ratios $\frac{V}{2A}$ for the front and side walls are 41.7 and 25 ft, respectively. If the quasi-steady overpressure on the front wall is 10 psig (pounds per square inch - gauge) and on the side wall 8 psig and if, further, the side wall opening becomes available 10 ms after the first blast impact, then the average inside pressure will be approximately as shown in Figure E-1 by the heavy line OAFG. In other words the room will fill in approximately 24 ms. Lines OAC and DE represent filling rates through front and side walls, respectively; and ordinates of OAC and DE are added to form the line OAF. Of course after the average inside pressure exceeds 8 psi there will be outflow through the side wall; to allow for this loss, the line FG has been placed between the outside pressure at the side wall (8 psig) and the outside pressure at the front wall (10 psig). The ordinate at FG is closer to 8 psig than to 10 psig because the area of the opening in the side wall is greater than that in the front wall. The line FG is intended to represent the final quasi-equilibrium pressure in the room. As outside pressure slowly falls to normal, room pressure will follow it.

---

* Empirical relationship, dimensionally inconsistent. Meanings of symbols as used in this Appendix are defined as introduced and under "Notation" at end of Appendix.

† The experimental justification of most of the procedures described in this section is demonstrated later in Figures E-4, E-5, E-6 and E-8.

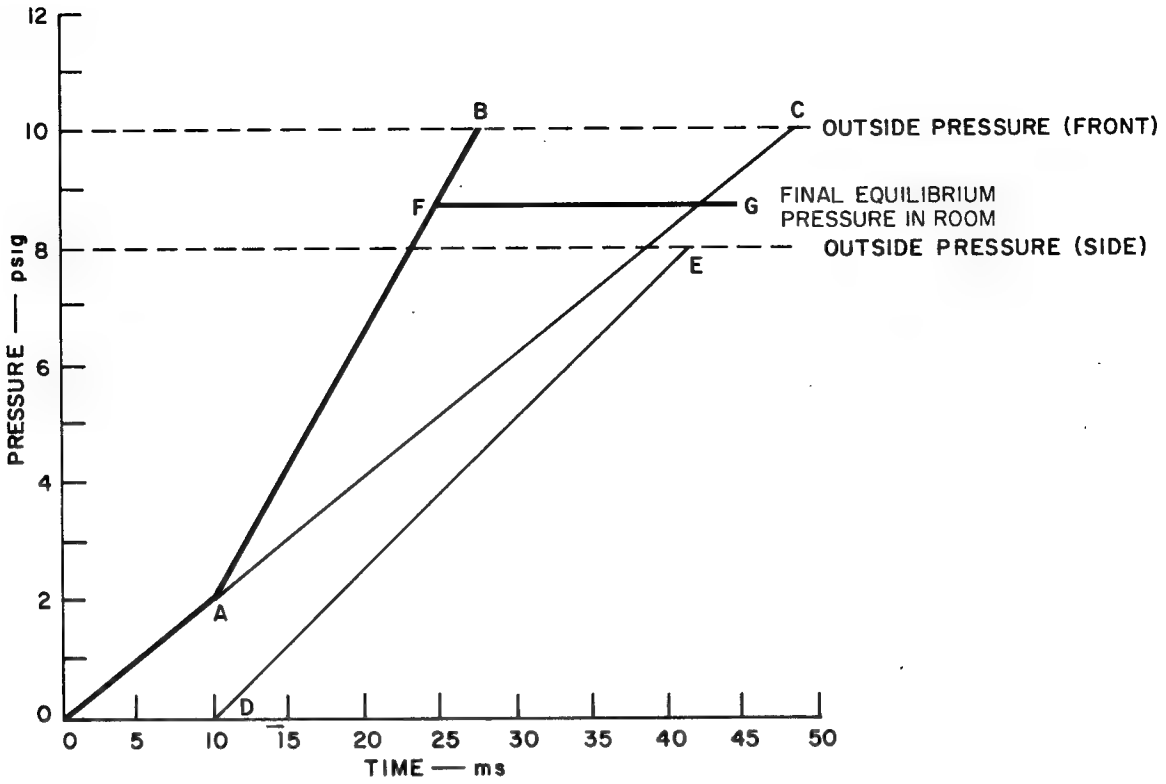

FIGURE E-1 APPROXIMATE FILLING RATE THROUGH TWO WALLS

These simple calculations do not apply when the reflected pressure lasts an appreciable length of time, or when the wave is nonclassical, such as it would be were a precursor present. Under these conditions the more detailed methods set forth below must be followed.

A theoretical justification due to Kriebel[24] of the approximate filling time $\Delta T = V/2A$ appears below in Section IIB1.

B. Detailed Calculation of Inside Pressure History

Confidence in the simple method noted above rests upon experience with a step-by-step calculation and comparison of its results with experiments. This calculation applies the principles of steady isentropic flow in ducts in successive, small time intervals. Conditions computed for the end of one time step become initial conditions for the next step. Conservation of energy, momentum and mass, along with the assumption that the air behaves as a perfect gas with constant specific heats, determine the thermodynamic variables, pressure, temperature and density, as well as the wind speed through the opening. Unique expressions lending themselves to simple calculation cannot be given for the laws of conservation of energy and momentum, so alternative forms leading to somewhat different results will be stated. All such expressions rely upon certain approximations to the conservation laws, and these approximations usually introduce errors into the results in comparison with which the approximations arising in the assumptions of isentropy, perfect gas behavior, and constant specific heats are negligible.

1. Inflow. Figure E-2 shows the idealized room with a single opening struck head-on by a blast wave. Three regions are noted: the outside ①, the doorway ②, which serves as a duct connecting the outside with the room ③. In order to make the calculations tractable, uniformity of conditions in each of the two regions ① and ③ and over the cross section of region ② is assumed; furthermore, during each small time interval Δt, steady conditions are assumed in each region. During the aforementioned quasi-steady state outside the building, these assumptions are probably valid for region ① but they clearly introduce error if the reflection or diffraction phase lasts an appreciable time, for during that episode relief waves are moving into the region from the edges of the building as well as from the doorway itself causing rapid fluctuations in wind speed and pressure. (Some account is taken of changes in pressure during the diffraction episode by the standard techniques of estimating outside pressure.) Similar remarks can be made concerning regions ② and ③, but if we are content to deal with "average" pressure and speed in those two regions, we may apply the step-by-step isentropic analysis. However, our present methods do not provide for any apportionment of gaseous energy in region ③ between streaming kinetic energy and internal energy; for simplicity of calculation it will be treated as entirely internal at all times, which will cause overestimation of pressure and neglect of winds within the chamber. In evaluating the wind threat, the speed and dynamic pressure in the duct ② must be regarded as the upper bounds on wind speed and dynamic pressure in region ③. Later, methods will be given for estimating change in dynamic pressure as the wind moves into the room.

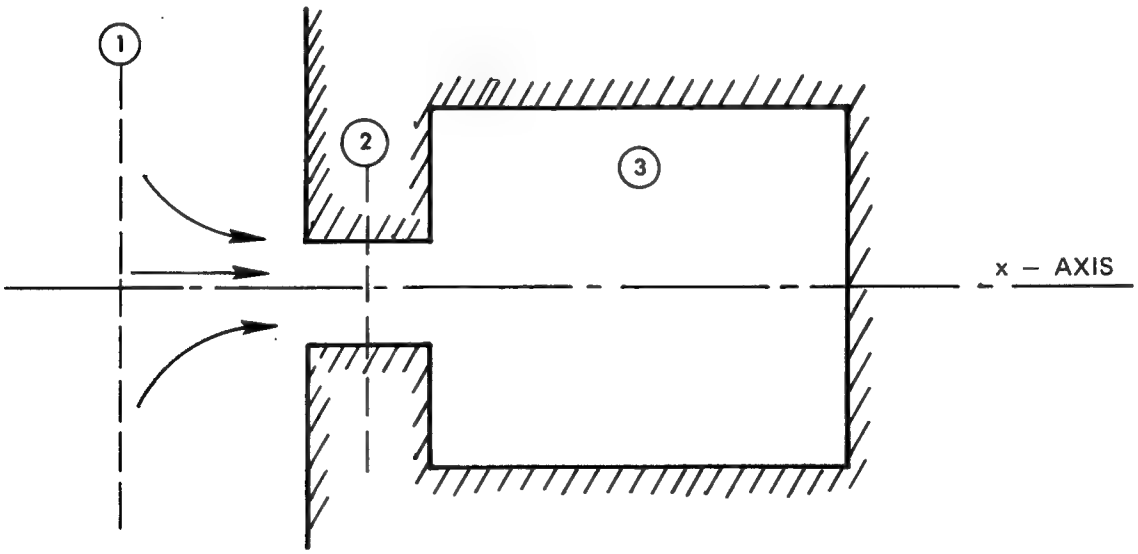

FIGURE E-2 THE FILLING CHAMBER

In writing the conservation equations, two views can be taken of conditions in region ①. On the one hand, pressure, density and wind speed may be those of the free field behind the blast front or, on the other hand, the air upstream of the opening may be treated as stagnate at a pressure above free field, either by the amount of the reflected pressure or by the amount of the product of the drag coefficient and dynamic pressure. Provided drag coefficients are known, the second view is more simply applied, especially when the blast front does not meet the wall head-on. In what follows, the pressure, P_1, and density, ρ_1, in region ① will be those of stagnate air outside the wall. The work done in moving a mass element Δm in region ① through a small distance Δx toward region ② is:

$$P_1 A_1 dx = P_1 \Delta V_1 = P_1 \cdot \frac{\Delta m}{\rho_1}$$

where A_1 is the cross sectional area, and ΔV is the volume occupied by Δm in region ①. The mass element carries with it the internal energy it had in region ①, i.e.,

$$\frac{1}{\gamma - 1} \cdot \frac{P_1}{\rho_1} \cdot \Delta m$$

where γ is the ratio of specific heat at constant pressure to the specific heat at constant volume. (The perfect gas equation of state is assumed; see Ref. 5.) If the flow into the room is steady, energy conservation requires that the same total energy, specifically, the sum

$$\frac{1}{\gamma - 1} \cdot \frac{P_1}{\rho_1} \cdot \Delta m + \frac{P_1}{\rho_1} \cdot \Delta m = \frac{\gamma}{\gamma - 1} \cdot \frac{P_1}{\rho_1} \cdot \Delta m$$

be given up within region ② during the same time interval. Furthermore, mass conservation asserts that the mass element moving through region ② toward region ③ equal Δm. The work done in region ② in pressing the mass element toward region ③ is

$$\frac{P_2}{\rho_2} \cdot \Delta m$$

and the internal energy in the element is

$$\frac{1}{\gamma - 1} \cdot \frac{P_2}{\rho_2} \cdot \Delta m$$

where the subscript 2 denotes conditions in region ②. Since the air is flowing into the room, however, the element in ② also carries (streaming) kinetic energy of amount

$$\frac{1}{2} u_2^2 \Delta m$$

where u designates particle or material speed. Thus, if conditions are not changing too fast, we can write (cancelling out the factor Δm):

$$\frac{\gamma}{\gamma - 1} \cdot \frac{P_1}{\rho_1} = \frac{\gamma}{\gamma - 1} \cdot \frac{P_2}{\rho_2} + \frac{1}{2} u_2^2 \qquad (1)$$

To apply conservation of linear momentum we consider a control surface, shown dashed in Figure E-3, enclosing an arbitrarily shaped volume outside the room and a portion of the entry duct (or doorway). Thus, a part of the control surface spans the duct throat where the air is moving rapidly into the room and consequently the air pressure P_2 is much lower

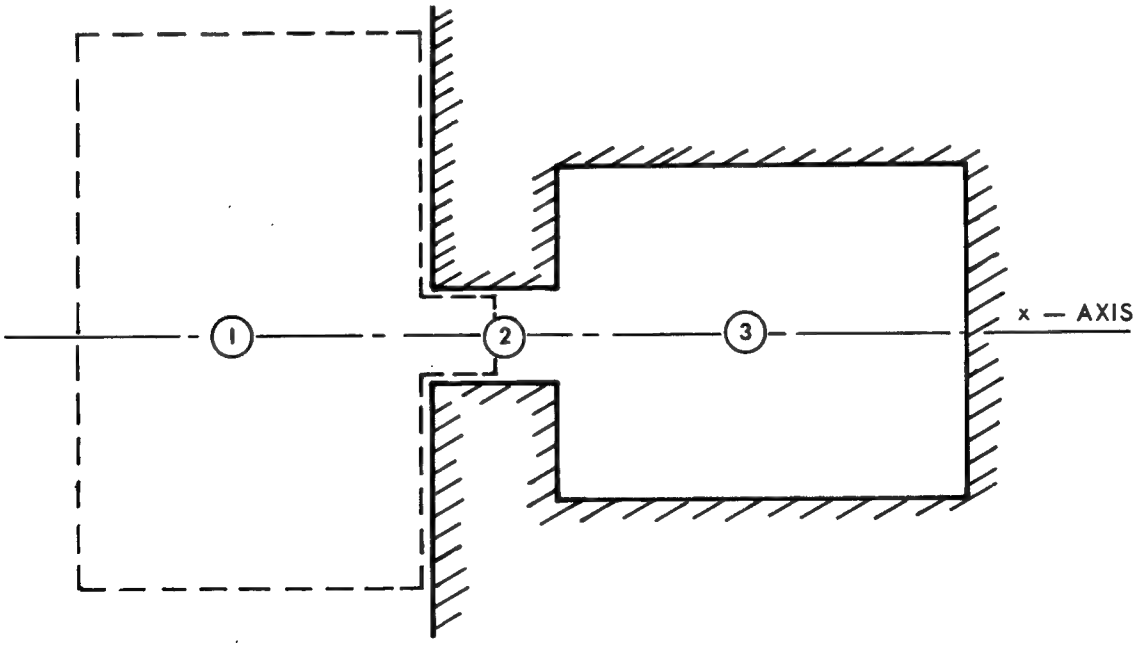

FIGURE E-3 FIRST CONTROL SURFACE

than the air pressure P_1 elsewhere within and on the control surface.* Newton's second law of motion states the net force in any direction on the air mass within the surface must equal the time rate of change of momentum in the same direction within the surface. Because of symmetry there is no net force in any but the x-direction; the net force (neglecting friction and viscous effects) in the x-direction is the difference between the high outside air pressure and the low duct air pressure integrated over the duct throat, i.e., the net force is:

$$\left(P_1 - P_2\right) A_2$$

This net force is balanced by a rate of change in momentum, which arises from two sources: (1) an acceleration of air within the control surface toward the open duct and (2) the high speed flow of air through the duct and out of the volume enclosed by the control surface altogether. After the initial diffraction of the shock wave through the doorway and after jet flow has been established into the room,† the second of these sources is the more important and we neglect the first in our calculation. The rate of flow of mass through the duct is:

$$\rho_2 \, u_2 \, A_2$$

hence, the rate of change of momentum (product of mass and speed) is:

$$\rho_2 \, u_2^2 \, A_2$$

Conservation of momentum (Newton's second law of motion) then implies:

$$\left(P_1 - P_2\right) A_2 = \rho_2 \, u_2^2 \, A_2$$

Canceling the factor A_2, we find:

$$P_1 - P_2 = \rho_2 \, u_2^2 \qquad (2)$$

---

* Pressure on the walls will be less than P_1, around the entrance to the duct, but the mass flow rate is not highly sensitive to corrections made for this effect; to simplify calculation, uniform pressure P_1 is assumed everywhere in 1. This assumption is conservative in assessing protective capability.

† See Section IIC.

Finally we note that, even in the presence of moderately strong or weak shocks, the isentropic equation of state of a perfect gas is accurate enough for this approximate calculation; hence,

$$\rho_2 = \rho_1 \left[\frac{P_2}{P_1}\right]^{1/\gamma} \tag{3}$$

(See Ref. 7).

Given P_1 and ρ_1, Eqs. (1), (2), and (3) may be solved for P_2, ρ_2, and u_2.* The result can be written as:

$$\frac{2\gamma}{\gamma + 1}\left[\frac{P_2}{P_1}\right]^{1/\gamma} = \frac{P_2}{P_1} + \frac{\gamma - 1}{\gamma + 1} \tag{4}$$

which is independent of ρ_1. If $y = \frac{P_2}{P_1}$, $A_o = \frac{\gamma - 1}{\gamma + 1}$

and $B = \frac{2\gamma}{\gamma + 1}$, Eq. (4) can be put in the form

$$By^{\frac{1}{\gamma}} = y + A_o \tag{5}$$

When A_o and B have the values stated above, Eq. (5) has two solutions one of which is y = 1 and the other is y = 0.1912. The second solution is the only one of interest here and will be designated y_o.

To continue the calculation ρ_1 must be known. This value can be found from the Rankine-Hugoniot relations and knowledge of the strength and angle of incidence of the original shock front (Ref. 1,2), or it can, with enough accuracy for incident shock strengths less than 15 psi, be computed from standard conditions† using the isentropic equation of state, i.e.,

---

* For diatomic gases like air, γ=1.4; see Ref. 8.

† Standard conditions (atmospheric) are defined in Table 6.1, Chapter 6, Volume 1 of the present work.

$$\rho_1 = \rho_o \left[\frac{P_1}{P_o}\right]^{1/\gamma} \tag{6}$$

where P_o and ρ_o are standard pressure and density, respectively. With ρ_1 known, air density and pressure in the opening can be calculated from:

$$\rho_2 = \rho_1 \, y_o^{\,1/\gamma} \tag{7}$$

$$P_2 = y_o \, P_1 \tag{8}$$

from which wind speed becomes:

$$u_2 = \left[\frac{P_1 - P_2}{\rho_2}\right]^{\frac{1}{2}} = \left[\frac{P_1 \, (1 - y_o)}{\rho_1 \, y_o^{\,1/\gamma}}\right]^{\frac{1}{2}} \tag{9}$$

The mass flow into the room (3) can be written

$$\Delta m = \rho_2 \, u_2 \, A_2 \Delta t$$

$$= \left[P_1 \, (1 - y_o) \, y_o^{\,\frac{1}{\gamma}} \, \rho_1\right]^{\frac{1}{2}} A_2 \, \Delta t \tag{10}$$

If V_3 is the volume of the room and the prime is used to denote conditions in the room at the beginning of time step Δt, then average density in the room ρ_3 at the end of Δt can be written as:

$$\rho_3 = \rho_3' + \frac{\Delta m}{V_3} \tag{11}$$

To find pressure in the room at the end of the time step we assume that all the energy lost in region (1) appears as an increase of internal energy of the gas in the room, i.e.,

$$\frac{\gamma}{\gamma - 1} \cdot \frac{P_1}{\rho_1} \cdot \Delta m = \frac{1}{\gamma - 1} \cdot \left(P_3 - P_3'\right) \; V_3$$

which can be solved to give P_3 in terms of known quantities:

$$P_3 = \frac{\gamma P_1}{\rho_1} \cdot \frac{\Delta m}{V_3} + P_3' \qquad (12)$$

At any time air temperature T_3 within the room can be calculated from the perfect gas law:

$$T_3 = \frac{P_3}{R\rho_3}$$

where R is the gas constant[5] for air in the appropriate units (e.g., in English units R = 2.329 Btu/slug-F). The quantity T_3 can reach high values as a result of the compression existing behind the shock and within the room; however, if airflow to the outside (outflow) is maintained, the relaxation of pressure following the passage of the front will return room gas temperatures to safe levels before injury to occupants is likely. Only the long-lasting increase in room temperature resulting from fires will normally be a threat to the shelterees.

Numerical Example No. 1 (Inflow by Method F). *The rate of pressure rise in a room of volume $V_3 = 15.0 \times 33.3 \times 8.0 = 4000$ cf containing openings into a single pressure field of total area $A_2 = 3 \times 7 = 21$ sf that faces side-on blast wave overpressure of 15 psi is calculated by taking the term P_3' to the left side of the Eq. (12) so that the equation reads:*

$$P_3 - P_3' = \frac{\gamma P_1}{\rho_1} \cdot \frac{\Delta m}{V_3}$$

Substituting for Δm, from Eq. (10) and dividing both sides by Δt, we find:

$$\frac{P_3 - P_3'}{\Delta t} = \frac{\gamma P_1}{\rho_1 V_3} \cdot A_2 P_1 (1-y_o) \rho_1 y_o^{1/\gamma} \, 0.5$$

In the limit of small Δt, this expression becomes the rate of pressure rise in the room, viz.,

$$\frac{P_3 - P_3'}{\Delta t} \rightarrow \frac{dP_3}{dt}$$

Assuming that ambient pressure before blast arrival is the standard value i.e., P_o = 14.7 psi, an outside overpressure of 15 psi means that

$$P_1 = 15 + 14.7 = 29.7 \text{ psi}$$

We approximate outside air density from Eq. (6) viz.:

$$\rho_1 = \rho_o \left[\frac{P_1}{P_o} \right]^{1/\gamma}$$

and (from Table 6.1 of Volume 1 of the present work) find the standard density of dry air at 14.7 psi and 59.0 F to be 0.002378 lb-sec^2/ft^4 (or slug/cf). Choosing this value as ambient (i.e., ρ_o), we calculate:

$$\rho_1 = 0.002378\ (29.7/14.7)^{1/1.4}$$
$$= 0.003930 \text{ lb-sec}^2/\text{ft}^4 \text{ (slug/cf)}$$

From page E-19

$$y_o = 0.1912$$

Hence, the initial rate of pressure increase in the room is:

$$\frac{dP_3}{dt} = \frac{1.4 \times 29.7}{0.00393 \times 4000} \left[29.7(1-0.1912)(0.1912)^{1/1.4}\ (0.00393)144. \right]^{0.5}_{21.}$$
$$= 231.5 \text{ psi/sec}$$

and this rate will remain constant as long as P_1 and ρ_1 are unchanging. If P_1 and ρ_1 do not change, then filling time ΔT becomes:

$$\Delta T = \frac{P_1 - P_o}{\frac{dP_3}{dt}} = \frac{15.0}{231.6} = 0.06476 \text{ sec}$$

$$= 64.8 \text{ ms}$$

An estimate by the simple method of Section IIA leads to a Value:

$$\Delta T = \frac{V}{2A} = \frac{4000}{2 \times 21} = 95.2 \text{ ms}$$

Conditions existing in the chamber at the beginning of a time step are used in the foregoing calculations only in Eqs. (11) and (12) and do not influence duct parameters because transients have been omitted from consideration. Transient phenomena, for example, determine the direction of flow; that is, if $P_1 > P_3$, flow is inward as discussed above, but otherwise flow is outward. Repeated neglect of signals originating from the room leads to an accumulation of error in the calculation of average pressure as can be seen from comparisons between calculation as above and measurement shown in Figures E-4, E-5, and E-6. The experiments[9] were carried out in a 24-inch shock tube; the configuration of each model chamber is shown in an inset in the figure; and the foregoing calculation produces Curve F of the figures. The curves in Figures E-5 and E-6 labelled "external history (A)" are measurements in the free stream by means of a pitot tube oriented with respect to the stream to conform with the orientation of the opening in the model room; "external history" in Figure E-4 is side-on overpressure in the unobstructed shock tube.[9] In each case the calculation initially yields pressure in agreement with observation but eventually shows room pressure during filling in excess of measurement, although the maximum difference is 20% or less. Magnitude of Δt for these calculations was one-quarter the transit time of a sound signal across the room.

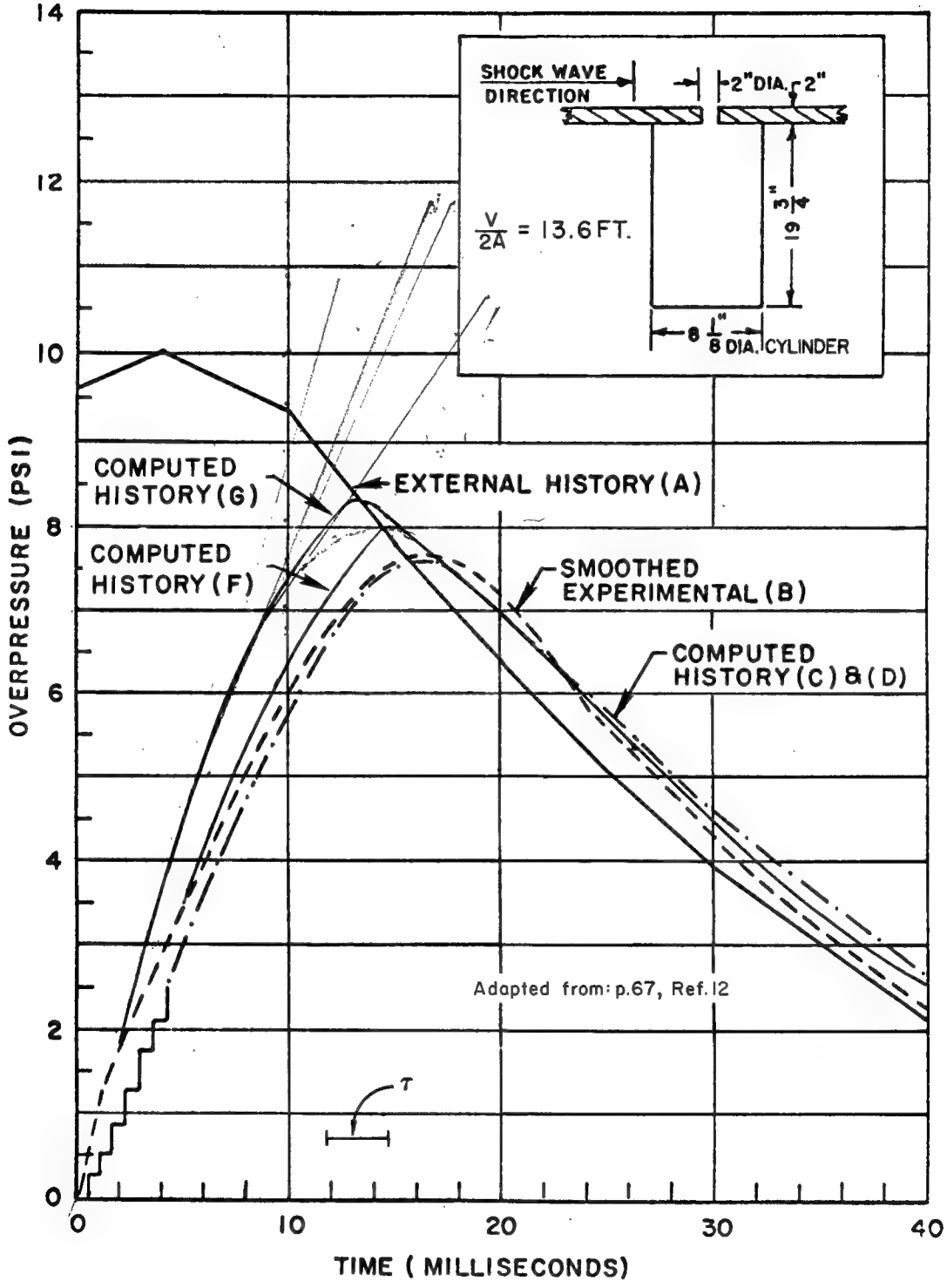

FIGURE E-4 FILL HISTORIES FOR SIDE-ON INCIDENCE

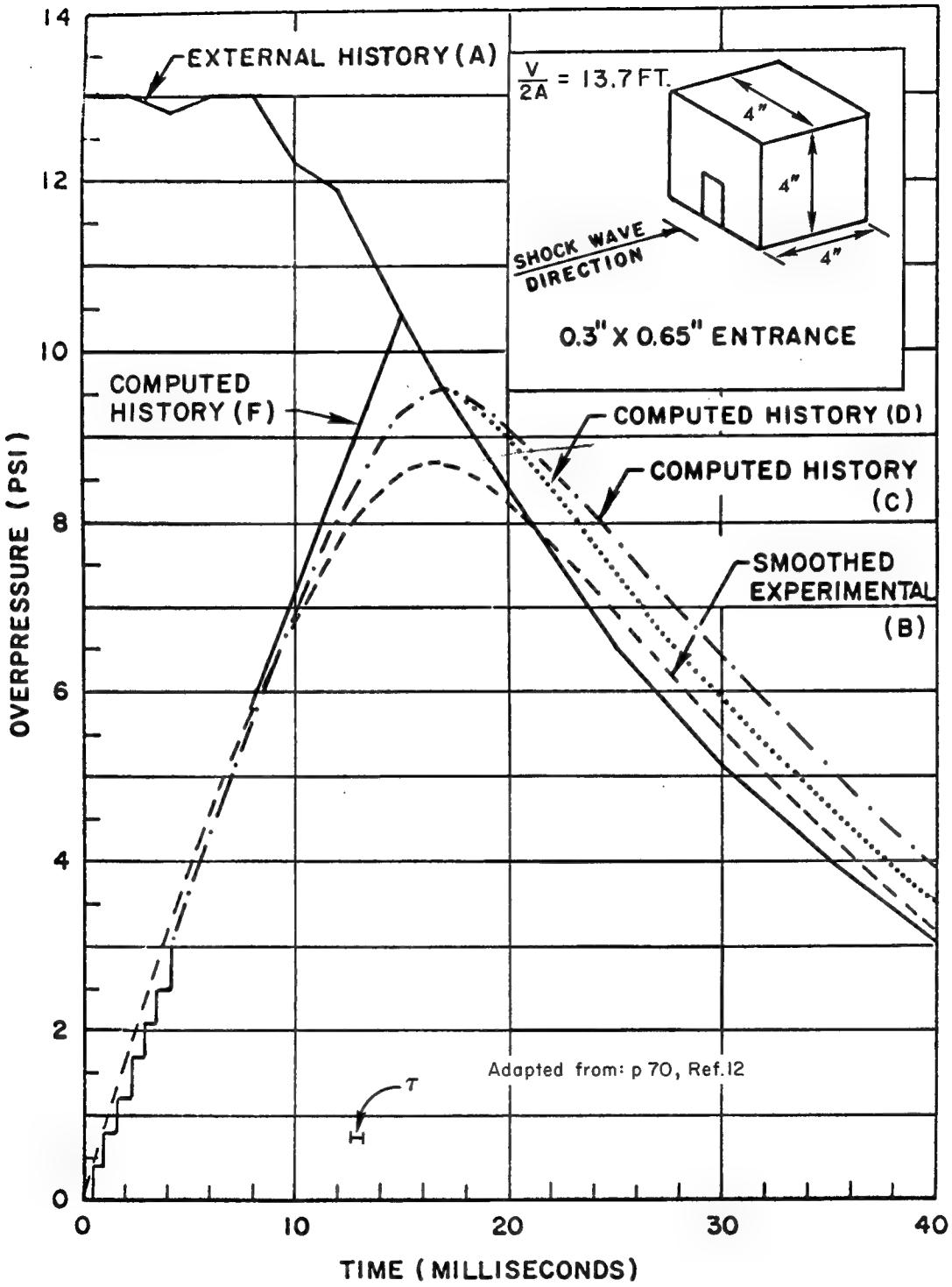

FIGURE E-5 FILL HISTORIES FOR A FACE-ON MODEL

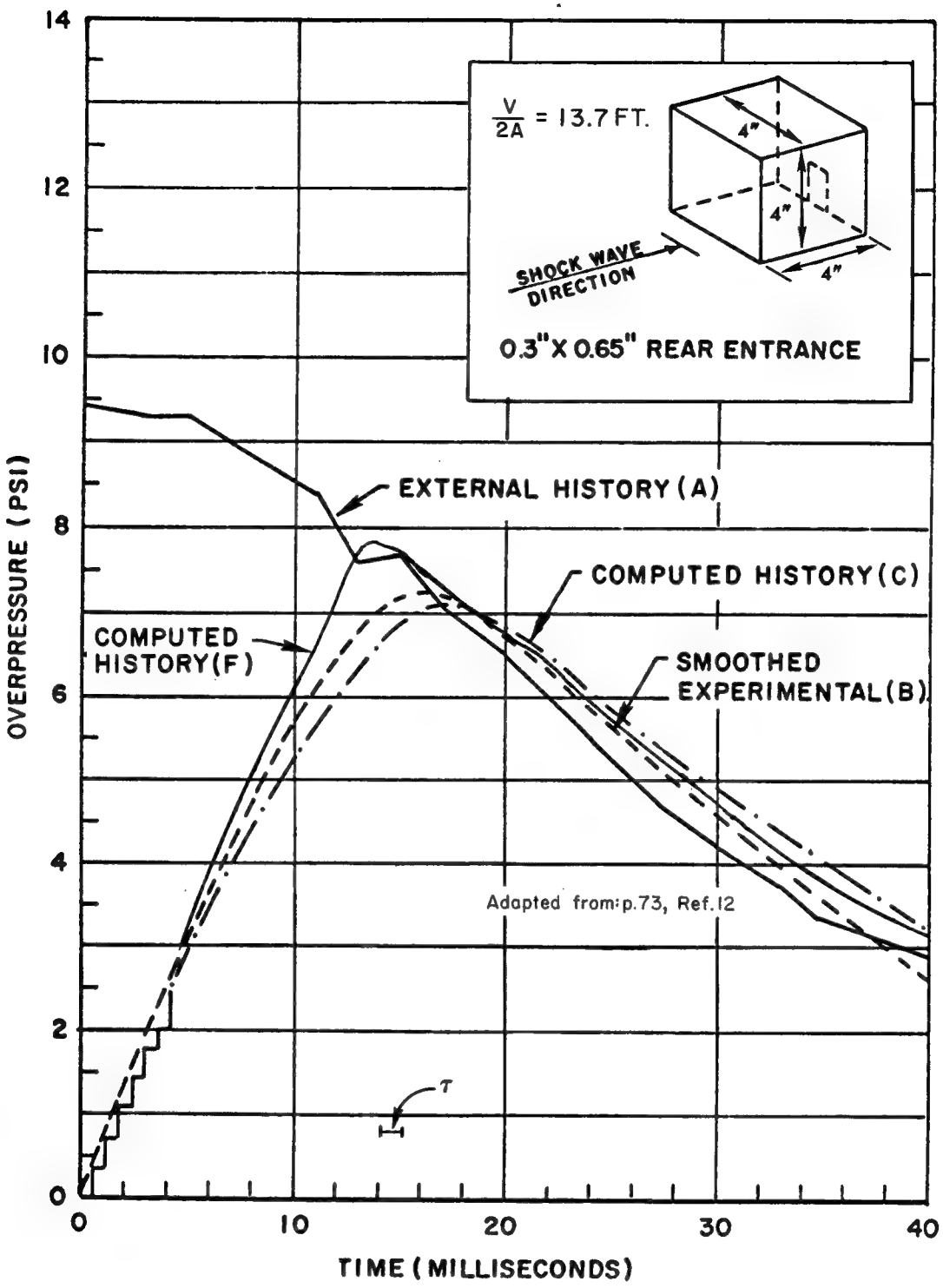

FIGURE E-6 FILL HISTORIES FOR A REAR FILL MODEL

Choice of the size of Δt is somewhat arbitrary except that (1) values much greater than sound transit time will give a false idea of the degree of irregularity in the fill process and (2) enough steps should be taken to make it possible for the influence of variations in P_1 to be shown in the results. The length of the bar labelled "τ" in Figures E-4, E-5, and E-6 represents the sound transit time across the longest room dimension.

A similar degree of comparison between calculation and measurement is found in the results shown in Figure E-8 stemming from a 27 cf model exposed to a large chemical explosion, except that the transient fluctuations associated with the entering shock front are more easily discerned in the larger model than in the small shock tube models. The parameter values used in the calculations summarized in Figure E-8 were:

$P_o = 13.58$ psia	ambient pressure
$\rho_o = 0.00209$ slug/cf	ambient density
$\gamma = 1.4$	ratio of specific heats
$A_2 = 0.821$ sf	area of opening
$V_3 = 27.0$ cf	volume of model room

The fraction of the impacted wall area occupied by the opening is slightly less than one-tenth.

From the results shown in Figures E-4, E-5, E-6, and E-8, some estimate can be made of the validity of the greatly simplified method of computing pressure rise in a filling room set forth in Section IIA. In each figure, the value of V/2A in feet has been entered. A constant pressure rise from zero time and zero overpressure to a pressure equal to outside pressure at a time equal to V/2A msec overestimates the fill pressure and underestimates the fill time in the small models but seems to give results in good agreement with both calculation and measurement in the three-foot cube model reported in Figure E-8, although the presence of important oscillations (caused by shock waves) in the pressure record in the large model makes clear assessment difficult. It should be noted also that the fraction of the wall struck by the blast that is occupied by the opening (opening fraction) is over 9 percent in the large model while only 1.2 percent in the small 4-inch cube models. The straight-line estimate explained in Section IIA would appear to be good also in Figure E-4 for which model size is intermediate and opening fraction is almost 6 percent.

The data from the models suggest that the simplified method of estimating pressure rise in a room, set forth in Section IIA, is adequate when outside pressure decay is slow as in a free-field nuclear blast wave. As will be noted later, when there exists an important diffraction phase in

the blast wave interaction with the structure, more sophisticated methods may be justified.

The existence of significant theoretical errors in our treatment of flow into a room by quasi-steady analysis is clearly revealed by considering the single control surface formed by superposition of that shown in Figure E-3 and that indicated with dashed lines in Figure E-7. Such a surface coincides with the inner surfaces of the room and passage and extends into quiescent air outside. Under our hypotheses there is no flow through this surface anywhere and no change of momentum within it, yet the surface integral of the x-component of pressure over the boundaries does not vanish.

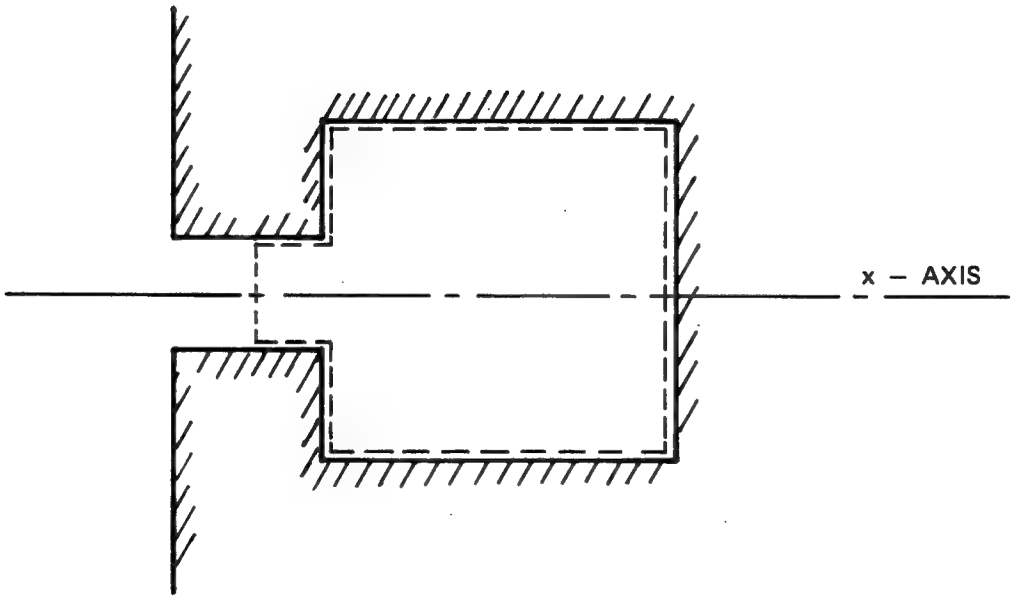

FIGURE E-7 SECOND CONTROL SURFACE

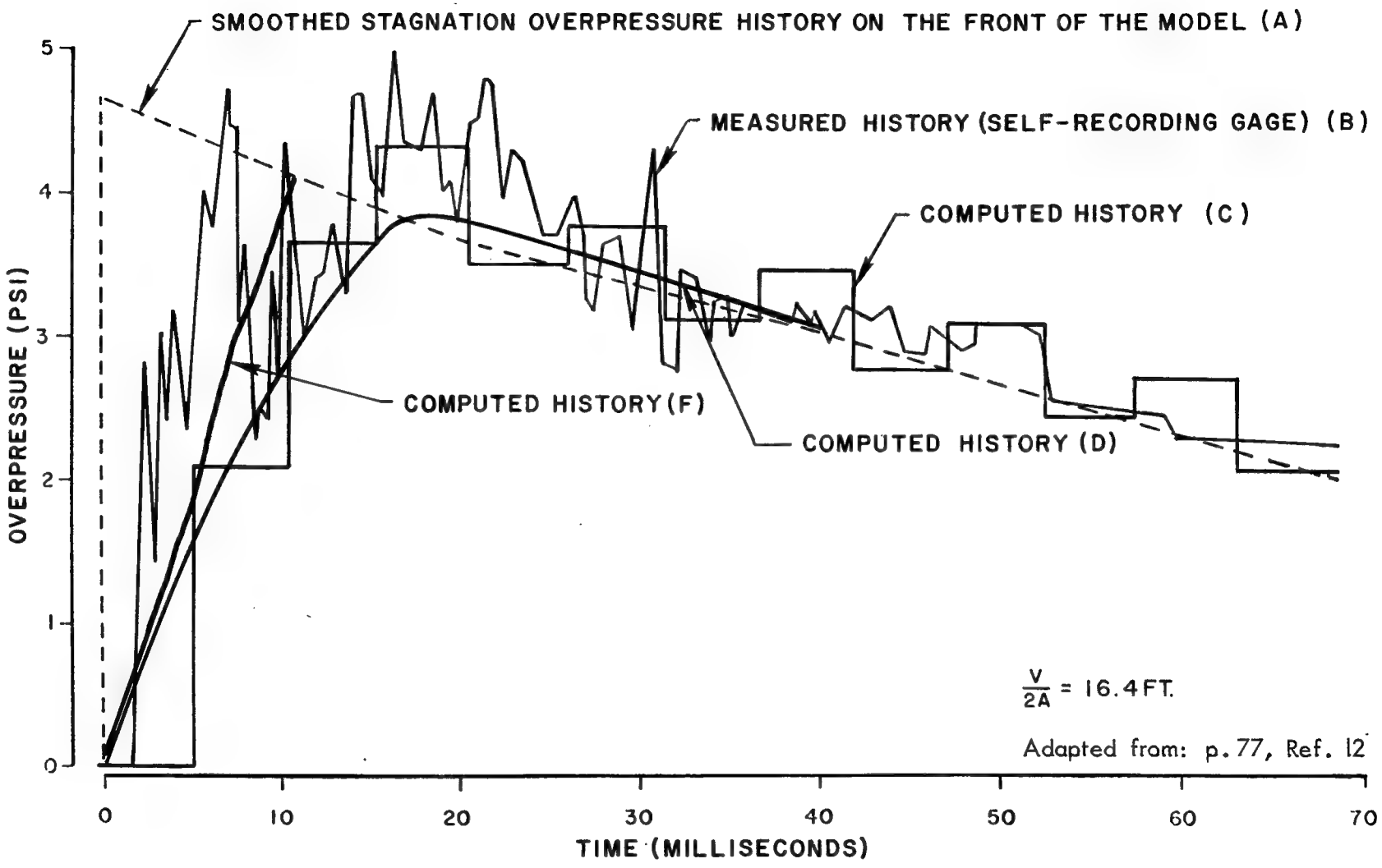

FIGURE E-8 COMPARISON OF THE COMPUTED VERSUS THE EXPERIMENTAL FILL HISTORY OF THE MODELED CHAMBER TESTED IN PROJECT DISTANT PLANE

This absurdity can be avoided in one or both of two ways. A term may be added to the right side of Eq. (2) to account for the changing flow pattern within the control surface shown in Figure E-3 or a term may be added to the left side of Eq. (2) to account for the possible nonuniformity of pressure over the boundaries of the surface. As the room begins to fill, a rarefaction wave moves back into the high pressure gas outside the first doorway bringing more and more gas into motion toward the opening. In other words, the neglect of the rate of change with time of the momentum within the control surface outside the room may be at least one cause of the contradiction noted above. Any attempt to calculate a correction for this effect would certainly add to the complexity of these simplified procedures; furthermore, the degree of agreement between observations and theory of Method F (shown in Figures E-4, E-5, and E-6) suggests that the added effort to account for the rarefaction wave may not be needed to achieve the desired degree of accuracy. Nevertheless, it is worthwhile to consider another method of estimating average pressure in a filling room.

Some writers[10,11,12,17] use the equation

$$P_2 = P_3' \tag{13}$$

instead of Eq. (2). Justification for Eq. (13) is based on analogy with the treatment of flow into a large chamber steadily being evacuated.[13] Equation (13) of course provides continual coupling between flow conditions and conditions in the room.

Using Eq. (13) we derive the pressure buildup inside the room in the following way. Substituting Eq. (3) into Eq. (1), then replacing P_2 with P_3' according to Eq. (13) and solving the resulting equation for u_2, we find:

$$u_2 = \left[\frac{2\gamma}{\gamma-1} \cdot \frac{P_1}{\rho_1} \left(1 - \left(\frac{P_3'}{P_1} \right)^{1-1/\gamma} \right) \right]^{1/2} \tag{14}$$

from which we calculate the mass inflow in the time increment Δt:

$$\begin{aligned} \Delta m &= K \rho_2 u_2 A_2 \Delta t \\ &= K \rho_1 \left(\frac{2\gamma}{\gamma-1} \cdot \frac{P_1}{\rho_1} \right)^{1/2} \left(\frac{P_3'}{P_1} \right)^{1/\gamma} \left[1 - \left(\frac{P_3'}{P_1} \right)^{1-1/\gamma} \right]^{1/2} A_2 \Delta t \end{aligned} \tag{15}$$

Whenever Eq. (13) is employed, empirical corrections are made to reduce the calculated inflow rate; the simplest correction is the discharge coefficient,[14] represented by the factor K in Eq. (15). Investigators at the IIT Research Institute[17] have found it necessary to use the value K=0.7 to reconcile computed pressure rises in small models with those measured; Curves D in Figures E-4 and E-5 have been produced by a calculation based on Eq. (13), with K=0.7 during inflow and K=1.00 during outflow.

The value of the discharge coefficient is usually discussed in connection with boundary layer thickness and the Reynolds number.[13] The relatively good agreement between the observed room pressures and Curves D was obtained in very small models, not in full-sized rooms. To estimate the influence of the value of K on calculated pressure rise, Curve G, based on the value of K=1.00 during both outflow and inflow, has been entered in Figure E-4. Presumably, the Reynolds number will be larger in the flow into full-sized rooms, and the discharge coefficient more nearly equal to 1.00 than in the flow into small models.

Finally, the pressure increment during the interval Δt is found by substitution of Eq. (15) into Eq. (12):

$$P_3 - P'_3 = K \gamma P_1 \left[\frac{2\gamma}{\gamma - 1} \cdot \frac{P_1}{\rho_1} \right]^{\frac{1}{2}} \left(\frac{P'_3}{P_1} \right)^{\frac{1}{\gamma}} \left[1 - \left(\frac{P'_3}{P_1} \right)^{1 - \frac{1}{\gamma}} \right]^{\frac{1}{2}} \frac{A_2 \, \Delta t}{V_3} \qquad (16)$$

Melichar[11,12] omits both the factors K and γ before the right-hand side of Eq. (16), which is equivalent numerically to making $K = 0.7$ and $\gamma = 1.4$. He attempts to justify this procedure on theoretical grounds unconnected with boundary layer theory.[12] Some of his numerical results are shown as Curves C in Figures E-4, E-5, E-6, and E-8. Melichar employs a value of Δt equal to the transit time of sound across the room.

Numerical Example No. 2 (Inflow by Method D). *We will apply Eq. (16) with K = 0.7 to the filling room considered in Numerical Example No. 1. The initial rate of pressure increase will be calculated by substituting* $P_3' = 14.7$ *psi,* $P_1 = 29.7$ *psi, and* $\rho_1 = 0.003930$ *slug/cf:*

$$\frac{dP_3}{dt} = 0.7 \times 1.4 \times 29.7 \left[\frac{2.8}{0.4}\,\frac{29.7\times144}{0.003930}\right]^{0.5} \left(\frac{14.7}{29.7}\right)^{1/1.4}$$

$$\times \left[1 - \left(\frac{14.7}{29.7}\right)^{1-1/1.4}\right]^{0.5} \frac{21}{4000} = 108.9 \text{ psi/sec}$$

Had we assumed K=1, then $\frac{dP_3}{dt} = 155.5$ *psi/sec*

Thus the initial pressure rise calculated under the assumptions $P_2 = P_3'$ *and* $K \leq 1$ *is lower than the rate calculated in the previous numerical example by Method F. However, the rate by Eq. (16) is not constant; it falls slowly from its initial value, so that in the conditions postulated in these examples Method F forecasts a markedly shorter fill time than does Eq. (16).*

Pursuing the analogy between room filling and steady flow into a chamber held at constant pressure, we expect to encounter the phenomenon of choking as the ratio of room pressure to outside pressure drops below the critical value.[13] Choking limits the rate at which mass flows into the room; hence, when inflow is choked, the rate of pressure rise dP_3/dt and wind speed u_2 in the entry will be limited.

For a given set of reservoir conditions, i.e., for each pair of values P_1 and ρ_1, the critical pressure ratio is that for which isentropic flow into the room achieves the maximum mass rate and for which the flow speed equals local sound speed. Therefore, to find this critical ratio, we can differentiate Eq. (15) with respect to P_3'/P_1, set the result equal to zero, and solve for $(P_3'/P_1)_{crit}$, which yields:

$$\left(\frac{P_3'}{P_1}\right)_{crit.} = \left(\frac{2}{\gamma+1}\right)^{\frac{\gamma}{\gamma-1}}$$

For every value of P_3' below the critical value as given above, mass flow into the room will be that obtained by substituting the critical ratio into Eq. (15), i.e.:

$$(\Delta m)_{choked} = K\left[\gamma\ \rho_1\ P_1\left(\frac{2}{\gamma+1}\right)^{\frac{\gamma+1}{\gamma-1}}\right]^{\frac{1}{2}} A_2\ \Delta t \qquad (17)$$

Because the mass flow rate is limited in this way independently of the value of P_3' it is called "choked" flow. Flow obeying Eq. (15) is called "unchoked" or "subsonic." Numerically, when $\gamma = 1.4$ the critical ratio equals 0.5283; thus, assuming ambient pressure is 14.7 psia,* the critical outside pressure is

$$\frac{14.7}{0.5283} = 27.83 \text{ psia or } 13.13 \text{ psig}$$

In none of the experiments reported in Figures E-4, E-5, and E-6 did peak overpressure rise above 13.13 psig; hence, according to the foregoing theory, choked flow should not have occurred.

Numerical Example No. 3 (Choked Inflow). *When inflow is choked, Eq. (17) replaces Eq. (15). Rate of pressure rise dP_3/dt is then found by substituting Eq. (17) into Eq. (12) and the wind speed u_2 is found by substituting into Eq. (14) the critical pressure ratio $(P_3/P_1)_{crit}$ as shown in the numerical example that follows.*

Consider a 4000-cf room filling side-on from a 20 psi overpressure blast wave through an opening 21 sf in area. Since the incident overpressure is greater than critical, viz., 13.13 psig, inflow is choked, and Eq. (17) applies until the difference between inside and outside pressures falls below critical.

The initial rate of pressure rise within the room depends on the following values:

$\gamma = 1.4$

$P_1 = 14.7 + 20 = 34.7$ psi

$K = 0.7$

$A_2 = 21$ sf

---

* Pounds per square inch, absolute.

Outside air density ρ_1 can be approximated by using the isentropic equation of state, Eq. (6), and standard conditions:

$$\rho_1 = \rho_o \left(\frac{P_1}{P_o}\right)^{1/\gamma} = 0.002378 \left(\frac{34.7}{14.7}\right)^{1/1.4}$$

$$= 0.004397 \text{ slugs/cf}$$

(According to p. 3.49 of Ref. 1 the air density ρ_1 behind a shock front of overpressure equal to p moving through air at pressure P_o and density ρ_o is:

$$\rho_1 = \rho_o \frac{7P_o+6p}{7P_o+p}$$

Substituting the values given, for ρ_o and P_o, we calculate:

$$\rho_1 = 0.002378 \frac{7\times14.7 + 20\times6}{7\times14.7 + 20}$$

$$= 0.004313 \text{ slug/cf}$$

Thus, the approximation based on the isentropic equation of state, Eq. (6), is only 2% higher than the correct value 0.004313 slug/cf.)

We now know everything necessary to compute the initial rate of pressure increase within the room. From Eqs. (17) and (12):

$$\frac{\Delta m}{\Delta t} = 0.7 \left[1.4 \times 0.004313 \times 34.7 \times 144 \left(\frac{2}{1.4+1}\right)^{\frac{1.4+1}{1.4-1}}\right]^{0.5} 21$$

$$\frac{dm}{dt} = 46.73 \text{ slug/sec}$$

Rewriting Eq. (12) in differential form:

$$\frac{dP_3}{dt} = \frac{\gamma P_1}{\rho_1 V_3} \frac{dm}{dt}$$

we calculate:

$$\frac{dP_3}{dt} = \frac{1.4 \times 34.7 \times 46.73}{0.004313\times4000} = 131.6 \text{ psi/sec}$$

Assuming P_1 remains constant, we can find the time $\Delta T'$ required to fill the room to the extent that flow is no longer choked as follows:

$$\Delta T' = \frac{20-13.13}{131.6} = 0.05220 \text{ sec}$$

$$= 52.0 \text{ ms}$$

After time $\Delta T'$, inflow is no longer choked and further pressure increase is calculated in time steps by Eq. (16) as follows:

We assume P_3' is constant during a small time increment Δt = 5 ms and, noting that P_3' = 20-13.13+14.7 = 21.57 psia, we calculate from Eq. (16):

$$P_3 = P_3' + 0.7 \times 1.4 \times 34.7 \left[\frac{2\times1.4}{0.4} \cdot \frac{34.7 \times 144}{.004313}\right]^{0.5} \left(\frac{21.57}{34.7}\right)^{1/1.4}$$

$$\times \left[1 - \left(\frac{21.57}{34.7}\right)^{1-1/1.4}\right]^{0.5} \quad \frac{21 \times .005}{4000}$$

$$P_3 = 21.57 + 0.6451 = 22.215 \text{ psig}$$

The calculation is now repeated with P_3' = 22.215 and a new value of P_3 found, which becomes P_3' in the next time step. The procedure is repeated until $P_3 > P_1$, at which time the room is considered filled.

For the case of choked inflow, Eq. (17), the simple estimate in Section IIA of rate of pressure rise and of filling time ΔT may be theoretically justified as follows.[24] Combining Eqs. (12) and (17), we find

$$\frac{P_3-P_3'}{\Delta t} = \frac{dP_3}{dt} = \frac{\gamma P_1}{\rho_1 V_3}\frac{dm}{dt} = \frac{A_2 K \gamma}{V_3}\left(\frac{P_1}{\rho_1}\right)^{1.5} P_1^{0.5}\left(\frac{2}{\gamma+1}\right)^{\frac{\gamma+1}{2(\gamma-1)}} \tag{18}$$

If P_1 remains constant and the inflow remains choked during most of the filling time, then

$$\Delta T \approx \frac{P_1-P_o}{\frac{dP_3}{dt}} = \frac{V_3}{KA_2}\frac{1}{\gamma}1.5\left(\frac{\gamma+1}{2}\right)^{\frac{\gamma+1}{2(\gamma-1)}}\left(\frac{\rho_o}{P_o}\right)^{0.5}\left(\frac{P_o}{P_1}\right)^{0.5}\left(\frac{P_1}{P_o}\right)^{\frac{1}{2\gamma}}\left(1-\frac{P_o}{P_1}\right)$$

Taking P_o = 14.7 psi, ρ_o = 0.002378 slugs/cf, γ = 1.4 and K = 1, we find the factor

$$\frac{1}{K\gamma^{1.5}} \left(\frac{\gamma+1}{2}\right)^{\frac{\gamma+1}{2(\gamma-1)}} \left(\frac{\rho_o}{P_o}\right)^{0.5}$$

takes on the value

$$\frac{1}{1.0\ (1.4)^{1.5}} \quad (1.2)^{3.0} \left(\frac{0.002378}{14.7} \quad \frac{\text{lb-sec}^2}{\text{ft}^4} \ \frac{\text{in}^2}{\text{lb}} \quad \frac{\text{ft}^2}{144\ \text{in}^2}\right)^{0.5}$$

$$= 0.001105 \text{ sec/ft}$$

$$= 1.10 \text{ ms/ft}$$

Hence,

$$\Delta T \approx 1.10 \ \frac{V_3}{A_2} \left(\frac{P_o}{P_1}\right)^{0.5} \left(\frac{P_1}{P_o}\right)^{\frac{1}{2\gamma}} \left(1 - \frac{P_o}{P_1}\right) \quad \text{ms/ft}$$

Evaluating this expression numerically, we find that in the range

$$0.528 \geq \frac{P_o}{P_1} \geq 0.25$$

the variation of ΔT is within

$$\frac{1}{2.11} \ \frac{V_3}{A_2} \geq \Delta T \geq \frac{1}{1.48} \ \frac{V_3}{A_2}$$

It turns out that when the inflow is unchoked, the simple estimate in Section IIA for filling time ΔT can also be shown, as follows, to be approximately true, at least until

$$\frac{P_o}{P_1} \geq 0.8$$

Substitution of Eq. (15) into Eq. (12) results in the expression for rate of pressure rise.

$$\frac{dP_3}{dt} = \frac{P_1 A_2 K}{\rho_1 V_3} \gamma \left(\frac{2\gamma}{\gamma-1}\right)^{0.5} \left(\rho_1 P_1\right)^{0.5} \left(\frac{P_3}{P_1}\right)^{\frac{1}{\gamma}} \left[1 - \left(\frac{P_3}{P_1}\right)^{\frac{\gamma-1}{\gamma}}\right]^{0.5}$$

Substituting the isentropic equation of state, Eq. (6), we find:

$$\frac{dP_3}{dt} = \frac{A_2 P_o^{1.5} K}{V_3 \rho_o^{0.5}} \left(\frac{P_o}{P_1}\right)^{\frac{1-3\gamma}{2\gamma}} \left(\frac{P_3}{P_1}\right)^{\frac{1}{\gamma}} \left[1 - \left(\frac{P_3}{P_1}\right)^{\frac{\gamma-1}{\gamma}}\right]^{0.5} \quad (19)$$

When P_o is substituted for P_3 on the right-hand side, this becomes the expression for the initial rate of pressure rise; furthermore, if this rate is assumed constant (as seems to be nearly true from the experimental observations), then

$$\Delta T = \frac{P_1 - P_o}{\left(\frac{dP_3}{dt}\right)} = \frac{V_3}{A_2 K} \frac{1}{\gamma} \left(\frac{\gamma-1}{2\gamma}\right)^{0.5} \left(\frac{\rho_o}{P_o}\right)^{0.5} \frac{\left(\frac{P_o}{P_1}\right)^{\frac{3\gamma-1}{2\gamma}} \left(\frac{P_1}{P_o} - 1\right)}{\left[1 - \left(\frac{P_o}{P_1}\right)^{\frac{\gamma-1}{\gamma}}\right]^{0.5}}$$

Evaluating the factor

$$\frac{1}{K\gamma} \left(\frac{\gamma-1}{2\gamma}\right)^{0.5} \left(\frac{\rho_o}{P_o}\right)^{0.5}$$

using the values K = 1.0, $\gamma = 1.4$, $P_o = 14.7$ psi and $\rho_o = 0.002378$ lb-sec^2/ft^4 we can write:

$$\Delta T = \frac{1}{1.4}\left(\frac{0.4}{2.8}\right)^{0.5}\left(\frac{0.002378}{(14.7)(144)}\right)^{0.5}\frac{V_3}{A_2}\;\frac{\left(\frac{P_o}{P_1}\right)^{\frac{3\gamma-1}{2\gamma}}\left(\frac{P_1}{P_o}-1\right)}{\left[1-\left(\frac{P_o}{P_1}\right)^{\frac{\gamma-1}{\gamma}}\right]^{0.5}}$$

$$= 0.286\;\frac{V_3}{A_2}\;\frac{\left(\frac{P_o}{P_1}\right)^{\frac{3\gamma-1}{2\gamma}}\left(\frac{P_1}{P_o}-1\right)}{\left[1-\left(\frac{P_o}{P_1}\right)^{\frac{\gamma-1}{\gamma}}\right]^{0.5}}\quad \text{ms/ft}$$

Over the interval $0.528 \le P_o/P_1 \le 0.8$, the calculated filling time ΔT according to the above formula lies between two values, viz:

$$\frac{1}{2.10}\frac{V_3}{A_2} \ge \Delta T \ge \frac{1}{3.83}\frac{V_3}{A_2}$$

The rate of pressure rise during choked inflow is of course independent of room pressure, Eq. (18), but even when the inflow is or becomes unchoked the rate is only weakly dependent on room pressure P_3, as we see by evaluating the last two factors on the right side of Eq. (19), viz:

$$\left(\frac{P_3}{P_1}\right)^{\frac{1}{\gamma}}\left[1-\left(\frac{P_3}{P_1}\right)^{\frac{\gamma-1}{\gamma}}\right]^{0.5}$$

and plotting the result as a function of P_3/P_1 in Figure E-9 The figure shows that rate of pressure rise varies between limits of ±10% as long as P_3/P_1 is within the bounds: $0.2 < P_3/P_1 < 0.8$.

The equations, derived from quasi-steady analysis, neglect the inertia of the inflowing column of air; therefore, we might expect a tendency for the rate of pressure rise to continue at the level established earlier to compete with a tendency to fall as forecast by the equations.

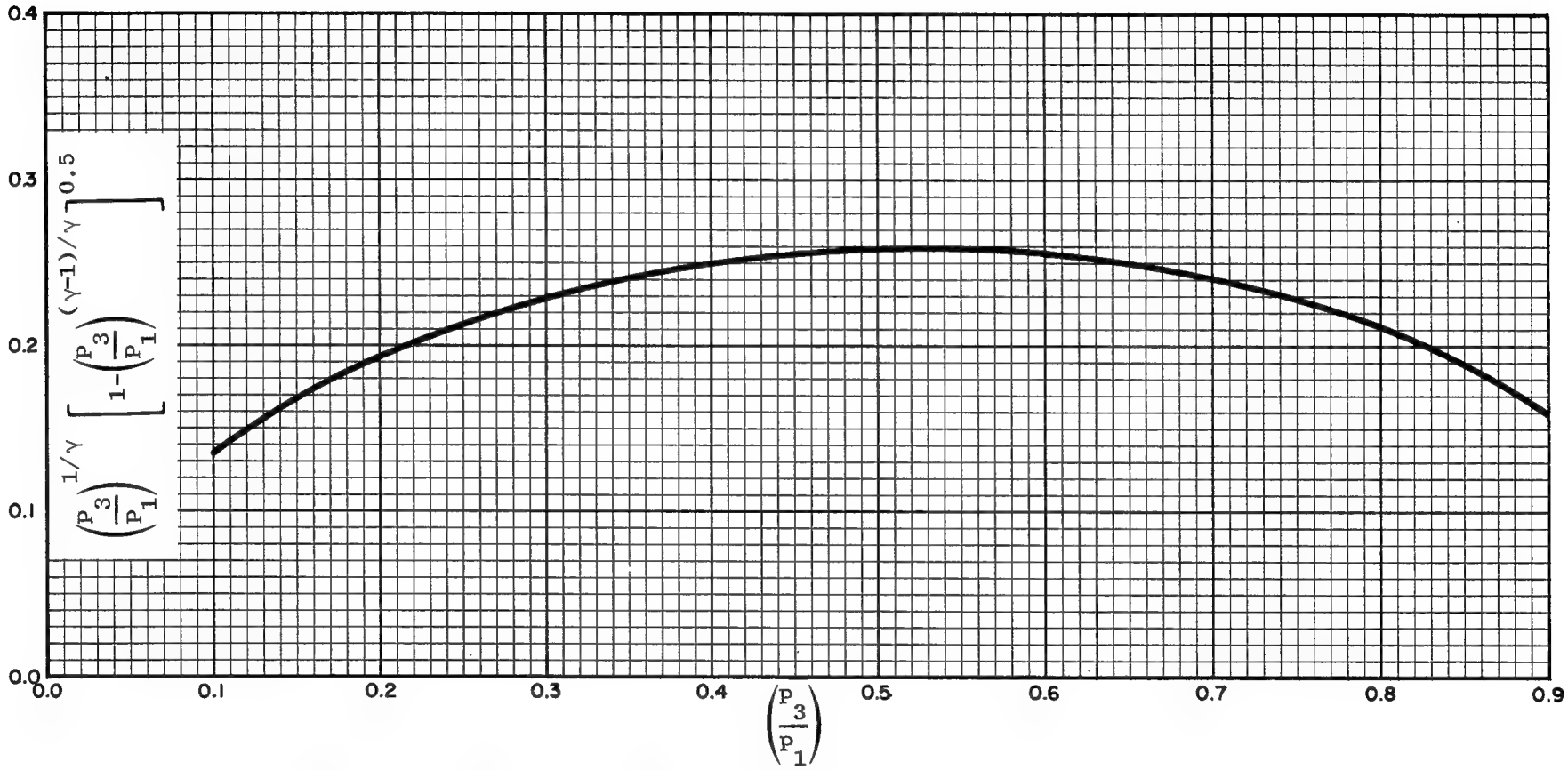

FIGURE E-9 VARIATION OF PRESSURE RATE DURING UNCHOKED FLOW (γ = 1.4)

Summary. Several distinct methods have been presented for estimating the rate of pressure rise in a room filling from a nuclear-induced air blast wave. All the methods are based on an analogy with steady flow in ducts and none applies to a room in which more than half of its exterior wall area is open to the blast. The simplest of the methods, given in Section IIA, demands only a knowledge of the room volume, the areas of the openings through which the blast enters, and the outside pressure against each opening during the filling. Should this outside pressure vary greatly during the filling, the methods of Section IIA will not in general be accurate.

A slightly more complicated method of calculating the rate of pressure rise takes into account the variation of outside pressure but not the resultant rise of inside pressure. This technique (Method F) uses Eqs. (9), (10) and (12). Despite their relative simplicity, both this method and the one outlined in Section IIA appear to give results in good agreement with observations in small and intermediate models.

The most sophisticated method of estimating rate of pressure rise within a room filling from an air blast and the wind speed in the entry comes from Eqs. (14), (16) and (17) (Method D) and makes use of the instantaneous pressures in the room and outside and requires the determination of whether the flow is choked as well as knowledge of an empirical discharge coefficient.

These methods are outlined in equation form in Section IIB3.

2. Outflow. All the experimental data discussed so far show that room pressure eventually exceeds outside pressure by a small amount. If all openings are into the same outside pressure field and if the fall of outside pressure is steady and slow, this "overshoot" is not likely to be of practical importance. However, as will be seen later, if a room has openings that are affected by different outside pressure histories, a significant outward pressure may develop on one or more walls of the room. To calculate this pressure, the rate of outflow of air through each opening must be found.

To compute inflow we treated the exterior atmosphere and the aperture leading into the room as parts of a system of ducts through which quasi-steady flow was maintained. Pressure increase within the room was computed as resulting from the transfer of mass and energy from the large outside reservoir into the room. Outflow may be treated in the same way, except that the direction of flow is reversed. For outflow, Eqs. (1) and

(2) still apply, but the air in the "duct" now originates in the room, and the adiabatic expansion law, Eq. (3), must be replaced by

$$\rho_2 = \rho_3' \left[\frac{P_2}{P_3'}\right]^{1/\gamma} \tag{20}$$

Equations (1), (2), and (20) can be combined to form an equation identical to Eq. (5) except that now

$$B = \frac{2\gamma}{\gamma + 1} \cdot \frac{\rho_3'}{\rho_1} \left[\frac{P_1}{P_3'}\right]^{1/\gamma} \tag{21}$$

But, as before,

$$y = \frac{P_2}{P_1} \quad \text{and} \quad A = \frac{\gamma - 1}{\gamma + 1} \tag{22}$$

In this form, Eq. (5) has two solutions in the range $0 \leq y \leq 1$ whenever $\gamma = 1.4$ and

$$\frac{\rho_3'}{\rho_1} \left[\frac{P_1}{P_3'}\right]^{1/\gamma} > 1$$

or

$$\frac{P_1}{\rho_1^{\gamma}} > \frac{P_3'}{\rho_3'^{\gamma}} \tag{23}$$

These two solutions merge into a single solution at $y = \left[\frac{B}{\gamma}\right]^{\frac{\gamma}{\gamma - 1}}$

if

$$\frac{P_1}{\rho_1^{\gamma}} = (0.9094) \frac{P_3'}{\rho_3'^{\gamma}}$$

Furthermore, if $\gamma = 1.4$, Eq. (5) has only one solution in the range of $0 \leq y \leq 1$ whenever

$$\frac{P_3'}{\rho_3'^{\gamma}} \geq \frac{P_1}{\rho_1^{\gamma}} > (0.9094) \frac{P_3'}{\rho_3'^{\gamma}} \tag{24}$$

Also, if

$$\frac{P_1}{\rho_1^{\gamma}} < (0.9094) \frac{P_3'}{\rho_3'^{\gamma}} \tag{25}$$

no solution to Eq. (5) exists.

Since the quantity P/ρ^{γ} is constant along an isentrope and increases with entropy, the truth of Inequality (25) implies that at the end of inflow specific entropy (i.e., entropy per unit mass) outside is less than approximately 0.9 the specific entropy within the room. Thus, in order to establish the existence of a solution to Eq. (5) during outflow, we must calculate the increase in specific entropy within the room during inflow and compare it with the increase in entropy through the shock front.

The increase in specific entropy in the room at any time during filling can be formally calculated as follows. First, we note that temperature of air in the room rises during the whole inflow period, as can be seen by treating Δm as a true differential and writing Eq. (12) as:

$$dP_3 = \frac{\gamma P_1}{\rho_1 V_3} \cdot dm$$

From the perfect gas law

$$P_3 = \frac{m_3 R T_3}{V_3},$$

where m_3 is the mass of air in the room, and R the gas constant for air, we write

$$dP_3 = \frac{R T_3}{V_3} \cdot dm + \frac{m_3 R}{V_3} \cdot dT_3$$

$$dP_3 = \frac{P_3}{m_3} \cdot dm + \frac{m_3 R}{V_3} \cdot dT_3 = \frac{\gamma P_1}{\rho_1 V_3} \cdot dm$$

Noting that $m_3 = \rho_3 V_3$ and collecting terms, we find

$$\frac{1}{V_3}\left[\frac{\gamma P_1}{\rho_1} - \frac{P_3}{\rho_3}\right] dm = \frac{m_3 R}{V_3} \cdot dT_3$$

Multiplying both sides of the equation by V_3/R and using the perfect gas law in the form $P/(R\rho) = T$, we find the following relation between inside and outside temperatures during filling:

$$\left[\gamma T_1 - T_3\right] \quad dm = m_3 \quad dT_3 \tag{26}$$

Clearly, at the start of filling $T_1 > T_3$; hence, at the start $dT_3 > 0$. Moreover Eq. (26) shows that T_3 can increase above T_1 while $dm > 0$ until T_3 approaches γT_1. Thus as temperature outside (T_1) falls due to the adiabatic relaxation behind the shock front, inflow and rising inside temperature continue.

Second, we can find a simple relation between the actual temperature increase within the room and a temperature increase in an isentropic process resulting in the same density increase.

In an isentropic process involving a certain mass of ideal gas the quantity $\rho/T^{1/(\gamma-1)}$ is constant; or taking differentials,

$$\frac{d\rho}{\rho} = \frac{dT}{\gamma T - T}$$

Rewriting Eq. (26) as

$$\frac{dm}{m_3} = \frac{dT_3}{\gamma T_1 - T_3}$$

then dividing (left-side) numerator and denominator by V_3 and noting that density $\rho_3 = m_3/V_3$, we find

$$\frac{d\rho_3}{\rho_3} = \frac{dT_3}{\gamma T_1 - T_3}$$

In other words the process of room filling during the time period t to t + dt results in a temperature increase dT_3 that bears the relation

$$\frac{dT_3}{(dT_3)_{\text{isentropic}}} = \frac{\gamma T_1 - T_3}{\gamma T_3 - T_3}$$

to the temperature increase in an isentropic process providing the same density increase. When $T_1 > T_3$, $\dfrac{dT_3}{(dT_3)_{\text{isentropic}}} > 1$

Finally, the entropy increase within the room is calculated from the specific heat at constant volume (or density).

$$dS = \frac{c_v\, dT}{T}$$

where c_v is specific heat at constant volume. If we imagine a return to the isentrope (after an increment of filling) by a process at constant density or volume, the specific entropy change within the room resulting from the filling increment becomes

$$dS_3 = \frac{c_v}{T_3} \left[dT_3 - (dT_3)_{\text{isentropic}} \right]$$

or,

$$dS_3 = \frac{c_v \gamma}{T_3} \left[\frac{T_1 - T_3}{\gamma T_1 - T_3} \right] dT_3 \qquad (27)$$

which on substitution of the quantity dT_3 from Eq. (26), becomes

$$dS_3 = \frac{c_v \gamma}{T_3 m_3} (T_1 - T_3) dm \qquad (28)$$

Therefore, during inflow (i.e., when $dm > 0$) specific entropy within the room will increase until $T_3 = T_1$ or $P_3 = P_1$, whichever occurs first.

Because of the passage of the shock front, air outside has greater than normal specific entropy. Hence, initially before inflow begins

$$\frac{P_1}{\rho_1^{\gamma}} > \frac{P_3}{\rho_3^{\gamma}}$$

however, Eq. (28) shows that the inflow process, according to the theory applied here, creates entropy within the room. Should enough entropy be so created, Inequality (25) may eventually be satisfied and solution of the outflow equations presented here may be impossible. The rise in specific entropy within the room as a result of inflow is:

$$\Delta S_3 = c_v \gamma \int_{t=0}^{P_3 = P_1} \frac{T_1 - T_3}{T_3 m_3} \frac{dm}{dt}\, dt$$

where t = time and T_1, T_3, and m_3 are functions of time. From Eq. (26) we know that T_3 rises asymptotically toward γT_1 until $P_1 = P_3$; thus, T_3 may be larger than T_1. For a given function $P_1(t)$ [which determines $T_1(t)$, $T_3(t)$, and $m_3(t)$], the maximum specific entropy within the room will be reached when

$$T_3 = T_1$$

If we assume that at this time inflow is still under way, then

$$P_1 > P_3$$

which implies, when $\gamma > 1$, that

$$P_1^{1-\frac{1}{\gamma}} > P_3^{1-\frac{1}{\gamma}}$$

or

$$P_1^{\frac{1}{\gamma}-1} < P_3^{\frac{1}{\gamma}-1}$$

Now from the equality of the temperatures at this time, the perfect gas law implies

$$\frac{P_1}{\rho_1} = \frac{P_3}{\rho_3}$$

Multiplying both sides by the last inequality above, we find

$$\frac{P_1}{\rho_1}^{1/\gamma} < \frac{P_3}{\rho_3}^{1/\gamma}$$

or

$$\frac{P_1}{\rho_1^{\gamma}} < \frac{P_3}{\rho_3^{\gamma}}$$

Hence, in general, the possibility may not be ruled out that Inequality (25) will be satisfied. Whether the outflow equations as presented here have a solution will depend on the nature of the function $P_1(t)$. If outflow is to be calculated, then to provide an initial disparity between specific entropy outside and inside, the inflow period must be treated using the initial density behind the shock front and computed from the Hugoniot relation:[1]

$$\rho_{1o} = \rho_o \frac{(\gamma+1)P_{1o} + (\gamma-1)P_o}{(\gamma-1)P_{1o} + (\gamma+1)P_o} \qquad (29)$$

Subsequent outside air densities may be calculated from the adiabatic law:

$$\rho_1 = \rho_{1o}\left[\frac{P_1}{P_{1o}}\right]^{1/\gamma} \tag{30}$$

In Eqs. (29) and (30), ρ_{1o} and P_{1o} refer to the air density and absolute pressure immediately behind the shock front. When peak pressure at an opening is reached by reflection of an incident shock wave from a wall, Eq. (30) is not correct regardless of whether P_{1o} is taken as peak incident absolute pressure or peak reflected absolute pressure, but the error in using Eq. (30) is small. We will arbitrarily consider ρ_{1o} and P_{1o} as representing conditions behind the free-field shock front. Use of Eqs. (29) and (30) may make it possible to satisfy the reverse of Inequality (25).

The outflow method discussed above and contained in Eqs. (5), (21) and (22) is analogous to Method F discussed in Section IIB1 for inflow. Should Inequality (25) be satisfied; other calculational methods must be used for the outflow phase, such as that proposed by Melichar[11,12] or that reported by IIT Research Institute.[17] These methods equate duct pressure P_2 with outside pressure during outflow; the IIT investigators then fit observed outflow pressure data by choosing values for the discharge coefficient and for the ratio of inside to outside pressure at the time of flow reversal. These methods are analogous to Method D discussed under Inflow in Section IIB1 and are treated in detail in the next subsection as a part of Method D.

3. Outline of Hand Calculation.* In constructing from the foregoing equations a calculational scheme for estimating the parameters of flow into and out of a single room with a single opening we start with a series of values of P_1, one for each time step. These may be obtained by linear interpolation from a given table of outside pressure as a function of time and each value should pertain to the center of the time interval. The size of the time interval, Δt, itself is arbitrary, but it should be no greater than the quantity τ; presumably up to a limit, greater accuracy results from smaller values of Δt. The size of Δt may be changed during the calculation when the rate of change of flow parameters changes. We also need values for ambient pressure P_o and density ρ_o.

* If the outside pressure is the result of a classical nuclear blast wave, the computer program described in Section V will perform this calculation.

As a general rule, Δt may be chosen to be one-tenth of γ. Certain tests incorporated into the calculation below will indicate when the value of Δt must be reduced.

Two methods of calculation are shown below. The first is that used to produce Curves F in Figures E-4, E-5, E-6, and E-8, namely, that based on Eqs. (1), (2) and (3) for inflow or Eqs. (1), (2) and (30) for outflow, and in the outline below it is called Method F. This method has the advantage of great simplicity and of not requiring knowledge of empirical constants; however, as will be explained later, values of wind speed and dynamic pressure computed by it are subject to doubt in some cases and for that reason a method given by IIT Research Institute is included also. The latter (and our second) method is responsible for Curves D in the Figures E-4, E-5, and E-8 and, therefore, in the outline below it is called Method D. As noted earlier, Method D for the unchoked flow case is numerically equivalent to the calculation used by Melichar[11,12] (Curves C in Figures E-4, -5, -6 and -8).

Average pressure inside a room and dynamic pressure in the single opening to an outside reservoir whose pressure variation in time is known may be calculated as functions of time by the sequential application of the steps stated below. Each cycle through a series of steps completes the calculation for one time interval. The first three steps are executed only during the first cycle; subsequent passes begin with step (4), as indicated in the outline. Step (5) is a branch point to separate sequences for inflow and outflow, chosen according to a criterion given in step (5). There are further branches: (a) to Method D or F, chosen at the discretion of the user at each time; and (b) under Method D to choked or unchoked flow, determined by stated criteria. Throughout the outline, the quantity γ has been set equal to 1.4.

(1) Set $P_3' = P_o$ and $\rho_3' = \rho_o$ and $t = 0$.

(2) Compute

$$\rho_{1o} = \rho_o \frac{6P_{1o} + P_o}{P_{1o} + 6P_o}$$

where P_{1o} is the absolute pressure immediately behind the shock front, and ρ_{10} is the associated air density.

(3) Choose value of Δt (see opening paragraph of this Section IIB3).

(4) Determine outside pressure at the current time; i.e., determine P_1, from the known reservoir pressure history (pressure variation with time). During first time interval $P_1 = P_{1o}$.

If the current value of P_1 differs from the immediately preceding value by more than 5% of itself, return time value to previous step (i.e., subtract Δt from current time), reduce Δt by half, and repeat preceding pass through this outline

(5) Determine direction of flow; i.e., if $P_1 > P_3'$, flow is inward; go to step (6). Otherwise flow is outward; go to step (28).

Inflow

(6) Compute

$$\rho_1 = \rho_{1o}\left[\frac{P_1}{P_{1o}}\right]^{0.7143}$$

Branch to selected Method below for step number (7D) (Method D) or step (7F) (Method F).

Method D (Inflow)

(7D) If $P_3'/P_1 \leq 0.5283$ inflow is choked; go to step (8D). Otherwise inflow is unchoked; go to step (18D).

Choked Inflow

(8D) $$\Delta m = K\left[1.4\,\rho_1 P_1 \left(\frac{2}{2.4}\right)^{\frac{2.4}{0.4}} F^*\right]^{1/2} A_2\,\Delta t$$

$$= 0.6847\ K\ [\rho_1 P_1 F]^{1/2} A_2\,\Delta t$$

Using the recommended value[17] of K = 0.70 this becomes

$$\Delta m = 0.4793\,[\rho_1 P_1 F]^{1/2} A_2\,\Delta t$$

The quantity A_2 is the sum of the areas of all openings into the pressure P_1.

(9D) $P_2 = P_3'$

(10D) $$\rho_2 = \rho_1\left[\frac{P_2}{P_1}\right]^{0.7143}$$

* The factor F is often necessary for consistency of units. For example, if u_2 is in ft/sec and P_1 is in lb/in^2 and ρ_1 in lb/cf, then F = 32. X 144. = 4,608.

(11D) $$u_2 = \frac{\Delta m}{\Delta t\, A_2 \rho_2 K}$$

(12D) $$P_3 = P_3' + 1.4 \frac{P_1}{\rho_1} \frac{\Delta m}{V_3}$$

(13D) Go to step (23D)

Unchoked Inflow

(18D) $$P_2 = P_3'$$

(19D) $$\rho_2 = \rho_1 \left[\frac{P_2}{P_1}\right]^{0.7143}$$

(20D) $$u_2^2 = 7 \left[\frac{P_1}{\rho_1} - \frac{P_2}{\rho_2}\right] F$$

(21D) $$\Delta m = \rho_2 u_2 A_2 \Delta t$$

(22D) $$P_3 = P_3' + 1.4 \frac{P_1}{\rho_1} \frac{\Delta m}{V_3}$$

If $\left|P_3 - P_3'\right| > .05\, P_3'$ return to immediately preceding time (i.e., subtract Δt from current time), reduce Δt by one-half, and return to step (4).

(23D) $$\rho_3 = \rho_3' + \frac{\Delta m}{V_3}$$

(24D) If desired, dynamic pressure, q_2, in the opening can be found from:

$$q_2 = \frac{1}{2} \frac{1}{A_2^2 \rho_1} \left(\frac{\Delta m}{\Delta t}\right)^2 \frac{1}{F} \left(\frac{P_1}{P_3'}\right)^{1/\gamma}$$ (See Section IIC)

(25D) $$P_3' = P_3$$

(26D) $\rho_3' = \rho_3$

(27D) Advance time by amount Δt and return to step (4).

Method F (Inflow)

(7F) $P_2 = 0.1912\ P_1$

(8F) $\rho_2 = \rho_1 \left[\frac{P_2}{P_1}\right]^{0.7143} = 0.3067\ \rho_1$

(9F) $u_2^2 = 7 \left[\frac{P_1}{\rho_1} - \frac{P_2}{\rho_2}\right] F = 2.637 \left[\frac{P_1}{\rho_1}\right] F$

(10F) $\Delta m_3 = u_2\ \rho_2 A_2\ \Delta t = 0.498\ (P_1\ \rho_1 F)^{1/2}\ A_2 \Delta t$

(11F) $P_3 = P_3' + 1.4\ \frac{P_1}{\rho_1}\ \frac{\Delta m_3}{V_3}$

(12F) $\rho_3 = \rho_3' + \frac{\Delta m_3}{V_3}$

(13F) If desired, the dynamic pressure, q_2, in the doorway can be calculated:

$$q_2 = \frac{1}{2A_2^2\rho_1} \left(\frac{\Delta m}{\Delta t}\right)^2 \frac{1}{F} \left(\frac{P_1}{P_3'}\right)^{1/\gamma}$$ (See Section IIC)

(14F) $\rho_3' = \rho_3$

(15F) $P_3' = P_3$

(16F) Advance time by amount Δt and return to step (4).

Outflow

(28) Branch to selected Method below for step (29D) (Method D) or step (29F) (Method F).

Method D (Outflow)

(29D) If $P_1/P'_3 \leq 0.5283$, outflow is choked; go to step (30D). Otherwise outflow is unchoked; go to step (39D).

Choked Outflow

(30D) $$\Delta m = -0.6847\ K\ [\rho'_3 P'_3 F]^{1/2}\ A_2 \Delta t$$

Using the recommended value[17] K = 1.0 for outflow this becomes

$$\Delta m = -0.6847\ [\rho'_3\ P'_3\ F]^{1/2}\ A_2 \Delta t$$

(31D) $$P_2 = P_1$$

(32D) $$\rho_2 = \rho'_3 \left[\frac{P_2}{P_1}\right]^{0.7143}$$

(33D) $$u_2 = \frac{\Delta m}{\Delta t\ A_2\ \rho_2\ K}$$

(34D) $$P_3 = P'_3 + 1.4\ \frac{\Delta m}{V_3}\ \frac{P'_3}{\rho'_3}$$

(35D) $$\rho_3 = \rho'_3 + \frac{\Delta m}{V_3}$$

(36D) $$P'_3 = P_3$$

(37D) $$\rho'_3 = \rho_3$$

(38D) Advance time by amount Δt and return to step (4).

Unchoked Outflow

(39D) $$P_2 = P_1$$

(40D) $$\rho_2 = \rho'_3 \left[\frac{P_2}{P'_3}\right]^{0.7143}$$

(41D) $$u_2^2 = 7 \left[\frac{P_1}{\rho_1} - \frac{P_2}{\rho_2}\right] F$$

(42D) $\Delta m = -\rho_2 \, u_2 \, A_2 \, \Delta t$

(43D) $P_3 = P_3' + 1.4 \dfrac{\Delta m}{V_3} \dfrac{P_3'}{\rho_3'}$

If $P_3 - P_3' > .05 \, P_3'$ return to immediately preceding time (i.e., subtract Δt from current time), reduce Δt by one-half, and return to step (4).

(44D) Go to step (35D)

Method F (Outflow)

(29F) If $P_1/\rho_1^{\gamma} < (0.9094)(P_3'/\rho_3^{\gamma})$, Method F cannot be used. Go to step (29D).

(30F) $B = \dfrac{7}{6} \dfrac{\rho_3'}{\rho_1} \left[\dfrac{P_3'}{P_1} \right]^{0.7143}$, $\qquad A = \dfrac{\gamma-1}{\gamma+1}$

(31F) Solve $By^{0.7143} = y + A$ for y.

(32F) $P_2 = yP_1$

(33F) $\rho_2 = \rho_3' \left[\dfrac{P_2}{P_3'} \right]^{0.7143}$

(34F) $\Delta m = -\rho_2 \, u_2 \, A_2 \, \Delta t$

(35F) $P_3 = P_3' + 1.4 \dfrac{P_1}{\rho_1} \dfrac{\Delta m}{V_3}$

If $P_3 - P_3' > .05 \, P_3'$ return to immediately preceding time (i.e., subtract Δt from current time), reduce Δt by one-half, and return to step (4).

(36F) $\rho_3 = \rho_3' + \dfrac{\Delta m}{V_3}$

(37F) $P_3' = P_3$

(38F) $\rho_3' = \rho_3$

(39F) Advance time by amount Δt and return to step (4).

C. Wind Speed and Dynamic Pressure (Jet Effect)

Should it become clear the shelter structure will withstand the pressure stemming from the shock wave and filling of interior spaces, interest will shift to the dynamic effects on the shelter contents of the filling stream itself, i.e., on the wind speed and, particularly, the dynamic pressure within the jet of air moving into the shelter space.

Unfortunately, direct measurements of wind speed and dynamic pressures in rooms filling from shock waves are even fewer than observations of room pressure. The differences among the predictions of speed of the several calculational methods are large, but the values of dynamic pressure are often in fair agreement. For estimates of the acceleration of objects in the stream, the dynamic pressure and wind direction are the only pertinent parameters.

1. Quantitive Description. Our recommended procedures for estimating dynamic pressures within a room consist of two parts: (1) calculation of core dynamic pressure, viz., that immediately inside the entry, and (2) quantitative description of the spread of the jet through the room.

Since the calculation of average pressure rise within the room are reasonably successful, especially by Methods D and F, our recommended procedures for estimating core dynamic pressure are derived from expressions for mass flow. Specifically, we define core dynamic pressure as

$$q_{core} = \frac{1}{2} \rho_{core} u_o^2$$

where ρ_{core} is air density in the jet core and u_o is wind speed just inside the entry. Now if we assume the core of the incoming jet just fills the doorway, we can express the mass rate of flow as:

$$\frac{\Delta m}{\Delta t} = \rho_{core} u_o A_2$$

After rearrangement, this becomes:

$$u_o = \frac{1}{\rho_{core} A_2} \left(\frac{\Delta m}{\Delta t}\right) \qquad (25)$$

Substituting this expression for u_o in the defining equation for core dynamic pressure, we find:

$$q_{core} = \frac{1}{2\rho_{core} A_2^2} \left(\frac{\Delta m}{\Delta t}\right)^2 \qquad (26)$$

Air density in the jet core is related to air density outside the room by the isentropic equation of state, Eq. (3), in which P_2 and ρ_2 are replaced by P_{core} and ρ_{core}, respectively.

Thus,

$$\rho_{core} = \rho_1 \left(\frac{P_{core}}{P_1}\right)^{1/\gamma} \tag{27}$$

However, it is a good approximation to assume*

$$P_{core} = P_3 \tag{28}$$

i.e., core pressure equals room pressure.

Substituting Eqs. (27) and (28) into Eq. (26), we find:

$$q_{core} = \frac{1}{2\rho_1 A_2^2} \left(\frac{P_1}{P_3}\right)^{1/\gamma} \left(\frac{\Delta m}{\Delta t}\right)^2 \tag{29}$$

Thus any of our previously developed expressions for mass flow rate $\Delta m/\Delta t$ (cf. Eqs. (10), (15), or (17) can be used in Eq. (26) to compute core dynamic pressure q_{core}. This calculation is not exact, because the area of the core will not in fact equal A_2, particularly when outside pressure is high (viz., inflow is choked according to Method D).

For information on the spread and attenuation of the jet within the room, we have relied on the steady jet characterized in such detail by Ambramovich[20] and illustrated in Figure E-10, where air is considered to be flowing from a reservoir at high pressure on the left through the aperture into the region of low pressure (i.e., the interior of the shelter) on the right. In the theory, the entry aperture may be slit of essentially infinite length and width b_o or it may be a circular opening of diameter b_o. Although the description of the jet is different for the slit than for the circle, the difference is not important here. Since most actual openings will be somewhere between the two, we assume that any actual opening has been approximated by a slit or by a circle and only one set of formulas is given. As shown in Figure E-10, inflowing air generally fans out into the receiving reservoir, slowing down after passing through a conical or wedge-shaped "core." Wind speed is constant everywhere within the core. The jet consists of the core and the surrounding fan, known as the mixing zone.

---

* It is also a good approximation at low overpressures to assume $\rho_{core} = \rho_3$.

Abramovich characterizes the jet by three parameters: width of the opening b_o; wind speed u_o in the axial direction at the initial cross section of the jet; and ratio θ between temperature in the core and that in the receiving reservoir (i.e., the shelter space). The flow is driven by a pressure difference between the two reservoirs, but it appears to be a fact that pressure everywhere within the usual subsonic jet itself is uniform and equal to that in the receiving reservoir. In other words, pressure equilibrium is quickly established between the jet and the air already in the reservoir. In most cases of room filling the ratio θ will be nearly 1, which implies that air density in the jet core nearly equals air density in the room; i.e.,

$$\rho_{core} \approx \rho_3$$

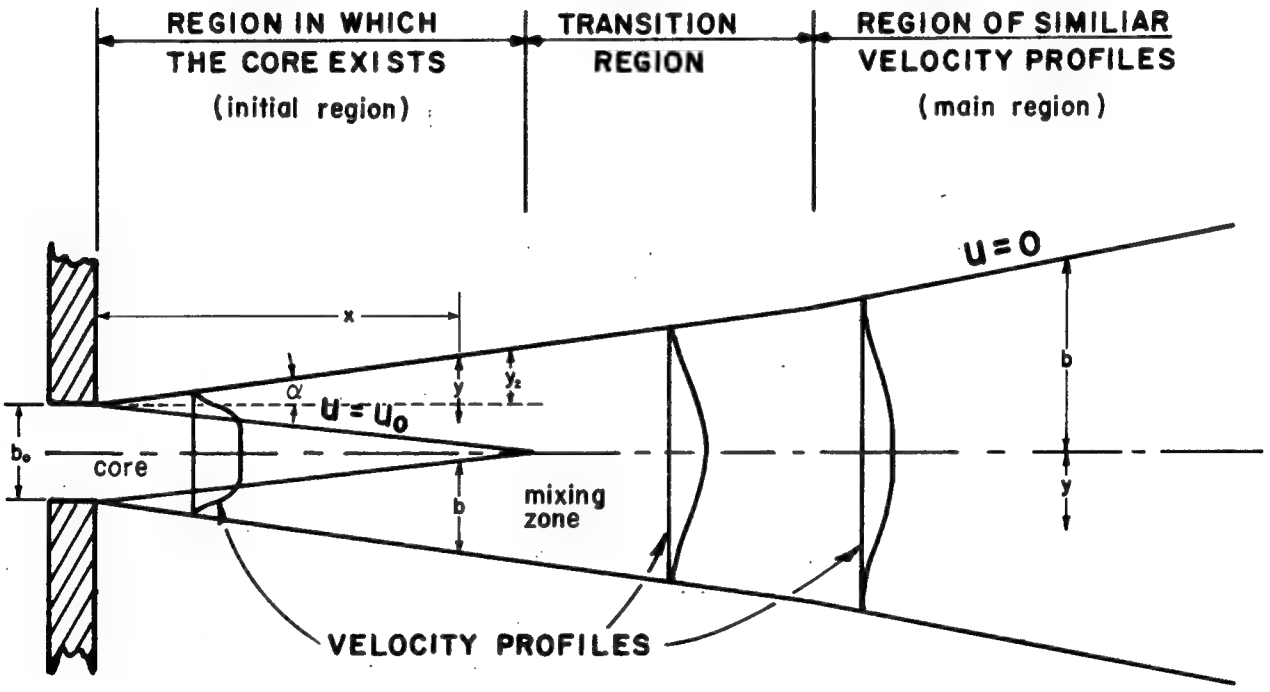

Source: Ref. 20

FIGURE E-10 SCHEMATIC OF JET FLOW

The description appearing below of the fully developed jet hinges on the value u_o of wind speed in the core, and calculations of the translation of objects on shelter floors by incoming air are based on values of q_{core} along with estimates of drag acceleration coefficients, as described further in Section IIC1. As in the treatment in Section IIB1 of the build-up of pressure within the shelter space, the parameters of the jet are here calculated quasi-statically. This procedure fails in the early stages and again in the late stages of room filling.

Before quasi-steady jet behavior is observed, air motion in the neighborhood of the opening is governed by the laws of shock waves. At that time, particle speed is relatively slow but as the diffracted waves reverberate in the opening, conditions for jet-like flow are established. This build-up of flow through the opening lasts a length of time

$$t_1 \approx \frac{4b_o}{c} \tag{30}$$

where c is the speed of sound in the opening. If this time interval is long enough to be important, it is recommended that mass flow rate in the opening be treated as varying linearly with time during t_o, from an initial value equaling that behind the incident shock:

$$\frac{\Delta m}{\Delta t} = \rho_s u_s A_2 = \rho_s \left(P_s - P_o\right)^{1/2} \left(\frac{1}{\rho_o} - \frac{1}{\rho_s}\right)^{1/2} A_2 \tag{31}$$

to that in the fully developed jet at time t_1. In Eq. (31) the subscript s designates conditions behind the incident shock, which may not be the same as conditions in the stagnated air outside the shelter, i.e., in that volume of air designated (1) in Figure E-3. This method of interpolating between shock or transient conditions and true quasi-steady conditions is used in the room filling computer program described in Section IVA.

The cessation of jet inflow at the conclusion of room filling shows a similar inertia. In confined spaces, inflow tends to establish a swirling pattern, which persists even after pressure equilibrium is reached between inside and outside environments.

The fully developed steady subsonic jet is described by the following three sets of formulas, each set valid in one of the three regions shown in Figure E-10. Only wind speed in the axial direction is calculated, since the horizontal speed exerts a comparatively negligible drag force.

Initial Region. The speed u in the mixing zone outside the core decreases with increasing distance from the core. At the jet boundary u = 0 and at the core boundary u = u_o. At a point in any plane at right angles to the jet axis and within the mixing zone

$$u = u_o \left\{1 - \left[1 - \eta^{1.5}\right]^2\right\} \qquad (32)$$

where $\eta = y/b$, y is the distance from the jet boundary (measured in a direction perpendicular to the jet axis) to any point outside the core, and b is the mixing zone half width also measured perpendicularly to the axis, both as shown in Figure E-10 (e.g., at the core boundary y = b and at the jet boundary y = 0). The quantity b varies linearly with distance x from the opening, i.e.,

$$b = 0.27x \qquad (33)$$

or, equivalently, the slope of the outer jet boundary (where u = 0) can be written

$$\tan \alpha = 0.158 \quad \text{or} \quad \alpha \approx 9^\circ$$

the length of the initial region (and the length of the core) is approximately $4.5b_o$.

Transition Region. Formulas valid for the transition region can be written, but they are not necessary for present purposes. If desired, values of quantities in this region may be interpolated between the initial and main regions. The length of the transition region, however, may be required and is approximately $2.2b_o$.

Main Region. Here, as in the transition region, there is no core: The jet is entirely mixing zone but the slope of the jet boundary is greater than in the initial region, i.e.,;

$$\alpha \approx 12.5^\circ$$

and the half-width of the jet is:

$$b = x \tan \alpha \approx 0.22\, x \qquad (34)$$

In any cross section of the jet made normal to its axis, wind speed is a maximum at the axis and falls to zero at the jet boundary. However, wind speed u_m along the axis decreases with distance from the opening;

$$u_m = u_o \frac{6.2 b_o}{x}$$

Now the variation in any cross section at a distance $y < b$ from the axis is:

$$u = u_m \left(1 - \eta^{1.5}\right)^2$$

where $\eta = y/b$ as shown before, except that y and b have slightly different meanings (Figure E-10). Hence, the dependence on both x and y is found by combining the last two expressions:

$$u = u_o \frac{6.2 b_o}{x} \left(1 - \eta^{1.5}\right)^2 \qquad (35)$$

Since density is nearly uniform throughout the jet, we can relate the dynamic pressure in the main region to that in the core by multiplying core dynamic pressure by the square of the ratio of wind speeds:

$$q = q_{core} \left(\frac{6.2 b_o}{x}\right)^2 \left(1 - \eta^{1.5}\right)^4 \qquad (36)$$

Numerical Example No. 4 (Jet Dynamic Pressure). Consider the room described in the numerical example of choked inflow on page E- 33. We will calculate the furthest extent of the jet core, the initial core dynamic pressure and the initial dynamic pressure in the established jet at a point 25 ft inside the door and 5 ft off the center line through the door.

Shock arrival at the door is followed by the diffraction phase, during which time the jet emerging from the doorway into the room is

established. If we consider the door as approximately circular, its radius will be

$$b_o \approx \left(\frac{21}{\pi}\right)^{0.5} = 2.58 \text{ ft.}$$

Since its area is 21 sf. to calculate the period of jet buildup using Eq. (30), we need a value for sound speed in the doorway, where initially the pressure is intermediate between that outside and that inside. As an approximation we can base our value of sound speed on initial conditions in the room (viz., pressure P_o = 14.7 psi and density ρ_o = 0.002378 slugs/cf) and apply the formula on page 10-38 of Ref. 5 viz.,

$$c = \left(\frac{\gamma P_o}{\rho_o}\right)^{0.5} = \left(\frac{1.4 \times 14.7 \times 144}{0.002378}\right)^{0.5}$$

$$= 1116. \text{ fps}$$

Thus $$t_1 = \frac{4 \times 2.58}{1116} = 0.00914 \text{ sec}$$

Since the duration of choked inflow is 52.0 ms (which is greater than t_1) the initial mass inflow rate after establishment of the jet will be (from Numerical Example No. 3):

$$\frac{dm}{dt} = 46.7 \text{ slug/sec}$$

and from Eq. (29) the initial core dynamic pressure becomes:

$$q_{core} = \frac{(46.7)^2}{2 \times 0.004397 \times (21)^2 \times 144} \left(\frac{34.7}{14.7}\right)^{1/1.4}$$

$$= 7.21 \text{ psi}$$

This core pressure reaches approximately

$$4.5\, b_o = 4.5 \times 2.58 = 11.6 \text{ ft}$$

in the room along the jet axis. Immediately following the core is the transition region extending a distance $2.2\, b_o = 2.2 \times 2.58 = 5.68$ ft

further into the room. The main region of the jet begins, then, at a point 11.6 + 5.68 = 17.3 ft inside the doorway. On the jet axis (y = o) at a distance 25 ft from the door x = 25 and Eq. (36) gives the dynamic pressure as:

$$q = 7.21 \left(\frac{6.2 \times 2.58}{25}\right)^2 = 2.96 \text{ psi.}$$

The half width of the mixing zone at this distance from the door is by Eq. (34):

$$b = 0.22 \times 25 = 5.5 \text{ ft}$$

so that at a point 5 ft off the axis $\eta = \frac{5}{5.5} = 0.909$ *and Eq. (36) gives the dynamic pressure as:*

$$q = 2.96 \left[1 - (0.909)^{1.5}\right]^4$$
$$= 0.000936 \text{ psi} \approx 0.0$$

2. Countermeasures Against the Jet. Obstacles to flow, such as corners or barriers, may be found in a shelter or can be deliberately designed into the structure. Coulter[21] has reportedly increased protection against the threat of the jet by placing a simple baffle inside the doorway to a small model of a shelter space, as illustrated in Figure E-11. Entry barriers or mazes certainly have the effect of increasing the duration of the diffraction phase, viz., the time during which the jet is building up to full intensity. Thus, if the driving pressure is of short duration or is rapidly decreasing, the average intensity of the jet flowing into the shelter can be reduced by the presence of a barrier at the entry. When the weapon yield is very small, i.e., a few kilotons, and peak overpressure larger than 1 psi, the delay in establishment of the jet resulting from the presence of a baffle or maze may have a measurable effect on the jet, but durations of moderate overpressures (1 to 15 psi) caused by megaton weapons are so long that the relatively brief delays offered by simple baffles are of little use in reducing the jet hazard. Another feature of baffles or mazes is the additional wall friction that might impede jet flow. Generally, to make friction effective at the high Reynolds numbers usually found in cases of blast room-filling, the length of constrained flow must be so great as to leave little space for shelter, as we shall see later in this section.

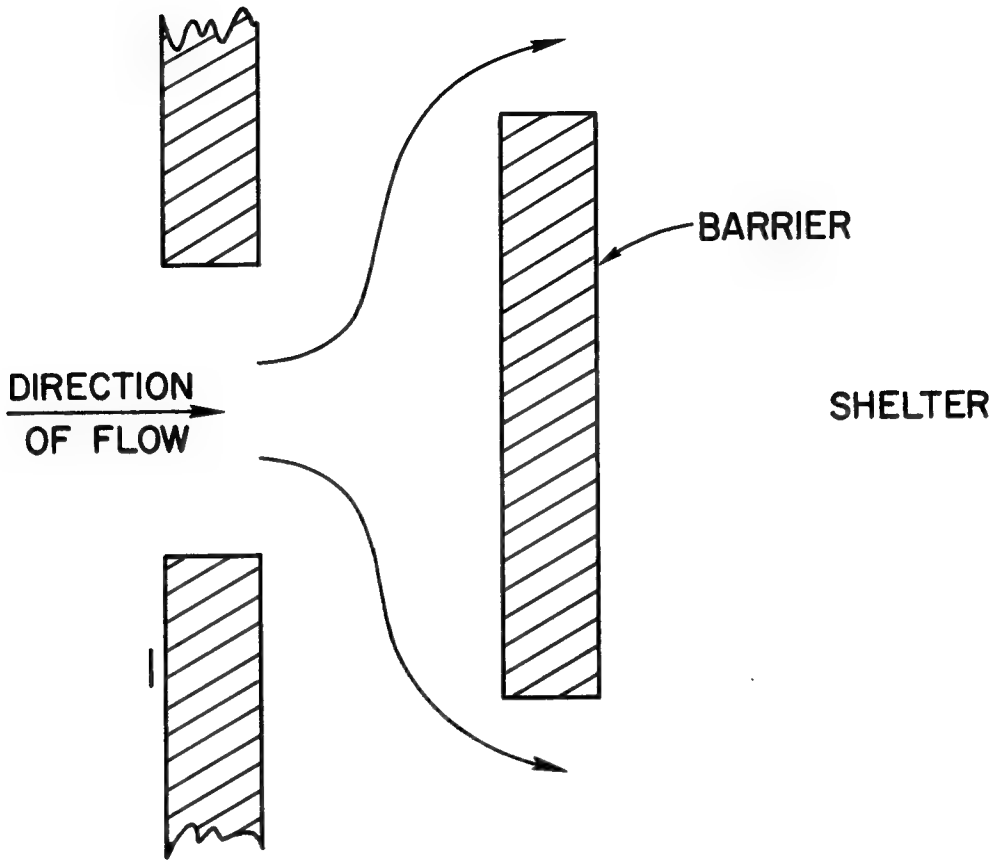

FIGURE E-11 SIMPLE BARRIER AT SHELTER ENTRY

Floor space usable for shelter might be increased by deliberate diffusion of the flow throughout the room, as suggested by the sketch in Figure E-12. In this case, the area A_2 appearing in the denominator of Eq. (29) may effectively be much greater than the area of the entry and the peak dynamic pressure in the room reduced below the danger level everywhere. A diffuser should also reduce vorticity, the presence of moving centers of high speed rotational flow extending over very limited areas at any one time. A vortex may be dangerous to human bodies in its path since wind speeds within the vortex may be considerably greater than in the jet core. Diffusion should not be considered unless the maximum or choked* flow rate $(\Delta m/\Delta t)_{choked}$ can be shown to be safe† when diffused

* See page 32.

† The general subject of hazard to shelterees in open shelter is discussed in Volume 1, pages 8-67 to 8-71, of the present work. The technical background necessary to calculation of the hazard is presented later in this section.

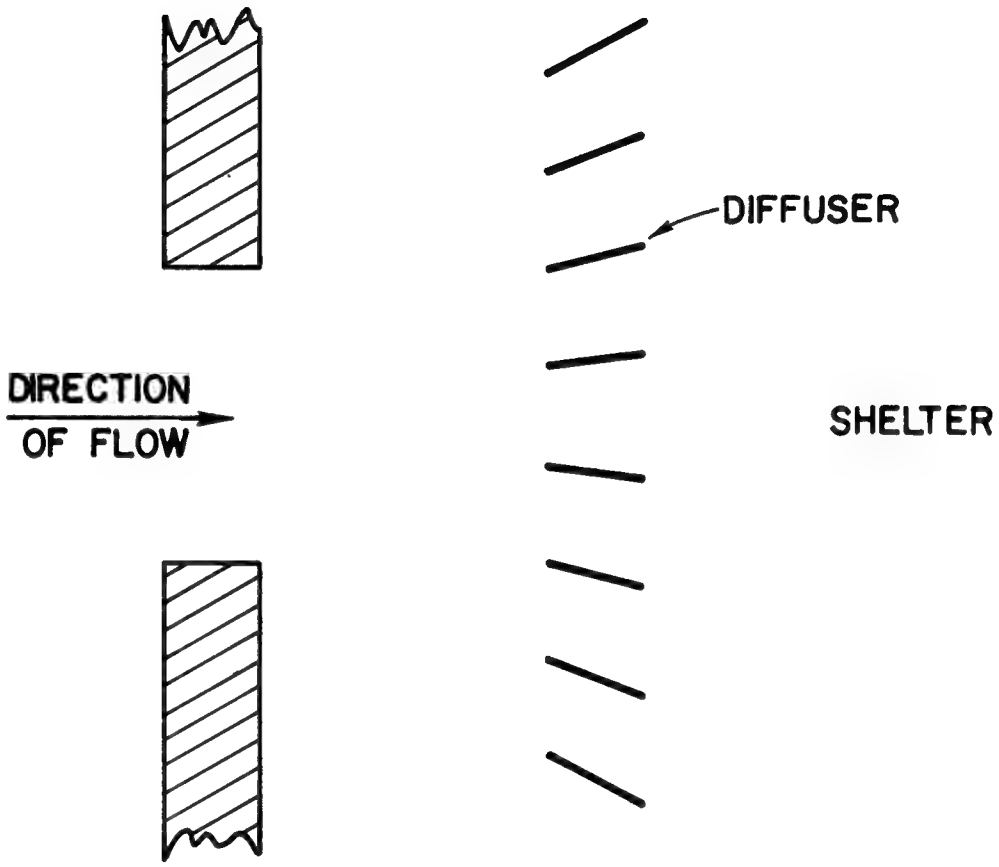

FIGURE E-12 DIFFUSER-BAFFLE SCHEME AT ENTRY

over a broad area at the entrance. Possibilities offered by deliberate diffusion are under study. The diffuser shown in Figure E-12 is schematic only and is not meant to suggest an actual device.

One kind of barrier that might reduce the jet intensity flowing over prone shelterees is a ramp to deflect part of the incoming stream toward the ceiling. No device of this kind has been studied.

Another seemingly useful characteristic of steady flow through pipes (and presumably of steady flow and quasi-steady flow through entry mazes) is a certain loss of momentum (or average wind speed) with distance traveled.[27] While it seems likely that, other things being equal, the loss through an entry maze would be greater than the loss through a pipe, the known loss rate through pipes of certain regular cross-sectional shapes

(with both rough and smooth walls) appears so slight that we are led to the belief that an entry maze effective for the protection of shelterees from translational hazard must be unreasonably long or that we must seek other protective mechanisms in the maze not found in pipes.

In order to demonstrate the frictional loss rate quantitatively we calculate it here for a pipe, which we imagine is serving as an entry to a shelter. The nondimensional coefficient of resistance λ is defined by the equation:[27]

$$\frac{dP}{dl} = \frac{\lambda}{d} q \qquad (37)$$

where dP/dl is the loss of pressure head per unit length of travel
d is the pipe diameter
q is the mean dynamic pressure in a cross section.

In smooth pipes the coefficient λ is a function only of the nondimensional group called the Reynolds number[5] Re which is a function of a linear dimension (in this case, the diameter d of the pipe), wind speed u, air viscosity η and air density ρ; i.e.,

$$Re = \frac{du\rho}{\eta}$$

Air viscosity is a function is a function of temperature, but in the range of our interest it can be taken[5,26] as approximately 4.0×10^{-5} lb sec/ft^2. If we assume that the pressure differential between inside and outside equals 10 psi, inside pressure P_3' is standard atmospheric* or 14.7 psi, air density in the entry and room is also standard* or 0.002378 slug/cf and $\gamma = 1.4$; then Eqs. (13) and (14) give the value of wind speed u_2 in the entry, i.e., $u_2 = 998$ fps. Also dynamic pressure, $q = (\rho u^2)/2 = 8.23$ psi. Hence, for the flow in our hypothetical pipe entry:

$$Re = 2.38 \times 10^5$$

where we have assumed a pipe diameter d of 4 ft.

Figure E-13 shows the dependence of frictional resistance λ on Re. The pronounced change in slope of the curve between RE = 2000 and Re = 4000 corresponds to the transition from laminar to turbulent flow.[27,28] Unfortunately, a 10-psi pressure differential across our hypothetical pipe entry leads to turbulent flow, where the value of λ is generally less than for laminar flow.

* See page 6-8 of Volume 1 of the present work.

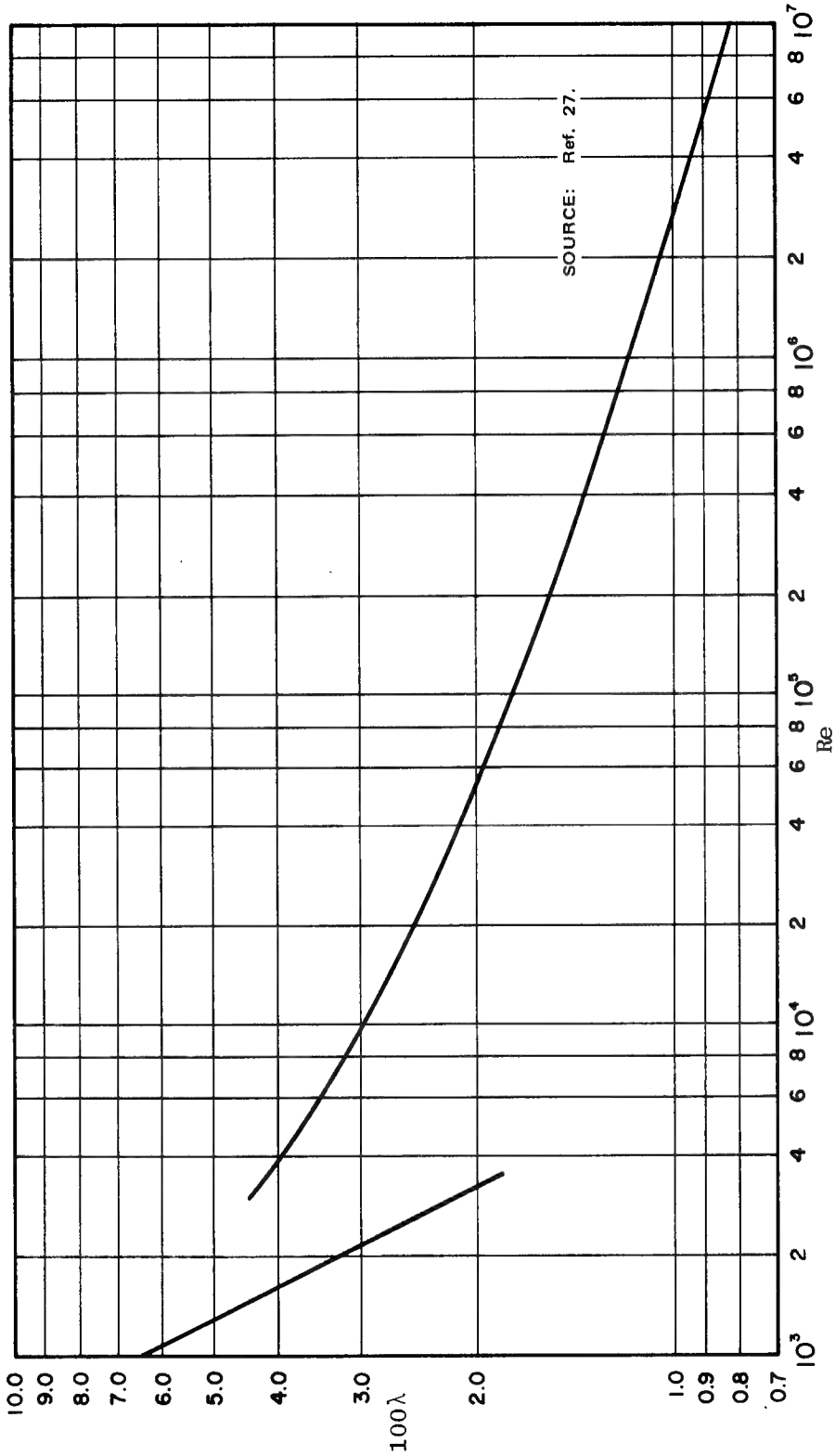

FIGURE E-13 FRICTIONAL RESISTANCE IN A SMOOTH PIPE

Reading Figure E-13 we expect the coefficient of resistance to be:

$$\lambda \approx 0.015$$

and Eq. (37) tells us immediately that the initial rate of loss of head is small. However, we can continue the quantitative estimate as follows.

Equation (1) can be written for any cross section in the pipe, which is another way of saying that the quantity

$$\frac{\gamma}{\gamma-1}\frac{P}{\rho} + \frac{1}{2}u^2 = c$$

is a constant along the length of the pipe. Since we know the values of the flow parameters at the intake cross section, we can evaluate this constant; i.e.,

$$c = \frac{\gamma}{\gamma-1}\frac{P_1}{\rho_1} + \frac{1}{2}u_1^2 \qquad (38)$$

where the subscripts refer to the initial cross section. Multiplying both sides of Eq. (38) by ρ and differentiating, we find:

$$-c\, d\rho + \frac{\gamma}{\gamma-1} dP + dq = 0 \qquad (39)$$

In steady flow another equation is available, since the mass passing through a cross section per unit time is the same everywhere along the pipe, or

$$\rho u = M, \text{ a constant} \qquad (40)$$

Squaring both sides of Eq. (40) and dividing by 2ρ, we can write:

$$\frac{1}{2}\rho u^2 = \frac{M^2}{2\rho}$$

Noting the definition, $q = (\rho u^2)/2$, and rearranging terms, we discover:

$$\rho = \frac{M^2}{2q}$$

After differentiation, this becomes:

$$d\rho = -\frac{M^2}{2q^2}$$

The last relation can be used in Eq. (39) to eliminate the density, so that we can rewrite Eq. (39) as follows:

$$dP = -\frac{\gamma-1}{\gamma}\left(1 + \frac{CM^2}{2q^2}\right) dq$$

To find the rate of change of dynamic pressure with distance of flow through the pipe, we substitute this expression for dP into the defining equation for λ, Eq. (37):

$$\frac{dq}{d\ell} = -\frac{\gamma}{1-\gamma} \frac{1}{1 + \frac{CM^2}{2q^2}} \frac{\lambda}{d} q$$

$$\left(\frac{1}{q} + \frac{CM^2}{2q^3}\right) dq = -\frac{\gamma}{1-\gamma} \frac{\lambda}{d} d\ell$$

This differential equation is easily integrated to give the relation we seek between the distance of travel ℓ and dynamic pressure q:

$$\ell n \frac{q_1}{q} + \frac{CM^2}{4}\left(\frac{1}{q^2} - \frac{1}{q_1^2}\right) = \frac{\gamma}{1-\gamma} \frac{\lambda}{d} \ell$$

Here q_1 is the dynamic pressure in the initial cross section. The constants C and M can be evaluated for our hypothetical pipe entry by using the previously calculated initial values of the flow parameters as follows:

$$P_1 = 14.7 + 10.0 = 24.7 \text{ psi}$$

$$\rho_1 = \rho_o \frac{7P_o + 6p^*}{7P_o + p}$$

$$= 0.002378 \text{ slug/cf} \frac{7 \times 14.7 + 6 \times 10}{7 \times 14.7 + 10}$$

$$= 0.00343 \text{ slug/cf}$$

$$u_1 = 998. \text{ fps}$$

$$\gamma = 1.4$$

Substituting these values in Eq. (38), we find:

$$c = 4.13 \times 10^6 \text{ ft}^2/\text{sec}^2$$

Equation (40) yields:

$$M = 3.42 \frac{\text{lb sec}}{\text{ft}^3}$$

Hence,

$$\frac{CM^2}{4} = 582 \text{ psi}^2$$

As noted above, the value of λ is initially 0.015; however as friction reduces wind speed, the Reynolds number will decrease and λ increase. However, the change in λ corresponding to a tenfold decrease in wind speed is less than a factor of 2, as is clear from Figure E-13. To find the length of flow required to reduce q to a value q/2, we will use Eq. (41) and assume λ is constant and equal to 0.02. Hence,

$$\ell n\ 2 + \frac{582}{(8.23)^2} \times 3 = \frac{7}{2}\ 0.002\ \frac{\ell}{d}$$

or,

$$\frac{\ell}{d} = 9820$$

---

* This is the air density behind a shock front of overpressure p in a standard atmosphere. See page 122 of Ref. 1. See page 6-8, Volume 1, of the present work for characteristics of the standard atmosphere.

In other words, a flow distance of nearly 10,000 diameters is needed to reduce the dynamic pressure in our hypothetical pipe entry to one-half its initial value.

Since increasing the value of λ tenfold, or even one hundredfold, would not make the results of our calculation significantly more optimistic, it appears doubtful that any sort of pipe friction in an entry maze will be of practical help in the design of open shelter. In fact, resistance in pipes of triangular and rectangular cross section is only slightly greater than in pipes of circular cross section.* Roughening the inside walls of pipes with sand increases λ no more than four times.†

It may be possible to increase the flow into a shelter (and thus reduce drag time) in a way not threatening to shelterees by using a porous wall; that is, admit the shelterees through a relatively small open doorway and fill the room with air from the blast wave through countless tiny ducts placed in an entire wall or walls. Such a method is a variation on the diffuser pictured in Figure E-12.

Within the shelter, friction will be important wherever the flow is caused to pass a corner, where the boundary layer will generally separate from the wall and a zone of turbulence will be created. Flow turning an inside corner, for example, will avoid the wall and pass outside a turbulent vortex zone, as sketched in Figure E-14. Flow past an outside corner, as in Figure E-15, will also be associated with a turbulent vortex zone, but there is no guarantee the zone will remain in one place as the room fills. In fact, the vortices may be shed from the corner and objects within the room buffeted as the very high speed winds within the vortices pass over them.

3. Calculation of the Drag Force on Objects. A still object in a stream of moving air is accelerated according to the formula

$$\frac{dv}{dt} = \frac{C_d A}{M} \quad q \qquad (42)$$

where C_d = drag coefficient of object
A = cross sectional area of object normal to flow
M = mass of object
q = dynamic pressure of moving air

---

* See Figure 20.12, page 517, Ref. 27

† See Figure 20.18, page 521, Ref. 27.

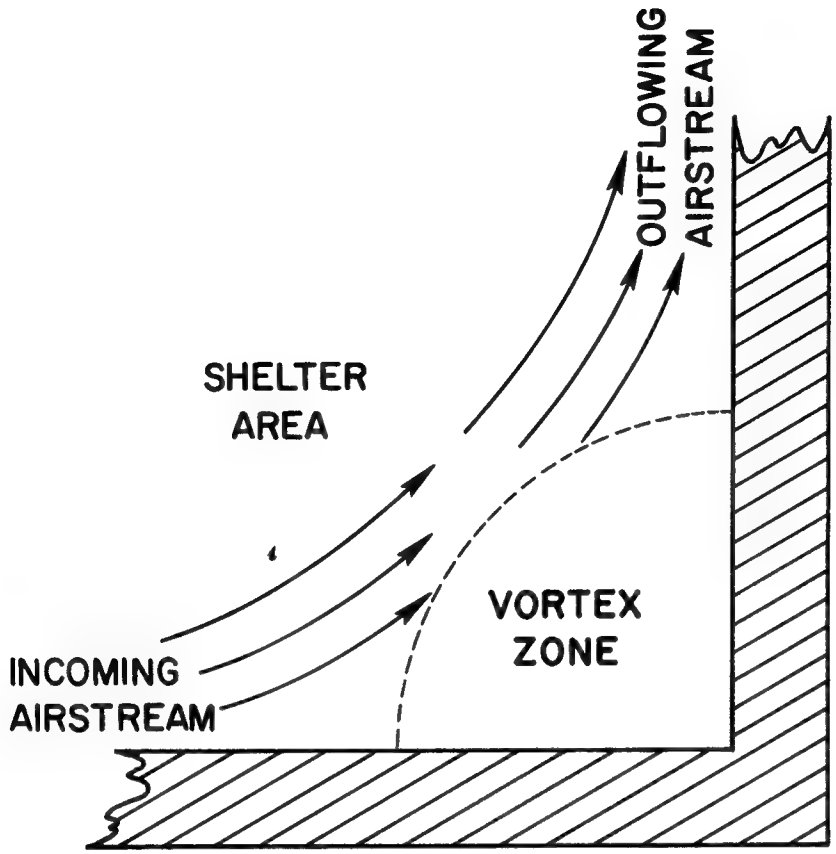

FIGURE E-14 DEFLECTION OF AIRSTREAM IN CORNER

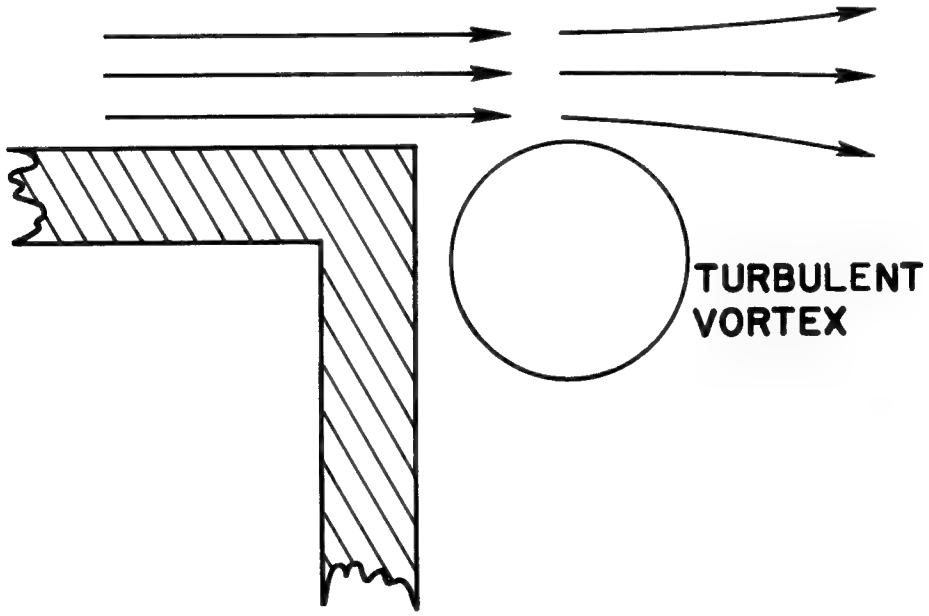

FIGURE E-15 FLOW PAST OUTSIDE CORNER

The drag coefficient C_d is a function of object shape and Reynolds number, Re, which is a dimensionless group depending on object size, L, wind speed, u, air viscosity, η, and air density, ρ:

$$Re = \frac{Lu\rho}{\eta} \tag{43}$$

Viscosity is a function of temperature but in the range of our interest it can be taken[5,26] as approximately 4.0×10^{-5} lb sec/ft^2.

Actually, there are two kinds of drag force exerted by moving air on a body: skin friction drag and pressure drag. Friction drag is important only when $Re < 10$, otherwise, only pressure drag need be considered. Both kinds of drag force are expressed by Eq. (42).

For pressure drag and for the spherical and cylindrical shapes, the coefficient C_d varies with Reynolds number as shown in Figures E-16 and E-17. The data in Figure E-17 apply to a cylinder whose axis is normal to the wind. Friction drag will not generally be important in blast filling of rooms. Since the Reynolds numbers corresponding to hazardous flows will usually be above 100, Figs. E-16 and E-17 show that the drag coefficient may conservatively be assumed constant at the value of 1. (The discontinuity shown near the value $Re = 10^6$ is associated with the onset of turbulence.)

Most of the measurements of dynamic pressure have been made indirectly by observing the motion of object accelerated by the drag force of an air jet. For example, Coulter has reported the acceleration of an 1/8-inch diameter nylon ball placed in the doorway of a small model room struck head-on by a weak shock wave[9]; in another series of experiments, Coulter has observed the motion of cylinders in a model basement filling from a shock wave.[25]

As illustrations of the calculation of acceleration of objects in a jet, we will attempt to account for Coulter's observations.

Our procedure will be as follows:

(1) Show the negligibility of any acceleration ascribable to the differential force on the object while the shock wave is still passing across the object.

(2) Estimate the acceleration of the object in the flow immediately behind the shock front. This will require knowledge of flow characteristics from articles 3.47 through 3.50 of Ref. 1, viz., wind speed, air density and dynamic pressure.

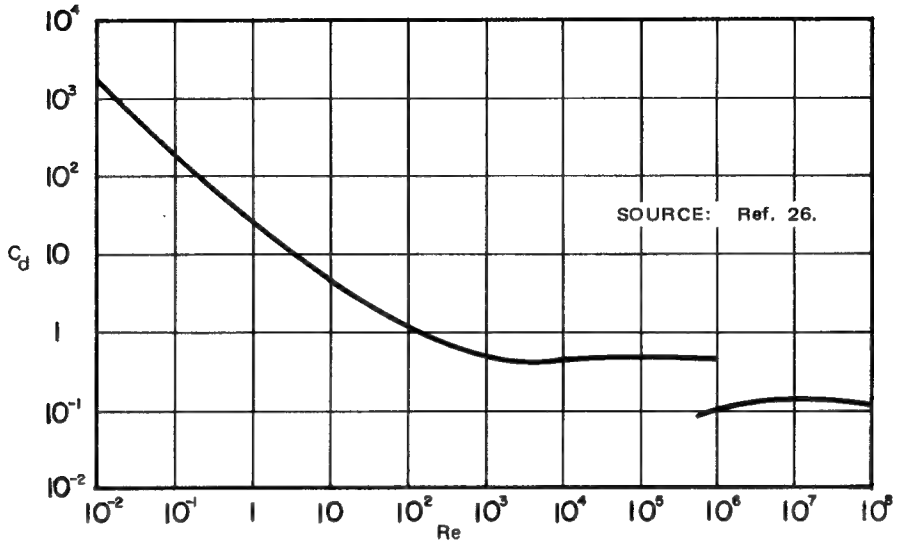

FIGURE E-16 EXPERIMENTAL DRAG COEFFICIENTS OF SPHERE

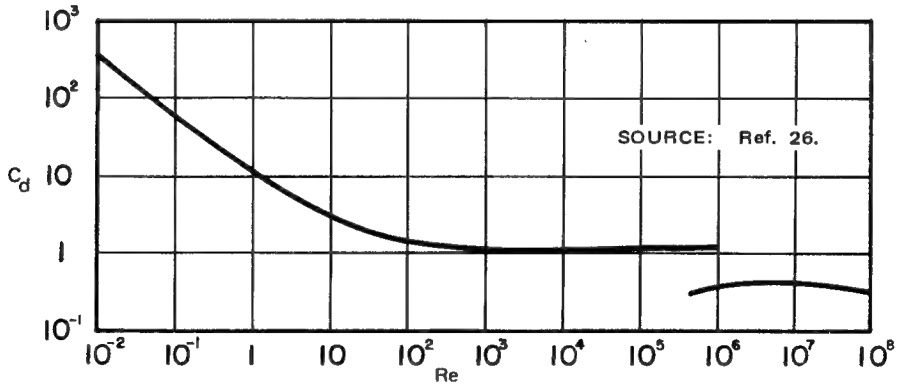

FIGURE E-17 DRAG COEFFICIENT OF CIRCULAR CYLINDER IN FLOW NORMAL TO AXIS (BETWEEN WALLS)

(3) Estimate duration of jet buildup from Eq. (30).

(4) Calculate acceleration of the object in the fully established jet using Eqs. (29) and (42).

(5) From the results of steps (2) and (4), approximate the speed gained during the buildup phase.

(6) Calculate the speed gained and distance travelled during the remainder of the room filling; hence, find the final speed and displacement of the ball to compare with observation.

Step (1) is accomplished by finding an upper bound to the impulse given to the ball by the pressure differential in the shock front during its passage across the ball diameter. The duration of the unbalanced shock pressure on the ball is less than the time of passage, T, of a sound signal across the ball diameter, D, i.e., $T=D/c_o$. The impulse, I, must be less than the overpressure $(P - P_o)$ times the ball cross sectional area $\pi D^2/A$ times T or:

$$I < (P - P_o) \frac{\pi D^2}{4} T = (P - P_o) \frac{\pi D^3}{4c_o}$$

If the specific gravity* of nylon is approximately unity, then the mass of the ball will be

$$M = \frac{\pi}{6} D^3 \rho_w$$

where ρ_w stands for the density of water. The speed, v, imparted to mass, M, by the impulse, I, can therefore not be greater than:

$$v = \frac{I}{M} < \frac{(P-P_o)\pi \frac{D^3}{4}}{\frac{\pi}{6} D^3 \rho_w c_o} = \frac{3}{2} \frac{P-P_o}{\rho_w c_o}$$

$$v < 0.488 \text{ fps}$$

where we have taken the density of water as 1.94 slugs/cf (page 6-04 of Ref. 5).

---

* See p. 13-48, Ref. 5, for a definition of specific gravity.

Thus the acceleration attributable directly to the shock is in this case and in most other cases completely negligible. As we will see, the drag force resulting from the wind immediately behind the shock front causes more acceleration than the front itself and the acceleration owing to the fully developed jet causes still greater acceleration

To begin step (2) we must write an expression for sound speed as a function of pressure and density. From Eq. (5) of Chapter 20 in Ref. 5, sound speed, c, can be written:

$$c = \left(\frac{\gamma P}{\rho}\right)^{0.5} = \left(\frac{1.4P}{\rho}\right)^{0.5}$$

where we have substituted the value $\gamma = 1.4$.

Then (from page 122 of Ref. 1) wind speed behind the shock of pressure, P, is

$$u = \frac{5}{7}\,\frac{P-P_o}{P_o}\,\frac{c_o}{\left[1 + \left(\frac{6(P-P_o)}{7P_o}\right)\right]^{0.5}}$$

where P_o = pressure ahead of shock front and

c_o = sound speed ahead of front.

From the same reference, density behind the front can be expressed as:

$$\rho = \frac{7 + \frac{6(P-P_o)}{P_o}}{7 + \frac{(P-P_o)}{P_o}}\,\rho_o \qquad (44)$$

and dynamic pressure (from Eq. (3.49.1) of Ref. 1) is

$$q = \frac{5}{2}\,\frac{(P-P_o)^2}{6P_0+P} \qquad (45)$$

In his experiment with the nylon ball, Coulter allowed a shock front of overpressure equal to 4.89 psig to strike a reflecting plate in which an entrance 1 x 4 inches was cut. Since the chamber behind the opening had a volume-to-opening area ratio (V/A) equal to 1.33, filling was essentially complete in 1.33/2 = 0.667 ms, during which time there was little or no decay of the incident wave. Hence, $P - P_o = 4.89$ psi, Table 6.1 on page 6-9 of Volume 1 of the present work gives standard atmospheric air density ρ_o at sea level and temperature of 59F as 0.002378 lb-sec^2/ft^4; and if we assume $P_o = 14.7$ psi, then air density behind the shock becomes:

$$\rho = 0.002917 \text{ lb-sec}^2/\text{ft}^4$$

and dynamic pressure

$$q = 0.5546 \text{ psi}$$

and sound speed, c_o, in standard air

$$c_o = 1116. \text{ fps}$$

Under these conditions, wind speed becomes:

$$u = 233.9 \text{ fps}$$

From these values of wind speed and air density we calculate the Reynolds number , Eq. (43), for the nylon ball caught in the wind immediately behind the shock:

$$Re = \frac{Lu\rho}{\eta} = \frac{(1/8) \times (1/12) \times 233.9 \times 0.002917}{4.0 \times 10^{-5}}$$

$$= 177.7$$

Finally, Figure E-16 suggests for Re = 178 a value of C_d near 0.9. We can now use Eq. (42) to calculate the initial acceleration of the nylon ball:

$$\frac{dv}{dt} = \frac{C_d A}{M} q = \frac{0.9\pi D^2/4}{\frac{\pi}{6} D^3 \rho_w} q = \frac{1.35}{D\rho_w} q$$

$$\frac{dv}{dt} = 5345. \text{ ft/sec}^2$$

For step (3) we estimate the duration t_o of the jet buildup from Eq. (30)

$$t_1 \sim \frac{4b_o}{c}$$

Here c should be the sound speed behind the shock front, where we have found air density to be

$$\rho = 0.002917 \text{ lb-sec}^2/\text{ft}^4$$

and where P = 14.7 + 4.89 = 19.6 psi;
hence,

$$c = \left(\frac{1.4P}{\rho}\right)^{0.5} = 1164. \text{ fps}$$

Taking b_o = 1 inch, the width of the opening, we find

$$t_1 = \frac{4 \times 1}{12 \times 1164} = 0.286 \text{ ms}$$

Since the filling time of the model, estimated by the simple rules of Section IIA, is approximately 0.667 ms, the buildup time t_1 is significant and we must consider the effect of the shock drag force on the object.

Step (4) begins with the calculation of reservoir conditions outside the entry to the model. Reflection at normal incidence of a 4.89-psig shock produces a reflected overpressure (cf. Eq. (3.50.1) of Ref. 1) equal to

$$P_1 = 2\ P\text{-}P_o + (\gamma+1)\ q$$

Substituting γ = 1.4 and q = 0.555 psi

$$P_1 = 25.8 \text{ psia}$$

Air density in the reservoir can be found from a second application of Eq. (44), where now ρ_o and P_o are the density and overpressure behind the incident shock and $P = P_1$. Hence,

$$\rho_1 = \frac{7 + \frac{6}{19.6}\ (25.8-19.6)}{7 + \frac{25.8-19.6}{19.6}}\ 0.0029717$$

$$\rho_1 = 0.003548 \text{ lb-sec}^2/\text{ft}^4$$

(We might have with enough accuracy found ρ_1 by using Eq. (6) and taking $P_o = 14.7$ psi and $\rho_o = 0.002378$ lb-sec^2/ft^4, the values in a normal atmosphere at sea level and temperature 59F.)

These reservoir conditions remain constant during the whole filling time.

From a knowledge of reservoir conditions alone, we can calculate mass inflow rate by Method F; specifically, from Eq. (10) we write:

$$\frac{\Delta m}{\Delta t} = \left[P_1 \left(1-y_o\right) y_o^{1/\gamma}\right]^{0.5} A_2$$

(Alternatively , we could use Method D and either Eq. (15) or Eq. (17).) The above expression for $\Delta m/\Delta t$ becomes upon substitution of numerical values for ρ_1 and P_1:

$$\frac{\Delta m}{\Delta t} = 1.809\ A_2 \text{ slugs/sec-ft}^2$$

Core dynamic pressure, then, comes from Eq. (29):

$$q_{core} = \frac{(1.809)^2}{2 \times 0.003548 \times 144} \left(\frac{P_1}{P_3}\right)^{0.7143} \text{ psi}$$

$$= 3.202\left(\frac{P_1}{P_3}\right)^{0.7143} \text{ psi}$$

As an approximation, we will use a mean value for the pressure ratio

$$\frac{P_1}{P_3} \approx \frac{25.8}{\frac{25.8 + 14.7}{2}} = 1.274$$

Hence,

$$q_{core} \approx 3.81 \text{ psi}$$

(Since $P_1 < 13.13$ psig, were we to use Method D, inflow would be unchoked and Eq. (15) would apply. Initially $P_3' = 14.7$ psi so that by Method D initial mass inflow rate for the same reservoir conditions becomes:

$$\frac{\Delta m}{\Delta t} = 1.733 \, A_2 \text{ slugs/sec-ft}^2$$

which compares fairly well with the mass inflow rate computed by Method F above.)

In order to find a value for the drag coefficient C_d in Figure E-16, we must determine the wind speed u from the mass flow rate and room air density. Again, taking a value for the density that is the mean between initial and final density in the chamber:

$$u = \frac{1.}{\rho_3 A_2} \quad \frac{\Delta m}{\Delta t} = \frac{1.809}{\frac{0.002378 + 0.003548}{2}}$$

$$\approx 610. \text{ fps}$$

from which we calculate the Reynolds number to be:

$$Re = \frac{Lu\rho}{\eta} = \frac{\frac{1}{8} \times \frac{1}{12} \times 610 \times 0.002963}{4 \times 10^{-5}}$$

$$= 472$$

From Figure E-16, C_d for the 1/8-inch sphere in such a flow is approximately 0.56. Combining these values in Eq. (42):

$$\frac{dv}{dt} = \frac{C_d A}{M} \, q_{core} = \frac{3}{2} \cdot \frac{C_d}{D\rho_w} \, q_{core}$$

$$= 22950 \text{ ft/sec}^2$$

Comparing this result with that of step (2), we see that acceleration in the fully established jet is four times greater than that immediately behind the incident shock front.

(The combination of constants C_dA/M is sometimes known as the "acceleration coefficient."[14] Over a wide range of Reynolds numbers it is characteristic only of the object being dragged. The interactive computer program listed in Table E-3 will ask the operator to enter a value for the acceleration coefficient before calculating slide trajectories.)

For step (5) we estimate the speed gain during the establishment of the jet by averaging the acceleration at the beginning of filling (viz., 5345 fps) and that in the fully established jet (viz., 22950 fps). Hence the speed gain Δv_1 during the time $t_o = 0.286$ ms becomes:

$$\Delta v_1 = \int_o^{t_o} \frac{dv}{dt} \, dt$$

$$\Delta v_1 = \frac{5345 + 22950}{2} \times 0.000286 \quad \text{fps}$$

$$\Delta v_1 = 4.05 \text{ fps}$$

Finally, in Step (6) we compute the additional speed gain Δv_2 from the fully established jet. For estimating an upper bound to this gain we can assume the drag force remains constant during the interval between t_o and the completion of filling, i.e., during a time 0.667 - 0.286 = 0.381 ms. In that case

$$\Delta v_2 < 22950 \times 0.000381 = 8.74 \text{ fps}$$

or the total speed $v = \Delta v_1 + \Delta v_2 < 8.74 + 4.05 = 12.8$ fps.

The distance moved s is bounded by the value:

$$s = \iint \frac{dv}{dt} \, dt \, dt$$

$$s < 0.5 \times 22950 \times (0.381)^2 \times 10^{-6} \times 0.000381$$

$$s < 0.0385 \text{ inch}$$

From this calculation we concluded that the ball stayed in the jet core until filling was complete.

Coulter, however, reported terminal speed of the nylon ball (after 0.700 ms) as 29.8 fps. The cause of the discrepancy between our upper bound $v < 12.8$ fps and Coulter's observation is not known. Had we postulated immediate jet establishment (that is, had we assumed $t_1 = 0$), we would calculate an upper bound on v somewhat larger than 12.8 fps as follows:

$$v < 22950 \times 0.000667 = 15.3 \text{ fps}$$

however, this upper bound is still only half as large as the speed reported.

In Eq. (42) the dynamic pressure q is a function of the time after shock arrival and of the position of the ball as it moves with the wind. (It is also a function of the ball speed, since drag force depends only on the difference between ball speed and wind speed. This dependence is not important when the ball speed is negligibly smaller than wind speed, as is the case in the example of the nylon ball.) By integrating Eq. (42) numerically the time and position dependence of dynamic pressure q can be taken into account, and in the case of a large room filling through a small opening time and position dependence of q must be taken into account. For example, Coulter[25] has observed the filling of a model basement from 5-, 10-, and 20-psig shock waves. Filling time was observed to be approximately 14 ms and jet establishment required between 1 and 2 ms. In these basement models, the room-filling wind swept over model barrels resting upright on the floor and simulating shelter supplies. The barrels moved the length of the room and their final speeds were measured approximately from motion pictures. Using a drag coefficient $C_d = 0.47$ (i.e., assuming an approximately spherical shape for the barrel) in a stepwise integration of Eq. (42), we calculate in the case of the 5-psig wave a final speed of 7.1 fps. Coulter measured a final speed equal to 7.5 fps. In this case then of relatively rapid jet establishment our calculation of drag acceleration of an object in a room-filling wind was fairly successful.

III. Multiple Rooms

A. Inflow

Although the algebra becomes increasingly cumbersom as rooms are added, the foregoing principles of calculation can be applied to a series of connected rooms. For example, two rooms are represented in Figure E-18 for which two control surfaces* can be employed. In the figure the

* The concept of control surfaces is explained in Section IIB1 above.

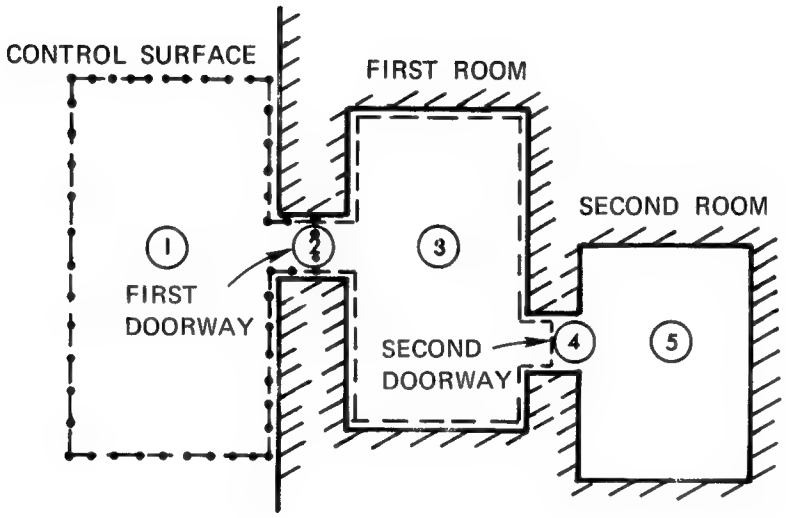

FIGURE E-18 CONTROL SURFACE USED IN CALCULATING FLOW INTO SECOND ROOM

larger control surface, shown dashed, includes the first or outer room as well as an arbitrary volume outside and the doorway between them. The smaller, shown dotted, embraces only the outside volume and the first doorway. In this section only inward flow through these surfaces will be considered; outflow, as well as inflow through one doorway combined with outflow in another, will be treated in the following section. Through the smaller surface the momentum flux is due to flow through the first doorway and the resulting conservation of momentum equation can be written exactly as in Eq. (2). In addition, conservation of energy, Eq. (1), and the isentropic equation of state, Eq. (3), both apply without change to the filling of the first or outer of two connected rooms from an outside blast wave. Equations (1), (2), and (3) constitute a solution by Method F. If Method D or G* is preferred, Eq. (13) replaces Eq. (2). In other words, within the accuracy of our approximation, the mass flow rate and wind speed through the first or outer doorway does not depend on the presence or absence of an inner room. Average pressure in the outer room, of course, is different when an inner room is present from what it is when an inner room is absent.

Calculation of the flow into the second or inner room by Method D or G requires obvious extensions of the foregoing set of equations. We may write conservation of energy as follows:

$$\frac{\gamma}{\gamma-1} \cdot \frac{p_3'}{\rho_3'} + \frac{1}{2} u_3^2 = \frac{\gamma}{\gamma-1} \cdot \frac{P_4}{\rho_4} + \frac{1}{2} u_4^2 \qquad (46)$$

where u_3 is the wind speed through the outer room. The analog of Eq. (13) in the inner room is:

$$P_4 = P_5' \qquad (47)$$

Conservation of mass implies the relation:

$$\rho_3 u_3 A_3 = \rho_4 u_4 A_4 \qquad (48)$$

where A_3 is an effective cross-sectional area of the outer room serving as a duct for flow into the inner room. Finally, we can write the isentropic equation of state for air in the second doorway:

---

* See Section IIB1 above. Method G is identical to Method D (described by Eqs. (16) and (17) above) except the discharge coefficient K is assumed to be unity.

$$\rho_4 = \rho_3' \left(\frac{P_4}{P_3'}\right)^{\frac{1}{\gamma}} \tag{49}$$

We thus have four equations - Eqs. (46), (47), (48), and (49) - to solve for four unknowns: ρ_4, u_4, P_4 and u_3. The mass flow through the second doorway can then be found from the equation:

$$\Delta m_5 = K_4 \rho_4 u_4 A_4 \Delta t \tag{50}$$

where K_4 is the discharge coefficient for the second or inner doorway. Flow will be choked* when the ratio $r = P_5'/P_3'$ reaches the critical value, determined by the vanishing of the derivative $d(\Delta m_5)/dr$.

Solving Eqs. (46) through (49) for u_4^2, we find

$$u_4^2 = \frac{2\gamma}{\gamma-1} \frac{P_3'}{\rho_3'} \left[-\left(\frac{P_5'}{P_3'}\right)^{1-1/\gamma} + 1 \right] \frac{1}{-\left(\frac{P_5'}{P_3'}\right)^{2/\gamma} \frac{A_4^2}{A_3^2} + 1}$$

Taking the square root and substituting this expression in Eq. (50), the analog to Eq. (15) is found to be:

$$\Delta m_5 = K_4 \left(\frac{2\gamma \rho_3' P_3'}{\gamma-1}\right)^{0.5} \left(\frac{P_5'}{P_3'}\right)^{1/\gamma} \left[-\left(\frac{P_5'}{P_3'}\right)^{1-1/\gamma} + 1 \right]^{0.5} \frac{A_4 \Delta t}{\left[-\left(\frac{P_5'}{P_3'}\right)^{2/\gamma} \left(\frac{A_4}{A_3}\right)^2 + 1 \right]^{0.5}} \tag{51}$$

Except for the final factor on the right side, Eq. (51) is equivalent to Eq. (15) with the substitutions $K \rightarrow K_4$, $\rho_1 \rightarrow \rho_3'$, $P_1 \rightarrow P_3'$, and $P_3' \rightarrow P_5'$. If we make the reasonable assumptions that $A_4 \ll A_3$ and $P_5' < P_3'$, then the final factor becomes unity and the similarity is exact. In this case,

---

* See Section IIB1 for a discussion of choking.

calculation of filling in the second room can be carried out by Method D or G as if the first room served as an outside reservoir for the second room treated as a single room. At each time step the pressure rise in the first room is found from Eq. (12), in which

$$\Delta m = \Delta m_3 - \Delta m_5$$

where Δm_3 is the mass increment flowing through the first doorway, calculated from Eqs. (1), (3) and (13).

Method F can be used to calculate pressure rise in the second room, but because of the logical absurdity mentioned in Section IIB1 provision must be made in the analysis for one or more correction terms Δ in equations expressing conservation of momentum.

To write conservation-of-momentum equations useful in solving for the flow into the second or inner room, we consider again the larger of the two control surfaces shown in Figure E-18, which embraces the same volume as the superposition of the two control surfaces drawn in Figures E-3 and E-7. Were the second doorway not present, the momentum flux through the surface would be zero; yet, the usual assumption of uniform pressure within the first room leaves us with a nonvanishing component of force in the x-direction after integration over the control surface. This is the logical absurdity presented in Section IIB1 above. To correct this inconsistency, we postulate the existence of a force symbolized by Δ_3 on the wall of the first room directly opposite the doorway; thus, when the second doorway is absent, the momentum balance becomes:

$$\left(P_1 - P_3'\right) A_2 + \Delta_3 = 0$$

Solving this equation for Δ_3, we find:

$$\Delta_3 = -\left(P_1 - P_3'\right) A_2 \tag{52}$$

Now in writing the momentum balance with the second doorway present we include the term Δ_3, as follows:

$$\left(P_1 - P_3'\right) A_2 + \Delta_3 + \left(P_3' - P_4\right) A_4 = \rho_4 u_4^2 A_4 \tag{53}$$

After substitution of the value of Δ, this equation reduces to:*

$$\left(P_3' - P_4\right) A_4 = \rho_4 u_4^2 A_2 \tag{54}$$

Combining Eqs. (46), (48), (49) and (51) we can solve for the four unknowns: u_3, P_4, ρ_4, and u_4.

The resulting solution for P_4 can be put in a form similar to that used in computing P_2 in Eq. (5)[4]:

$$\frac{2\gamma}{\gamma+1}\left(\frac{P_4}{P_3'}\right)^{1/\gamma} = \frac{P_4}{P_3'} + \frac{\gamma-1}{\gamma+1}\left[1 - \left(\frac{A_4}{A_3}\right)^2 \left(\frac{P_4}{P_3'}\right)^{2/\gamma}\right] + \frac{\gamma-1}{\gamma+1}\left[\frac{A_4}{A_3}\left(\frac{P_4}{P_3'}\right)^{1/\gamma}\right]^2 \frac{P_4}{P_3'} \tag{55}$$

If $y = \dfrac{P_4}{P_3'}$

$$A_o = \frac{\gamma-1}{\gamma+1}\left\{\left[1 - \left(\frac{A_4}{A_3}\right)^2 \left(\frac{P_4}{P_3'}\right)^{2/\gamma}\right] + \left[\frac{A_4}{A_3}\left(\frac{P_4}{P_3'}\right)^{1/\gamma}\right]^2 \frac{P_4}{P_3'}\right\}$$

---

* The use of Eq. (51) is equivalent to neglecting the possibility of continuous flow through the "maze" or pipe consisting of the first doorway, the first room, and the second doorway, such as was considered in Section IIC2 above. Presumably, were the first room small enough, such continuous pipe-like flow would be established, making it more sensible to treat the two connected rooms as a single room of volume equaling the sum of the volumes of its two components. The means of calculating which of the two analytical treatments (viz., analysis as two connected rooms, or as a single room) is appropriate are not available. As we shall see in a numerical calculation later (cf. Figure E-19), treatment as two connected rooms may reveal no significant pressure difference between the two rooms and yield essentially the same pressure history in the blast-filled volume as does treatment as a single room.

and $B = \dfrac{2\gamma}{\gamma + 1}$

then Eq. (43) can be written in the same form as Eq. (5); viz.,

$$B\, y^{1/\gamma} = y + A_o$$

Since $P_4 \leq P_3'$ and usually $A_4 \ll A_3$,

$$A_o \cong \frac{\gamma-1}{\gamma+1} \tag{56}$$

Use of Eq. (56) is equivalent to neglecting the average wind speed in the first room; i.e., if $u_3 = o$ is substituted in Eq. (46), Eq. (56) is exact.

After the duct parameters, i.e., ρ_2, P_2, u_2, ρ_4, u_4, and, if desired, u_3, have been found from the foregoing equations, then the new room pressures P_3 and P_5 and densities ρ_3 and ρ_5 are calculated as follows:

$$\Delta m_5 \left(\frac{\gamma}{\gamma-1} \cdot \frac{P_3'}{\rho_3'} + \frac{1}{2} u_3^2 \right) = \frac{1}{\gamma-1} (P_5 - P_5')\, V_5 \tag{57}$$

where $\Delta m_5 = u_4 \cdot \rho_4 \, A_4 \cdot \Delta t$, mass increment in second room

$$\frac{\gamma}{\gamma-1} \cdot \frac{P_1}{\rho_1} \cdot \Delta m = \frac{1}{\gamma-1} \cdot (P_3 - P_3')\, V_3 + \frac{1}{\gamma-1} \cdot (P_5 - P_5') \cdot V_5 \tag{58}$$

where $\Delta m = u_2 \cdot \rho_2 \, A_2 \cdot \Delta t$, mass increment in first room;

$$\rho_5 = \rho_5' + \frac{\Delta m_5}{V_5} \tag{59}$$

and

$$\rho_3 = \rho_3' + \frac{\Delta m - \Delta m_5}{V_3} \tag{60}$$

Numerical Example No. 5 (Flow into Two Connected Rooms). Assume that the room considered in Numerical Example No. 3 has within it a small storage compartment of 800 cf volume opening onto the main room through a small passage 10 sf in area. We compute the pressure rise in both portions of the 4000-cf volume in the first time increment $\Delta t = 5$ ms.

Before making the detailed calculations however, we can see from the simple rule in Section IIA that there will never be significant pressure difference between the two volumes. The approximate filling time of the larger volume is:

$$\Delta T_1 = \frac{4000 - 800}{2 \times 21} = 76.2 \text{ ms}$$

and for the smaller volume:

$$\Delta T_2 = \frac{800}{2 \times 10} = 40.0 \text{ ms}$$

The fact that $\Delta T_2 < \Delta T_1$ means that the smaller volume will keep pace with the larger volume in filling, as we can understand from the detailed calculation below by Method D.

The initial mass flow rate through the outer doorway (calculated in Numerical Example No. 3) is:

$$\frac{dm}{dt} = 46.73 \text{ slug/sec}$$

which means that in the first time increment

$$\Delta m_3 = 46.73 \times 0.005 = 0.2336 \text{ slug}$$

Such a mass increment means, according to Eq. (12), that the average pressure rise in the outer room without flow into the inner room will be:

$$\Delta P_3 = P_3 - P_3' = \frac{1.4 \times 34.7 \times 0.2336}{0.004313(4000-800)} = 0.8222 \text{ psi}$$

In applying Eq. (51) we use the values $P_5' = 14.7$ psi, $K_4 = 0.7$, and provisionally assume $P_3' = 14.7 + 0.822 = 15.51$ psi. Also by Eq. (11) the provisional value of outer room density is:

$$\rho_3' = 0.002378 + \frac{0.2336}{3200} = 0.002451 \text{ slug/cf.}$$

Hence,

$$\Delta m_5 = 0.7 \left(\frac{2 \times 1.4 \times 0.002451 \times 15.52 \times 144}{1.4 - 1}\right)^{0.5} \left(\frac{14.7}{15.52}\right)^{1/1.4}$$

$$\times \left[1 - \left(\frac{14.7}{15.52}\right)^{1-1/1.4}\right]^{0.5} \quad \frac{10 \times 0.005}{\left[1 - \left(\frac{14.7}{15.52}\right)^{2/1.4} \left(\frac{10}{21}\right)^2\right]^{0.5}}$$

$$= 0.02910 \text{ slug}$$

The mass remaining in the main room then is:

$$\Delta m = 0.2336 - 0.02910 = 0.2045 \text{ slug}$$

and the corrected density in the main room at the end of the first time step is:

$$\rho_3 = 0.002378 + \frac{0.2045}{3200} = 0.002442 \text{ slug/cf}$$

and in the small room:

$$\rho_5 = 0.002378 + \frac{0.02910}{800} = 0.002414 \text{ slug/cf}$$

Corrected pressure in the main room at the end of the first time step is by Eq. (12):

$$P_3 = 14.7 + \frac{1.4 \times 34.7 \times 0.2045}{0.004313 \times 3200} = 15.42 \text{ psi}$$

and using an analogy to Eq. (12) in which P_1 and ρ_1 have been replaced by P_3' and ρ_3', respectively, we calculate the pressure in the small connected volume to be:

$$P_5 = 14.7 + \frac{1.4 \times 14.7 \times 0.02910}{0.002378 \times 800} = 15.01 \text{ psi}$$

For the second time increment time is advanced to t = 0.005 sec and any change in outside conditions must be reflected in the values of P_1 and ρ_1. If we assume P_1 and ρ_1 are unchanged during the first time step, then dm/dt through the outer doorway is the same as it was initially; the preliminary increases in P_3 and ρ_3 are the same, i.e.,

$$P_3' = 15.42 + 0.8222 = 16.24 \text{ psi}$$

and

$$\rho_3' = 0.002442 + \frac{0.2336}{3200} = 0.002515 \text{ slug/cf}$$

Again applying Eq. (51) we find:

$$\Delta m_5 = 0.7 \left(\frac{2.8 \times 0.002515 \times 16.24 \times 144}{0.4}\right)^{0.5} \left(\frac{15.01}{16.24}\right)^{1/1.4} \left[1 - \left(\frac{15.01}{1624}\right)^{1-1/1.4}\right]^{0.5} \frac{}{\left[\left(\frac{15.01}{16.24}\right)^{1/0.7} \left(\frac{10}{21}\right)^2\right]^{0.5}}$$

$$= 0.03546 \text{ slug}$$

The net increase in the main room is then:

$$\Delta m = 0.2336 - 0.03546 = 0.1981 \text{ slug}$$

So that at the end of the second time increment:

$$P_3 = 15.42 + \frac{1.4 \times 34.7 \times 0.1981}{0.004313 \times 3200} = 16.12 \text{ psi}$$

$$P_5 = 15.01 + \frac{1.4 \times 16.24 \times 0.03546}{0.002515 \times 800} = 15.41 \text{ psi}$$

$$\rho_3 = 0.002515 + \frac{0.1981}{3200} = 0.002577 \text{ slug/cf}$$

$$\rho_5 = 0.002414 + \frac{0.03546}{800} = 0.002458 \text{ slug/cf}$$

As we forecast, the pressure differential between the two connected volumes is decreasing in time and will remain small.

B. Outflow

The foregoing section considered inward flow through both doorways. The principles for studying outflow through one or both doorways are the same but certain equations must be rewritten. Two statements can be made:

First, outflow (like inflow) through the first or outer doorway can be calculated exactly as set forth for a single room. In the case of outflow, Eqs. (1), (2), and (20) are required, as explained in Section IIB2.

Second, both inflow and outflow through the second or inner doorway are affected by the direction of flow through the first doorway. There are therefore three cases remaining to be treated in discussing flow

through the second doorway: (1) flow through the second doorway is outward while flow through the first is inward, (2) flow through the second doorway is outward while flow through the first is outward, and (3) flow through the second doorway is inward while flow through the first is outward. The case of inward flow through both doorways has been treated in the preceding section.

In Case (1), $u_3 = 0$ and Eq. (46) simplifies to:

$$\frac{\gamma}{\gamma-1} \cdot \frac{P_3'}{\rho_3'} = \frac{\gamma}{\gamma-1} \cdot \frac{P_4}{\rho_4} + \frac{1}{2} u_4^2 \tag{61}$$

but a momentum balance such as Eq. (53) must contain two correction terms, Δ_3 and Δ_5, to account for excess force against the righthand and lefthand walls, respectively, of the first room; Δ_3 is given by Eq. (52) and by analogy we can write:

$$\Delta_5 = (P_5' - P_3') A_4 \tag{62}$$

Hence, writing the momentum balance as follows:

$$(P_1 - P_3') A_2 + \Delta_3 + (P_3' - P_4) A_4 + \Delta_5 = \rho_4 u_4^2 A_4 \tag{63}$$

and substituting for Δ_3 and Δ_5, we find:

$$P_5' - P_4 = \rho_4 u_4^2 \tag{64}$$

To the outflow through the second or inner doorway we can apply the isentropic equation of state in analogy with Eq. (6):

$$\rho_4 = \rho_5' \left(\frac{P_4}{P_5'}\right)^{1/\gamma} \tag{65}$$

Combining Eqs. (61), (64), and (65), we find:

$$By^{1/\gamma} = y + A_o$$

where

$$y = \frac{P_4}{P_5'} \tag{66}$$

$$B = \frac{2\gamma}{\gamma+1} \cdot \frac{\rho_5'}{\rho_3'} \cdot \frac{P_3'}{P_5'} \tag{67}$$

$$A_o = \frac{\gamma-1}{\gamma+1} \tag{68}$$

In Case (2), there is net flow through the first room (i.e., $u_3 \neq 0$); Eq. (46) is unchanged but the analog of Eq. (53) is:

$$(P_1 - P_3') A_2 + (P_3' - P_4) A_4 + \Delta_5' = \rho_4 u_4^2 A_4 \tag{69}$$

where

$$\Delta_5' = (P_5' - P_3') A_4 - (P_1 - P_3') A_2 \tag{70}$$

This value of Δ_5' is computed by noting that the momentum flux through a control surface embracing both rooms and the outside reservoir is zero, i.e.:

$$(P_5'-P_3') A_4 - \Delta_5' + (P_3'-P_1) A_2 = 0$$

Combination of Eqs. (69) and (70) leads again to Eq. (64).

Solving Eqs. (46), (48), (64), and (65), we find again that

$$By^{1/\gamma} = y + A_o$$

where x and B are given by Eqs. (66) and (67), but now

$$A_o = \frac{\gamma+1}{\gamma-1} \left\{ (1-\alpha^2) \left[\frac{P_1 - P_3'}{P_5'} \cdot \frac{A_2}{A_4} + \frac{P_3' + \Delta_5'}{P_5'} \right] + \alpha^2 y \right\} \tag{71}$$

and

$$\alpha = \frac{A_4}{A_3} \cdot \frac{\rho_5'}{\rho_3'} \cdot y^{1/\gamma} \tag{72}$$

$$A_o = \frac{\gamma-1}{\gamma+1} \{(1-\alpha^2) + \alpha^2 y\} \tag{73}$$

Since, ordinarily, $A_3 \gg A_4$, and $y < 1$, $\alpha^2 \ll 1$, from which we conclude:

$$A_o \approx \frac{\gamma-1}{\gamma+1} \tag{74}$$

An alternative expression for A in Case (2) can be found by writing the excess force on the wall against which the outflow from the second room is directed as the pressure differential across the duct times the duct area:

$$\Delta_5'' = (P_5' - P_3') A_4 \tag{75}$$

Substituting Δ_5'' from Eq. (75) for Δ_5' in Eq. (71), we compute for the constant term

$$A_o = \frac{\gamma-1}{\gamma+1} \left\{ (1-\alpha^2) \left[\frac{P_1 - P_3'}{P_5'} \cdot \frac{A_2}{A_4} + 1 \right] + \alpha^2 y \right\} \tag{76}$$

which for small α becomes

$$A_o = \frac{\gamma-1}{\gamma+1} \left[\frac{P_1 - P_3'}{P_5'} \cdot \frac{A_2}{A_4} + 1 \right] \tag{77}$$

In Case (3), namely, outflow through the first doorway combined with inflow through the second, conditions in the second doorway are computed by solving Eq. (46) with $u_3 = 0$, Eq. (49) and

$$(P_1 - P_3') A_2 + (P_3' - P_4) A_4 = \rho_4 u_4^2 A_4$$

(There is no excess force on the walls of the first room hence no correction terms appear in Eq. (78).

These equations lead to Eq.(5), in which

$$y = \frac{P_4}{P_3'}$$

$$B = \frac{2\gamma}{\gamma+1}$$

$$= \frac{\gamma-1}{\gamma+1} \left[\left(\frac{P_1}{P_3'} - 1 \right) \frac{A_2}{A_4} + 1 \right]$$

In summary then we see that in every case an equation of the form $By^{1/\gamma} = y + A$ must be solved for y. This equation is encountered also in the first doorway if Method F is used. In Table E-1 the meanings of y, A, and B for each case are listed. Since conditions in the first doorway under Method F are independent of conditions inside, the definitions for the first duct appear separately.

Table E-1

MEANINGS OF y, A_o, AND B IN THE EQUATION $By^{1/\gamma} = y + A_o$ WHEN METHOD F IS USED

First doorway

Inflow

$$y = \frac{P_2}{P_1}$$

$$B = \frac{2\gamma}{\gamma + 1}$$

$$A_o = \frac{\gamma - 1}{\gamma + 1}$$

Outflow

$$y = \frac{P_2}{P_3'}$$

$$B = \frac{2\gamma}{\gamma + 1} \cdot \frac{\rho_3'}{\rho_1} \cdot \frac{P_1}{P_3'}$$

$$A_o = \frac{\gamma - 1}{\gamma + 1} \cdot \frac{P_1}{P_3'}$$

Second doorway

Inflow Both Doorways

$$y = \frac{P_4}{P_3'}$$

$$B = \frac{2\gamma}{\gamma + 1}$$

$$A_o = \frac{\gamma - 1}{\gamma + 1} \left[1 - \left(\frac{A_4}{A_3} y^{1/\gamma} \right)^2 (1 - y) \right]$$

Outflow Both Doorways

$$y = \frac{P_4}{P_5'}$$

$$B = \frac{2\gamma}{\gamma + 1} \cdot \frac{\rho_5'}{\rho_3'} \cdot \frac{P_3'}{P_5'}$$

$$A_o = \frac{\gamma - 1}{\gamma + 1} [1 - \alpha^2 (1 - y)]$$

$$\alpha = \frac{A_4}{A_3} \cdot \frac{\rho_5'}{\rho_3'} y^{1/\gamma}$$

or alternatively

$$A_o = \frac{\gamma - 1}{\gamma + 1} \left\{ (1 - \alpha^2) \left[\frac{P_1 - P_3'}{P_5'} \cdot \frac{A_2}{A_4} + 1 \right] + \alpha^2 y \right\}$$

Inflow First Doorway/Outflow Second Doorway

$$y = \frac{P_4}{P_5'}$$

$$B = \frac{2\gamma}{\gamma + 1} \cdot \frac{\rho_5'}{\rho_3'} \cdot \frac{P_3'}{P_5'}$$

$$A_o = \frac{\gamma - 1}{\gamma + 1}$$

Outflow First Doorway/Inflow Second Doorway

$$y = \frac{P_4}{P_3'}$$

$$B = \frac{2\gamma}{\gamma + 1}$$

$$A_o = \frac{\gamma - 1}{\gamma + 1} \left[\left(\frac{P_1}{P_3'} - 1 \right) \frac{A_2}{A_4} + 1 \right]$$

In Figure E-19 results of a calculation carried out by Method F for two rooms are compared with measurement[23] of average pressure in the first room. The two rooms consisted of two small models such as those illustrated in Figures E-5 and E-6 placed back to back with a connecting door exactly like the outside door. The experiment was performed in a shock tube in which the wave struck the first doorway head-on. Also in Figure E-19 appears the result of a calculation treating the whole volume of the two model rooms as if it were in a single room. In Figure E-20 measured and calculated results for the second room in the model appear. At least in this one example, all three calculated pressure rises, i.e., in the first room, in the second room, and in the whole volume of both rooms treated as a single room, are quite similar and there appears to be no advantage in using the complicated procedures for computing the fill of two connected rooms.

The calculated histories shown in Figures E-19 and -20 have not been carried beyond the time of equilibrium between inside and outside pressures.

Figure E-21 shows pressure history calculated by Method D ignoring the wall between rooms. For this calculation the discharge coefficient has been set equal to 0.7 on inflow and 1.0 for outflow.*

The outside pressure, in Figures E-19, E-20, and E-21, labeled "input history," was measured as a pressure on the front face of the model simultaneously with the measurements of interior pressures. The short-lived reflected wave does not appear in these external histories.

IV Openings into Different Pressure Fields

The detailed calculations of inside pressure history considered in Section IIB above can easily be extended to the case of simultaneous flow into a single room through several openings, each of which is exposed to a separate outside pressure history. This situation will arise, for example, when a nuclear blast wave sweeps over a building, striking one of the four walls head-on, two side-on and exposing the fourth to the wake of the wave. If the burst is above the ground and the roof is in the regular reflection region,† the roof will be struck partly head-on; otherwise, it will be struck side-on. Head-on impact produces a strong but brief reflected wave followed by a quasi-steady wind and an associated

---

* CAVFIL, a FORTRAN program written at IIT Research Institute, was used to make the computation

† See pages 109-115, Ref. 1.

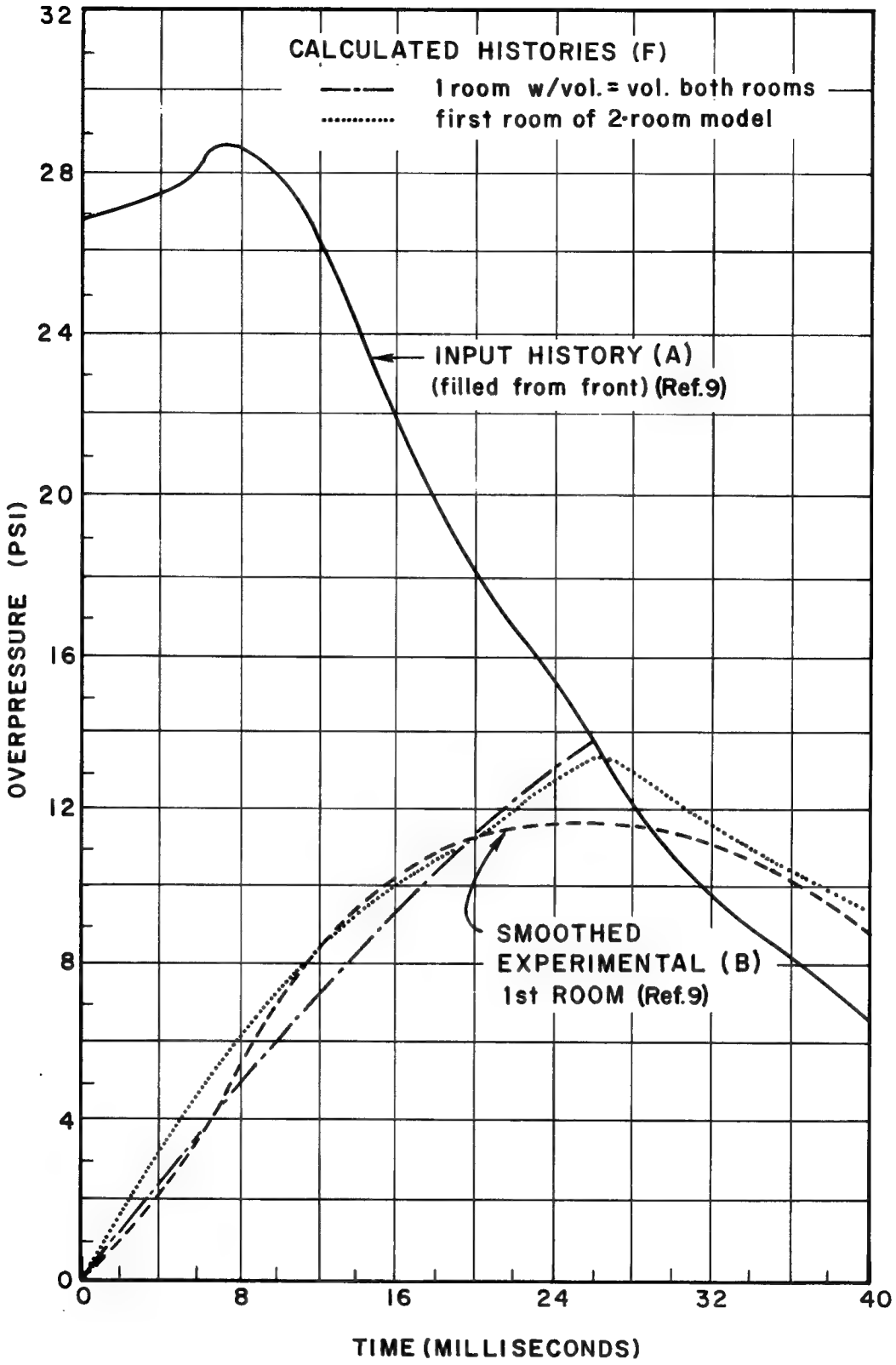

FIGURE E-19 COMPARISON OF OBSERVATIONS IN THE FIRST ROOM OF A TWO-ROOM MODEL WITH CALCULATIONS BY METHOD F

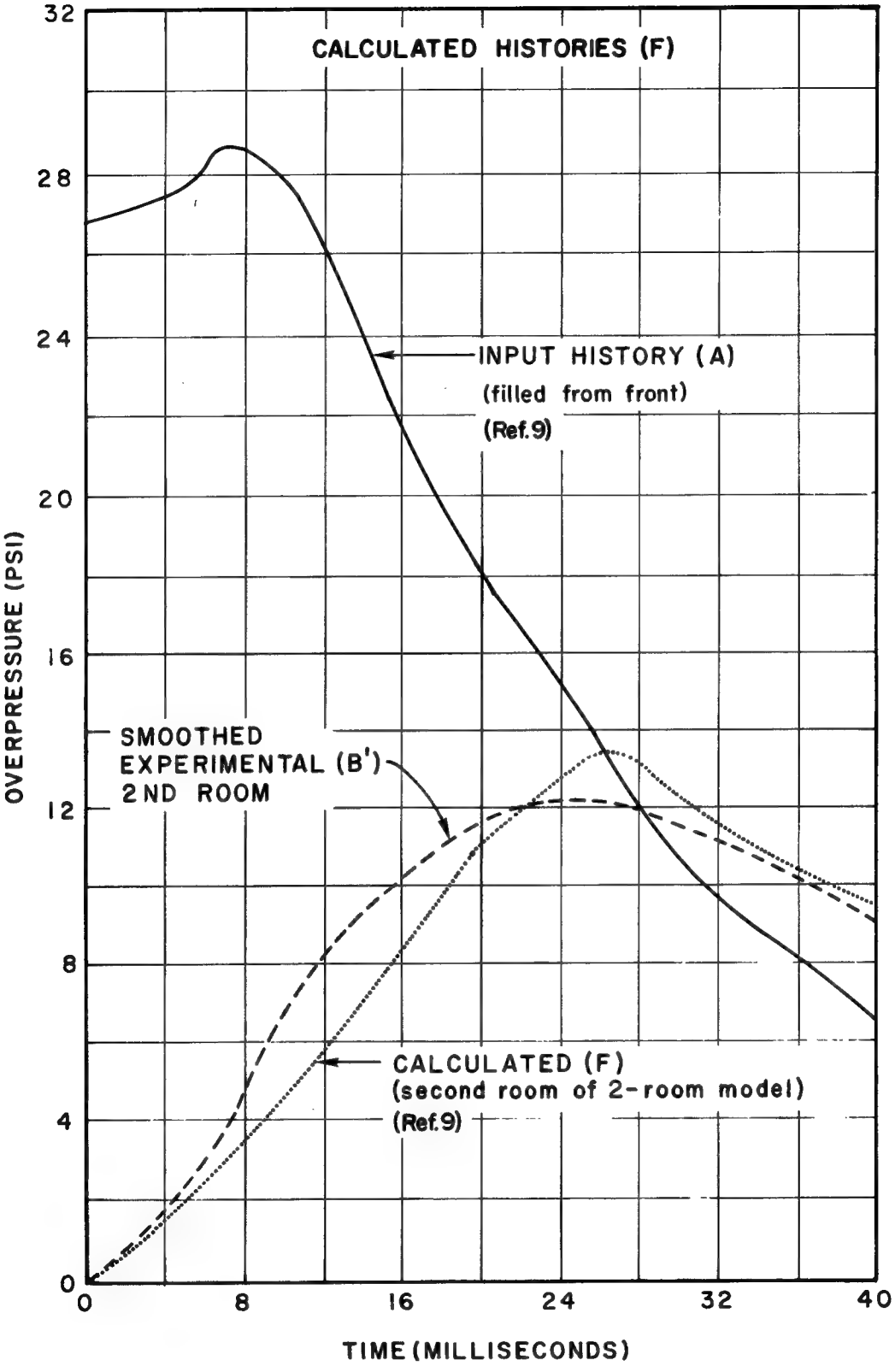

FIGURE E-20 COMPARISON OF OBSERVATIONS IN THE SECOND ROOM OF A TWO-ROOM MODEL WITH CALCULATIONS BY METHOD F

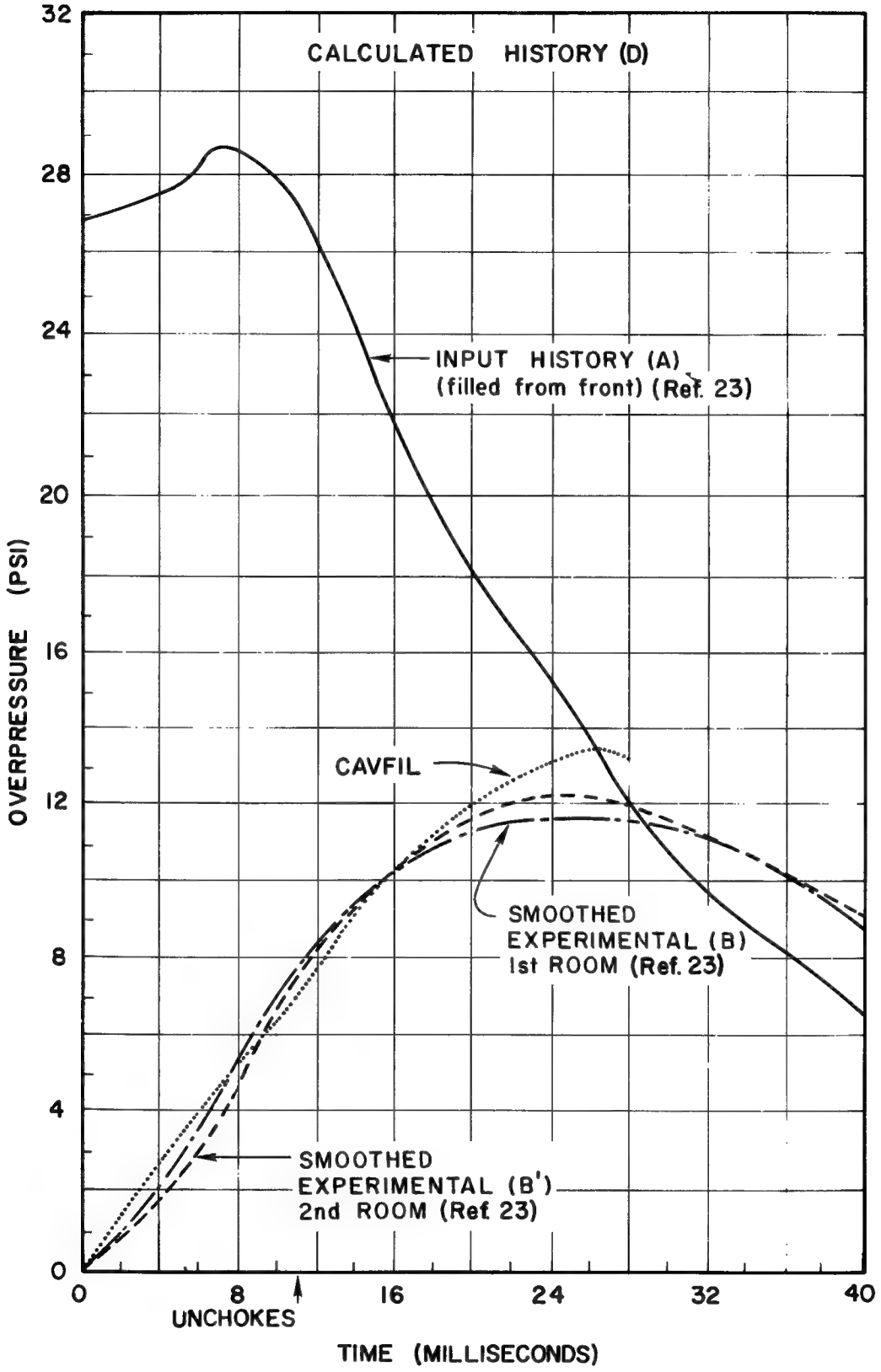

FIGURE E-21 COMPARISON OF OBSERVATIONS IN TWO-ROOM MODEL WITH CALCULATIONS BY METHOD D

strong drag force superimposed upon the free-field overpressure. When impact is not head-on, only the drag and free-field overpressures are ordinarily taken into account. References 1 and 3 contain discussions of methods of estimating outside pressure in these cases. (Reference 2 of Volume 1 of the present work gives detailed information about the drag forces exerted by wind.)

A head-on blast or shock wave striking a wall is first reflected at the surface to a peak overpressure 2 to 8 times as great as the incident. This high pressure lasts a relatively short time as rarefactions from regions of low pressure at the sides of the wall erode the reflected pressure; the erosion takes a length of time called the "clearing time." At the conclusion of clearing, pressure against the wall is the sum of free-field pressure plus a "drag" arising from the flow pattern, which has by now been established around the wall.

A wall oriented side-on to the shock front experiences no reflected pressure; and sometimes the free-field pressure against the wall is reduced by the flow past the wall. This reduction may be accounted for by assigning the wall a negative "drag" coefficient (although true drag is of course exerted in a direction parallel to the flow and is completely negligible for a more or less smooth wall). In our numerical example to follow we assume the drag coefficient of the wide walls to be zero. The pressure against walls struck completely side-on is the free-field pressure.

The wall of a rectangular building opposite to the wall struck head-on (we will call it the rear wall) will always feel a pressure less than free-field pressure, as long as the front wall stands to shield it. Here again, the drag force and drag coefficient are negative.

These principles are illustrated quantitatively in the numerical example below.

Numerical Example No. 6. As an indication of how the foregoing general procedures may be modified to account for several openings a brief numerical example is presented here.

Consider a volume contained in two rooms connected to each other by an open doorway and consider each room connected to the outside by a single doorway, as shown in Figure E-22. The blast wave that sweeps over the structure will be characterized by a free-field overpressure of 10 psig, head-on incidence upon the opening to the larger room, and

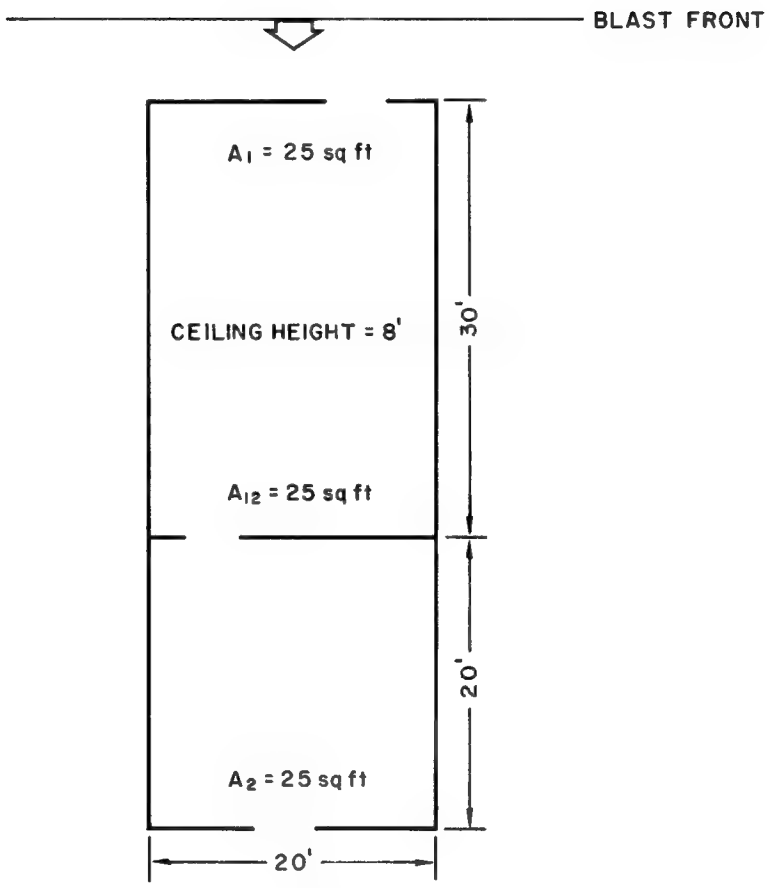

FIGURE E-22 SKETCH ILLUSTRATING NUMERICAL EXAMPLE

positive phase duration of 1 sec. Standard conditions will be assumed, i.e., P_o = 14.7 psia and ρ_o = 0.0761 lb/ft^3. In the front wall the opening area is 25 sf^2 and there is a like opening in the rear wall. Because the door between the rooms has an area comparable to the area of each of the outside doors, the presence of the partition will be ignored and the volume to be filled taken as

$$V_3 = 50 \times 20 \times 8 = 8000 \text{ cf}$$

As a first step the pressure histories outside the two doors will be calculated, according to the procedures recommended by Ref. 1. Since the first window is struck head-on, there will be no time delay there and the peak pressure will be the reflected pressure P_R, which is calculated as:

$$P_R = 2 \ P_{so} \cdot \frac{7 \ P_o + 4 \ P_{so}}{7 \ P_o + P_{so}}$$

Here

P_{so} = 10 psi and P_o = 14.7 psi; hence

P_R = 25.3 psi

This reflected pressure will be felt in declining strength for the duration of the clearing time, t_c, which is estimated as

$$t_c = \frac{3s}{c}$$

where s is a dimension of the wall undergoing pressure clearing and c is sound speed. In this case

$$c = \left(\gamma \ P_o/\rho_o\right)^{1/2} = \left(1.4 \times 14.7 \times 32 \times 144/0.076096\right)^{1/2} = 1116 \text{ ft/sec}$$

and $s = 20$

so that

t_c = 53.7 ms

As an approximation, the decline of reflected pressure during the interval

$$0 \leq t \leq t_c$$

is treated as linear; that is, at $t = t_c$ *the pressure* P_c *on the first wall is simply the sum of the free-field overpressure* P_{sc} *and the drag* P_{dc} *arising from the winds behind the shock front. Since during the time* t_c *free-field pressure has fallen exponentially*[1] *from* $P_{so} = 10$ *psi:*

$$P_{sc} = P_{so} \left(1 - \frac{t_c}{t_o}\right) e^{-t_c/t_o}$$

where t_o *is the free-field duration of positive overpressure; in this case* $t_o = 1$ *sec so that*

$$P_{sc} = 8.97 \text{ psi}$$

Peak drag pressure P_{do} *is computed from the formula*

$$P_{do} = \frac{5}{2} \cdot \frac{(P_{so})^2}{7\,P_o + P_{so}} = \frac{5}{2} \cdot \frac{100}{7 \times 14.7 + 10} = 2.21 \text{ psi}$$

so that drag pressure at $t = t_c$ *is:*[1]

$$P_{dc} = P_{do} \left(1 - \frac{t_c}{t_o}\right)^2 e^{-2\,t_c/t_o}$$

Numerically, this is

$$P_{dc} = 1.78 \text{ psi}$$

Therefore the pressure outside the first opening at $t = t_c$ *is:*

$$P_c = P_{sc} + P_{dc} = 8.97 + 1.78 = 10.75$$

and, assuming a linear fall from P_{so} *to* P_c*, for* $0 \le t \le t_c$*, pressure* P_1 *outside first wall as a function of time becomes:*

$$P_1 = P_c + \frac{(t_c - t)}{t_c} (P_R - P_c) \qquad (79)$$

For the remainder of the positive phase duration, outside pressure at the first opening is simply the sum of the decayed side-on pressure

$$P_s = P_{so} \left(1 - \frac{t}{t_o}\right) e^{-t/t_o} \tag{80}$$

and decayed dynamic pressure

$$P_d = P_{do} \left(1 - \frac{t}{t_o}\right)^2 e^{-2t/t_o} \tag{81}$$

so that for $t_o > t > t_c$

$$P_1 = P_s + P_d \tag{82}$$

For the first wall a drag coefficient equal to + 1.0 has been tacitly assumed above but for the second opening this coefficient will be different from 1, and according to Ref. 1, a value of -0.4 can be assumed. At the rear opening there is no reflected pressure and the delay is equal to the time taken by the front to traverse the building (assuming that the opening is already open upon blast arrival or that it is immediately forced open by the blast). Blast front speed can be found from the formula[1]

$$U = c_o \left(1 + \frac{\gamma + 1}{2} \cdot \frac{P_{so} - P_o}{P_o}\right)^{1/2}$$

where c_o = sound speed in ambient air, i.e.,

$$c_o = \left(\gamma P_o \, 32 \times 144/\rho_o\right)^{1/2} = 1116 \text{ ft/sec}$$

Hence,

$$U = 1116 \times \left(1 + \frac{2.4}{2.8} \times \frac{10}{14.7}\right)^{1/2} = 1148 \text{ ft/sec}$$

so that delay at the rear entrance is $\frac{50}{1148} = 43.5$ ms.

Beginning at $t = 43.5$ ms the room starts to fill through the rear opening. (Outflow through openings other than the first can ordinarily be neglected during the delay period: either the other openings are closed to the blast for a certain period or, if not, the blast travel time to them is much shorter than the time required to start outflow through them.)

Filling through the rear opening takes place however from a reservoir at lower pressure than that outside the front opening, i.e., outside pressure P_{1r} at the rear is:

$$P_{1r} = P_s - 0.4\ P_d \qquad (83)$$

The decline in P_{so} and P_{do} that occurs while the blast front travels from front to rear opening is negligibly small and can be safely neglected for buildings of ordinary size.

For this sample case, the quantities P_1 (pressure outside the front opening) and P_{1r} (pressure outside the rear opening) have been calculated as functions of time and plotted in Figure E-23. The figure shows the discontinuity in the derivative of P_1 with respect to time at the point (t_c, P_c) when the reflected pressure is assumed to disappear and the outside pressure takes on its quasi-steady value.

Also plotted in the figure are inside pressure histories P_3 calculated by two methods: the greatly simplified procedure given in Section IIA of this report and the step-by-step Method F explained in Section IIB. In the first of these two procedures, the estimated history is given by the line segments ODFG obtained as follows. When the blast arrives at the front opening, filling immediately begins along line OA, where point A is the intersection of the outside pressure history and the abscissa

$$t = \frac{V_3}{2A_1} = \frac{8000}{2 \times 25} = 160 \text{ ms}$$

Line BC is a similar line representing filling through the rear opening, beginning after the delay time of 43.5 ms. Ordinates under the line BC have been added to ordinates of OA to produce the line DE. Since areas of both openings are equal, the point F is placed halfway between current outside pressures outside the front and rear openings and the decline of P_3 represented schematically by the line FG.

The step-by-step calculation results in the curve labelled "Method F" in Figure E-23. Because of the high reflected pressure during the interval $0 \le t \le t_c$ (which does not influence the results of the simplified method in this example), the more careful calculation shows a faster build-up of

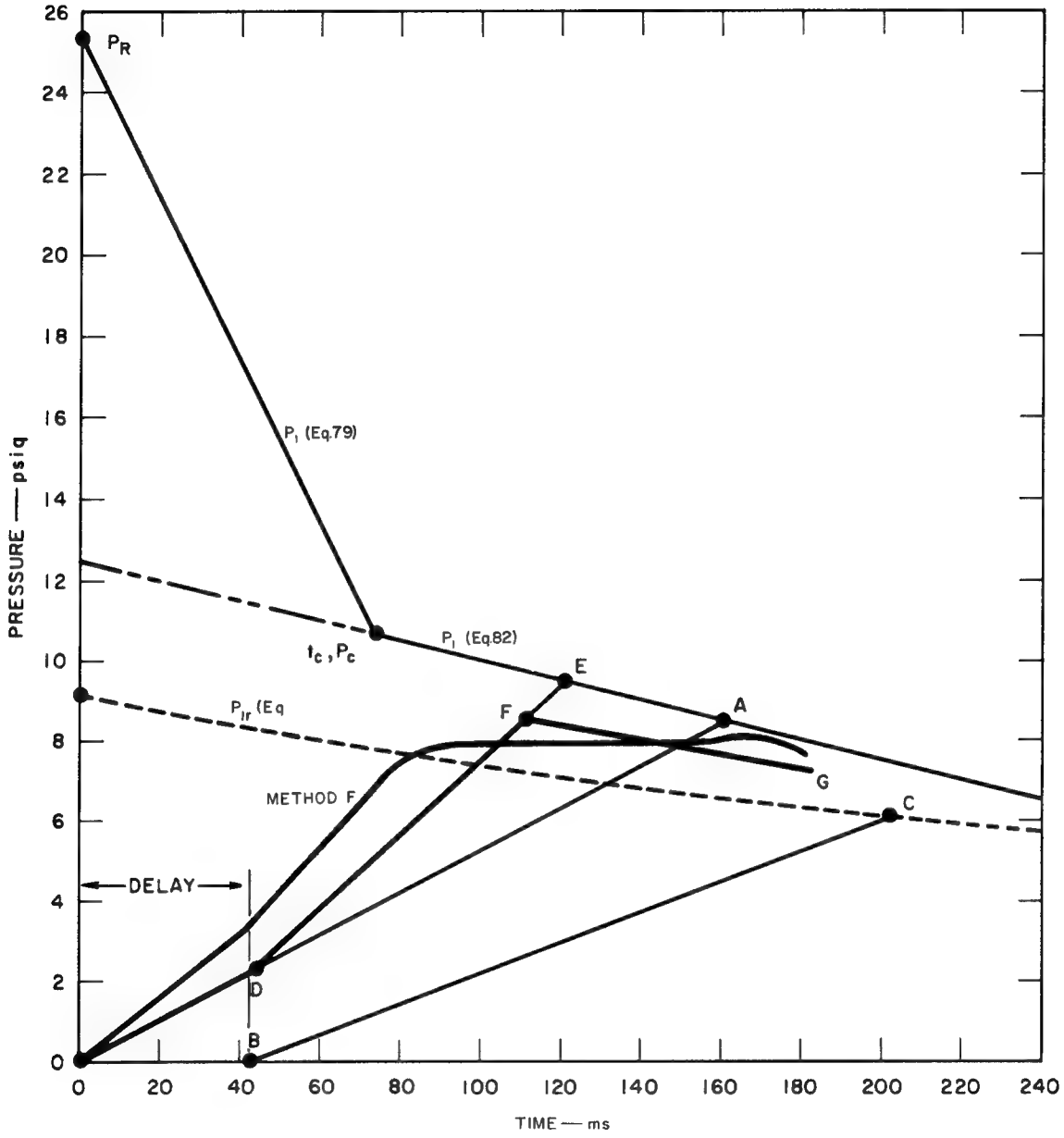

FIGURE E-23 ILLUSTRATIVE EXAMPLE

room pressure than the line ODF. To demonstrate the method the first step of the stepwise solution will be calculated below. In this sample calculation the reverberation time t_1 (Eq. (30)) is assumed to be zero for simplicity.

Since the least sound transit time across the room is approximately 20 ms we will choose a value of $\Delta t = 5$ ms. At $t = 0$ there is only one opening, that in the front wall. Outside pressure there at that time is $P_R = 25.3$ psig. Inside pressure $P_3' = P_o = 14.7$ psia and density is $\rho_3' = \rho_o = 0.002378$ slug/cf.

1. $P_1 = 25.3 + 14.7 = 40.0$ psia.

2. $\rho_1 = \left(\frac{P_1}{P_0}\right)^{1/\gamma} \rho_o = \left(\frac{40.0}{14.7}\right)^{1/1.4} (0.002378) = 0.004861$ slug/cf

3. $P_2 = 0.1912 \quad P_1 = (0.1912) \times (40.0) = 7.65$ psia

4. $\rho_2 = \left(\frac{P_2}{P_1}\right)^{1/\gamma} \rho_1 = (0.307) \times (0.004861) = 0.001492$ slug/cf

5. $u_2^2 = \frac{2\gamma}{\gamma - 1}\left(\frac{P_1}{\rho_1} - \frac{P_2}{\rho_2}\right) = \frac{2.8}{0.4}\left(\frac{40.0}{0.004861} - \frac{7.65}{0.001492}\right) \times 144 = 3.13 \times 10^6 \frac{ft^2}{sec^2}$

6. *Since $P_1 > P_3'$: $u_2 > 0$, i.e., flow is inward. Were $P_3' > P_1$, u_2 would be negative.*

7. $\Delta m_{31} = u_2 \rho_2 A_1 \Delta t = 0.3298$ slug.

8. $q_{core} = \left(\frac{\Delta m_{31}}{\Delta t}\right)^2 / 2 \rho_3' A_1^2 (144) = 10.0$ psi

9. $\Delta w_{31} = \frac{P_1 \Delta m_{31}}{\left(\frac{\gamma - 1}{\gamma}\right) \rho_1} = \frac{(40.0)(0.3298)}{\frac{0.4}{1.4}(0.004861)} \times 144 = 1.36 \times 10^6$ ft lb

10. *Since the rear opening is closed at this time:*

$$\Delta m_{32} = \Delta w_{32} = 0$$

Were the second opening available, Steps 1 - 9 would be repeated using initial outside pressure at rear opening to calculate Δm_{32} *and* Δw_{32}

11. $\Delta m_3 = \Delta m_{31} + \Delta m_{32} = 0.3298$ *slug*

12. $\Delta w_3 = \Delta w_{31} + \Delta w_{32} = 1.36 \times 10^6$ *ft lb*

13. $P_3 = P_3' + \dfrac{(\gamma - 1)\,\Delta w_3}{V_3} = 14.7 + \dfrac{(0.4)(1.36 \times 10^6)}{8000 \times 144} = 15.17$ *psia (room pressure)*

14. $\rho_3 = \rho_3' + \dfrac{\Delta m_3}{V_3} = 0.002378 + \dfrac{0.3298}{8000} = 0.002419$ *slug/cf (air density in room)*

15. P_3' *equal to* P_3 *and* ρ_3' *equal to* ρ_3 *and return to Step 1 with value of* P_1 *at* $t = \Delta t = 5$ *ms*

V. Computer Program

The time-sharing computer program listed in Table E-2 will calculate and report average pressure inside an open room exposed to a nuclear blast wave. Dynamic pressures of winds entering the room and translation speeds of objects caught in a jet(s) may be obtained also. The program is interactive or conversational, that is, the user provides necessary input data by typing responses to questions. A sample input and output listing is shown in Table E-3. The user's responses are underlined.

Provision is made in the program for a maximum of eight openings into the room from the outside; delay times between wave front arrival (at the blastward face of the room) and the start of flow through the opening must be applied. Delays will be caused by shock travel time

Table E-2
COMPUTER PROGRAM

```
100C INTERACTIVE FØRTRAN PRØGRAM TØ CØMPUTE HISTØRY ØF AVERAGE PRESSURE
101C AND DYNAMIC PRESSURE DISTRIBUTIØN WITHIN A SINGLE RØØM WHICH IS
102C FILLING FRØM A NUCLEAR BLAST WAVE THRØUGH AS MANY AS EIGHT
103C ØPENINGS IN ANY WALL ØR WALLS ØF RØØM. IF DESIRED, PRØVIDES
104C SØME TRANSLATIØNAL EFFECTS ØN AN ØBJECT CAUGHT IN JET.
105C USES METHØD F. CANNØT CØMPUTE BEYØND END ØF PØSITIVE PHASE.
110       CØMMØN G2,G3,L3,Q(500,8),T(500),A(8,2),NWIN,NTI,C,AB
120       LØGICAL L1,L2,L3,L4,L5,L6,L7,L8
130       DIMENSIØN P(500),N(8),Q2(8),PØUT(8)
140       DIMENSIØN Q3(8),DREV(8),TREV(8)
150       PRINT,"AMBIENT AIR PRESSURE (PSIA)"
160       INPUT,P0
170       PRINT,"AMBIENT AIR DENSITY (SLUGS/CF)"
180       INPUT,RH00
190       PRINT,"RØØM VØLUME (CF)"
200       INPUT,V3
210       PRINT,"NUMBER ØF ØPENINGS (NØT MØRE THAN 8)"
220       INPUT,NWIN
230       PRINT,"AREAS ØF EACH ØPENING (SF)"
240       INPUT,(A(I,1),I=1,NWIN)
250       PRINT,"LØCATIØN CØDE FØR EACH ØPENING"
260       INPUT,(N(I),I=1,NWIN)
270       PRINT,"DELAY IN ENTRY AT EACH ØPENING (MS)"
280       INPUT,(A(I,2),I=1,NWIN)
290       PRINT,"CØMMUNICATIØN DISTANCE (FT) FØR EACH ØPENING"
300       INPUT,(DREV(I),I=1,NWIN)
310       PRINT,"CLEARING TIME (MS)"
320       INPUT,TC
330       PRINT,"DRAG CØEFFS FØR LØCATIØN CØDES 1, 2 AND 3"
340       INPUT,CDFF,CDFS,CDFR
350       PRINT,"PEAK FREE FIELD ØVERPRESSURE (PSIG)"
360       INPUT, PS0
370       PRINT, "DURATIØN ØF PØSITIVE PHASE (SEC)"
380       INPUT, T0
390       TC=TC/1000.
400       PRINT,"WANT PEAK VALUES ØNLY (.TRUE. ØR .FALSE.)"
410       INPUT,L1
420       IF(L1)GØ TØ 3
430       PRINT,"INTERVAL BETWEEN VALUES ØF ØUTPUT (MS)"
440       INPUT,TI
450       TI=TI/1000.
460       PRINT,"WANT  DECLINE ØF RØØM PRESSURE (.TRUE. ØR .FALSE.)"
470       INPUT,L2
480       GØ TØ 5
490     3 TI=T0/99.
500       L2=.FALSE.
510     5 L3=.FALSE.
520       L7=.FALSE.
530       PRINT,"WANT ØUTSIDE PRESSURE (.TRUE. ØR .FALSE.)"
540       INPUT,L5
550       PRINT,"WANT DYNAMIC PRESSURES (.TRUE. ØR .FALSE.)"
560       INPUT,L4
570       PRINT,"WANT TRANSLATIØN EFFECTS (.TRUE. ØR .FALSE.)"
580       INPUT,L6
590       IF(.NØT.L6)GØTØ 6
600       PRINT,"ACCELERATIØN CØEFFICIENT (SF/SLUG)"
610       INPUT,AB
620     6 IF(L5)PRINT 26
630       PR=2.*PS0*(7.*P0+4.*PS0)/(7.*P0+PS0)
640       PD0=2.5*PS0*PS0/(7.*P0+PS0)
650       PSC=PS0*(1.-TC/T0)*EXP(-TC/T0)
660       PDC=PD0*(1.-TC/T0)*(1.-TC/T0)*EXP(-2.*TC/T0)
670       PC=PSC+PDC
680       NT=T0/TI+1
690       NTI=NT
700       IF(NT.LE.500)GØTØ 13
710       TMAX=500.*TI
720       PRINT,"***VECTØR ØVERLØADED - TIME INTERVAL TRUNCATED"
730       PRINT,"MAX. TIME= ",TMAX," (SEC)"
740       NTI=500
750    13 G=1.4; G2=1./G ; G3=1.-G2 ; G4=2./G3
760       G5=G+1.; G6=2.*G/G5; G7=(G-1.)/G5
770       G9=.1912**G2
780       GP0=2.*G*P0 ; GPS=2.*G*(PS0+P0)
785       PCRIT=(2./G5)**(G/(G-1.))
790       RH010=RH00*(GP0+G5*PS0)/(GP0+(G-1.)*PS0)
800       RH011=RH010*(GPS+G5*(PR-PS0))/(GPS+(G-1.)*(PR-PS0))
810       C=SQRT(G*P0*144./RH00)
820       DØ 7 I=1,NWIN
830       TREV(I)=4.*DREV(I)/C
840       Q2(I)=0.
850       A(I,2)=A(I,2)/1000.
860     7 CØNTINUE
870       DØ 8 I=1,NWIN
880       DØ 8 J=1,NTI
890     8 Q(J,I)=0.0
895       I2=0
900       P30=P0 ; RH030=RH00
910       TT=0. ; T0=0.
920       TAU=2.*(V3**(1./3.))/C
930       DT=TAU/10.
940       DDT=DT
950     9 IF(TI-2.*DDT)10.11,11
960    10 DDT=DDT/2.
970       GØ TØ 9
980    11 IF(DDT-.0005*T0)31,32,32
982    32 DDT=DDT/2.
984       GØ TØ 11
986    31 IST0P=TI/DDT+1
990       DDT=TI/IST0P
1000       MC=-1
1010       DØ 990 J=1,NT1
1020       IF(J.GT.500)GØTØ 992
1030       DØ 99 I=1,IST0P
1040       MC=MC+1
1050       MD=2 ; II=I
1060       IF(MC.NE.0)GØ TØ 62
1070       II=I-1 ; MD=1
```

```
1080   62  TT=T0+II*DDT
1090       IF(TT.GT.T0)G0 T0 99
1100       R=TT/T0 ; RR=1.-R
1110       PD=PD0*RR*RR*EXP(-2.*R)
1120       PS=PS0*RR*EXP(-R)
1130       DM=0. ; W=0.
1140       D0 500 K=1,NWIN
1150       M=N(K) ; DLY=A(K,2)
1160       IF(DLY.GT.TT)G0 T0 500
1170       PS1=PS0+P0
1180       RH012=RH010
1190       G0 T0 (15,16,17),M
1200   15  CDF=CDFF
1205       IF(TC.EQ.0.)G0 T0 21
1210       IF(TT-TC)20,20,21
1220   20  P11=(TC-TT)*(PR-PC)/TC+PC
1230       RH012=RH011
1240       PS1=PR+P0
1250       G0 T0 30
1260   16  CDF=CDFS
1270       G0 T0 21
1280   17  CDF=CDFR
1290   21  P11=PS+CDF*PD
1300   30  P0UT(K)=P11
1310       P11=P11+P0
1320       RH01=RH012*((P11/PS1)**G2)
1330       L8=.FALSE.
1340       US=0.
1350       DDM1=0.
1360       IF(TT.GE.TREV(K))G0T0 1
1370       US=(C*PS/(G*P0))/SQRT(1.+PS/(G6*P0))
1380       DDM1=RH01*US
1390       L8=.TRUE.
1400    1  IF(P11-P30)36,35,37
1410   35  U22=0.
1420       G0 T0 39
1430   36  JSIGN=-1
1440       AA=G7*P11/P30
1450       BB=G6*RH030*P11/(RH01*P30)
1460       Z=P11/(RH01**G)
1470       Y=.9094*P30/(RH030**G)
1480       IF(Y.GT.Z)G0 T0 60
1490       CALL EQ(AA,BB,P2)
1500       IF(.N0T.L3)G0 T0 303
1510       NT1=J
1520       G0 T0 19
1530   60  X=P30/RH030
1532       Y=P11/P30
1534       IF(Y.GT.PCRIT)Y=PCRIT
1536       RH02=RH030*(Y**G2)
1540       P2=P11
1542       IF(I2.EQ.0) PRINT, "Y.GT.Z, METH0D D USED IN S0ME CALCULATI0NS"
1544       I2=1
1546       G0 T0 44
1550  303  RH02=((P2)**G2)*RH030
1560       P2=P2*P30
1570       X=P30/RH030
1580       G0 T0 38
1590   37  JSIGN=+1
1600       P2=.1912*P11
1610       RH02=G9*RH01
1620       X=P11/RH01
1630   38  U22=G4*(X-P2/RH02)*144.
1635   44  CONTINUE
1640       IF(U22)40,39,39
1650   40  PRINT,"U22 NEGATIVE",U22
1660       PRINT,"JSIGN=",JSIGN
1670       G0 T0 999
1680   39  U2=SQRT(U22)*JSIGN
1690       Q2(K)=0.
1700       G0 T0 (500,65),MD
1710   65  DDM=U2*RH02
1720       IF(L8)G0T0 4
1730       Q2(K)=JSIGN*DDM*DDM/(2.*RH01*144.*((P30/P11)**G2))
1740       DDM=DDM*A(K,1)*DDT
1750       G0T0 2
1760    4  DDM=DDM1+(DDM-DDM1)*TT/TREV(K)
1770       Q2(K)=JSIGN*DDM*DDM/(2.*RH01*144.*((P30/P11)**G2))
1780       DDM=DDM*A(K,1)*DDT
1790       G0T0 2
1800    2  DM=DM+DDM
1810       W=W+P11*DDM/(G3*RH01)
1820   500 CONTINUE
1830       P3A=P30
1840       RH030=RH030+DM/V3
1850       P30=P30+(G-1.)*W/V3
1860       IF(.N0T.L2.AND.P30.LT.P3A)G0T0 80
1870       G0 T0 (19,99),MD
1880   80  L7=.TRUE.
1890       NT1=J
1891       P30=P3A
1892       TT=TT-II*DDT
1900       G0 T0 19
1910   99  CONTINUE
1920   19  T0=TT
1930       P(J)=P30-P0
1940       T(J)=TT
1950       IF(L5)PRINT 27,J,(P0UT(K),K=1,NWIN)
1960       D0 18 L=1,NWIN
1970       IF(Q2(L))41,42,42
1980   41  Q(J,L)=0.
1990       G0T0 43
2000   42  Q(J,L)=Q2(L)
2005       IF(L7) Q(J,L)=Q3(L)
2010   43  Q2(L)=0.
2020   18  CONTINUE
2030       IF(L3)G0 T0 992
2040       IF(L7)G0T0 800
2050  990  CONTINUE
```

Table E-2 (Continued)

```
2060 800   IF(L1)G0T0 991
2070       G0 T0 992
2080 991   PRINT 50,T(NT1),P(NT1),(Q(2,K),K=1,NWIN)
2090  50   F0RMAT(1H0,30X,11HPEAK VALUES//1H 6HTIME= ,E11.4,1X,
2100      &3HSEC,4X,10HPRESSURE= ,E11.4,1X,4HPSIG//
2110      &18H DYNAMIC PRESSURES,1X,5H(PSI)/8(1H E11.4/))
2120       ST0P
2130 992   PRINT 22
2140       D0 993 I=1,NT1
2150       PRINT 51,I,T(I),P(I)
2160 993   C0NTINUE
2170  22   F0RMAT(1H-///14H TIME STEP N0.,3X,9HTIME(SEC),7X,7HINSIDE
2180&      15HPRESSURE (PSIG)//)
2190  51   F0RMAT(1H ,I10,5X,E11.4,5X,E11.4)
2200       PRINT," "
2210       IF(.N0T.L4)G0 T0 995
2220       PRINT 23
2230       D0 994 I=1,NT1
2240       PRINT 24,T(I),(Q(I,K),K=1,NWIN)
2250 994   C0NTINUE
2260
2270 995   IF(L6)CALL SLIDE
2280  23   F0RMAT(1H-///1H 15X,40HC0RE DYNAMIC PRESSURES (PSI) AT EACH 0PE
2290&      ,4HNING//12H 0PENING N0.,2X,1H1,7X,1H2,7X,1H3,7X,1H4,7X,1H5,7X,
2300&      1H6,7X,1H7,7X,1H8//10H TIME(SEC)//)
2310  24   F0RMAT(1H F7.3,1X,8F8.2)
2320  26   F0RMAT(1H0,14X,40H0UTSIDE PRESSURES (PSIG) AT EACH 0PENING//
2330&      12H 0PENING N0.,5X,1H1,6X,1H2,6X,1H3,6X,1H4,6X,1H5,6X,1H6,
2340&      6X,1H7,6X,1H8//14H TIME STEP N0.//)
2350  27   F0RMAT(1H ,I6,7X,8(F6.2,1X))
2360 999   ST0P
2370       END
2380       SUBR0UTINE EQ(A,B,X)
2390C SOLVES THE EQUATION B*(X**G2)=X+A F0R X
2400       C0MM0N G2,G3,L3
2410       L0GICAL L3
2420       X0=(B*G2)**(1./G3)
2430       F1=X0+A
2440       F2=B*(X0**G2)
2450       IF(F1-F2)1,2,3
2460   3   PRINT,"N0 S0LN IN EQ"
2470       L3=.TRUE.
2480       RETURN
2490   2   IF(X0-1.)4,5,5
2500   5   PRINT,"N0 S0LN IN EQ LT 1"
2510       L3=.TRUE. ; RETURN
2520   4   X=X0 ; RETURN
2530   1   N=0
2540       IF(X0-1.)8,42,7
2550   7   N=1
2560   8   F1=1.+A
2570       IF(F1-B)9,10,11
2580   9   N=N+3 ; G0 T0 12
2590  10   N=N+1 ; G0 T0 12
2600  11   N=N+5
2610  12   G0 T0 (40,5,40,42,39,5),N
2620  39   XU=1. ; XL=X0 ; G0T0 21
2630  40   XU=X0 ; XL=0. ; G0 T0 21
2640  42   XU=1. ; XL=0. ; G0 T0 21
2650  21   XM=(XU+XL)/2.
2660       R=(XU-XL)/XU
2670       IF(R-0.001)22,23,23
2680  23   F1=XM+A
2690       F2=B*(XM**G2)
2700       IF(F1-F2)24,22,25
2710  24   XU=XM
2720       G0 T0 21
2730  25   XL=XM ; G0 T0 21
2740  22   X=XM
2750  99   RETURN
2760       END
2770  SUBR0UTINE SLIDE
2780  C0MM0N G2,G3,L3,Q3(500,8),T(500),A(8,2),NWIN,NT,C,AA
2790  PRINT 7
2800  3  F0RMAT(1H ////)
2810  PRINT 4, AA
2820  AA=AA*144.
2830  4  F0RMAT(1H-,22X,27H***TRANSLATI0N 0F 0BJECT***//
2840&     27H ACCELERATI0N C0EFFICIENT =,F9.4,2X,9H(SF/SLUG)/
2850&     32H C00RDINATES CENTERED IN 0PENING)
2860  NT2=NT-1
2870  D0 900 I=1,NWIN
2880  PRINT 3
2890  PRINT 5,I
2900  5  F0RMAT(13H 0PENING N0. ,I1////16H INITIAL C00RDS.,6X,
2910  & 13HFINAL C00RDS.,9X,11HFINAL SPEED/16H   X (FT)   Y (FT),5X,
2920  &  16H   X (FT)   Y (FT),8X,5H(FPS)//)
2930  7  F0RMAT(1H //////)
2940  B0=2.*SQRT(A(I,1)/3.14158)
2950  X1=4.5*B0
2960  X2=X1+2.2*B0
2970  X3=5.*X2
2980  DELX=X1/10.
2990  DELY=X1/2.
3000  NJ=1000
3010  NK=1000
3020  D0 895 J=1,NK
3030  X0=(J-1)*DELY
3040  PRINT," "
3050  Y=0.
3060  M=0
3070  D0 890 K=1,NJ
3080  Y=(K-1)*DELX
3090  X=X0
3100  V=0.
3110  D0 880 L=1,NT2
3120  Q0=(Q3(L,I)+Q3(L+1,I))/2.
3130  IF(Q0)15,18,18
```

Table E-2 (Continued)

```
      15  Q0=0.
      18  IF(X.GE.X1)G0T0 50
      IF(Y.GT.(.1577*X+B0/2.))G0T0 20
      IF(Y.GT.B0/2.)G0T0 30
      G0T0 40
      20  Q=0.
      M=1
      G0T0 100
      30  B=.27*X
      QA=Q0
      10  E=(B-(Y-(X1-X)/9.))/B
      Q=QA*(1.-(1.-E**1.5)**2.)**2.
      G0T0 100
      40  R=Y/(X1-X)
      IF(R-.1111)42,42,30
      42  Q=Q0
      G0T0 100
      50  IF(X-X2)60,60,70
      60  B=.27*X1+(.22*X2-.27*X1)*(X-X1)/(X2-X1)
      F=Y/B
      IF(F.GT.1)G0T0 20
      E=B0/(1.08*X)+.584
      QA=Q0*(1.-(1.-E**1.5)**2.)**2.
      G0 T0 10
      62  E=Y/B
      IF(E.GT.1)G0T0 20
      Q=Q0*((1.-E**1.5)**4.)*((6.2*B0/X)**2.)
      G0T0 100
      70  B=.22*X
      G0T0 62
      100  DT=T(L+1)-T(L)
      V=V+AA*Q*DT
      X=X+V*DT
      IF(M-1)880,220,220
      220  PRINT 25,X0,Y,X,Y,V
      G0T0 895
      880  C0NTINUE
      PRINT 25,X0,Y,X,Y,V
      IF(V-10.)891,891,890
      891  K=NJ
      IF(Y.LT.DELX)J=NK
      25  F0RMAT(1H ,F6.1,2X,F6.1,6X,F6.1,2X,F6.1,8X,F6.1/)
      890  C0NTINUE
      895  C0NTINUE
      900  C0NTINUE
      RETURN
      END
```

Table E-2 (Concluded)

```
 1. AMBIENT AIR PRESSURE (PSIA)?14.7
 2. AMBIENT AIR DENSITY (SLUGS/CF)?.002378
 3. R00M V0LUME (CF)?1.311E6
 4. NUMBER 0F 0PENINGS (N0T M0RE THAN 8)?8
 5. AREAS 0F EACH 0PENING (SF)?25,25,12.6,77,139.8,125,125,229.4
 6. L0CATI0N C0DE F0R EACH 0PENING?2,2,2,2,2,2,2,2
 7. DELAY IN ENTRY AT EACH 0PENING (MS)?22,208,0,0,0,22,208,241
 8. C0MMUNICATI0N DISTANCE (FT) F0R EACH 0PENING?3.5,3.5,2,7.6,3.5,3.5,6
 9. CLEARING TIME (MS)?0
10. DRAG C0EFFS F0R L0CATI0N C0DES 1, 2 AND 3?1.0,-.4
11. PEAK FREE FIELD 0VERPRESSURE (PSIG)?10
12. DURATI0N 0F P0SITIVE PHASE (SEC)?4
13. WANT PEAK VALUES 0NLY (.TRUE. 0R .FALSE.)?F
14. INTERVAL BETWEEN VALUES 0F 0UTPUT (MS)?50
15. WANT  DECLINE 0F R00M PRESSURE (.TRUE. 0R .FALSE.)?F
16. WANT 0UTSIDE PRESSURE (.TRUE. 0R .FALSE.)?T
17. WANT DYNAMIC PRESSURES (.TRUE. 0R .FALSE.)?T
18. WANT TRANSLATI0N EFFECTS (.TRUE. 0R .FALSE.)?T
19. ACCELERATI0N C0EFFICIENT (SF/SLUG)?.708
```

0UTSIDE PRESSURES (PSIG) AT EACH 0PENING

0PENING N0. / TIME STEP N0.	1	2	3	4	5	6	7	8
1	0.	0.	10.00	10.00	10.00	0.	0.	0.
2	9.75	0.	9.75	9.75	9.75	9.75	0.	0.
3	9.51	0.	9.51	9.51	9.51	9.51	0.	0.
4	9.27	0.	9.27	9.27	9.27	9.27	0.	0.
5	9.04	0.	9.04	9.04	9.04	9.04	0.	0.
6	8.81	8.81	8.81	8.81	8.81	8.81	8.81	8.81
7	8.58	8.58	8.58	8.58	8.58	8.58	8.58	8.58
8	8.36	8.36	8.36	8.36	8.36	8.36	8.36	8.36
9	8.14	8.14	8.14	8.14	8.14	8.14	8.14	8.14
10	7.93	7.93	7.93	7.93	7.93	7.93	7.93	7.93
11	7.72	7.72	7.72	7.72	7.72	7.72	7.72	7.72
12	7.52	7.52	7.52	7.52	7.52	7.52	7.52	7.52
13	7.32	7.32	7.32	7.32	7.32	7.32	7.32	7.32
14	7.12	7.12	7.12	7.12	7.12	7.12	7.12	7.12
15	6.93	6.93	6.93	6.93	6.93	6.93	6.93	6.93
16	6.74	6.74	6.74	6.74	6.74	6.74	6.74	6.74
17	6.55	6.55	6.55	6.55	6.55	6.55	6.55	6.55
18	6.43	6.43	6.43	6.43	6.43	6.43	6.43	6.43

TIME STEP N0.	TIME(SEC)	INSIDE PRESSURE (PSIG)
1	0.	0.
2	0.5000E-01	0.2165E+00
3	0.1000E+00	0.4655E+00
4	0.1500E+00	0.7116E+00
5	0.2000E+00	0.9550E+00
6	0.2500E+00	0.1339E+01
7	0.3000E+00	0.1815E+01
8	0.3500E+00	0.2286E+01
9	0.4000E+00	0.2752E+01
10	0.4500E+00	0.3213E+01
11	0.5000E+00	0.3669E+01
12	0.5500E+00	0.4120E+01
13	0.6000E+00	0.4567E+01
14	0.6500E+00	0.5008E+01
15	0.7000E+00	0.5446E+01
16	0.7500E+00	0.5879E+01
17	0.8000E+00	0.6308E+01
18	0.8333E+00	0.6256E+01

C0RE DYNAMIC PRESSURES (PSI) AT EACH 0PENING

0PENING N0. / TIME(SEC)	1	2	3	4	5	6	7	8
0.	0.	0.	0.	0.	0.	0.	0.	0.
0.050	4.33	0.	4.33	4.33	4.33	4.33	0.	0.
0.100	4.21	0.	4.21	4.21	4.21	4.21	0.	0.
0.150	4.09	0.	4.09	4.09	4.09	4.09	0.	0.
0.200	3.98	0.	3.98	3.98	3.98	3.98	0.	0.
0.250	3.86	3.86	3.86	3.86	3.86	3.86	3.86	3.86
0.300	3.72	3.72	3.72	3.72	3.72	3.72	3.72	3.72
0.350	3.58	3.58	3.58	3.58	3.58	3.58	3.58	3.58

Table E-3
SAMPLE PROBLEM LISTING TO SHOW TYPICAL INPUT AND OUTPUT

0.400	3.46	3.46	3.46	3.46	3.46	3.46	3.46	3.46
0.450	3.34	3.34	3.34	3.34	3.34	3.34	3.34	3.34
0.500	3.23	3.23	3.23	3.23	3.23	3.23	3.23	3.23
0.550	3.12	3.12	3.12	3.12	3.12	3.12	3.12	3.12
0.600	3.02	3.02	3.02	3.02	3.02	3.02	3.02	3.02
0.650	2.93	2.93	2.93	2.93	2.93	2.93	2.93	2.93
0.700	2.84	2.84	2.84	2.84	2.84	2.84	2.84	2.84
0.750	2.75	2.75	2.75	2.75	2.75	2.75	2.75	2.75
0.800	2.67	2.67	2.67	2.67	2.67	2.67	2.67	2.67
0.833	0.	0.	0.	0.	0.	0.	0.	0.

TRANSLATION OF OBJECT

ACCELERATION COEFFICIENT = 0.7080 (SF/SLUG)
COORDINATES CENTERED IN OPENING

OPENING NO. 1

INITIAL COORDS. X (FT)	Y (FT)	FINAL COORDS. X (FT)	Y (FT)	FINAL SPEED (FPS)
0.	0.	113.1	0.	197.1
0.	2.5	91.1	2.5	154.8
0.	5.1	0.	5.1	0.
12.7	0.	115.6	0.	173.7
12.7	2.5	80.7	2.5	123.1
12.7	5.1	12.7	5.1	0.
25.4	0.	110.0	0.	145.2
25.4	2.5	76.0	2.5	97.0
25.4	5.1	31.7	5.1	12.9
25.4	7.6	25.4	7.6	0.
38.1	0.	110.6	0.	121.2
38.1	2.5	83.6	2.5	85.5
38.1	5.1	47.7	5.1	21.8
38.1	7.6	38.1	7.6	0.1
50.8	0.	99.6	0.	88.4
50.8	2.5	85.5	2.5	67.1
50.8	5.1	65.5	5.1	31.3
50.8	7.6	53.1	7.6	5.2
63.5	0.	97.9	0.	65.8
63.5	2.5	89.9	2.5	52.3
63.5	5.1	78.1	5.1	30.6
63.5	7.6	68.7	7.6	11.2
63.5	10.2	64.3	10.2	1.8
76.2	0.	101.4	0.	49.9
76.2	2.5	96.6	2.5	41.2
76.2	5.1	89.2	5.1	27.2
76.2	7.6	82.6	7.6	13.8
76.2	10.2	78.4	10.2	4.7
88.9	0.	108.0	0.	38.7
88.9	2.5	104.9	2.5	32.9
88.9	5.1	100.2	5.1	23.6
88.9	7.6	95.5	7.6	14.1
88.9	10.2	92.0	10.2	6.7
101.6	0.	116.5	0.	30.6
101.6	2.5	114.5	2.5	26.6
101.6	5.1	111.2	5.1	20.2
101.6	7.6	107.9	7.6	13.5
101.6	10.2	105.2	10.2	7.7
114.2	0.	126.2	0.	24.7
114.2	2.5	124.8	2.5	21.9
114.2	5.1	122.5	5.1	17.4
114.2	7.6	120.2	7.6	12.4
114.2	10.2	118.0	10.2	8.0
126.9	0.	136.7	0.	20.3
126.9	2.5	135.7	2.5	18.3
126.9	5.1	134.1	5.1	15.0
126.9	7.6	132.3	7.6	11.3
126.9	10.2	130.6	10.2	7.8
139.6	0.	147.7	0.	16.9
139.6	2.5	147.0	2.5	15.5
139.6	5.1	145.8	5.1	13.0
139.6	7.6	144.5	7.6	10.2
139.6	10.2	143.2	10.2	7.5
152.3	0.	159.2	0.	14.3
152.3	2.5	158.6	2.5	13.2
152.3	5.1	157.7	5.1	11.3
152.3	7.6	156.7	7.6	9.2
165.0	0.	170.9	0.	12.3
165.0	2.5	170.5	2.5	11.4
165.0	5.1	169.8	5.1	10.0

Table E-3 (Continued)

Table E-3 (Concluded)

177.7	0.	182.8	0.	10.6
177.7	2.5	182.5	2.5	10.0
190.4	0.	194.8	0.	9.3

OPENING NO. 2

INITIAL COORDS. X (FT)	Y (FT)	FINAL COORDS. X (FT)	Y (FT)	FINAL SPEED (FPS)
0.	0.	66.2	0.	169.9
0.	2.5	54.2	2.5	128.7
0.	5.1	0.	5.1	0.
12.7	0.	75.1	0.	153.0
12.7	2.5	51.8	2.5	99.5
12.7	5.1	12.7	5.1	0.
25.4	0.	75.9	0.	124.9
25.4	2.5	53.8	2.5	75.6
25.4	5.1	28.8	5.1	9.3

between the blastward face and the opening, and an additional delay may be caused if a door or window resists blast entry for a certain time. Also, the user must type in the free-field duration of the positive overpressure, from which the program calculates the decay of the outside pressure by methods described in Refs. 1 and 3. Since both peak free-field overpressure and positive phase duration are specified, a specific value of weapon yield is tacitly implied.

Only three different pressure-time histories may be used in any one problem. The user must specify the history appropriate to each opening by the use of a "location code." The code number 1 means the history contains a reflected pressure pulse that clears during the "clearing time" (which also must be specified). The code numbers 2 and 3 are both for pressure-time histories that have no reflected pulse.

Corresponding to each location code number the user must specify a "drag coefficient," which is used by the program to calculate the drag pressure on the outside wall containing the opening (methodology is described in Section IIC3). The total pressure against an opening is the free-field pressure plus any pressure increments due to reflection and any increments or decrements due to drag. If the location code is 2 or 3 and the drag coefficient is zero, the total pressure is the free-field pressure (e.g., a fully buried structure's cover slab, in a Mach region). The program cannot compute pressure increments when the impact of the blast wave is not head-on. The user must estimate whether the conditions of impact at each wall of his problem are more nearly head-on or side-on.

Referring to Table E-3:

- The first two questions ask for the outside pressure and air density immediately before the arrival of the blast wave. In the sample these questions have been answered from information for the standard sea level atmosphere listed in Table 6.1 of Volume 1.

- In the third and fourth questions the program obtains pertinent physical parameters of the open shelter: room volume in cubic feet and number of openings through which it fills. If the user does not want translational (jet effect) information in the neighborhood of two or more openings, and if these openings are in the same wall, he should add their areas together and consider the several openings as a single opening. The computer output formats are arranged for a maximum of eight openings but the program will accept any integral number. The response to "Number of openings (not more than 8)?" must be an integer, typed with no decimal point.

- In answering the next four questions the user must enter data for each of the openings included in the response to the fourth question. The sequence of items in each list must be such that the openings to which the items pertain are in the same order after each question. Opening areas are entered in square feet, Location code for each opening must be an integer: 1, 2, or 3, typed without a decimal. Delay in entry at each opening is in milliseconds; in the absence of resistance to entry at the opening, the delay may be calculated by dividing the distance to the opening (measured along the line of blast travel from the blastward wall) by the shock speed. Such a delay for any opening in the blastward wall will be zero. Shock speed in standard air may be found in Table E-4 as a function of peak overpressure. Whenever the blast wave must break a structure, such as a door or window, to gain entry to the room, a breakage time delay must be included in the delay time. Breakage time for ordinary window glass is approximately 4 ms[4]. An independent estimate of time to failure must be made by the engineer for each door and wall subjected to blast. Communication distance (eighth question) is that distance over which sound waves must "communicate" to the entering wave the shape and size of the opening. Were there to be no effect on the blast wave arising from the edges of the aperture or entry channel, the entering air flow would remain what it is initially, that is, shock afterflow. At free-field overpressures above about 20 psig this afterflow is usually stronger than jet flow; below approximately 20 psig afterflow is usually weaker. The program interpolates between afterflow and jet flow, based on a "communication" time, or time to establish jet flow as described in Section IIC1, which in turn is based on the program user's input value of "communication distance." In the case of a simple opening, this distance is the shortest dimension of the opening. For baffled openings or entry channels through mazes the best estimate of communication distance is the distance along the shortest channel into the room. In the case of a composite opening, that is, an opening consisting of two or more actual windows or other apertures, the communication distance should be found by averaging the distances for all openings included in the composite opening. Each distance is entered in feet.

- The ninth question refers to clearing time of the reflected blast wave from the blastward face of the structure. It is used in calculating the outside pressure on all openings assigned location code number 1. If there is no such opening, any value whatever may be entered for "clearing time." There will be no such openings, for example, in an underground structure. Clearing time

Table E-4

SHOCK SPEEDS IN STANDARD ATMOSPHERE*

P Peak Overpressure (psig)	U Shock Speed (fps)
5.	1268.
10.	1404.
15.	1528.
20.	1714.
25	1750.
30.	1850.
50.	2208.
100.	2917.

---

* Computed from the formula given in Ref. 1:

$$U = c_o \left(1 + \frac{6p}{7P_o}\right)^{0.5}$$

in which P_o = 14.7 psi and c_o = 1116. fps

may be calculated by multiplying by three the shorter of the following two distances: the height of the blastward wall or half its width; and dividing the product by the free-field shock speed from Table E-4. Clearing time is expressed in milliseconds.

- The computer program will assign the three drag coefficients of the tenth question to the three location code numbers in ascending order. The three values shown in the tenth question in Table E-3 are those recommended by Ref. 1 for the reflecting blastward wall (location code 1), the slab at ground level over an underground structure (assigned location code 2 in this example), and the rear or side wall of an above ground structure located at a free-field pressure below 25 psig (assigned location code 3 in this example), respectively. The recommended values are: 1 for a front wall, 0 for a ground level slab in the Mach region, and -0.4 for a roof and walls other than the blastward wall.

- The eleventh and twelfth questions describe the free-field blast wave at the same range or position as the structure. Overpressure is in pounds per square inch and positive phase duration is in seconds. If weapon yield and overpressure are known, positive phase duration can be found in Ref. 1.

- The next seven questions provide the user some choice of output. By answering .TRUE. to the thirteenth question "Want peak values only?", the program will omit intermediate values of inside pressure and print out only the maximum pressure and the time it first occurs. In the answer to the fourteenth question the user specifies the time interval (milliseconds) for which he wants the inside pressure. If the positive phase duration divided by the specified time interval is greater than 500, the calculation will be stopped before the end of the positive phase duration and a warning message containing the value of the time at the end of the calculation printed out. Ordinarily the user will have no need for the inside pressure during the relatively long outflow phase and he may save computer time and shorten the output by answering the fifteenth question, "Want decline of room pressure?" by typing .FALSE. Should the user need the pressure difference across an exterior wall (outside face minus inside face), he will probably want to answer the sixteenth question, "Want outside pressure?" with .TRUE. The pressure difference is then found at any opening in that wall. Ordinarily dynamic pressures in the various openings will not be needed, and the user will answer the seventeenth question, "Want values of dynamic pressure?" by

typing .FALSE. However, the sample output in Table E-3 contains dynamic pressures at each of the eight specified openings. These are "core" values, viz., dynamic pressures in the heart of the jet just inside the opening, as illustrated in Figure E-10.

- The eighteenth question, "Want translation effects?" should be answered .TRUE. if the user wants to estimate the hazard to a shelteree, stores, equipment, or other object arising from the translation of the object by the winds entering through the openings (jet effect). In Table E-3 this question has been answered .TRUE. so that the next question asks for the value of Acceleration Coefficient of the object (in square feet per slug). Acceleration coefficient is defined briefly in Section IIC3 and in great detail in Ref. 14. Table E-5 is a list of some typical values, particularly those for a human body in various postures in relation to the wind. In estimating translation hazard to the human body in a shelter the value for the prone body athwart the wind stream is recommended: 0.708 sf/slug. Values for objects not listed in Table E-5 may in some cases be estimated by the calculations described in Section IIC3.

When computing translation, the program places the body initially at a number of different points on a grid or coordinate system centered at the center of each opening and compute a time-history of displacement and speed for each starting grid point. The x-coordinate lies in the direction of the wind; the y-coordinate lies in any direction normal to the wind. The final coordinates and final speed correspond to the position and speed the unimpeded object has reached at the time the pressure difference between inside and outside becomes zero and the air flow first ceases. Since no decelerating forces are taken into account, the reported speed will be an upper limit on the speed achieved by an actual object.

VI. Edge Diffraction of an Acoustic Wave

A weak planar shock striking a semi-infinite wall head-on can be treated approximately as a self-similar acoustic wave in the manner demonstrated by Ludloff.[16] By this means we can estimate the pressure distribution within an open room during the diffraction phase immediately following blast arrival. Hitherto in this Appendix we have tried to calculate only an average air pressure in the filling room. Such an average may be grossly inadequate in determining the interior pressure load on the blast-struck wall, which is strongly affected immediately after blast arrival and long before the room fills appreciably, by the shock front as it diffracts through openings in that wall.

Table E-6

TYPICAL ACCELERATION COEFFICIENTS[14]

	sf/slug
168-lb man:	
Standing facing wind	1.67
Standing sidewise to wind	0.708
Crouching facing wind	0.676
Crouching sidewise to wind	0.547
Prone aligned with wind	0.203
Prone perpendicular to wind	0.708
Average value for tumbling man in straight, rigid position	0.966
21-g mice, maximum presented area	12.2
180-g rats, maximum presented area	6.12
530-g guinea pigs, maximum presented area	4.83
2100-g rabbits, maximum presented area	2.54
Typical stones:	
0.1 g	21.6
1.0 g	10.3
10.0 g	4.83
Window-glass fragments, 1/8 in. thick:	
0.1 g, all orientations	25.1
1.0 g, edgewise and broadside to wind	15.4-18.4
10.0 g, edgewise and broadside to wind	10.9-23.2
Steel spheres:	
1/8 in. diameter	4.48
1/4 in. diameter	2.24
7/16 in. diameter	1.28
1/2 in. diameter	1.12
9/16 in. diameter	0.998

This acoustic treatment is deficient in several ways. Shock waves do not behave like sound waves but only approach acoustic behavior at low overpressure. However, up to 5 psi free-field overpressure the differences (for our purposes) are not serious, and even above that level acoustic behavior is suggestive of shock behavior. A more restrictive limitation on the usefulness of the acoustic treatment is its two-dimensionality. We find here solutions valid only in a plane normal to an infinite reflecting half-plane and normal to the edge of this half-plane. In other words, the influences of other edges of the opening and of other walls of the room cannot be properly taken into account. However, there may be situations when the two-dimensional acoustic solution presented here will give useful insight into the shock pressure distribution on the inside of a blast-struck wall during the critical period immediately after blast arrival when the exterior air pressure load on the wall is at its peak.

The derivation that follows requires an understanding of the theory of functions of a complex variable. Reference 29 can provide guidance to a reader unfamiliar with the subject. The reader not wishing to pursue the derivation appearing below may turn immediately to Figure E-27, where the results of the calculation will be found in graphic form. A numerical example illustrating the use of Figure E-27 follows the figure.

In the acoustic approximation, all disturbances of effects are assumed to be propagated with sound speed.* Thus, after the incoming wave front strikes the semi-infinite wall, the influence of the edge will be felt only within a cylinder whose axis is the edge and whose radius is

$$c\ t$$

where c is sound speed and t is elapsed time after initial impact. If a Cartesian coordinate system is placed so that the edge of the semi-infinite plane becomes the z-axis and the negative y-axis lies in the plane, the location of the circle of influence of the edge is

$$x^2 + y^2 = c^2 t^2$$

and the equation satisfied by the overpressure p is

$$\frac{\partial^2 p}{\partial x^2} + \frac{\partial^2 p}{\partial y^2} = \frac{1}{c^2} \frac{\partial^2 p}{\partial t^2} \qquad (84)$$

The orientation of the circle and the wall is shown in Figure E-24. If a change of variables is made:

* Which is assumed constant throughout the calculation. In an actual blast the temperature - and hence the sound speed - will change from time to time and place to place.

$$\eta = \frac{y}{ct}, \quad \sigma = \frac{x}{ct}, \quad \text{and} \quad \tan \theta = \frac{y}{x} = \frac{\eta}{\sigma} \tag{85}$$

then in the new coordinates (η, σ, θ) the disturbance is confined to a circle of unit radius. If, further, radii are changed in scale according to the formula:

$$\rho = \frac{r}{1 + (1 - r^2)^{1/2}} \tag{86}$$

where ρ is the new radius and $r^2 = \eta^2 + \sigma^2$, then the equation satisfied by p in the cylindrical polar coordinates (ρ, θ) can be written

$$\rho \frac{\partial}{\partial \rho} \left(\rho \frac{\partial p}{\partial \rho} \right) + \frac{\partial^2 p}{\partial \theta^2} = 0 \tag{87}$$

This is Laplace's equation and is satisfied by the imaginary component of any analytic function of the complex variable.

$$\zeta = \rho \, e^{i\theta}$$

In the case of edge diffraction of a weak shock this method yields a solution for $0 \le r \le 1$ (or $0 \le \rho \le 1$). The angle θ lies in the range $-\pi/2 \le \theta \le 3\pi/2$, as illustrated in Figure E-24. The origin of coordinates labeled 0.

The boundary conditions are determined by physical considerations. Because the acoustic Eq. (84) or (87) is linear, the incident overpressure may be taken as unity and the pressure reflected from the wall, as 2. The overpressure in the undisturbed air is of course zero. These conditions imply the following pressure values on the circumference of the circle of influence:

$$\left.\begin{array}{ll} -\frac{\pi}{2} \le \theta \le 0 & p = 0 \\ 0 \le \theta \le \pi & p = 1 \\ \pi \le \theta \le \frac{3\pi}{2} & p = 2 \end{array}\right\} \tag{88}$$

Outside the circle pressure takes on uniform values within certain areas, as marked in Figure E-24.

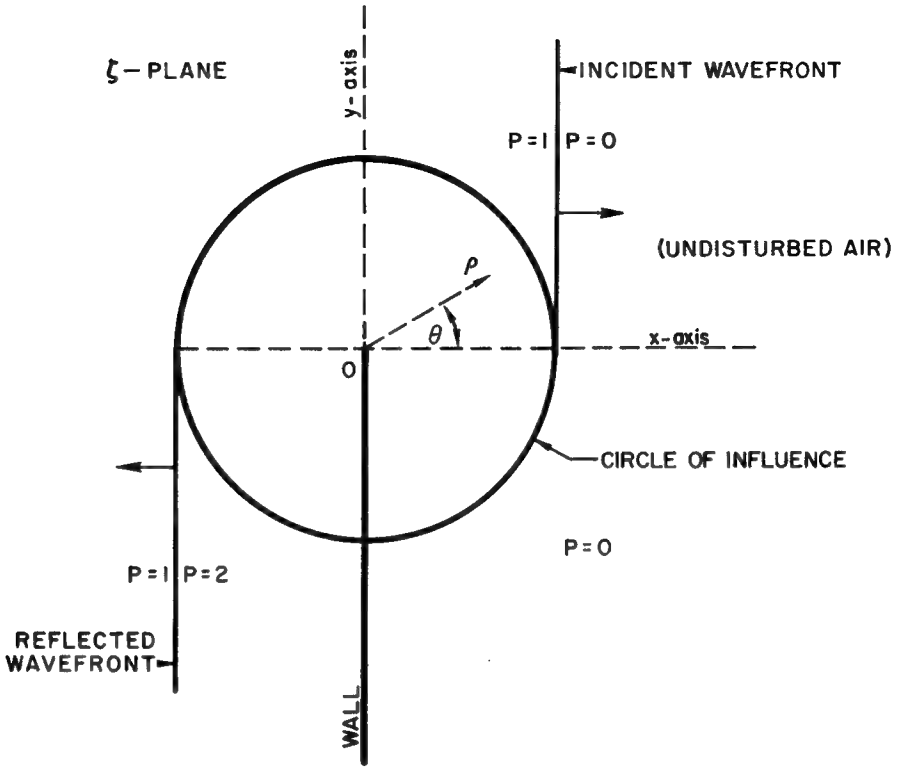

FIGURE E-24 BOUNDARY CONDITIONS ON CIRCLE OF INFLUENCE

Potential theory guarantees that there is only one pressure distribution within the unit circle that satisfies Eq. (87) and meets the foregoing boundary conditions. Equation (87) will be satisfied by any distribution function that is analytic.

A further transformation of variable will make the choice of the correct pressure distribution function clear. Let w be a complex variable defined by:

$$w = (i\zeta)^{1/2} = Re^{i\Phi} \tag{89}$$

where $R = \rho^{1/2}$ and $\Phi = \left(\frac{\pi}{2} + \theta\right)\frac{1}{2}$

In the w-plane, the unit circle of influence becomes a semicircle of radius 1; the back side of the wall lies along the line $\Phi = 0$ while the front side falls along $\Phi = \pi$. The line $\theta = 0$ in the ζ-plane rotates to $\Phi = \pi/4$ and the line $\theta = \pi$ is found along $\Phi = 3\pi/4$. Thus in the w-plane the boundary conditions on the semicircle R = 1 become

$$\left.\begin{array}{ll} p = 0 & 0 \le \Phi \le \frac{\pi}{4} \\ p = 1 & \frac{\pi}{4} \le \Phi \le \frac{3\pi}{4} \\ p = 2 & \frac{3\pi}{4} \le \Phi \le \pi \end{array}\right\} \qquad (90)$$

Any analytic function of w will also be an analytic function of ζ.

The function $w = -e^{\pi i/4}$ is represented by the line BA in Figure E-25 and its argument by the angle α. When A falls on the unit circle, α increased discontinuously from $-\pi/4$ to $3\pi/4$ as A moves counter-clockwise through the point B. The function $w = -e^{5\pi i/4}$ is continuous within and on the upper semicircle DBE. Furthermore the included angle γ is

$$\gamma = \alpha + \beta$$

where $\text{Arg}\left[w - e^{i\frac{\pi}{4}}\right] = -\alpha$ and $\text{Arg}\left[w - e^{i\frac{5\pi}{4}}\right] = \beta$. But along the arc EB, $\gamma = \frac{\pi}{2}$. Hence the function

$$f_1 = \frac{1}{\pi}\left\{\text{Arg}\left[\frac{w - e^{i\frac{5\pi}{4}}}{w - e^{i\frac{\pi}{4}}}\right] - \frac{\pi}{2}\right\}$$

is zero along EB and one along BD.

By a similar argument based on Figure E-26 it is clear that the function

$$f_2 = \frac{1}{\pi}\left\{\text{Arg}\left[\frac{w - e^{i\frac{7\pi}{4}}}{w - e^{i\frac{3\pi}{4}}}\right] - \frac{\pi}{2}\right\}$$

is zero along the arc EB′ and one along B′D.

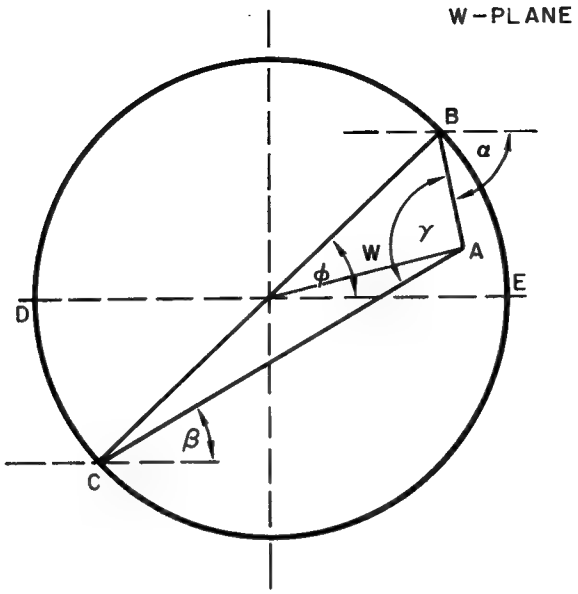

FIGURE E-25 COMPUTATION OF ARGUMENT $\left[\frac{w - e^{5\pi i/4}}{w - e^{\pi i/4}}\right]$

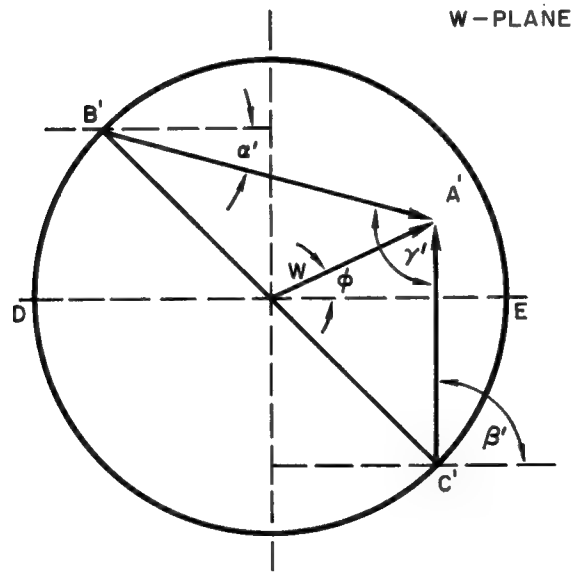

FIGURE E-26 COMPUTATION OF ARGUMENT $\left[\frac{w - e^{7\pi i/4}}{w - e^{3\pi i/4}}\right]$

Thus the sum

$$f_1 + f_2 = \frac{1}{\pi}\left\{ \mathrm{Arg}\left[\frac{w - e^{i\frac{5\pi}{4}}}{w - e^{i\frac{\pi}{4}}} \cdot \frac{w - e^{i\frac{7\pi}{4}}}{w - e^{i\frac{3\pi}{4}}} \right] - \pi \right\} \qquad (91)$$

meets the required boundary conditions along the semicircle EBD in the w-plane. But

$$F(w) = \frac{1}{\pi}\left\{ \ell n \left[\frac{w - e^{i\frac{5\pi}{4}}}{w - e^{i\frac{\pi}{4}}} \cdot \frac{w - e^{i\frac{7\pi}{4}}}{w - e^{i\frac{3\pi}{4}}} \right] - i\pi \right\}$$

is analytic in w and z and since $f_1 + f_2$ in Eq. (91) is evidently the imaginary part of F(w), Eq. (91) provides the sought-for expression giving the pressure distribution within and on the circle of disturbance $\rho = R = 1$.

Equation (91) can be written as

$$\pi p = \tan^{-1}\left(\frac{R \sin \Phi + \frac{1}{\sqrt{2}}}{R \cos \Phi - \frac{1}{\sqrt{2}}} \right) + \tan^{-1}\left(\frac{R \sin \Phi + \frac{1}{\sqrt{2}}}{R \cos \Phi - \frac{1}{\sqrt{2}}} \right)$$

$$- \tan^{-1}\left(\frac{R \sin \Phi - \frac{1}{\sqrt{2}}}{R \cos \Phi - \frac{1}{\sqrt{2}}} \right) - \tan^{-1}\left(\frac{R \sin \Phi - \frac{1}{\sqrt{2}}}{R \cos \Phi + \frac{1}{\sqrt{2}}} \right) - \pi \qquad (92)$$

where

$$R = \rho^{1/2} = \left[\frac{r}{1 + (1 - r^2)^{1/2}} \right]^{1/2}$$

and

$$\Phi = \frac{\pi}{4} + \frac{\theta}{2}$$

The denominators of the four arctangents in Eq. (92) have real roots in the range $0 \le \Phi \le \pi$ when $\rho \ge 1/2$; and care must be taken to evaluate the inverse functions in such a way that p is continuous within the unit circle. There are no zeros in the denominators when $\rho < \frac{1}{2}$.

If $R \cos \Phi_1 + \frac{1}{\sqrt{2}} = 0$ and

$$R \cos \Phi_2 - \frac{1}{\sqrt{2}} = 0$$

then $\frac{3\pi}{4} \leq \Phi_1 \leq \pi$

and $0 \leq \Phi_2 \leq \frac{\pi}{4}$

If the FORTRAN algorithm is used to evaluate the arctangent terms in Eq. (92) then for

$$\Phi > \Phi_2 \text{ and } R > \frac{1}{\sqrt{2}}$$

the second term,

$$\tan^{-1}\left(\frac{R \sin \Phi + \frac{1}{\sqrt{2}}}{R \cos \Phi - \frac{1}{\sqrt{2}}}\right)$$

can be increased by π, and the third term

$$\tan^{-1}\left(\frac{R \sin \Phi - \frac{1}{\sqrt{2}}}{R \cos \Phi - \frac{1}{\sqrt{2}}}\right)$$

must be decreased by π, or the sum in Eq. (92) increased by 2π. When $\Phi > \Phi_1$ and $R > \frac{1}{\sqrt{2}}$ we must add another 2π to keep the expression for p continuous and insure the existence of its derivatives.

In order to assure continuity with respect to radius the foregoing choices limit the arctangents to certain quadrants where radius R is such that no zeros in the denominators exist, i.e., when $R < \frac{1}{2}$. Thus, since we have chosen to add π to

$$\tan^{-1}\left(\frac{R \sin \Phi + \frac{1}{\sqrt{2}}}{R \cos \Phi - \frac{1}{\sqrt{2}}}\right)$$

for $\Phi > \Phi_2$ and $R > \frac{1}{2}$, we must, when using the FORTRAN algorithm, add π to the same inverse tangent for all Φ when $R < \frac{1}{2}$ in order to place the angle computed in the second quadrant. Similarly, by subtracting π from

$$\tan^{-1}\left(\frac{R \sin \Phi - \frac{1}{\sqrt{2}}}{R \cos \Phi - \frac{1}{\sqrt{2}}}\right)$$

when $\Phi > \Phi_2$ and $R > \frac{1}{2}$ we are placing the arctangent in the range $-\frac{\pi}{2}$ to $-\pi$; hence the same function, when $R < \frac{1}{2}$, must be computed in the same range by subtracting π from the angle as computed by FORTAN. When $R < \frac{1}{2}$ the denominator

$$R \cos \Phi + \frac{1}{\sqrt{2}}$$

is always positive and when $R < \frac{1}{2}$ the FORTRAN choices of quadrant for the two arctangents containing it are consistent with those for $R > \frac{1}{2}$.

Pressure contours, located as outlined above, are shown in Figure E-27, in which the planar acoustic front is moving from left to right past the parallel wall shown as the heavy vertical line in the lower center of the Figure. The reflected wave is moving right to left off the wall (lower left); the incident wave (upper right) has passed the wall. The zone of influence of the edge is a circle centered at the edge.

Numerical Example No. 7 (Pressure Distribution over a Wall Near an Edge). Consider a large opening in a wall struck head-on by a 5-psig blast wave. Taking time t = o at the moment of impact, we estimate the pressure history over the inside and outside surfaces of the wall along a line normal to any edge of the opening. Standard atmospheric conditions are assumed to prevail inside and outside the wall before blast arrival.

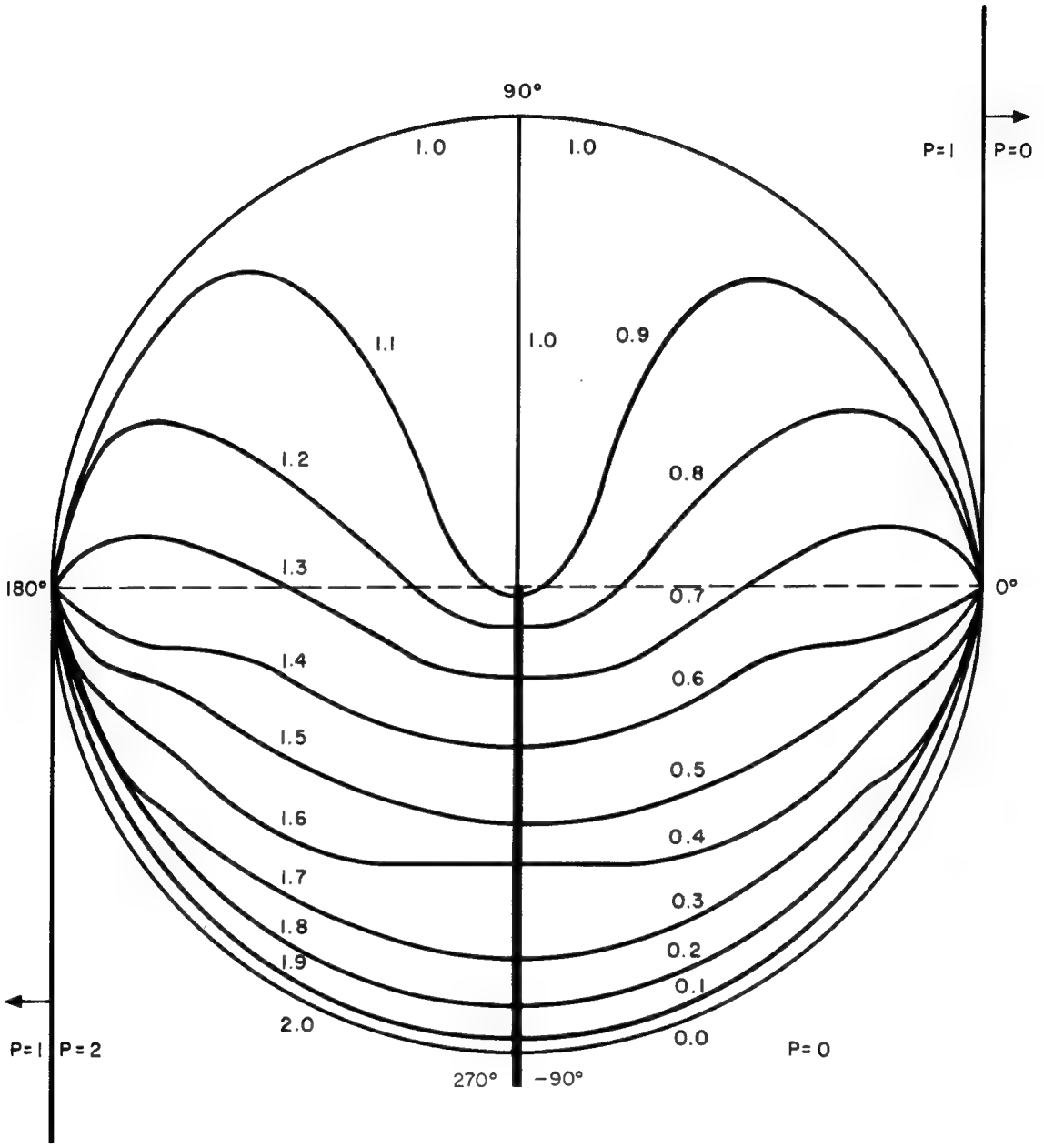

FIGURE E-27 PRESSURE CONTOURS WITHIN CIRCLE OF INFLUENCE

*The extent of the penetration y of the shock front is estimated from the speed of sound**

$$c = 1116 \text{ fps}$$

so that

$$y = ct = 1116\ t.$$

At t = 10 ms, for example, a distance of 11.2 ft along the wall inside the opening has been affected by the entering blast. The pressure distribution within that 11.2 ft can be found by reference to Figure E-27, in which the outermost (circular) contour now corresponds to 11.2 ft. The pressure along the lower right quadrant of that contour is zero. At a distance from the edge of the opening equal to 10.7 ft the pressure is 0.1 × 5 = 0.5 psig. This is where the 0.1 contour intersects the wall. At 5.68 ft from the edge the pressure at t = 10 ms is 0.5 × 5 = 2.5 psig, as given by the intersection of the 0.5 contour and the wall. Outside the wall these same contours are associated with pressures less than the pressure prevailing outside after reflection; that is, outside the wall the 0.1 contour becomes the 2- 0.1 = 1.9 contour, so that the pressure difference across the wall at t = 10 ms and y = 10.7 ft is (1.9 - 0.1) × 5 = 9.0 psig. Beyond the circle of influence, for example at y = 12, the pressure difference is (2.0 - 0.0) × 5 = 10.0 psig.

---

* *Calculated in Numerical Example No. 4.*

NOTATION*

A	Area
A_o	An additive term appearing in Eq. (5)
B	Constant equal to various functions of γ and/or of interior and exterior conditions, appearing in Eq. (5)
b	Half width of jet mixing zone
b_o	Maximum width of jet core
C	Constant
C_d	Drag coefficient
c	Speed of sound in air
c_o	Speed of sound in the standard atmosphere
c_v	Specific heat at constant volume for air
D	Diameter
F	Numerical factor for consistency of units
I	Integral
I	Impulse
K	Discharge coefficient
L	Linear dimension
ℓ	Distance along jet axis measured from opening
ℓ	Distance of travel along pipe

---

* Numerical subscripts may be used with variables to refer to a particular space or volume; see Preface.

M Mass of object

M Constant

m Mass of air

Δm Increment of air mass corresponding to time increment Δt

P Air pressure

P' Air pressure during immediately preceding time step

P_{1o} Peak overpressure outside front or first wall

P_{1r} Total overpressure outside rear wall

P_c Sum of dynamic and side-on air pressure at time t_c

P_d Free-field dynamic pressure

P_{dc} Dynamic pressure in blast wave at time t_c

P_{do} Peak dynamic pressure in blast wave

P_o Ambient air pressure

P_R Reflected pressure at a wall struck by blast wave

P_s Free-field side-on overpressure

P_{sc} Free-field side-on blast overpressure at time t_c

P_{so} Free-field peak side-on overpressure

p Overpressure

q Dynamic pressure of air

q_{core} Dynamic pressure of air in jet core

$\bar{q}$ (Spatial) average dynamic pressure in jet at one cross section

R Gas constant for air (See Ref. 5)

R Radius of jet of streming air

Re Reynolds number

r Radial coordinate, i.e., $r = (\eta^2 + \sigma^2)^{1/2}$

r Radial coordinate measured from axis of jet

r Ratio of pressures

S Specific entropy of air

ΔS Increment of entropy

s Wall dimension used to compute clearing time

s Distance

T Absolute temperature

T Time of passage of sound across object

ΔT Filling time or interval between first arrival of blast and achievement of pressure equilibrium

t Time measured from first arrival of blast at structure

t_c Clearing time of structure in blast wave

t_o Duration of positive side-on overpressure

t_1 Time required to establish jet flow through an opening

Δt Increment of time

U Blast front speed

u Particle speed of air

u_m Air particle speed along jet axis

u_o Air particle (wind) speed in jet core

V Volume of room or other space to be filled

ΔV Increment of air volume

v Speed of object in air stream

x Cartesian coordinate

y Cartesian coordinate

y Unknown variable in Eq. (5)

y Distance from outer jet boundary along normal to jet axis to point within mixing zone

y_o A specific solution of Eq. (5), i.e., $y_o = 0.1912$

w Complex variable $Re^{i\Phi}$

Δw Energy increment

α Angle in complex w-plane

α A certain function of y

α Angle between outer jet boundary and jet axis

β Angle in complex w-plane

γ Ratio of specific heat at constant pressure to specific heat at constant volume

γ Angle in complex w-plane

Δ Correction term applied to momentum balance associated with one control surface

ξ Complex variable $\rho e^{i\theta}$

λ Coefficient of resistance to flow in pipes

η Viscosity of air

η Coordinate of point in jet mixing zone; equal to y/b

η Time independent coordinate, i.e., $\eta = y/ct$

θ Angle between inward normal to surface and the positive direction of the x-axis

θ Angular coordinate, i.e., tan $\theta = y/x$

θ Ratio between temperature in jet core and that in room

ρ Density of air

ρ Reduced radial coordinate

ρ' Air density during immediately preceding time step

ρ_{core} Air density in jet core

ρ_o Ambient air density

ρ_w Density of water

σ Time independent coordinate, i.e., $\sigma = x/ct$

τ Time required to transmit a sound signal over the longest room dimension

π Ratio of circumference to diameter of circle

REFERENCES

1. Glasstone, S., editor, The Effects of Nuclear Weapons, U.S. Dept. of Defense and Atomic Energy Commission, Feb. 1964 reprint (with changes) of 1962 edition; Govt. Printing Office, Washington, D.C. 20402

2. Moulton, J., editor, Nuclear Weapons Blast Phenomena, Defense Atomic Support Agency (now Defense Nuclear Agency), Washington, D.C., DASA 1200 Vol. I, March 1960

3. Design of Structures to Resist the Effects of Atomic Weapons, EM 1110-345-413, Weapons Effects Data, Manuals - Corps of Engineers, U.S. Army, Washington, D.C., 1 July 1959

4. Iverson, J., Existing Structures Evaluation, Part II: Window Glass and Applications, Stanford Research Institute for the Office of Civil Defense, Menlo Park, Calif., December 1968 (AD-687 294)

5. Eshbach, O. W., editor, Handbook of Engineering Fundamentals, 2nd edition, John Wiley & Sons, 1952 (see chapter 8 for discussion of entropy and internal energy)

6. Oswatitsch, K., Gas Dynamics, Academic Press, 1956 (for a discussion of the concept and use of control surfaces in the study of flowing compressible fluids)

7. Eshbach, O. W., op. cit., pg 8-23

8. Eshbach, O. W., op. cit., pg 8-21

9. Coulter, G. A., Air Shock Filling of Model Rooms, Ballistic Research Laboratories Memorandum Report No. 1916, Aberdeen Proving Ground, Md., March 1968, Figure 28, pg 54 (AD-670 937)

10. Childers, H. M., C. A. Vansant and D. F. Mokrauer, Open Shelter Feasibility Study, The Vertex Corp. for the Office of Civil Defense, Kensington, Md., October 1968

11. Melichar, J. F., Air-Blast-Induced Aerodynamic Effects in Blast-Slanted Basement Shelters, URS Corporation for Office of Civil Defense, URS 692-3, OCD Work Unit 1126E, Burlingame, Calif., Jan. 1969 (AD-691 773)

12. Melichar, J. F., The Propagation of Blast Waves into Chambers: Aerodynamic Mechanisms, Terminal Ballistics Laboratory, Ballistic Research Laboratories, Aberdeen Proving Ground, Md., November 1967

13. Shapiro, A., The Dynamics and Thermodynamics of Compressible Fluid Flow, Volume I, The Ronald Press Co., 1953 (art. 4.7 for treating flow into a large reservoir which is steadily being evacuated)

14. Bowen, I. G., et al., A Model Designed to Predict the Motion of Objects Translated By Classical Blast Waves, Lovelace Foundation for Medical Education and Research, Albuquerque, N.M., U.S. Atomic Energy Commission CEX-58.9, June 29, 1961

15. Brode, H. L., Point Source Explosion in Air, RM-1824-AEC, the RAND Corporation, December 3, 1956

16. Ludloff, A. F., "On Aerodynamics of Blasts," Advances in Applied Mechanics, Vol. III, R. V. Mises, T. V. Kármán, editors, Academic Press, 1953

17. Air Blast Attentuation, IIT Research Institute for the Office of the Chief of Engineers, U.S. Army, Technical Manuscript S-1R, February 1971 (AD-729 425)

18. Coulter, G. A., op. cit., Figures 19 and 20, pp 43 and 44

19. Coulter, G. A., op. cit., Fig. 7, pg 27

20. Abramovich, G. N., The Theory of Turbulent Jets, M.I.T. Press, 1963

21. Coulter G. A., Flow in Model Rooms Caused by Air Shock Waves, Ballistic Research Laboratories Memorandum Report No. 2044, Aberdeen Proving Ground, Md., July 1970 (AD-711 885)

22. Melichar, J. F., Analysis of the Effect of Shelter Openings on Blast Protection, URS Research Company, San Mateo, Calif., for U.S. Office of Civil Defense, September 1970 (AD-724 710)

23. Taylor, W. J., Ballistic Research Laboratories, Aberdeen Proving Ground, Maryland, personal communication, March 1971

24. Kriebel, A. R., Airblast in Tunnels and Chambers, URS Research Company, San Mateo, Calif., for U.S. Defense Nuclear Agency, DRAFT Final Report, February 1972

25. Coulter, G. A., Blast Loading in Existing Structures - Basement Models, Ballistic Research Laboratories Memorandum Report No. 2208, Aberdeen Proving Ground, Md., August 1972 (AD-751 769)

26. Hoerner, S., Fluid Dynamic Drag, published by the author, Midland Park, N.J., Second Edition, 1958

27. Schlichting, H., Boundary Layer Theory, Fourth Edition, McGraw-Hill, 1960

28. Rouse, H., Elementary Mechanics of Fluids, John Wiley & Sons, 1953

29. Churchill, R. V., Complex Variables and Applications, Second Edition, McGraw-Hill, 1960

DISTRIBUTION LIST

Organization	No. of Copies
Defense Civil Preparedness Agency Research and Engineering Attention: Administrative Officer Washington, D.C. 20301	50
Assistant Secretary of the Army (R&D) Attention: Assistant for Research Washington, D.C. 20310	1
Chief of Naval Research Washington, D.C. 20360	1
Commander, Naval Supply Systems Command (Code 0652) Department of the Navy Washington, D.C. 20390	1
Commander Naval Facilities Engineering Command Research and Development (Code 0322C) Department of the Navy Washington, D.C. 20390	1
Advisory Committee on Civil Defense National Academy of Sciences Attention: Mr. Richard Park 2101 Constitution Avenue, N.W. Washington, D.C. 20418	1
Defense Documentation Center Cameron Station Alexandria, Virginia 22314	12
Civil Defense Research Project Oak Ridge National Laboratory Attention: Librarian P. O. Box X Oak Ridge, Tennessee 37830	1
Chief of Naval Personnel (Code Pers M12) Department of the Navy Washington, D.C. 20360	1
U.S. Naval Civil Engineering Laboratory Attention: Document Library Port Hueneme, California 93041	1
Director, Civil Effects Branch Division of Biology and Medicine Atomic Energy Commission Attention: Mr. L. J. Deal Washington, D.C. 20545	1
Air Force Special Weapons Laboratory Attention: Technical Library Kirtland Air Force Base Albuquerque, New Mexico 87117	1
AFWL/Civil Engineering Division Kirtland AFB, New Mexico 87117	1
Civil Engineering Center/AF/PRECET Wright-Patterson AFB, Ohio 45433	1
Chief of Engineers Department of the Army Attention: ENGME-RD Washington, D.C. 20314	1
Office of the Chief of Engineers Department of the Army Attention: Mr. Roy T. Spurlock Washington, D.C. 20314	50
Director, U.S. Army Engineer Waterways Experiment Station P. O. 631 Attention: Document Library Vicksburg, Mississippi 39180	1
Director, U. S. Army Engineer Waterways Experiment Station P. O. Box 631 Attention: Nuclear Weapons Effects Branch Vicksburg, Mississippi 39180	1
Director, Defense Nuclear Agency Attention: Technical Library Washington, D.C. 20305	1
Director, Defense Nuclear Agency Attention: Mr. Jack R. Kelso Washington, D.C. 20305	1

Organization	No. of Copies
Director, U.S. Army Ballistic Research Laboratories Attention: Document Library Aberdeen Proving Ground, Md. 21005	1
Director, U.S. Army Ballistic Research Laboratories Attention: Mr. William Taylor Aberdeen Proving Ground, Md. 21005	1
Agbabian Associates 250 N. Nash St. El Segundo, California 90245	1
Professor Robert Bailey Nuclear Engineering Department Duncan Annex Purdue University Lafayette, Indiana 47907	1
Miss Nancy K. Barberii OCD Professional Advisory Service Center University of Arizona Tucson, Arizona 85721	1 1
Dr. Harold Brode The RAND Corporation 1700 Main Street Santa Monica, California 90401	1
The Dikewood Corporation 1009 Bradbury Drive, S.E. University Research Park Albuquerque, New Mexico 87106	1
Mr. J. W. Foss Supervisor, Buildings Studies Group Bell Telephone Laboratories, Inc. Whippany Road Whippany, New Jersey 07981	1
Professor Raymond R. Fox Nuclear Defense Design Center School of Engineering & Applied Science George Washington University Washington, D.C. 20006	1
General American Transportation Corporation General American Research Division 7449 North Natchez Avenue Niles, Illinois 60648	1
Dr. William J. Hall University of Illinois 111 Talbot Laboratory Urbana, Illinois 61801	1
Professor Carl H. Koontz Department of Civil Engineering Worcester Polytechnic Institute Worcester, Massachusetts 01609	1
Mr. Samuel Kramer Chief Office of Federal Building Technology Center for Building Technology National Bureau of Standards Washington, D.C. 20234	1
Professor Richard E. Kummer 101 Eng. A Pennsylvania State University University Park, Pennsylvania 16802	1
Mr. John G. Lewis Defense Nuclear Agency Washington, D.C 20305	1
Mr. Anatole Longinow IIT Research Institute 10 West 35th Street Chicago, Illinois 60616	1
Dr. Stanley B. Martin Stanford Research Institute 333 Ravenswood Avenue Menlo Park, California 94025	1
Mr. R. W. Mayo Bell Telephone Laboratories, Inc. Whippany Road Whippany, New Jersey 07981	1
Dr. Clarence R. Mehl Dept. 5230 Sandia Corporation Sandia Base Albuquerque, New Mexico 87115	1
Professor William M. Miller Department of Civil Engineering 307 More Hall University of Washington Seattle, Washington 98105	1

Organization	No. of Copies
Mr. H. L. Murphy Stanford Research Institute 333 Ravenswood Avenue Menlo Park, California 94025	1
Research Triangle Institute P. O. Box 12194 Research Triangle Park, North Carolina 27709	1
Mr. James E. Roembke Research and Engineering Directorate Defense Civil Preparedness Agency Washington, D.C. 20301	1
Dr. Abner Sachs Institute for Defense Analysis 400 Army-Navy Drive Arlington, Virginia 22202	1
Professor John A. Samuel Department of Mechanical Engineering University of Florida Gainesville, Florida 32601	1
Mr. M. B. Scott Purdue Research Foundation School of Civil Engineering Civil Engineering Building Purdue University Lafayette, Indiana 47907	1
Mr. George N. Sisson Research and Engineering Directorate Defense Civil Preparedness Agency Washington, D.C. 20301	1
Dr. Lewis V. Spencer National Bureau of Standards Room C313 - Building 245 Washington, D.C. 20234	1
Dr. Robert G. Spicher Department of Civil Engineering San Jose State University San Jose, California 95114	1
URS Research Company 155 Bovet Road San Mateo, California 94402	1
Professor Gale K. Vetter School of Architecture University of Colorado Boulder, Colorado 80302	1
Mr. Luke J. Vortman Division 5412 Sandia Corporation Box 5800, Sandia Base Albuquerque, New Mexico 87115	1
Mr. Henry S. Wakabayashi Research and Engineering Directorate Defense Civil Preparedness Agency Washington, D.C. 20301	51
Mr. Thomas E. Waterman IIT Research Institute Technology Center 10 West 35th Street Chicago, Illinois 60616	1
Mr. Lyndon Welch Eberle Smith Associates, Inc. 950 West Fort Street Detroit, Michigan 48226	1
Dr. Clayton S. White President-Director Lovelace Foundation 5200 Gibson Boulevard, S.E. Albuquerque, New Mexico 87108	1
Dr. Merit P. White University of Massachussetts School of Engineering Amherst, Massachusetts 01002	1
Mr. Carl K. Wiehle Stanford Research Institute 333 Ravenswood Avenue Menlo Park, California 94025	1
Mr. Eugene F. Witt Bell Telephone Laboratories, Inc. Whippany Road Whippany, New Jersey 07981	1
Mr. Milton D. Wright Research Triangle Institute P. O. Box 12194 Research Triangle Park, North Carolina 27709	1

Organization	No. of Copies
Mr. Paul Zigman Environmental Science Associates 1291 E. Hillsdale Blvd. Foster City, California 94404	1
Mr. Hakan Axelsson	1
Dr. Nils Gylden	1
Mr. Vilhelm Sjolin Research Institute of National Defense Stockholm 80, SWEDEN	1
Dr. Benjamin Ma Dept. of Nuclear Engineering Iowa State University Ames, Iowa 50010	1
J. P. Nielsen Civil Emergency Measures Organization Department of National Defense 125 Elgin Street Ottawa, Ontario, CANADA K1A, OK2	1
Mr. Serge B. Pretre Dorfstrasse 11 CH-8954 GEROLDSWIL SWITZERLAND	1
Research Instiute for Protective Construction (FMB) Auf der Mauer 2 8001 Zurich, SWITZERLAND	1
Dr. Philip Thomas Fire Research Station Boreham Wood, HERTS. ENGLAND	1
Dr. Michel A. Toyer Chef du Laboratoire des Effets des Reyonnements Centre Scientifique et Technique du Batiment Avenue Jean Jaurès 77 Champs-Sur-Marne FRANCE	1
Dr. F. J. Agardy c/o URS Research Company 155 Bovet Road San Mateo, California 94402	1
Mr. Thomas Carrol Fairbank Research Station Federal Highway Administration 6300 Georgetown Pike Langley, Virginia 23365	1
Dr. A. F. Dill 601 Running Water Circle, S.E. Albuquerque, New Mexico 87123	1
Professor Bruce G. Johnston Civil Engineering Department University of Arizona Tucson, Arizona 85721	1
Dr. Nathan M. Newmark University of Illinois Civil Engineering Building Urbana, Illinois 61801	1
Biggers-Scarbrough-Neal-Crisp & Clark Architects and Engineers Attention: Mr. J.J.W. Biggers 1353 13th Avenue Columbus,	1
Mr. J. D. Latimer John D. Latimer & Associates Architects - Engineers P. O. Box 177 Durham, North Carolina 27702	1
E. Oren Smith, Architect 1505 Elmwood Drive Columbus, Georgia 31906	1
Stevens & Wilkinson Architects and Engineers Attention: Mr. P. S. Stevens 157 Lucky Street Atlanta, Georgia 30304	1
Mr. J. R. Janney c/o Wiss, Janney, Elstner & Associates 330 Pfinsten Road Northbrook, Illinois 60062	1
Mr. M. Kudroff Daniel, Mann, Johnson & Mendenhall 3325 Wilshire Boulevard Los Angeles, California 90005	1

Organization	No. of Copies	Organization	No. of Copies
Dr. Mete A. Sozen 3112 Civil Engineering Building University of Illinois Urbana, Illinois 61801	1		
Mr. R. G. Carroll c/o C. A. Hill & Associates P. O. Box 2088 Redding, California 96001	1		
Mr. J. H. Iverson 1410 Stephen Way San Jose, California 95129	1		
D. L. Leitner	2		
J. E. Trevor	1		
Org. 475 Info Center	1		
W. L. White	1		
C. K. Wiehle	1		
J. R. Rempel	1		
F. C. Allen	1		
G. G. Hoskins	1		
J. E. Beck	1		
H. L. Murphy Stanford Research Institute Menlo Park, California 94025			

Slanting for Combined Nuclear Weapons Effects: EXAMPLES WITH ESTIMATES, AND AIR BLAST ROOM FILLING (UNCLASSIFIED)

By: H. L. Murphy and J. E. Beck (with an Appendix by J. R. Rempel)

Stanford Research Institute, Menlo Park, California 94025
June 1973, 280 pages
Contract DAHC20-71-C-0292, DCPA Work Unit 1154H

This report provides updated and expanded versions of, and thus replacements for, Chapter 8 (Slanting the Building) and Appendix E (Room Filling from Air Blast) in the latest of a series of feasibility studies* on slanting (design modification) of basements in new buildings, to provide shelter against combined nuclear weapons effects - air blast and initial nuclear, thermal and fallout radiation. As in the overall feasibility study, the two parts of this report were written solely for the guidance of building design professionals (architects and engineers). *Full slanted basement shelters, as presented in these reports, more than meet requirements for protection against all natural disasters except floods, even those designed for as low as 5 or 10 psi air blast overpressure and related radiation effects.*

This first part of this report, entitled Chapter 8 (Slanting the Building), uses the study Scope and Stipulations sections, plus weapons effects data and engineering protective design guidance provided by earlier chapters, applying such data and guidance to slanting four buildings in a total of eighteen modifications from the buildings as originally designed. The first eight modifications are for 15 psi design peak overpressure and related effects; additional slanting applications are

Slanting for Combined Nuclear Weapons Effects: EXAMPLES WITH ESTIMATES, AND AIR BLAST ROOM FILLING (UNCLASSIFIED)

By: H. L. Murphy and J. E. Beck (with an Appendix by J. R. Rempel)

Stanford Research Institute, Menlo Park, California 94025
June 1973, 280 pages
Contract DAHC20-71-C-0292, DCPA Work Unit 1154H

This report provides updated and expanded versions of, and thus replacements for, Chapter 8 (Slanting the Building) and Appendix E (Room Filling from Air Blast) in the latest of a series of feasibility studies* on slanting (design modification) of basements in new buildings, to provide shelter against combined nuclear weapons effects - air blast and initial nuclear, thermal and fallout radiation. As in the overall feasibility study, the two parts of this report were written solely for the guidance of building design professionals (architects and engineers). *Full slanted basement shelters, as presented in these reports, more than meet requirements for protection against all natural disasters except floods, even those designed for as low as 5 or 10 psi air blast overpressure and related radiation effects.*

This first part of this report, entitled Chapter 8 (Slanting the Building), uses the study Scope and Stipulations sections, plus weapons effects data and engineering protective design guidance provided by earlier chapters, applying such data and guidance to slanting four buildings in a total of eighteen modifications from the buildings as originally designed. The first eight modifications are for 15 psi design peak overpressure and related effects; additional slanting applications are

Slanting for Combined Nuclear Weapons Effects: EXAMPLES WITH ESTIMATES, AND AIR BLAST ROOM FILLING (UNCLASSIFIED)

By: H. L. Murphy and J. E. Beck (with an Appendix by J. R. Rempel)

Stanford Research Institute, Menlo Park, California 94025
June 1973, 280 pages
Contract DAHC20-71-C-0292, DCPA Work Unit 1154H

This report provides updated and expanded versions of, and thus replacements for, Chapter 8 (Slanting the Building) and Appendix E (Room Filling from Air Blast) in the latest of a series of feasibility studies* on slanting (design modification) of basements in new buildings, to provide shelter against combined nuclear weapons effects - air blast and initial nuclear, thermal and fallout radiation. As in the overall feasibility study, the two parts of this report were written solely for the guidance of building design professionals (architects and engineers). *Full slanted basement shelters, as presented in these reports, more than meet requirements for protection against all natural disasters except floods, even those designed for as low as 5 or 10 psi air blast overpressure and related radiation effects.*

This first part of this report, entitled Chapter 8 (Slanting the Building), uses the study Scope and Stipulations sections, plus weapons effects data and engineering protective design guidance provided by earlier chapters, applying such data and guidance to slanting four buildings in a total of eighteen modifications from the buildings as originally designed. The first eight modifications are for 15 psi design peak overpressure and related effects; additional slanting applications are

Slanting for Combined Nuclear Weapons Effects: EXAMPLES WITH ESTIMATES, AND AIR BLAST ROOM FILLING (UNCLASSIFIED)

By: H. L. Murphy and J. E. Beck (with an Appendix by J. R. Rempel)

Stanford Research Institute, Menlo Park, California 94025
June 1973, 280 pages
Contract DAHC20-71-C-0292, DCPA Work Unit 1154H

This report provides updated and expanded versions of, and thus replacements for, Chapter 8 (Slanting the Building) and Appendix E (Room Filling from Air Blast) in the latest of a series of feasibility studies* on slanting (design modification) of basements in new buildings, to provide shelter against combined nuclear weapons effects - air blast and initial nuclear, thermal and fallout radiation. As in the overall feasibility study, the two parts of this report were written solely for the guidance of building design professionals (architects and engineers). *Full slanted basement shelters, as presented in these reports, more than meet requirements for protection against all natural disasters except floods, even those designed for as low as 5 or 10 psi air blast overpressure and related radiation effects.*

This first part of this report, entitled Chapter 8 (Slanting the Building), uses the study Scope and Stipulations sections, plus weapons effects data and engineering protective design guidance provided by earlier chapters, applying such data and guidance to slanting four buildings in a total of eighteen modifications from the buildings as originally designed. The first eight modifications are for 15 psi design peak overpressure and related effects; additional slanting applications are

for 5, 10 and 20 psi on two buildings ("open" shelter), and 20 and 30 psi on two others of the four buildings ("closed" shelter). Floor plans show both original layouts and slanting layouts, with the latter keyed to tables showing the specific modifications and the additional estimated cost of each.

The second part of the report, entitled Appendix E (Room Filling from Air Blast), provides the theory, equations, and practical simplifications necessary to solve the problem of estimating the behavior of air blast inside shelters, including locating zones of drag pressure or wind hazard (jet effect) and developing the pressure/time history of the average overpressure buildup and subsidence within the shelter (room filling). An interactive computer program (FORTRAN) listing is included.

---

*Murphy, H. L., Feasibility Study of Slanting for Combined Nuclear Weapons Effects (Revised), Volumes 1 and 2, SRI Technical Report for OCD (DCPA), July 1971 (AD-734 831 and 2), and an updating report:
Murphy, H. L., and J. R. Rempel, Slanting for Combined Nuclear Weapons Effects: FIRE HAZARD REDUCTION, Stanford Research Institute Technical Report for Defense Civil Preparedness Agency, August 1971 (AD-762 472).

for 5, 10 and 20 psi on two buildings ("open" shelter), and 20 and 30 psi on two others of the four buildings ("closed" shelter). Floor plans show both original layouts and slanting layouts, with the latter keyed to tables showing the specific modifications and the additional estimated cost of each.

The second part of the report, entitled Appendix E (Room Filling from Air Blast), provides the theory, equations, and practical simplifications necessary to solve the problem of estimating the behavior of air blast inside shelters, including locating zones of drag pressure or wind hazard (jet effect) and developing the pressure/time history of the average overpressure buildup and subsidence within the shelter (room filling). An interactive computer program (FORTRAN) listing is included.

*Murphy, H. L., Feasibility Study of Slanting for Combined Nuclear Weapons Effects (Revised), Volumes 1 and 2, SRI Technical Report for OCD (DCPA), July 1971 (AD-734 831 and 2), and an updating report:
Murphy, H. L., and J. R. Rempel, Slanting for Combined Nuclear Weapons Effects: FIRE HAZARD REDUCTION, Stanford Research Institute Technical Report for Defense Civil Preparedness Agency, August 1971 (AD-762 472).

for 5, 10 and 20 psi on two buildings ("open" shelter), and 20 and 30 psi on two others of the four buildings ("closed" shelter). Floor plans show both original layouts and slanting layouts, with the latter keyed to tables showing the specific modifications and the additional estimated cost of each.

The second part of the report, entitled Appendix E (Room Filling from Air Blast), provides the theory, equations, and practical simplifications necessary to solve the problem of estimating the behavior of air blast inside shelters, including locating zones of drag pressure or wind hazard (jet effect) and developing the pressure/time history of the average overpressure buildup and subsidence within the shelter (room filling). An interactive computer program (FORTRAN) listing is included.

*Murphy, H. L., Feasibility Study of Slanting for Combined Nuclear Weapons Effects (Revised), Volumes 1 and 2, SRI Technical Report for OCD (DCPA), July 1971 (AD-734 831 and 2), and an updating report:
Murphy, H. L., and J. R. Rempel, Slanting for Combined Nuclear Weapons Effects: FIRE HAZARD REDUCTION, Stanford Research Institute Technical Report for Defense Civil Preparedness Agency, August 1971 (AD-762 472).

for 5, 10 and 20 psi on two buildings ("open" shelter), and 20 and 30 psi on two others of the four buildings ("closed" shelter). Floor plans show both original layouts and slanting layouts, with the latter keyed to tables showing the specific modifications and the additional estimated cost of each.

The second part of the report, entitled Appendix E (Room Filling from Air Blast), provides the theory, equations, and practical simplifications necessary to solve the problem of estimating the behavior of air blast inside shelters, including locating zones of drag pressure or wind hazard (jet effect) and developing the pressure/time history of the average overpressure buildup and subsidence within the shelter (room filling). An interactive computer program (FORTRAN) listing is included.

*Murphy, H. L., Feasibility Study of Slanting for Combined Nuclear Weapons Effects (Revised), Volumes 1 and 2, SRI Technical Report for OCD (DCPA), July 1971 (AD-734 831 and 2), and an updating report:
Murphy, H. L., and J. R. Rempel, Slanting for Combined Nuclear Weapons Effects: FIRE HAZARD REDUCTION, Stanford Research Institute Technical Report for Defense Civil Preparedness Agency, August 1971 (AD-762 472).